The systematics, evolution, and extinction risks of tropical bees

A thesis submitted for the degree of Doctor of Philosophy

By

James Bryce Dorey

College of Science and Engineering
Flinders University
South Australia, Australia

Earth and Biological Sciences
South Australian Museum
South Australia, Australia

25th January 2022

Table of Contents

Thesis summary

Bees are a diverse group of insects that are ecologically and agriculturally crucial. Despite this, the taxonomy and biology of most bee species are poorly understood. Such knowledge is foundational for higher level questions and its paucity limits research and conservation of bee species. In this thesis, my first three chapters focus on a relatively simple ecological system — the endemic Fijian bee species in the genus *Homalictus* (Hymenoptera: Halictidae). My fourth chapter examines another tropical bee species, *Pharohylaeus lactiferus* (Cockerell, 1910) (Hymenoptera: Colletidae).

The endemic Fijian bee fauna was previously considered to be depauperate, with only four described species of *Homalictus*. However, recent sampling has uncovered surprising cryptic species diversity. In my first chapter, I used mitochondrial DNA (mtDNA) gene sequences and morphology to described nine new species. This chapter also highlights that the majority of the Fijian *Homalictus* diversity is found in highland regions (>800 m above sea level) and that there are more species requiring description. The total diversity is at least 22 species, all of which have arisen relatively recently from a single Fijian colonisation event. How this diversity has arisen in Fiji so quickly and predominantly in the highlands is of great interest. In my second chapter, I used phylogenetic analyses of mtDNA and single nucleotide polymorphism (SNP) data to contrast two ecological models of speciation: (i) the taxon cycle model and (ii) phylogenetic niche conservatism. Across most speciation events elevational state was conserved, providing support for phylogenetic niche conservatism over the taxon cycle model. This diversity likely arose through repeated contractions to, and expansions from, the highlands over past climate cycles, encouraging repeated isolation (vicariance) and admixture. With a strong phylogenetic signal across the phylogeny, it is likely that past climate cycles impacted the demography of even lowland Fijian *Homalictus* species. In my third chapter, I use COI, SNPs, and improved analytical methods to examine the past demography of *H. fijiensis* on two Fijian islands, Viti Levu and Kadavu. I found that the *H. fijiensis* population on Viti Levu has undergone a recent population increase that broadly coincided with the arrival and modification of the environment by humans (~3,000 years ago), but not with changing climates. In contrast to this, the Kadavu population has remained stable for the past 11,500 years and acts as a control for human impacts due to its limited history of anthropogenic disturbance. I show that the Fijian *Homalictus* are (i) species rich, (ii) most diversity in the highlands, (iii) have been impacted by past climate cycles, (iv) likely vulnerable to future climate change, and (v) have been impacted by human modification of the environment.

My final chapter describes the rediscovery, after 100 years, of the Australian tropical bee, *Pharohylaeus lactiferus*. It reviews the current knowledge of the genus. Then provides novel information about potential host and habitat specialisation and associated anthropogenic threats to *P. lactiferus*.

This thesis highlights the importance of taxonomy and the utility of tropical bees in studying the impacts of climate and humans on insect evolution, ecology, and conservation.

Declaration

I certify that this thesis:

1. does not incorporate without acknowledgment any material previously submitted for a degree or diploma in any university;
2. to the best of my knowledge and belief, does not contain any material previously published or written by another person except where due reference is made in the text; and
3. did not incorporate the services of any professional editors.

James Bryce Dorey

List of contributors/contributions

Primary supervisor	Associate Professor Michael P. Schwarz College of Science and Engineering Flinders University
Associate supervisor	Professor Michael S.Y. Lee College of Science and Engineering Flinders University, and Biological and Earth Sciences South Australian Museum
Adjunct supervisor	Associate Professor Mark I. Stevens Earth and Biological Sciences South Australian Museum, and School of Biological Sciences The University of Adelaide
Internal Committee	Professor Luciano B. Beheregaray College of Science and Engineering Flinders University
	Associate Professor Trevor H. Worthy College of Science and Engineering Flinders University

Division of labour table

JBD — James B. Dorey; MPS — Michael P. Schwarz; MSYL — Michael S.Y. Lee; MIS — Mark I. Stevens; SVCG — Scott V.C. Groom; EHF — Elisha H. Freedman; CSM — Cale S. Matthews; OKD — Olivia K. Davies; EJD — Ella J. Deans; CR — Celina Rebola; and AVC — Alejandro Velasco-Castrillón.

	Chapter 1	**Chapter 2**	**Chapter 3**	**Chapter 4**
Concept and design	JBD	JBD, MPS, MIS	JBD	JBD
Planning and implementation	JBD, MPS, MIS	JBD, MPS, MSYL, MIS	JBD, MPS, MSYL	JBD
Data collection	JBD, MPS, MIS	JBD, MPS, MIS, EHF, CSM, SVCG, CR, OKD	JBD, MPS, MIS, SVCG, AVC	JBD
Analysis	JBD	JBD, MPS, MSYL, EHF, CSM	JBD, MSYL, MPS	JBD
Interpretation	JBD	JBD, MPS, MSYL, MIS, EHF, CSM	JBD, MSYL, MPS	JBD
Writing and figures	JBD	JBD	JBD, SVCG	JBD
Editing	All authors	All authors	All authors	JBD
Overall responsibility	JBD	JBD	JBD	JBD

*In all chapters, I completed the vast majority of the work.

Acknowledgements

My first and greatest thanks must go to my primary supervisor Michael Schwarz, whose knowledge, passion and fascinating research drew me from the subtropics to the alternatingly boiling and freezing Adelaide. Four years of researching under your tutelage has certainly helped me grow as both a person and as a researcher. I hope that the results of your efforts are both evident and satisfying to see.

I also owe an incredible thanks to my associate and adjunct supervisors. Because most of my thesis is built around the results of phylogenetic analyses, Mike Lee's expertise in this field has been invaluable. Mike has always been very happy to provide well-considered help and advice. He has also put a lot of time and energy into helping me throughout my candidature and I have learned a lot about analysis, writing and science from him. Finally, Mark Stevens played a large role in recruiting me to Adelaide for my honours year and helped out with much of my early work, particularly chapter one.

But of course, as the age-old saying goes: *it takes a village to raise a thesis*. I assure you *they've* been saying that for years. No need to look it up.

Hence, my next most immense thanks goes to my lab-mates in the LEGS who, over the course of my project, were always available with an ear or advice. My long-term co-inmates and close friends have included: Olivia Davies, my partner and continual support network who has provided unfathomable assistance for both my project and my life in general; Ben Parslow, who was always keeping us all on-track, providing coffees, advice and a fantastic work and play environment in general; Robert O'Reilly, who has sought shelter with us bee-people for many years and indeed, blessed us with his friendship, chats, hangs and council; Justin Holder, one of Schwarz's last PhD students, who has quickly grown to be an integral and stalwart part of the lab always willing to have a chat, hang, provide advice and just be a good dude; Lucas Hearn, whose calm demeanour and terrifically-cutting humour has always been appreciated and enjoyable; Jess Clayton, while we were separated by offices you have always brightened my days with cheeky conversations, usually shared over lunch or coffee.

Of course, other students who might not have stayed as long have also had a massive and positive impact on me, including: Rebecca Dew, who was only present for the start of my time in Adelaide but nonetheless made me feel incredibly welcome and supported as a friend; Alice Woodward, who shared the lab with me for my honours year and, along with our other honours friends, made that year incredibly wonderful and enjoyable; Cale Matthews and Elisha Freedman, both joined us for two trips to Fiji meaning that we managed to have two wonderful years of Fiji work to become friends in; Bonnie Dern and Lucy Clive, our labs drifted apart somewhat during my time at Flinders but I will always have very fond memories of hanging out together and exchanging friendly and sometimes creative words; and Matthew Elmer, was already a close friend that I afforded much fondness and respect and his year in our lab (and home) only strengthened that bond.

Outside of this immediate university network, many others have inspired me during my thesis. Some of these people include: Stefan Caddy-Retalic and Emrys Leitch (plus their border-collie, Benny) with whom we shared countless stress-relieving walks, meals, and chats; Remko Leijs and Katja Hogendoorn, who have together and independently inspired my research in native bees and freely provided support, advice, and company in my learning; the Hogendoorn lab, including Jay Iwaski, Beth Fung, Jorgiane Parish, and Dona Kireta. Additionally, the many wonderful researchers and students who have inspired me at conferences and workshops.

Of course, most of the science behind my thesis would have been impossible without the support of quite a few funding bodies. To these organisations and their committees, I am eternally grateful. Not just for the help that they gave to me, but for the funding that they provide to support young researchers around the country. The bodies who funded me during my candidature were: Flinders University, for providing my PhD stipend through the AJ and IM Naylon PhD Scholarship; the Playford Trust for funding me during both my honours and PhD. Both of these funders have been very kind and have helped me put more into my research than I possibly could have done otherwise. The bodies that funded my actual research include: the Ecological Society of Australia through the Holsworth Wildlife Research Endowment which funded the majority of my doctoral work over three years and for which much research is still forthcoming; the Linnean Society of NSW through the Joyce W. Vickery Research Fund; the Flinders University Student Association through their FUSA development grant; the Royal Society of South Australia through their Small Research Grants Scheme; the Field Naturalists Society of South Australia through their Lirabenda Endowment Fund; and the Society of Australian Systematic Biologists for their Student Travel Award.

I would like to give thanks to the many researchers who reviewed my manuscripts [unfortunately] free of charge. Additionally, I thank the editors who similarly put in a lot of effort to improve my manuscripts and see that they were published. These editor were, in order of chapters: Jason Gibbs, Loeske Kruuk, Benjamin Sibbett, and Jack Neff. Their comments and suggestions improved the rigour of my research and therefore, my thesis.

There are just so many people that have helped me during my thesis or at the very least lessened the load of stress through their presence and kindness. I will try to mention more of those now. Of course, I must thank my family for not only providing literal refuge and support, but also for providing the open offer of fall-back support. This is not something that all candidates are privileged to have. My many house-mates during this time, including: Nicole Langley, Aidan Lee, Naja Dohm, [somehow] Deb Ide, Liv Davies, Lettee Dametto, Bella Davies, Matt Elmer, Leese Nelson, and Karo Lutkiewicz. I have had much help and company during my field work in Australia and my explicit thanks goes to Ben Parslow, Liv Davies, Erinn Fagan-Jeffries, Peter Rühr, Maddi Giannotta, Karl Magnacca, Lucas Hearn, Nadia Meakin, Jenny Thynne, Marie Laretive Siccard, and Carmen da Silva. My Fiji project's field work had many more helpers, primary amongst them were Scott Groom, Mark Stevens, Michael Schwarz, Meli Naiqama (as well as his family and Navai village), Marika Tuiwawa, Cale Matthews, Justin Biddle, Rebecca Schober, Matthew Elmer, Justin Holder, Elisha Freedman, Olivia Davies, and Ben Parslow. And finally, I would like to thank some Flinders support staff. Tania Bawden helped immensely with media releases for my publications and Brad Budgen was indispensable for help with just about everything else Flinders-related. Even though I rarely had to reach out to Tara Brabazon, her support of those around me, weekly vlogs, and vehement advocacy for HDR students and colleagues was a huge comfort and simply incredible to see.

I am certain that I will have forgotten many people who are doubtless worthy of appreciation and explicit acknowledgment here. Hopefully, you know who you are and will accept my accidentally-omitted thanks.

Thank you all.

PhD publication list

Bolded publications indicate thesis chapters

1. Naaz ZT, Bibi R, Dorey JB. 2021 Current status of bees in Fiji; geographical distribution and role in pollination of crop plants. Orient. Insects. (doi:https://doi.org/10.1080/00305316.2021.1982043)
2. Dorey JB, et al. 2021 Continental risk assessment for understudied taxa post catastrophic wildfire indicates severe impacts on the Australian bee fauna (ID: GCB-21-1545). *Global Change Biol.* **27**. (doi:https://doi.org/10.1111/gcb.15879)
3. **Dorey JB, Groom SVC, Velasco-Castrillon A, Stevens MI, Lee MSY, Schwarz MP. 2021 Holocene population expansion of a tropical bee coincides with early human colonisation of Fiji rather than climate change. *Mol. Ecol.* (doi:https://doi.org/10.1111/mec.16034)**
4. **Dorey JB. 2021 Missing for almost 100 years: the rare and potentially threatened bee *Pharohylaeus lactiferus* (Hymenoptera, Colltidae). *J. Hymenoptera Res.* 81, 165-180. (doi:https://doi.org/10.3897/jhr.81.59365)**
5. Dorey JB. 2021 Phantom of the forest: after 100 years in hiding, I rediscovered the rare cloaked bee in Australia. The Conversation. (https://theconversation.com/phantom-of-the-forest-after-100-years-in-hiding-i-rediscovered-the-rare-cloaked-bee-in-australia-156026)
6. Dorey JB. 2021 The story of how the Australian cloaked bee was re-discovered. *Aust. Geogr*. **162**, 18-19.
7. da Silva CRB, et al. 2021 Climate change and invasive species: a physiological performance comparison of invasive and endemic bees in Fiji. *J. Exp. Biol.* **224**, jeb230326. (doi:https://doi.org/10.1242/jeb.230326)
8. O’Connor P, Dorey JB, Glatz RV. 2020 Buzz off honey industry, our national parks shouldn’t be milked for money. The Conversation.
9. Leijs R, Dorey J, Hogendoorn K. 2020 The genus *Amegilla* (Hymenoptera, Apidae, Anthophorini) in Australia: a revision of the subgenus *Asaropoda*. *ZooKeys* **908**, 45–122. (doi:https://doi.org/10.3897/zookeys.908.47375)
10. Ibalim S, Groom SVC, Dorey JB, Velasco-Castrillon A, Schwarz MP, Stevens MI. 2020 Origin and dispersal of *Homalictus* (Apoidea: Halictidae) across Australia, Papua New Guinea and Pacific. *Trans. R. Soc. S. Aust.*, 1–14. (doi:https://doi.org/10.1080/03721426.2020.1740957)
11. **Dorey JB, Groom SVC, Freedman EH, Matthews CS, Davies OK, Deans EJ, Rebola C, Stevens MI, Lee MSY, Schwarz MP. 2020 Radiation of tropical island bees and the role of phylogenetic niche conservatism as an important driver of**

biodiversity. *Proc Biol Sci* 287, 20200045. (doi:https://doi.org/10.1098/rspb.2020.0045)

12. Dorey JB, Fagan-Jeffries EP, Stevens MI, Schwarz MP. 2020 Morphometric comparisons and novel observations of diurnal and low-light-foraging bees. *J. Hymenoptera Res.* **79**, 117–144. (doi:https://doi.org/10.3897/jhr.79.57308)
13. **Dorey JB, Schwarz MP, Stevens MI. 2019 Review of the bee genus *Homalictus* Cockerell (Hymenoptera: Halictidae) from Fiji with description of nine new species. *Zootaxa* 4674, 1–46. (doi:https://doi.org/10.11646/zootaxa.4674.1.1)**
14. Leijs R, Dorey J, Hogendoorn K. 2018 Twenty six new species of *Leioproctus (Colletellus)*: Australian Neopasiphaeinae, all but one with two submarginal cells (Hymenoptera, Colletidae, Leioproctus). *ZooKeys* **811**, 109–168. (doi:https://doi.org/10.3897/zookeys.811.28924)
15. Lee MSY, Dorey JB. 2018 Evolution: dampening the cambrian explosion. *Curr. Biol.* **28**, R1353–R1355. (doi:https://doi.org/10.1016/j.cub.2018.10.012)
16. Dorey JB. 2018 *Bees of Australia: A Photographic Exploration*. Clayton, Australia, CSIRO Publishing; 224 p.
17. Dorey JB, Merritt DJ. 2017 First observations on the life cycle and mass eclosion events in a mantis fly (Family Mantispidae) in the subfamily Drepanicinae. *Biodivers. Data J.* **5**. (doi:https://dx.doi.org/10.3897%2FBDJ.5.e21206)
18. Dorey JB. 2017 In pursuit of pollinators. *Aust. Geogr.* **139**, 44-51.

General introduction

Pollination is a vital ecosystem service that is provided by many animals; bees, however, are considered to be the single most-important contributors [1-6]. Much pollination research has focussed on pollination by the European honeybee (*Apis mellifera*; Hymenoptera: Apidae). But this research often ignores the estimated 25,000 other bee species that are found worldwide [7-9]. Despite their importance, the taxonomy of many bee groups remains poorly-resolved [8,10,11]. For example, prior to my research, only four of the 22 currently known Fijian *Homalictus* (Hymenoptera: Halictidae) species were recognized and covered by taxonomic keys [12,13]. Taxonomic knowledge is foundational to most biological research and conservation. Hence, taxonomic gaps must be addressed before complex and novel evolutionary and ecological questions can be reliably addressed.

The framework of island biogeography theory has often been used to explore evolutionary and ecological hypotheses. At its core, island biogeography theory aims to explain the development and maintenance of species richness on islands, with implications for continental taxa [14-16]. Considering past climate cycles in island biogeography theory is an important addition to the theory [17,18], yet it has received relatively little empirical attention [50]. Shifts in climate, sea level, wind regimes, and ocean currents will all have impacted island biogeography [19]. The scale of climatic changes is predicted to be less in the tropics than at higher latitudes [51]. However, because tropical ectotherms have evolved as thermal specialists, they are generally more sensitive to climatic variations than their temperate or boreal counterparts [52,53]. This suggests that the impacts of (i) past climate cycles on species richness, and (ii) future climate change on extinction risks, might be greater at lower latitudes.

In addition to species richness, past climate cycles have also been hypothesised to have impacted past population sizes. However, studies that attempt to address such demographic questions are often confounded by the potential impacts of human alteration of the environment [20-24]. Pacific archipelagos are likely ideal systems to answer these hypotheses because many have relatively recent, varied, and tractable histories of human activity; Fiji is one such archipelago [25-27]. Answering these questions could also indicate the degree to which human modification of the environment can impact insect populations — currently a hotly-debated topic [28-31]. Parallels can then be drawn between Fiji and continental regions such as Australia.

In this thesis I aim to address several knowledge gaps about tropical bee systematics, evolution, and extinction risks. Primarily, I have collected and analysed molecular and distributional data from the only known endemic bee species in Fiji, *Homalictus*. The relative simplicity of the Fijian archipelago means that my aims can be addressed in the absence of many potential confounding factors present on continents. Firstly, I aimed to describe several of the Fijian *Homalictus* species — those where we had both male and female specimens. Secondly, I aimed to empirically compare and contrast the relative importance of the taxon cycle and phylogenetic niche conservatism models of speciation in generating Fiji's *Homalictus* diversity. Thirdly, I aimed to examine if past climate or human modification of the environment was associated with a sudden population increase in the predominant lowland Fijian bee species, *H. fijiensis* (Perkins & Cheesman, 1928). And finally, I aimed to locate the tropical bee species, *Pharohylaeus lactiferus* (Cockerell, 1910) (Hymenoptera: Colletidae) and explore if human modification of the environment might have influenced its extreme rarity.

My thesis is comprised of four data chapters. Chapter one was published in the journal *Zootaxa* (doi: https://doi.org/10.11646/zootaxa.4674.1.1); chapter two was published in the journal *Proceedings of the Royal Society B: Biological Sciences* (doi: https://doi.org/10.1098/rspb.2020.0045), chapter three was published in *Molecular Ecology* (doi: https://doi.org/10.1111/mec.16034), and chapter four was published in the *Journal of Hymenoptera Research* (doi: https://doi.org/10.3897/jhr.81.59365). While all four chapters have been published in separate journals, they all share a common reference format and list in this thesis.

A chapter-by-chapter break-down of author contributions can be found in the division of labor table (above). For all chapters, I was the first author and responsible for the majority of all work undertaken. Notable exceptions to this are: (i) most Fijian specimen collection was shared with other authors (SVCG, MIS, MPS, EJD, and CR) prior to and during my field work, which began in 2017; (ii) most molecular laboratory work was undertaken by other authors (SVCG, EJD, CR, and AVC); (iii) the concept, design, planning and implementation of chapter two was carried out by myself with advice from MPS and MIS; and (iv) the initial SNP filtering and analysis for chapter two was aided by EHF, with inputs from CSM. All authors made inputs into the chapters that they co-authored, but MPS and MSYL were particularly instrumental in the analysis and interpretation of chapters two and three. With this in mind, each chapter is briefly outlined below.

Chapter 1: Review of the bee genus *Homalictus* Cockerell (Hymenoptera: Halictidae) from Fiji with description of nine new species

In this chapter, I redescribe the four named Fijian *Homalictus* species and describe an additional nine species — those for which we have specimens of both sexes. I used both morphology and phylogenetics to delimit species. The new species described here are *H. atritergus* **sp. nov.**, *H. concavus* **sp. nov.**, *H. groomi* **sp. nov.**, *H. kaicolo* **sp. nov.**, *H. nadarivatu* **sp. nov.**, *H. ostridorsum* **sp. nov.**, *H. taveuni* **sp. nov.** *H. terminalis* **sp. nov.**, and *H. tuiwawae* **sp. nov.**. I provide an identification key for all species examined. Species descriptions include the (i) material examined, (ii) a species diagnosis for both sexes, (iii) a species description for both sexes (including an image plate), (iv) comments (if applicable), (v) distribution (including a map), and (vi) the etymology of new species names. I also discuss the distributional patterns of *Homalictus* diversity in Fiji, as well as potential risks associated with climate change.

Chapter 2: Radiation of tropical island bees and the role of phylogenetic niche conservatism as an important driver of biodiversity

My second chapter aimed to address why the newly recognized (Chapter 1) *Homalictus* species richness in Fiji is so high compared to studies prior to my PhD. From a single colonization event, Fiji now has at least 22 species of *Homalictus*, most of which are restricted to only a few topographically-complex islands. In this chapter, I use extensive phylogenetic analyses to compare the contributions of the taxon cycle (adaptive radiation in insular regions) and phylogenetic niche conservatism models of speciation to *Homalictus* species richness in Fiji. I argue that poor adaptive capacities of many Fijian *Homalictus* species have combined with past climate cycles and Fiji's topographic complexity to encourage climate-driven cycles of speciation. I suggest that phylogenetic niche conservatism is likely an important driver of diversity in tropical ectotherms and that it also might lead to major extinction risks under future climate change scenarios.

Chapter 3: Holocene population expansion of a tropical bee coincides with early human colonisation of Fiji rather than climate change

In chapter two I inferred that the Fijian *Homalictus* fauna has been strongly impacted by past climate cycles; particularly the numerous highland species. Hence, it seems likely that the most-common lowland bee species, *H. fijiensis*, might also have been impacted in the past by changing climates as suggested by Groom, *et al.* [32]. However, the methods used in that study were flawed. In this chapter I use an expanded mitochondrial DNA (mtDNA) dataset, as well as a large single nucleotide polymorphism (SNP) dataset, more advanced analyses, and carefully filtered data, to examine the past demography of *H. fijiensis*. In contrast to Groom, *et al.* [32], I found that the timing of population increase on the largest island of Viti Levu broadly coincided with the arrival of humans in the archipelago (~3,000 years ago) and not climatic changes. Unlike Viti Levu, the nearby island of Kadavu — which has a limited history of human clearing — shows no change in past demography in the past 11,500 years. Over this same time period there has been very little change in sea surface temperatures, but I estimated an approximate halving of available land area. Together, these results indicate that (i) human modification of the environment had a large, and positive, impact on *H. fijiensis* population size on Viti Levu and (ii) climatic changes in the last 11,500 years have not had a major impact of *H. fijiensis* demography. Importantly, these results indicate that tropical ectotherms can be used to uncover very recent demographic patterns and compare the relative impacts of climate change and human dispersals. Additionally, it provides empirical evidence that human modification of the environment, through habitat alteration, can have a large impact on bee populations in pre-modern times.

Chapter 4: Missing for almost 100 years: the rare and potentially threatened bee, *Pharohylaeus lactiferus* (Hymenoptera, Colletidae)

Reliable empirical evidence of anthropogenically-induced insect declines is important, but difficult to provide [33]. Like the Fijian bees, the foundational research for many Australian bee groups is absent [10]. In my final chapter, I report on the rediscovery, after almost 100 years, of the colletid bee species, *P. lactiferus*. This tropical species is particularly important as it is the only Australian species in the genus and has only one close relative — *P. papuaensis*, in Papua New Guinea. I provide the first biological information about the species, including: associated plant species, known distribution, potential habitat specialization, and behaviour. I also undertake exploratory GIS analyses to identify possible reasons for the rarity of *P. lactiferus* and its potential threats. So far, *P. lactiferus* has been found on only two plant species — *Stenocarpus sinuatus* (Proteaceae) and *Brachychiton acerifolius* (Malvaceae) — and near a single habitat type (tropical or subtropical rainforest). Despite extensive sampling, a lack of data makes drawing conclusions difficult. To this end, I highlight avenues of future research that could provide a stronger understanding of the species and its threats, particularly: the (i) use of trap nests, (ii) targeted sampling with an *a priori* sampling regime, (iii) species distribution modelling, and importantly (iv) genetic sampling for demographic reconstruction.

I conclude my thesis with a general discussion of my key research results and their broader implications.

Thesis structure

The thesis is broken into four chapters. These chapters are, most-importantly, preceded by a thesis summary and general introduction and succeeded by the general discussion. These sections are kept brief as important introduction and discussion materials are included within each chapter.

Each of these four chapters have been published in separate journals and are reproduced here with slight variations and permission from the publishers, where permission was required. While all of these journals have their own referencing style, this thesis shares one reference style and the single reference list is placed near the end of this thesis. Each of these journals also has their own formatting requirements. While I have made much of the formatting consistent across the thesis, I have intentionally maintained some journal formatting where I thought appropriate. For example, my thesis chapter names remain the same as the journal publications, I have kept figures embedded in chapter one for ease of reading, and other nuances might remain the same. Hence, the style of published chapters may vary from other thesis sections.

This thesis can easily be navigated by finding the page number of relevant sections and their headings in the table of contents.

Chapter 1: Review of the bee genus *Homalictus* Cockerell (Hymenoptera: Halictidae) from Fiji with description of nine new species

James B. Dorey[a,b,1], Michael P. Schwarz[a], and Mark I. Stevens[b,c]

[a]*College of Science and Engineering, Flinders University, GPO Box 2100, SA 5001, Adelaide, Australia*

[b]*Earth and Biological Sciences, South Australian Museum, GPO Box 234, SA 5001, Adelaide, Australia*

[c]*School of Pharmacy and Medical Sciences, University of South Australia, Adelaide, Australia*

[1] *Corresponding author. E-mail: jbdorey@me.com*

Published in Zootaxa (https://doi.org/10.11646/zootaxa.4674.1.1).

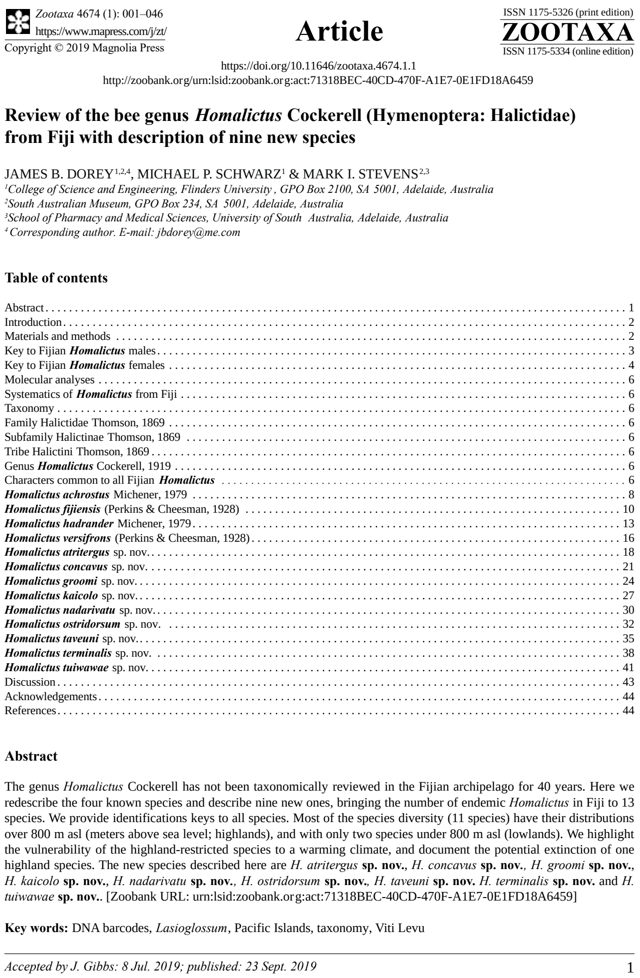

Zootaxa 4674 (1): 001–046
https://www.mapress.com/j/zt/

Article

ISSN 1175-5326 (print edition)
ZOOTAXA
ISSN 1175-5334 (online edition)

https://doi.org/10.11646/zootaxa.4674.1.1
http://zoobank.org/urn:lsid:zoobank.org:act:71318BEC-40CD-470F-A1E7-0E1FD18A6459

Review of the bee genus *Homalictus* Cockerell (Hymenoptera: Halictidae) from Fiji with description of nine new species

JAMES B. DOREY[1,2,4], MICHAEL P. SCHWARZ[1] & MARK I. STEVENS[2,3]
[1]*College of Science and Engineering, Flinders University , GPO Box 2100, SA 5001, Adelaide, Australia*
[2]*South Australian Museum, GPO Box 234, SA 5001, Adelaide, Australia*
[3]*School of Pharmacy and Medical Sciences, University of South Australia, Adelaide, Australia*
[4] *Corresponding author. E-mail: jbdorey@me.com*

Table of contents

Abstract

The genus *Homalictus* Cockerell has not been taxonomically reviewed in the Fijian archipelago for 40 years. Here we redescribe the four known species and describe nine new ones, bringing the number of endemic *Homalictus* in Fiji to 13 species. We provide identifications keys to all species. Most of the species diversity (11 species) have their distributions over 800 m asl (meters above sea level; highlands), and with only two species under 800 m asl (lowlands). We highlight the vulnerability of the highland-restricted species to a warming climate, and document the potential extinction of one highland species. The new species described here are *H. atritergus* **sp. nov.**, *H. concavus* **sp. nov.**, *H. groomi* **sp. nov.**, *H. kaicolo* **sp. nov.**, *H. nadarivatu* **sp. nov.**, *H. ostridorsum* **sp. nov.**, *H. taveuni* **sp. nov.** *H. terminalis* **sp. nov.** and *H. tuiwawae* **sp. nov.**. [Zoobank URL: urn:lsid:zoobank.org:act:71318BEC-40CD-470F-A1E7-0E1FD18A6459]

Key words: DNA barcodes, *Lasioglossum*, Pacific Islands, taxonomy, Viti Levu

---

Accepted by J. Gibbs: 8 Jul. 2019; published: 23 Sept. 2019

Abstract

The genus *Homalictus* Cockerell has not been taxonomically reviewed in the Fijian archipelago for 40 years. Here we redescribe the four known species and describe nine new ones, bringing the number of endemic *Homalictus* in Fiji to 13 species. We provide identifications keys to all species. Most of the species diversity (11 species) have their distributions over 800 m asl (meters above sea level; highlands), and with only two species under 800 m asl (lowlands). We highlight the vulnerability of the highland-restricted species to a warming climate and document the potential extinction of one highland species. The new species described here are *H. atritergus* **sp. nov.**, *H. concavus* **sp. nov.**, *H. groomi* **sp. nov.**, *H. kaicolo* **sp. nov.**, *H. nadarivatu* **sp. nov.**, *H. ostridorsum* **sp. nov.**, *H. taveuni* **sp. nov.**, *H. terminalis* **sp. nov.**, and *H. tuiwawae* **sp. nov.**. [Zoobank URL: urn:lsid:zoobank.org:act:71318BEC-40CD-470F-A1E7-0E1FD18A6459]

Introduction

The genus *Homalictus* Cockerell (Hymenoptera: Halictidae) was established by Cockerell [34] almost a century ago. More recently *Homalictus* has been suggested to be a subgenus of *Lasioglossum* Curtis based on phylogenetic analysis that renders *Lasioglossum sensu lato* paraphyletic [35,36]. However, *Homalictus* was not formally revised and placed as a subgenus of *Lasioglossum*. Most authors have retained the generic status *Homalictus* [8,37-44], while others place it within *Lasioglossum* [35,36,45,46]. Without a formal revision of the tribe Halictini, we are uncertain if *Homalictus* is indeed a subgenus of *Lasioglossum* or if *Lasioglossum*, as currently recognized, comprises multiple clades that may warrant generic status. While we treat *Homalictus* as a distinct genus, we recognise and highlight the need for comprehensive formal revision of the group and the new species names proposed here would survive relegation of *Homalictus* to subgeneric status.

The Fijian *Homalictus* form a monophyletic group resulting from a single colonisation event, with an estimated crown age of ~400 ka [47]. Only four endemic Fijian species of *Homalictus* have been described: *H. fijiensis* (Perkins & Cheesman 1928), *H. versifrons* (Perkins & Cheesman 1928), *H. hadrander* Michener, 1979 and *H. achrostus* Michener, 1979. Based on recent molecular analysis (using a fragment of the mitochondrial (mtDNA) cytochrome oxidase *c* subunit I (COI) gene) and morphological (male genitalia) characters many more species of *Homalictus* are present in Fiji, with most of these still undescribed [49].

Here we describe nine new *Homalictus* species for which both male and female specimens are currently available.

Materials and methods

DNA extraction and sequencing. Tissue samples for DNA extraction were obtained by removing a single hind leg from a specimen of each species (n = 764) except for *H. versifrons* as material could not be acquired. DNA extraction and PCR amplification prior to the 2014 samples was completed at the Canadian Centre for DNA Barcoding (CCDB) at the Biodiversity Institute of Ontario [32] and amplification used the universal C0I barcoding primers (LepF1 and LepR2 [32,50]). For all samples obtained after 2014, DNA extraction and PCR amplification was completed at the South Australian Regional Facility for Molecular Ecology and Evolution (SARFMEE); PCR amplification of the 710 bp fragment of the DNA (COI) was completed using the primers LCO1490 (forward) and HCO2198 (reverse) [51]. DNA extractions for post 2014 samples followed protocols described by Ivanova*, et al.* [52] with the subsequent DNA eluted into 75 μL of TLE buffer. The 25 μL PCR reactions comprised the following reagents: sterile H2O (15.9 μL), MRT buffer (5 μL), 1 μL (5 μM) of LCO1490, 1 μL (5 μM) of HCO2198, Immolase Taq (0.1 μL), and DNA from specimen (2 μL). The thermocycling regime comprised of one cycle at 94℃ for 10 min for initial denaturation, followed by five cycles at 94 C for 1 min, annealing at 46℃ for 90 sec, and extension at 72℃ for 75 sec, followed by 35 cycles at 94℃ for 60 sec, 51℃ for 90 sec, 72℃ for 75 sec. Finalising with one cycle at 72℃ for 10 min, and 25℃ for 2 min.

Sequences were checked against the NCBI BLAST database to screen for non-*Homalictus* mtDNA. Forward and reverse sequences of *Homalictus* specimens were aligned and checked using chromatograms for nucleotide assignment errors before creating final consensus sequences in *Geneious* version 10.2.2 [53]. All chromatograms sequence files were manually checked and all base calls were unambiguous. The *Homalictus* alignment was trimmed to 630 bp to avoid spurious results that could arise from missing data [54,55].

Phylogenetic analyses. Parameters for phylogenetic analyses were set using *BEAUti* version 1.8.4 [56]. Sequences were divided into three partitions based on codon position with substitution models unlinked, but tree and uncorrelated relaxed clock [57] models were linked for all partitions. The first and second codon positions were assigned an HKY+I+Γ substitution model, while the third codon position was given an HKY+Γ substitution model because those non-coding positions are not subject to selection. A Yule Process [58,59] speciation tree model was applied for the single specimen phylogeny while Bayesian skyline [60] was implemented for the multiple specimen phylogeny. Phylogenetic analyses were implemented in *BEAST* version 1.10.0 [60] with 500 million iterations, sampled every 50,000th iteration. Resulting log files were analysed in *Tracer* version 1.6 [61] and a burnin of 5x10^{7} iterations was employed, which was always after stationarity had been achieved. Maximum credibility trees and posterior probability (PP) support values were obtained using *TreeAnnotator* Version 1.8.4 [56].

Morphological analyses. Morphological characters were visualised using a Nikon SMZ1000 microscope and an LED ring light scored digitally and checked for their reliability and relevance before inclusion in descriptions or dichotomous keys. Surface puncture terminology was scored following Leijs, *et al.* [62] and Houston [63] and surface sculpture terminology follows Harris [64]. The ventral surfaces of male genitalia were imaged and examined, with a focus on the gonostylus and dorsoapical crest of the gonocoxite. Where some specimens were missing part of their metasoma, body length measurements have been omitted. Existing *Homalictus* species were identified using the key from Michener [65]. We were unable to identify any specimens of *H. versifrons* from the key or from the descriptions, so only the type specimen was examined. The type specimens of *H. achrostus*, *H. fijiensis*, and *H. hadrander* were each examined using a series of focus-stacked images provided by curators in CNC, NHMUK and SEMC, respectively.

Images were taken with a Canon EOS 5D MK iv or Canon EOS 5DSR using macro (dorsal, lateral, and rear; Canon MP-E 65 mm f 2.8 1–5x macro) and microscopic (head; Nikon 4x plan achromat, pygidial plate, propodeum, vertex, and supraclypeal area; Nikon 10x plan achromat) lenses, while male genitalia were imaged using a Nikon Eclipse 50i with the same camera attached. Measurements were taken using a dissecting microscope or using size-calibrated images.

Maps of Fiji were produced in *ArcMap* [66] and a Fiji digital elevation model (DEM) was provided by Fiji Lands Information System [67].

Terminology

The terminology used broadly follows Michener [68]:

UID: upper interorbital distance: shortest distance between upper inner margins of eyes.
LID: lower interorbital distance: shortest distance between lower inner margins of eyes.
AOD: antennocular distance: shortest distance from inner eye margin to rim of antennal socket.
IAD: interantennal distance: shortest distance between inner margins of antennal sockets.
OAD: ocellantennal distance: shortest distance between posterior margin of antennal socket and anterior margin of median ocellus.
IOD: interocellar distance: shortest distance between inner margins of rear ocelli.
OOD: ocellocular distance: shortest distance between upper inner margin of eye and ipsilateral rear ocellus.
EW: eye width: greatest width of eye in side view.
GW: genal width: greatest width of gena in side view.
ML: metanotum length: greatest width of metanotum measured anterioposteriorly.
SL: scutellum length: greatest width of scutellum measured anterioposteriorly.
BL: body length: distance from antennal sockets to posterior end of metasoma.
FL: forewing length: proximal end of costal vein to distal tip of wing.
m asl: metres above sea level
T1: first metasomal tergite

NHMUK – Natural History Museum UK
CNC - Canadian National Collection of Insects, Arachnids, and Nematodes, Ottawa.
SEMC - Snow Entomological Museum Collection, University of Kansas.
BPBM - Bernice Pauahi Bishop Museum, Honolulu.

The holotype and allotype specimens are deposited in the South Australian Museum, Adelaide (SAMA), while paratypes are on loan to Museums Victoria.

Key to Fijian Homalictus males

1. Fovea along anterior inner margin of eye present (Fig. 1d) 2

- Fovea along anterior inner margin of eye absent (Fig. 1h) 3

2. Habitus mostly blue and propodeum moderately strigate-rugose (Fig. 8) *H. hadrander*

- Habitus mostly black and propodeum has strong striae dorsally (Fig. 4) *H. achrostus*

3. Supraclypeal area mostly finely colliculate (Fig. 1f–g) 4

- Supraclypeal area mostly moderately colliculate (Fig. 1e) 8

4. Posterior or margin of scutum about straight (Fig. 11a) 5

- Posterior margin of scutum concave (Fig. 13a) *H. concavus* **sp. nov.**

5. Transverse striae along proximal margin of compound eyes, scutum and scutellum mostly golden, purple, blue and/or Pink *H. ostridorsum* **sp. nov.**

- Mostly colliculate along proximal margin of compound eyes, scutum and scutellum mostly golden green and metallic 6

6. T1 black or nearly so (Fig. 11a–c) *H. atritergus* **sp. nov.**

- T1 green (Figs 17 & 23a–c) 7.

7. Scutellum to forewing length ratio 1:14, supraclypeal area and scutum completely golden green and metallic *H. taveuni* **sp. nov.**

- Scutellum to forewing length ratio 1:16.5, supraclypeal area and scutum with golden and orange colouration *H. kaicolo* **sp. nov.**

8. Antennal sockets and paraocular area not strongly depressed, clypeus mostly finely colliculate 9

- Antennal sockets and paraocular area strongly depressed, clypeus finely and moderately colliculate 12

9. Frons with vertical striae 10

- Frons with many diagonal striae 11

10. Scape extends to or below anterior margin of medial ocellus and T1 green *H. fijiensis*

- Scape extends above head and T1 black or nearly so *H. terminalis* **sp. nov.**

11. Labrum with two medial projections, clypeus shiny and almost smooth *H. nadarivatu* **sp. nov.**

- Labrum simple, clypeus finely colliculate *H. tuiwawae* **sp. nov.**

12. Scutum mostly purple, striae on frons mostly transverse, posterior surface of the propodeum does not have transverse striae and metasoma “shining blackish brown and metallic” [48]

H. versifrons

- Scutum mostly green, striae on frons mostly longitudinal, posterior surface of the propodeum with diagonal striae ventrally and proximally and joins dorsal striae and metasoma dark green or green, dark along posterior edges *H. groomi* **sp. nov.**

Key to Fijian *Homalictus* females

1. Habitus mostly blue or black (Fig. 4, 8) 2
- Habitus mostly green (Fig. 11) 3
2. Habitus mostly blue and propodeum moderately strigate-rugose (Fig. 8g) *H. hadrander*
- Habitus mostly black and propodeum with strong striae dorsally (Fig. 4) *H. achrostus*
3. Supraclypeal area mostly finely colliculate (Fig. 1f–g) 4
- Supraclypeal area mostly moderately colliculate (Fig 1e) 8
4. Pygidial plate with few minute sparse punctures or open to dense fine punctures medially (Fig. 2), Scutum and scutellum golden, green or reddish 5
- Pygidial plate with close fine punctures (Figs 2, 21i), Scutum and scutellum mostly purple, with some orange and green (Fig. 21f) *H. ostridorsum* **sp. nov.**
5. Posterior margin of scutum about straight, propodeum coarsely strigate-rugose dorsally (Fig. 1a) 6
- Posterior margin of scutum concave, propodeum moderately strigate-rugose dorsally (Fig. 1b) *H. concavus* **sp. nov.**
6. Pygidial plate smooth (Fig. 11j), frons striate immediately above antennal sockets 7
- Dense line of medial hairs on pygidial plate (Figs 2, 27j), frons colliculate immediately above antennal sockets *H. tuiwawae* **sp. nov.**
7. Striae on dorsal, posterior margin of propodeum not forming a triangular pattern (Fig. 11f) *H. atritergus* **sp. nov.**
- Striae on dorsal, posterior margin of propodeum forms triangular pattern (Fig. 17f) *H. kaicolo* **sp. nov.**
8. Scape extends above head 9
- Scape does not extend beyond posterior margin of medial ocellus 10
9. Sculpturing on anterior of scutum colliculate but not lineolate, if there are punctures on the pygidial plate they are found in a medial line *H. terminalis* **sp. nov.**
- Sculpturing on anterior of scutum is colliculate and lineolate, minute punctures on pygidial plate (Figs 2, 19j) *H. nadarivatu* **sp. nov.**
10. Propodeum coarsely strigate-rugose (Fig. 1a), posterior margin of scutum straight and posterior surface of propodeum with transverse striae ventrally and proximally 11

- Propodeum moderately strigate-rugose dorsally (Fig. 1b), posterior margin of scutum concave and posterior surface of propodeum with diagonal striae originating ventrally and proximally *H. groomi* **sp. nov.**

11. Propodeum with a strong anterior medial groove dorsally (Fig. 6f) *H. fijiensis*

- Propodeum without a medial anterior groove dorsally (Fig. 23f) *H. taveuni* **sp. nov.**

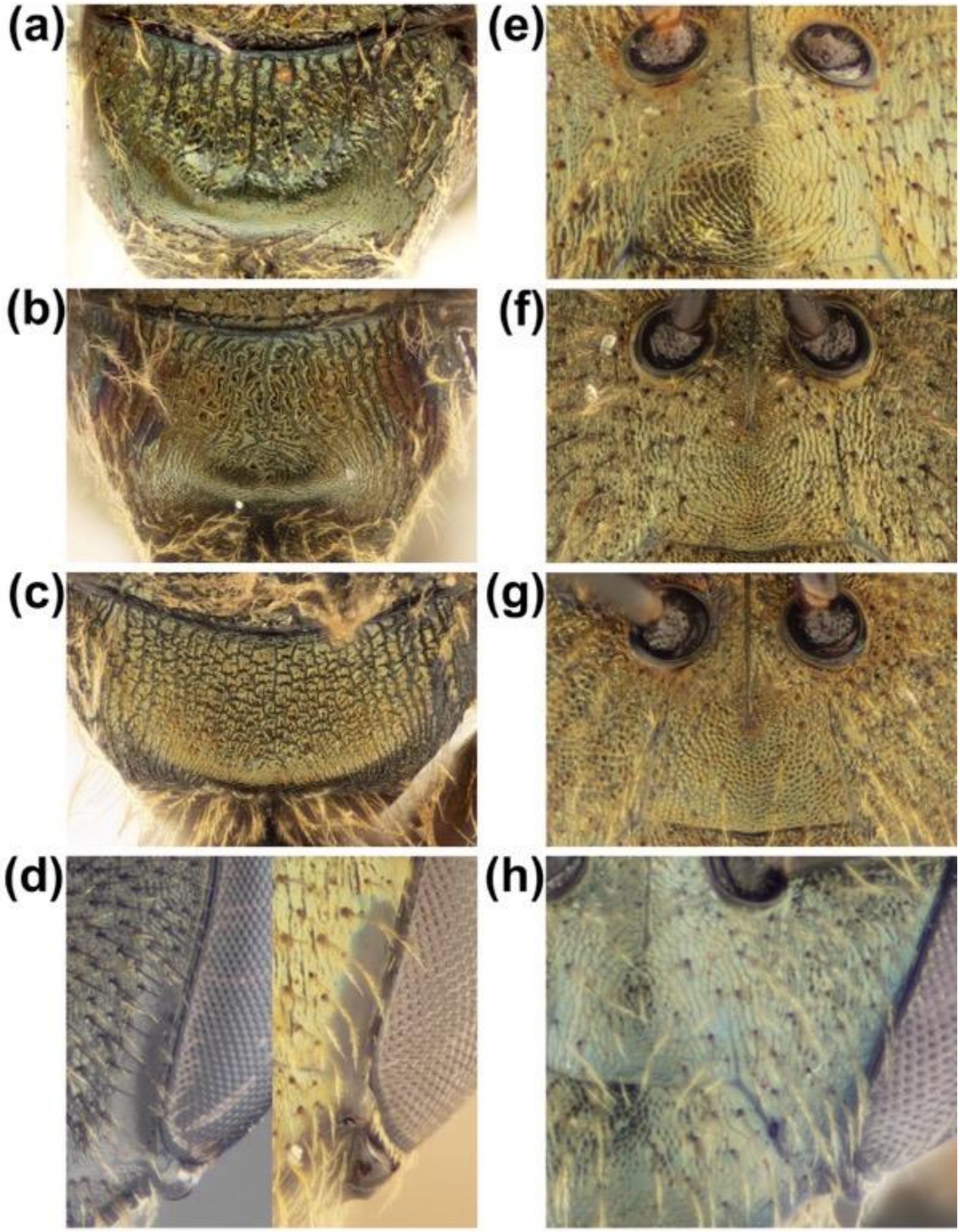

Figure 1. Propodeum dorsally showing (a) coarsely, (b) moderately, and (c) finely strigate-rugose sculpturing. Fovea along anterior inner margin of eye (d) present and (h) absent. Supraclypeal area showing (e) mostly moderately, (f) mostly finely, and (g) entirely finely sculpturing.

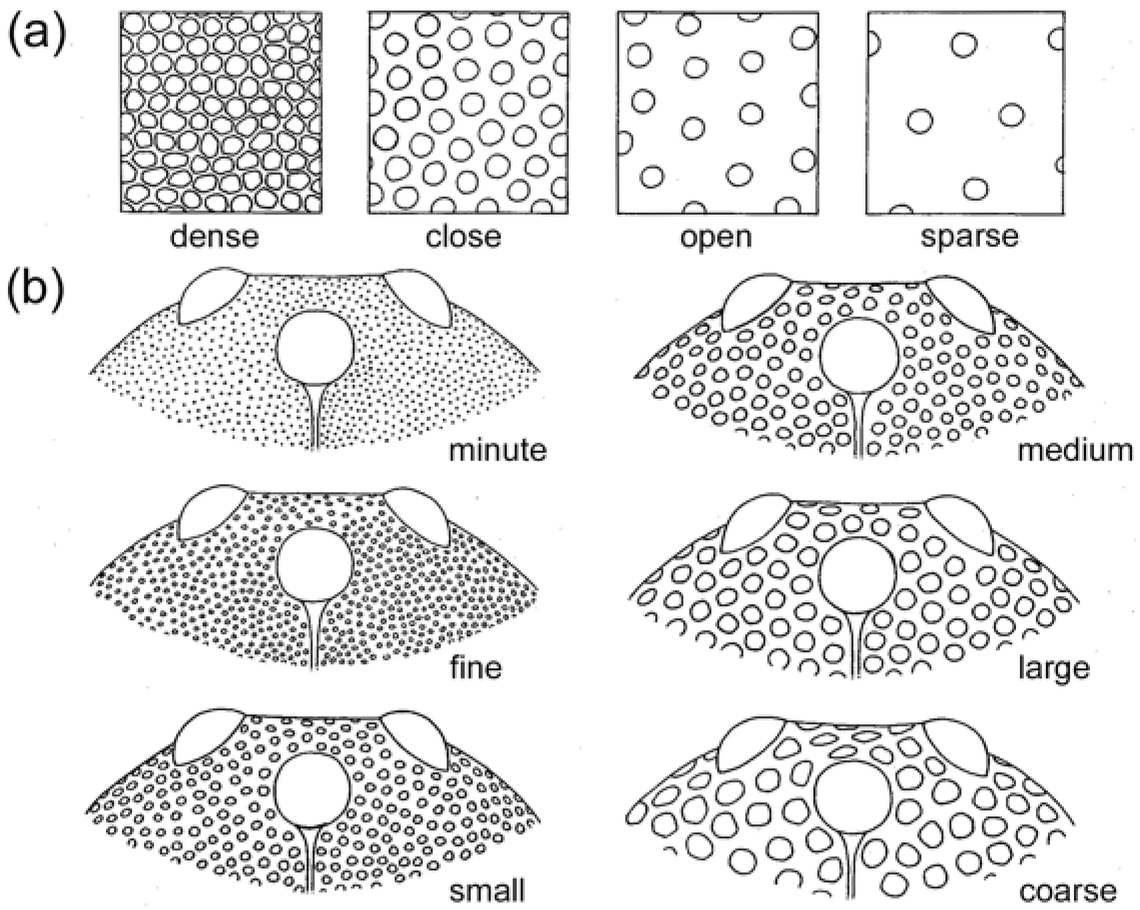

Figure 2. Grades of (a) pit density, and (b) pit size. Reproduced from Houston (1975) with permission from CSIRO Publishing.

Molecular analyses

The maximum credibility tree of the mtDNA (COI) gene from our BEAST analysis (Figs. 3 and S1) indicates the existence of 12 distinct clades. Distal clades generally had higher posterior probability support than basal clades, except for *H. achrostus*. Seven of the 11 clades in our BEAST analysis are restricted to single geographical highland regions (>800 m asl), while *H. taveuni* sp. nov. is restricted to a single island.

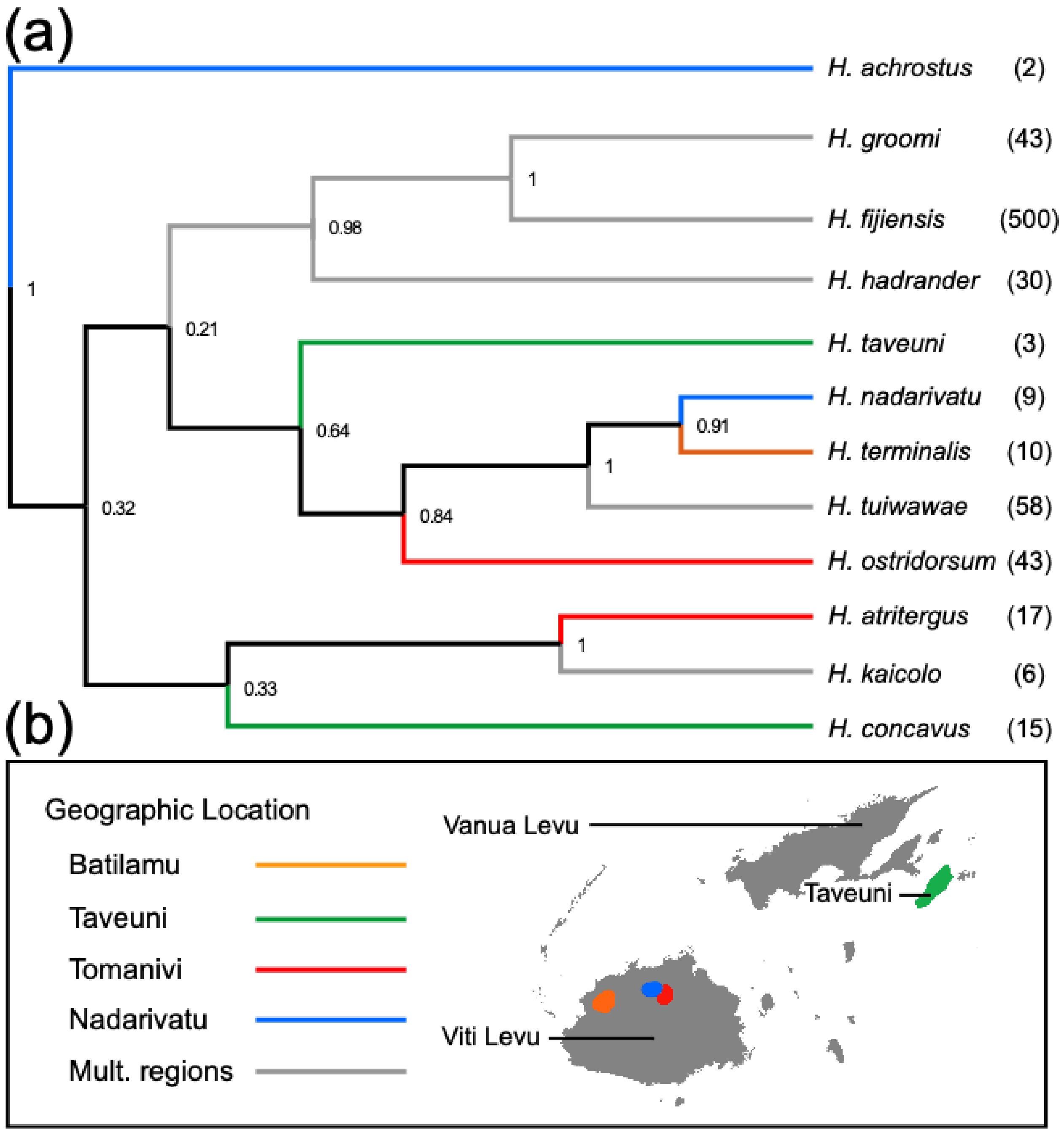

Figure 3. (a) maximum credibility tree of the Fijian *Homalictus* where branch colour represents (b) geographic location. Numbers at tree nodes show posterior probability and numbers in parentheses indicate sample sizes.

Systematics of *Homalictus* from Fiji

Taxonomy

Family Halictidae Thomson, 1869

Subfamily Halictinae Thomson, 1869

Tribe Halictini Thomson, 1869

Genus *Homalictus* Cockerell, 1919

Characters common to all Fijian *Homalictus*

The diagnosis for *Homalictus* remains unchanged, see Cockerell (1919). Here we summarise characters common to all Fijian *Homalictus* (male and female). The Fijian *Homalictus* have open to sparse (Fig. 2), moderate to long hairs covering their heads and thoraces; some hairs on the dorsal side of the metasoma becoming denser posteriorly and long to very long hairs on the ventral surface of the metasoma, with the longest and densest hairs on females. All females possess a black fovea along the proximal anterior margin of the eyes; this feature was also found in some males and might indicate feminization in some species. Mandibles of both males and females can be simple or bidentate and vary within species, perhaps the result of wear. The propodeum has a weak carina along the posterior dorsal margin, this can be depressed medially, or not, and can vary in breadth. The number of spines on the inner hind tibial spur varies greatly with 4-18 spines found on *H. fijiensis* alone and a range of one or two for other species. The claws of all specimens examined were cleft. The redescriptions below for *H. fijiensis*, *H. hadrander*, *H. achrostus*, and *H. versifrons* are provided to standardise the descriptions of Fijian *Homalictus*.

Homalictus achrostus Michener, 1979

(Figs 4-5)

Material examined

Type material ♂: Fiji, Viti Levu Nandaravatu, 1100m Microwave Stn. 16-23.VIII.78 S.&J. Peck-Mal. Trap. Holotype *Homalictus achrostus* C.D. Michener. Holotype *Homalictus achrostus* Michener CNC No. 15918.

Allotype ♀, and 4 ♀ paratypes: FIJI: Viti Levu: malaise trap at telecom tower, Nadarivatu, 1,100 m altitude, 1-16.VIII.1978, S & J Peck (after Michener 1979). Holotype and allotype in SEMC, paratypes deposited in CNC, BPBM and NHMUK. The material below is consistent with the type specimen described by Michener (1979).

Other material examined

1 ♂: AFO055, 1/9/10, 10:03 AM, 1,040 m asl, -17.5762, 177.9350, SVC Groom, Viti Levu.

1 ♀: AFO056, 1/9/10, 10:03 AM, 1,040 m asl, -17.5762, 177.9350, SVC Groom, Viti Levu.

Diagnosis

Males: Bee mostly black. Additionally, males of H. achrostus also have comparatively large mandibles (Fig. 4d), a strong medial depression of their clypeus (Fig. 4d), strong striations on the dorsal surface of their propodeum (Fig. 4a) and comparatively elongate gonostylus (Fig. 4e).

Females: Bee mostly black. Additionally, females of H. achrostus have a weaker medial depression of their clypeus (Fig. 4i), strong striations on the dorsal surface of their propodeum (Fig 3f) and a longitudinal medial carina on the pygidial plate (Fig. 4j).

Description

Males:

Measurements: UID 0.95 mm. LID 0.91 mm. AOD 0.31 mm. IAD 0.19 mm. OAD 0.37 mm. IOD 0.24 mm. OOD 0.32 mm. GW 0.36 mm. EW 0.33 mm. BL 5.61 mm. ML 0.14 mm. SL 0.3 mm. FL 4.51 mm.

Colouration: Body (including clypeus, supraclypeal area, frons, paraocular area, scutum, scutellum, propodeum dorsally and metasoma) black. Fovea along anterior and proximal margin of eye present.

Sculpturing: Paraocular area fine striae and colliculate along margin of compound eyes. Frons mostly longitudinal striae and transverse striae under ocelli. Supraclypeal area mostly finely colliculate. Clypeus finely colliculate. Vertex punctures small and sparse. Scutum anteriorly finely colliculate and lineolate; medially moderately fine colliculate and almost smooth; posteriorly finely colliculate and almost smooth. Scutellum almost entirely smooth except for punctation. Scutellum punctation open and sparse. Propodeum dorsal striae close and strong and weak medial anterior groove present; laterally finely colliculate, some striae anteriorly, dorsally, and ventrally; posteriorly finely colliculate and diagonal striae ventrally and proximally.

Morphology: Scape extends to posterior margin of medial ocellus. Interantennal distance greater than diameter of socket. Clypeus strongly depressed medially. Posterior margin of scutum shape mostly straight. Gonostylus elongate, gonocoxite with dorsoapical crest weak (Michener 1979).

Females:

Measurements: UID 0.82 mm. LID 0.83 mm. AOD 0.25 mm. IAD 0.15 mm. OAD 0.43 mm. IOD 0.19 mm. OOD 0.26 mm. GW 0.27 mm. EW 0.35 mm. BL 5.56 mm. ML 0.18 mm. SL 0.34 mm. FL 4.75 mm.

Colouration: Body (including frons, propodeum dorsally, metasoma) black except clypeus, supraclypeal areas, paraocular area, scutum, and scutellum black or partially sub-metallic.

Sculpturing: Paraocular area fine striae and colliculate along margin of compound eyes. Frons mostly longitudinal striae and colliculate above antennal sockets. Supraclypeal area mostly finely colliculate. Clypeus finely colliculate. Vertex punctures small and sparse. Scutum anteriorly moderately fine colliculate and lineolate; medially and posteriorly moderately fine colliculate. Scutellum punctation open and sparse. Propodeum dorsally strong striae close and weak medial anterior groove; laterally finely colliculate and posteroventral and anterior striae curve towards each other and can meet; posteriorly finely colliculate and transverse striae ventrally and proximally.

Morphology: Scape extends to or below anterior margin of medial ocellus. Interantennal distance greater than diameter of socket. Labrum simple. Clypeus moderately depressed medially. Area posterior of vertex with strong and close striae. Posterior margin of scutum shape mostly straight.

Comments

This species was last collected in 2010, where a single male and female were sampled from their type locality near Nadarivatu. When the species was described by Michener [65] only one male and five females where collected at 1,100 m asl — the highest elevation in the Nadarivatu region. That no more specimens have been collected since 2010, despite intensive searching most years between 2010 and 2018, suggests that this species might have become extinct, perhaps due to the combination of its limited range on a single high mountain peak and global climate warming.

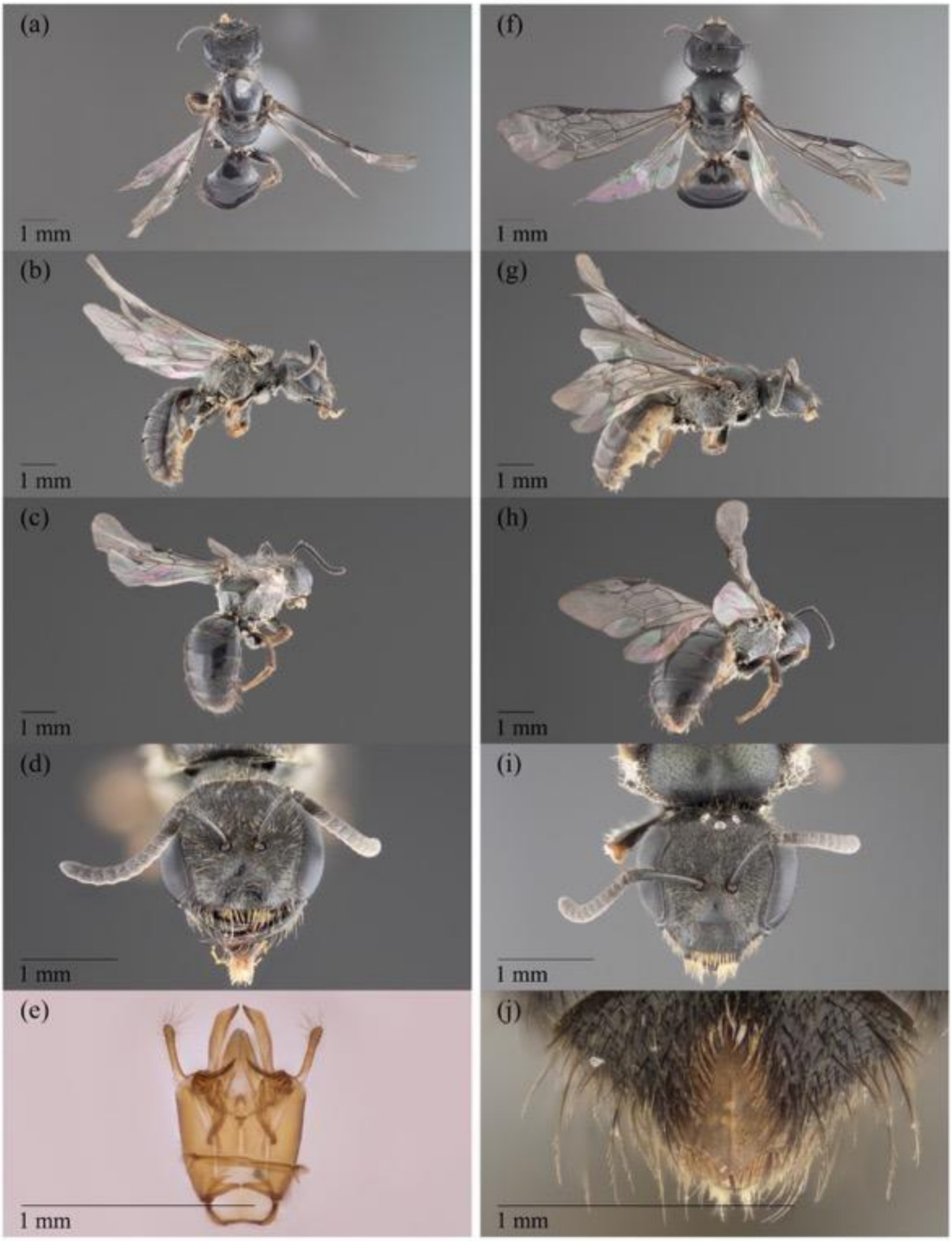

Figure 4. *Homalictus achrostus* male (a) dorsal habitus, (b) lateral habitus, (c) dorso posterior, (d) anteriorly frontal face and (e) ventral genitalia. Female (f) dorsal habitus, (g) lateral habitus, (h) dorso posterior, (i) anteriorly frontal face, and (j) pygidial plate.

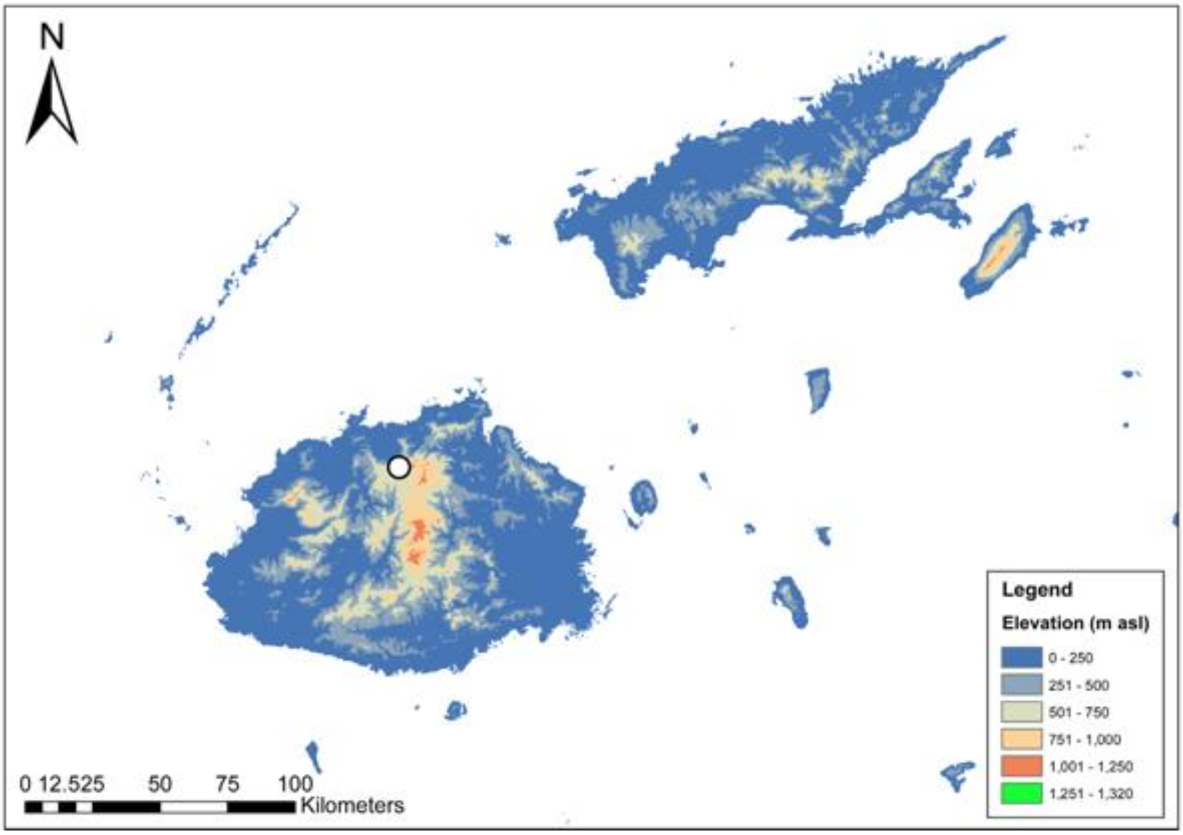

Figure 5. Collection map of *Homalictus achrostus* from specimens with identity confirmed by mtDNA COI gene. Sample size is 2.

Distribution

Homalictus achrostus has only ever been sampled from the telecom towers at Nadarivatu on the largest island, Viti Levu [65], with only two specimens sampled in this study, both in 2010 (Fig. 5). Our specimens of *H. achrostus* were sampled at 1,040 m asl.

Homalictus fijiensis (Perkins & Cheesman)

(Figs 6-7)

Halictus fijiensis Perkins & Cheesman 1928: 21.
Halictus suvaensis Cockerell 1929: 357.
Homalictus fijiensis: Michener 1965: 180 (new combination); Michener 1979: 229.
Homalictus suvaensis: Michener 1965: 181 (new combination); Michener 1979: 229 (synonymy).

Material examined

Type material: Holotype — Fiji, ♂, Fiji 1.1905 R.C.L.P, *Halictus fijiensis* type. Cheesman and Perkins. R.C.L. Perkins Coll. B.M. 1942-95. B.M. TYPE HYM. 17A2586. [Specimen collection number] NHMUK010576228.

Fiji: Cuvu (5 ♂, 6 ♀),24, 25.vi.1915 (Veitch), Suva (1 ♀), 22.ix.1920, Yasawa (1 ♂), 14.x.1921, Ovalau, (1 ♂), 21.x.1921, and Taveuni (1 ♀), 19.xii.1921 (Simmonds) (after Perkins & Cheesman 1928). Types deposited in NHMUK. The material below is consistent with the type specimen described by Perkins & Cheesman [48].

Other material examined

5 ♂: 17FJ81 (SAMA 32-036189), 28/4/17, 12:00 PM, 612 m asl, -17.67438, 177.53976, JB Dorey, Mt. Batilamu, long grass and weeds on the path down the mountain. 17FJ188 (SAMA 32-036190), 28/4/17, 12:08 PM, 543 m asl, -17.61783, 177.53863, JB Dorey & OK Davies, Mt. Batilamu, cleared embankment with purple weed flowers. Near a possible nesting site with substantial areas of exposed clay, down the mountain track. 17FJ211 (SAMA 32-036191), 19/4/17, 934 m asl, -17.5826, 177.93654, BA Parslow, Nadarivatu Rd, towards telecom tower. ABT008 (SAMA 32-036192), 8/8/10, 11:01 AM, 71 m asl, -19.038, 178.170, SVC Groom, Kadavu. AAO043 (SAMA 32-036193), 19/7/11, 11:59 AM, 7 m asl, -18.247, 178.080, SVC Groom, Viti Levu — Coastal.

5 ♀: 17FJ24 (SAMA 32-036184), 28/4/17, 11:30 AM, 664 m asl, -17.67602, 177.54025, JB Dorey & OK Davies, Mt. Batilamu, swept off long grass with no canopy, used for cattle and goat farming. Overcast but warm. Swept off flowering weeds amongst grass. 17FJ187 (SAMA 32-036185), 17/4/17, 12:08 PM, 872 m asl, -17.73819, 178.06611, OK Davies, Monasavu Rd, swept off low grass where they were flying in a group in front of the clay nesting site. 17FJ210 (SAMA 32-036186), 19/4/17, 934 m asl, -17.5826, 177.93654, BA Parslow, Nadarivatu Rd, towards telecom tower. ABT005 (SAMA 32-036187), 7/8/10, 11:01 AM, 71 m asl, -19.038, 178.170, SVC Groom, Kadavu. AAO042 (SAMA 32-036188), 19/7/11, 11:59 AM, 7 m asl, -18.247, 178.080, SVC Groom, Viti Levu — Coastal.

Diagnosis

Male: In combination: Bee mostly green, supraclypeal area mostly moderately colliculate (Fig. 1e), antennal sockets and paraocular area not strongly depressed, antennal sockets and paraocular area not strongly depressed, clypeus mostly finely colliculate, frons has vertical striae and scape extends at or below anterior margin of medial ocellus. Additionally, the genitalia of *H. fijiensis* are unique in having both a proximally and posteriorly-directed gonostylus (Fig. 6e).

Female: In combination: Bee mostly green, supraclypeal area mostly moderately colliculate (Fig. 1e), scape does not extend beyond posterior margin of medial ocellus and propodeum has a strong anterior medial groove dorsally (Fig. 6i). Additionally, females can be distinguished from some species (except *H. hadrander, H. ostridorsum,* and *H. tuiwawae*) by a dense (Fig. 2) medial line of hair on the pygidial plate (Fig. 6j).

Description

Males:

Measurements: UID 0.66–0.87 mm. LID 0.59–0.68 mm. AOD 0.15–0.22 mm. IAD 0.13–0.17 mm. OAD 0.34–0.47 mm. IOD 0.18–0.42 mm. OOD 0.18–0.38 mm. GW 0.25–0.32 mm. EW 0.35–0.39 mm. BL 4.55–4.9 mm. ML 0.11–0.16 mm. SL 0.25–0.32 mm. FL 3.14–3.72 mm.

Colouration: Whole clypeus golden green and metallic. Supraclypeal and paraocular area metallic green or golden green. Frons, scutum, scutellum, and dorsal area of propodeum golden green and metallic. Metasoma green, dark green along posterior edges.

Sculpturing: Paraocular area colliculate, longitudinal striae posteriorly and proximally above antennal socket or striae and colliculate along margin of compound eyes. Frons mostly longitudinal striae, transverse striae under ocelli and colliculate above antennal sockets. Supraclypeal area mostly moderately colliculate. Clypeus finely colliculate. Vertex punctures small, close, and open. Scutum anteriorly moderately colliculate and lineolate; medially moderately fine colliculate, rarely lineolate; posteriorly moderately fine colliculate. Scutellum punctation close, open, and sparse. Propodeum dorsally linear pattern, strong striae, weak or strong medial anterior groove, and coarsely strigate-rugose; laterally finely or moderately colliculate, lineolate, ventral, and anterior striae curve towards each other and can meet or some striae anteriorly and dorsally; posteriorly moderately fine colliculate, transverse striae medially and ventrally and proximally.

Morphology: Scape extends to or below anterior margin of medial ocellus. Interantennal distance greater than diameter of socket. Labrum simple. Clypeus not depressed medially. Area posterior of vertex with strong striae or striae close. Posterior margin of scutum straight.

Gonostylus with posterior and proximal projections, dorsoapical crest of gonocoxite well developed. Gonocoxite relatively broad and penis valves strongly hooked.

Females:

Measurements: LID 0.84–1.01 mm. AOD 0.29–0.38 mm. IAD 0.11–0.14 mm. OAD 0.29–0.65 mm. IOD 0.22–0.28 mm. OOD 0.22–0.30 mm. GW 0.30–0.67 mm. EW 0.39–0.45 mm. BL 5.32–5.80 mm. ML 0.11–0.18 mm. SL 0.28–0.36 mm. FL 3.75–3.94 mm.

Colouration: Clypeus anteriorly black; middle iridescent; posteriorly green, golden green, and metallic, rarely orange. Supraclypeal area green or golden green and metallic. Frons green, golden green, and metallic, rarely orange. Paraocular area green, golden green, and metallic, rarely orange. Scutum golden green and metallic, rarely red and orange. Scutellum golden green and metallic, rarely orange and red. Propodeum dorsally golden green and metallic. Metasoma green and dark green along posterior edges or rarely almost black.

Sculpturing: Paraocular area colliculate, longitudinal striae posteriorly and proximally above antennal socket or striate and colliculate along margin of compound eyes. Frons mostly longitudinal striae, having transverse striae under ocelli and colliculate above antennal sockets. Supraclypeal area moderately colliculate, medial area finely colliculate, rarely finely colliculate anteriorly. Clypeus mostly finely colliculate. Vertex punctures small and close, rarely small and open. Scutum anteriorly moderately colliculate and lineolate; medially finely colliculate, moderately fine colliculate, rarely lineolate; posteriorly moderately fine colliculate. Scutellum punctation close and open. Propodeum dorsally linear pattern, strong striae, strong medial anterior groove or coarsely strigate-rugose; laterally finely colliculate, moderately colliculate, lineolate, ventral and anterior striae curve towards each other and meet or some striae ventrally; posteriorly moderately fine colliculate, transverse striae medially and ventrally and proximally, rarely transverse striae dorsally. Pygidial plate close fine punctures medially.

Morphology: Scape extends to posterior margin of medial ocellus. Interantennal distance about equal to diameter of socket. Labrum with two medial projections parallel from one another. Clypeus not depressed medially. Area posterior of vertex strong or weak close striae. Posterior margin of scutum straight.

Comments

Homalictus fijiensis exhibits a significant amount of morphological variation. Female body and wing length can vary from 4.9–7.0 mm and 3.7–5.0 mm, respectively, while male body and wing length varies from 4.5–6.0 mm and 3.1–4.2 mm respectively [65]. Colour can also vary greatly in *H. fijiensis*, with most individuals being mostly green, but others can be more orange and golden (e.g. ABT005 from Kadavu). Some individuals can have a blue scutum, but never have an essentially entirely blue thorax as seen in *H. hadrander*. This variation is the reason that Michener [68] synonymised *H. suvaensis* with *H. fijiensis*.

Homalictus fijiensis is the most common bee found in the Fijian lowlands and can be found in both disturbed and undisturbed areas, often in great local abundance.

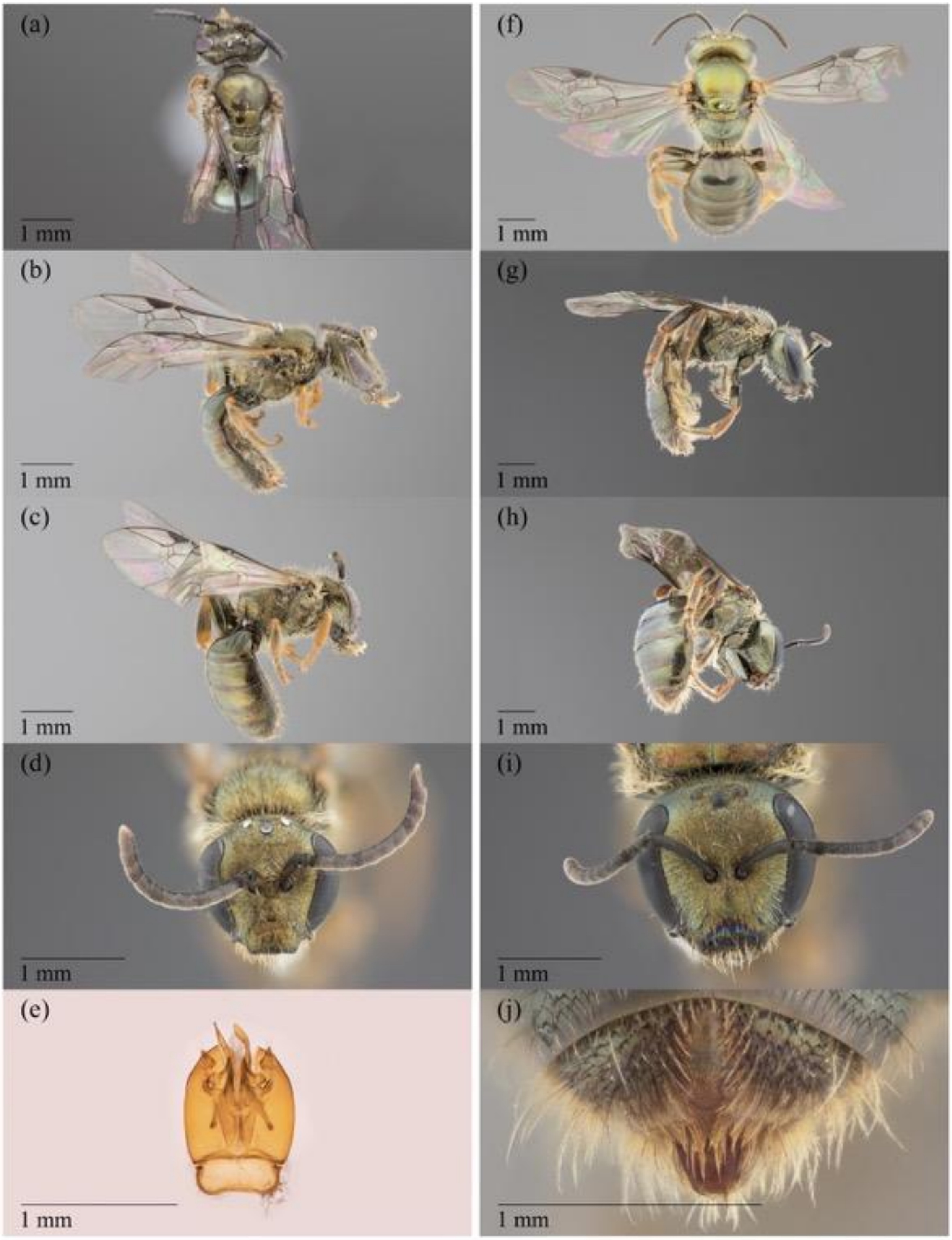

Figure 6. *Homalictus fijiensis* male (a) dorsal habitus (b) lateral habitus, (c) dorsoposterior view, (d) face frontal view and (e) ventral genitalia. Female (f) dorsal habitus, (g) lateral habitus, (h) dorso posterior, (i) anteriorly frontal face, and (j) pygidial plate.

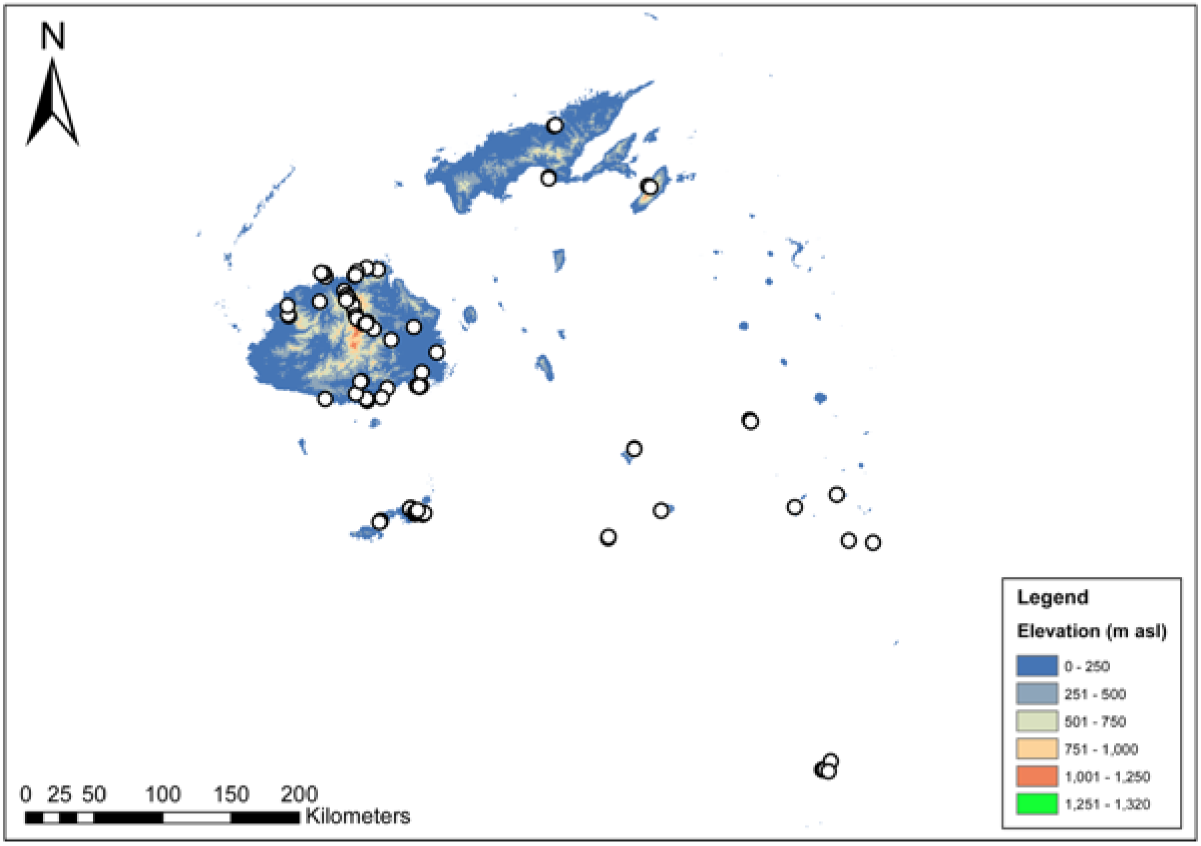

Figure 7. Collection map of *Homalictus fijiensis* from specimens with identity confirmed by mtDNA COI gene. Sample size is 500.

Distribution

Homalictus fijiensis has the widest distribution of any of the Fijian *Homalictus* species, being found on every island where we have sampled (Fig. 7). While most common at lower elevations, *H. fijiensis* has been found up to 1,120 m asl.

Homalictus hadrander Michener, 1979

(Figs 8–9)

Material examined

Type material: Holotype and allotype — Fiji — Viti Levu, Nadarivatu 2700 ft. 25 June 1959 C.D. Michener. Specimens held at The University of Kansas Biodiversity institute.

Holotype ♂, allotype ♀, and 43 ♂, 4 ♀ paratypes: FIJI: Viti Levu: Nadarivatu, 823 m (2,700 ft) altitude, 23.VI.1959, CD Michener, 5 ♀ paratypes, same locality but from malaise trap at telecom tower, 1,100 m altitude, 1-16.VIII.1978, S & J Peck (after Michener 1979). Holotype and allotype lodged in the SEMC, paratypes in NHMUK, CNC, and BPBM. The material below is consistent with the type specimen described by Michener (1979).

Other material examined

1 ♂: 17FJ16 (SAMA 32-036208), 28/4/17, 12:00 PM, 612 m asl, -17.67438, 177.53976, JB Dorey, Mt. Batilamu, long grass and weeds on the path down the mountain.

2 ♀: 17FJ162 (SAMA 32-036206) and 17FJ7 (SAMA 32-036207), 19/4/17, 10:35 AM, 865 m asl, -17.609817, 177.979867, JB Biddle, RK Schober, JB Dorey & CS Matthews, Navai village, caught amongst weeds and grass above a kava plantation (cleared but surrounded by forest). Sunny, little to no breeze in clearing.

Diagnosis

Males: Fovea along anterior inner margin of eye is present (Fig. 1d) and habitus is mostly blue.

Females: Habitus mostly blue and propodeum moderately strigate-rugose (Fig. 8g).

Description

Males:

Measurements: UID 0.85 mm. LID 0.86 mm. AOD 0.3 mm. IAD 0.14 mm. OAD 0.5 mm. IOD 0.25 mm. OOD 0.24 mm. GW 0.32 mm. EW 0.38 mm. BL 6.22 mm. ML 0.16 mm. SL 0.32 mm. FL 4.56 mm.

Colouration: Clypeus anteriorly black; middle blue. Whole clypeus partly iridescent. Supraclypeal area blue, yellowish medially. Fovea along anterior and proximal margin of eye present. Frons, paraocular area, scutum, scutellum, and dorsal area of propodeum blue. Metasoma black or some iridescence.

Sculpturing: Paraocular area striae, colliculate along margin of compound eyes. Frons mostly longitudinal striae, transverse striae under ocelli, and colliculate above antennal sockets.

Supraclypeal area mostly moderately colliculate, medial area finely colliculate. Clypeus finely colliculate. Vertex punctures small and close. Scutum anteriorly finely colliculate and lineolate; medially and posteriorly finely colliculate. Scutellum punctation close, open, and close posteriorly. Propodeum dorsally linear pattern, weak medial anterior groove, and moderately strigate-rugose; laterally finely colliculate and posteroventral and anterior striae curve towards each other and can meet; posteriorly finely colliculate and diagonal striae ventrally and proximally.

Morphology: Scape extends to above vertex. Interantennal distance about equal to diameter of socket. Labrum simple. Clypeus strongly or moderately depressed medially. Area posterior of vertex with strong and close striae. Posterior margin of scutum shape about straight. Gonostylus well developed with a slight constriction at its base, dorsoapical crest of gonocoxite is well developed. Penis valves strongly hooked.

Females:

Measurements: UID 0.86–0.88 mm. LID 0.92–0.94 mm. AOD 0.31–0.32 mm. IAD 0.12–0.13 mm. OAD 0.48–0.49 mm. IOD 0.23–0.25 mm. OOD 0.22–0.25 mm. GW 0.36–0.4 mm. EW 0.34–0.36 mm. BL 6.1–6.41 mm. ML 0.18–0.19 mm. SL 0.35–0.38 mm. FL 5.04–5.46 mm.

Colouration: Clypeus, partly iridescent, lower black; middle blue. Supraclypeal area blue, yellow, orange and purple. Frons blue. Paraocular area blue. Fovea along anterior and proximal margin of eye present or has some iridescence. Scutum blue. Scutellum blue. Propodeum dorsally blue or partly black. Metasoma black, some iridescent purple or iridescence.

Sculpturing: Paraocular area fine striae, colliculate along margin of compound eyes. Frons mostly fine and dense longitudinal striae and colliculate above antennal sockets. Supraclypeal area mostly moderately colliculate, medial area finely colliculate. Clypeus finely colliculate. Vertex punctures small and close or open. Scutum anteriorly finely colliculate, moderately colliculate or lineolate; medially and posteriorly finely colliculate. Scutellum punctation close or open. Propodeum dorsally no linear pattern or linear pattern, posterior striae triangular, weak medial anterior groove and moderately strigate-rugose; laterally finely colliculate, some striae anteriorly and dorsally or some striae ventrally; posteriorly finely colliculate and diagonal striae ventrally and proximally. Pygidial plate close and fine punctures medially and hairs emerging on ventral 1/3.

Morphology: Scape extends to above vertex. Interantennal distance less than diameter of socket. Labrum with two medial projections parallel from one another. Clypeus not depressed medially. Area posterior of vertex with weak striae, lineolate or finely colliculate. Posterior margin of Scutum shape concave or about straight.

Comments

Homalictus hadrander has a wide-spread distribution for a mostly highland species and yet is found in small numbers in some lowland regions in the southern parts of Viti Levu. It is possible that climate (or some other factor) in this region is more like that at higher elevations.

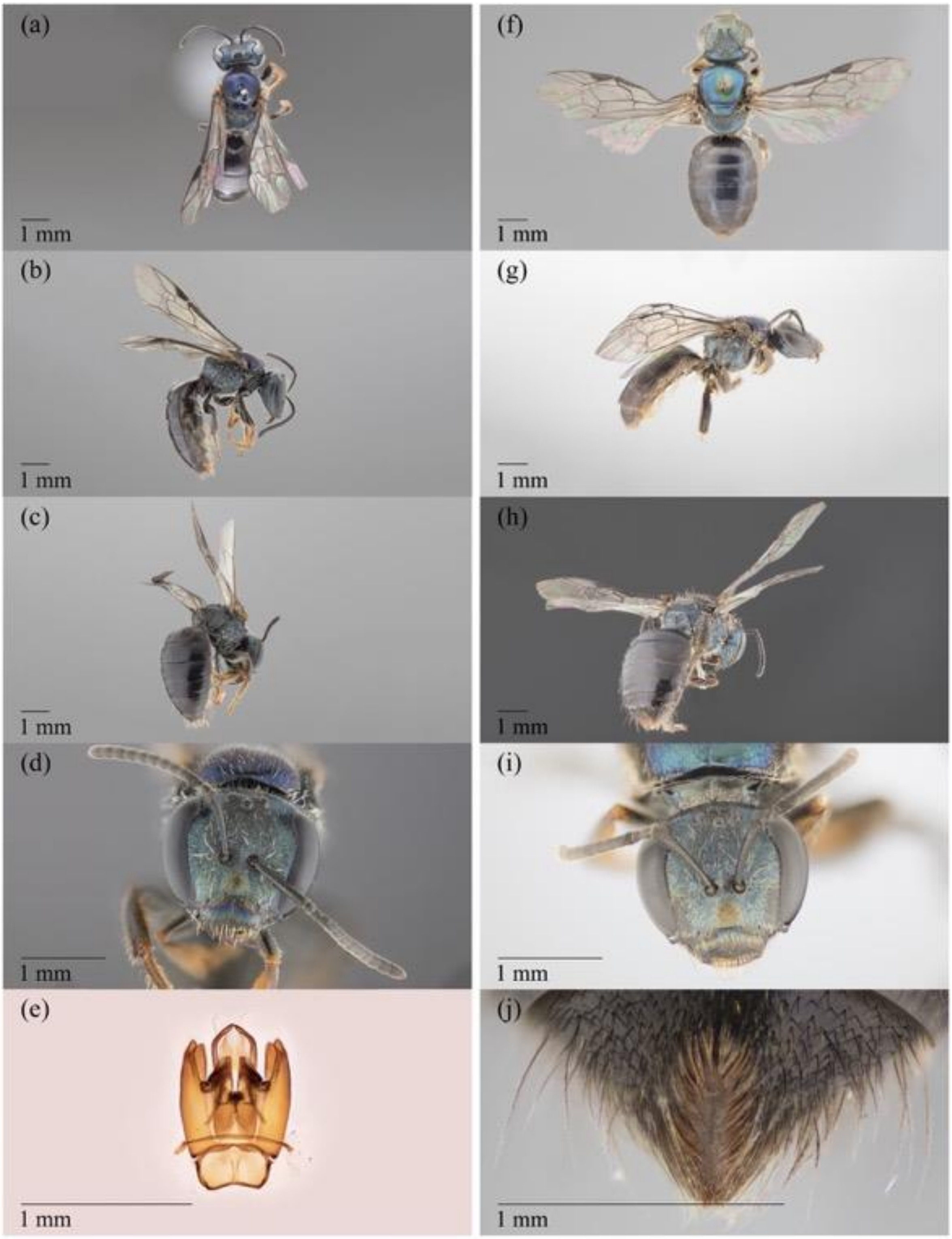

Figure 8. *Homalictus hadrander* male (a) dorsal habitus, (b) lateral habitus, (c) dorso posterior, (d) anteriorly frontal face and (e) ventral genitalia. Female (f) dorsal habitus, (g) lateral habitus, (h) dorso posterior, (i) anteriorly frontal face, and (j) pygidial plate.

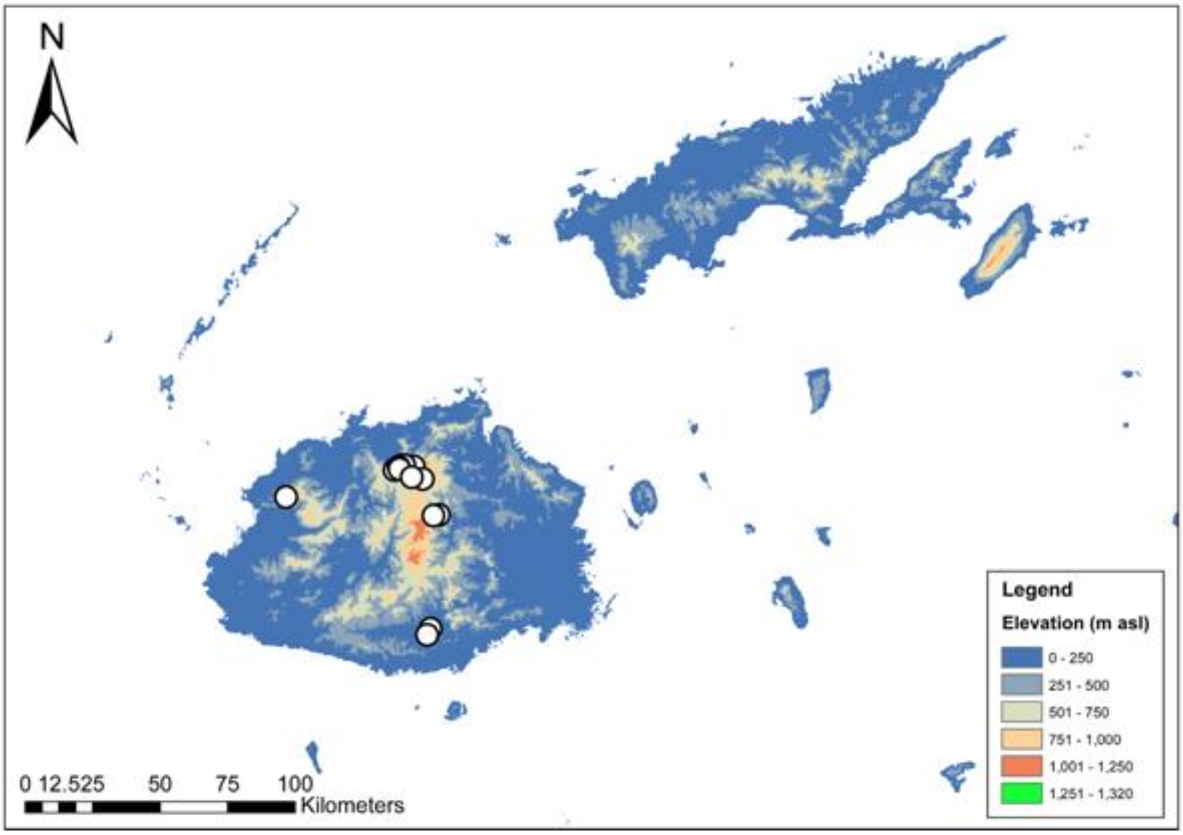

Figure 9. Collection map of *Homalictus hadrander* from specimens with identity confirmed by mtDNA COI gene. Sample size is 30.

Distribution

Homalictus hadrander has only been sampled on the largest island, Viti Levu (Fig. 9). While *H. hadrander* is mostly found between 600 m asl and 1,290 m asl, two individuals have been found at lower elevations (150 m asl) in the cooler and wetter forested areas of Viti Levu.

Homalictus versifrons (Perkins & Cheesman)

(Fig. 10)

Halictus versifrons (Perkins & Cheesman 1928): 22.
Homalictus versifrons (Michener 1965): 181.

Material examined (1 ♂)

Holotype — Fiji, a single ♂, i.1905 (after Perkins & Cheesman 1928). Located and examined in NHMUK. [Specimen collection number] NHMUK013455808.

Diagnosis

Male: In combination: Antennal sockets and paraocular area strongly depressed, striae on frons are mostly transverse. Additionally, the abdomen is "shining blackish brown and metallic" **[48]**, which appears to be unique amongst the Fijian *Homalictus* described here.

Description

Male:

Measurements: UID 0.67 mm. LID 0.52 mm. AOD 0.17 mm. IAD 0.12 mm. OAD 0.35 mm. IOD 0.16 mm. OOD 0.19 mm. GW 0.16 mm. EW 0.33 mm. BL 3.8 mm. ML 0.16 mm. SL 0.42 mm. FL 2.97 mm.

Colouration: Clypeus, supraclypeal area, frons, paraocular area, and propodeum dorsally golden green and metallic. Scutum mostly purple. Scutellum strongly iridescent purple and pink. Metasoma brown.

Sculpturing: Paraocular area striae not straight. Frons striae transverse tapering towards frontal line. Supraclypeal area mostly moderately colliculate, finely colliculate medially. Clypeus finely and moderately colliculate. Clypeus not depressed medially. Scutum anteriorly finely and moderately colliculate and lineolate; medially and posteriorly finely colliculate. Punctures on scutum and scutellum sparse. Propodeum dorsally coarsely strigate-rugose and moderately colliculate between grooves; laterally ventral and anterior striae curve towards each other and can meet; posteriorly moderately fine colliculate.

Morphology: Scape extends to posterior margin of medial ocellus. Interantennal distance about equal to diameter of socket. Labrum simple. Vertex has very few punctures small and open. Area posterior of vertex strong striae strong and close. Region around antennal sockets extending to paraocular area depressed. Posterior margin of scutum shape mostly straight. Dorsal subapical crest of gonocoxite weakly developed compared to *H. fijiensis* (Michener 1979).

Comments

Only a single specimen of this species is available and it is kept at the NHMUK, and type locality is simply recorded as "Fiji" by Perkins & Cheesman (1928). Michener (1979) collected from the telecom tower at 1,100 m asl (Nadarivatu) where he found this species to be quite numerous. Seventeen pinned specimens labelled as *H. versifrons* (1 ♂ and 16 ♀) are at SEMC, all but one female of which I have been able to examine. None of these specimens matched the description of *H. versifrons* although, without DNA, association of males and females is unlikely. The 16 females that were examined keyed to *H. tuiwawae*, *H. nadarivatu, H. kaicolo,* and two undescribed species. We have not collected any individuals that are consistent with the description for this species and it is therefore omitted from any phylogenetic analysis.

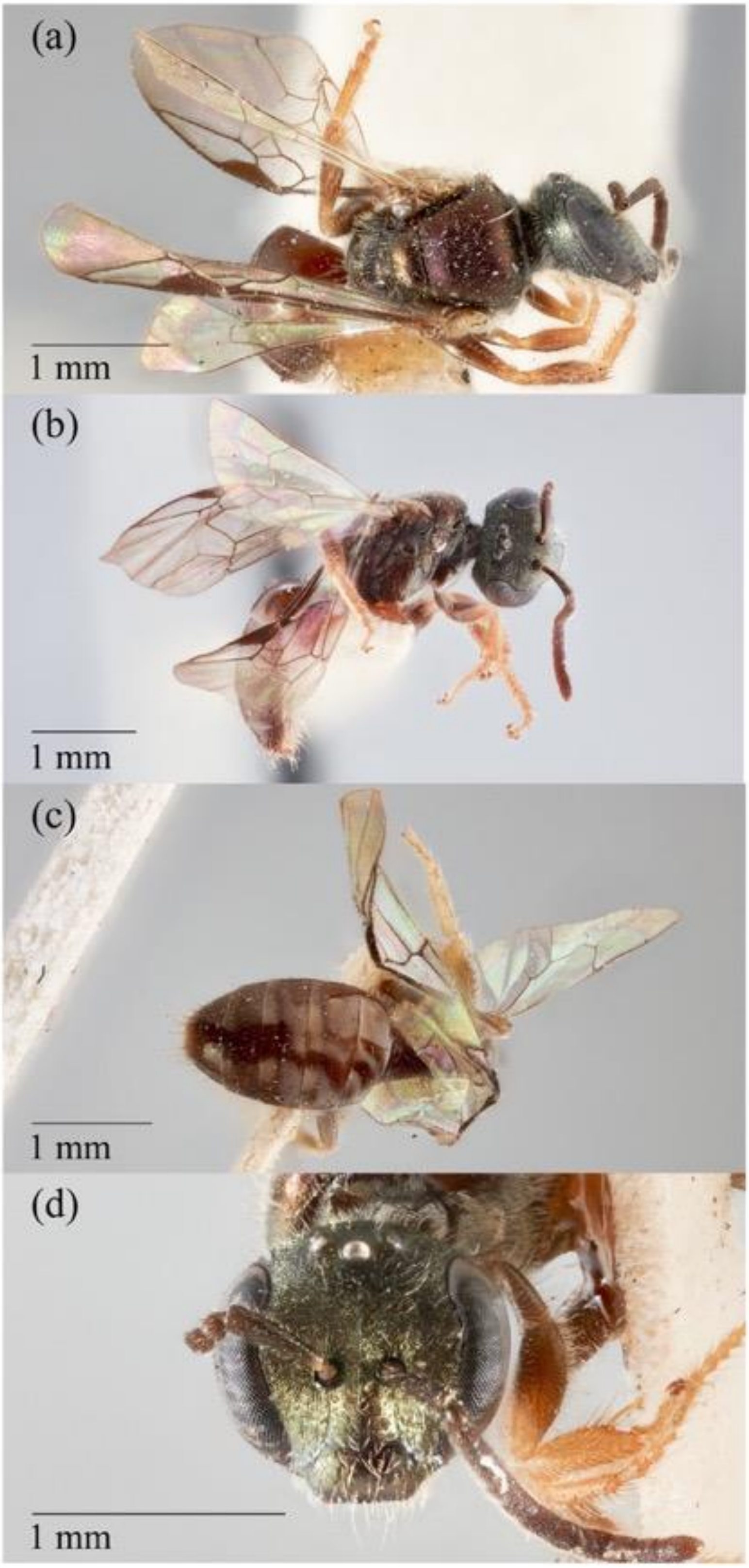

Figure 10. *Homalictus versifrons* male (a) dorsal habitus, (b) lateral habitus, (c) dorso posterior, (d) anteriorly frontal face, and (e) ventral genitalia.

Distribution

Fiji.

Homalictus atritergus sp. nov.

(Figs 11-12)

Material examined

Holotype ♂: 17FJ140 (SAMA 32-036172), 17/4/17, 10:45 AM, 1,328 m asl, -17.614762, 178.018284, JB Biddle, JB Dorey, CS Matthews & RK Schober, peak of Mt. Tomanivi, general sweep of grasses and flowers.

Allotype ♀: 17FJ135 (SAMA 32-036173), Mt. Tomanivi, Fiji, -17.614762, 178.018284, 17.04.2017, 10:45 AM, 1,328 m asl, JB Dorey, JB Biddle, CS Matthews, RS Schober, HG17JB33, peak of Mt. Tomanivi, cleared patch of grass, no flowers, general sweep, sunny, light breeze.

Paratypes 2 ♂: 17FJ133 (SAMA 32-036174), 17/4/17, 10:45 AM, 1,328 m asl, -17.614762, 178.018284, JB Biddle, JB Dorey, CS Matthews & RK Schober, peak of Mt. Tomanivi, cleared patch of grass, no flowers, general sweep, sunny, light breeze. 17FJ148 (SAMA 32-036175), 17/4/17, 10:45 AM, 1,328 m asl, -17.614762, 178.018284, JB Biddle, JB Dorey, CS Matthews & RK Schober, cleared patch of grass with no flowers at top of Mt. Tomanivi, sunny and a light breeze. General sweep of grasses and flowers, and 2 ♀, 17FJ125 (SAMA 32-036176) and 17FJ126 (SAMA 32-036177), 17/4/17, 10:45 AM, 1,328 m asl, -17.614762, 178.018284, JB Biddle, JB Dorey, CS Matthews & RK Schober, cleared patch of grass with no flowers at top of Mt. Tomanivi, sunny and a light breeze. General sweep of grasses and flowers.

Other material examined

1 ♂: 17FJ105, 18/4/17, 12:31 PM, 1,289 m asl, -17.615347, 178.017228, JB Biddle, JB Dorey & RK Schober, Mt. Tomanivi — open area along ridge between peaks, sun out, low wind, clear weather grassy open area.

2 ♀: 17FJ98 and 17FJ99, 18/4/17, 12:31 PM, 1,289 m asl, -17.615347, 178.017228, JB Biddle, JB Dorey & RK Schober, Mt. Tomanivi — open area along ridge between peaks, sun out, low wind, clear weather grassy open area.

Diagnosis

Males: T1 black or nearly so (Figs. 11a-c).

Females: In combination: Supraclypeal area mostly finely colliculate (Fig. 1f-g), scutum reddish, posterior margin of scutum abought straight, pygidial plate smooth (Fig. 11j), and posterior margin of propodeum does not form a triangular pattern (Fig. 11f).

Description

Males:

Measurements: UID 0.7-0.88 mm. LID 0.55-0.69 mm. AOD 0.2-0.5 mm. IAD 0.12-0.16 mm. OAD 0.36-0.44 mm. IOD 0.2-0.27 mm. OOD 0.21-2.7 mm. GW 0.22-0.25 mm. EW 0.3-0.39 mm. BL 4.1-4.7 mm. ML 0.09-0.13 mm. SL 0.21-0.26 mm. FL 4.18-4.23 mm.

Colouration: Clypeus golden green and metallic can be partly iridescent. Supraclypeal area golden green and metallic. Frons golden. Paraocular area golden green and metallic can be partly iridescent. Scutum golden green and metallic, can have some orange and appear reddish. Scutellum and propodeum dorsally golden green and metallic. Metasoma T1 black or nearly so, T2 onwards dark green or green, dark along posterior edges.

Sculpturing: Paraocular area colliculate, longitudinal striae posteriorly and proximally above antennal socket. Frons longitudinal and rarely diagonal striae posteriorly and anterior striae messy. Supraclypeal area mostly finely colliculate. Clypeus finely colliculate. Vertex punctures fine, close, and sparse. Scutum anteriorly and posteriorly finely or moderately colliculate; medially finely colliculate. Scutellum punctation open and sparse. Propodeum dorsally strong striae, weak medial anterior groove coarsely strigate-rugose; laterally fine to moderately colliculate and some striae anteriorly, dorsally and can meet; posteriorly finely colliculate, transverse striae medially and ventrally and proximally.

Morphology: Scape extends to or below anterior margin of medial ocellus. Interantennal distance about equal to diameter of socket. Labrum simple. Clypeus not depressed medially. Area posterior of vertex with strong and close striae. Posterior margin of Scutum shape mostly straight or convex. Gonostylus short and broad, dorsoapical crest of gonocoxite moderate with proximal hooks.

Females:

Measurements: UID 0.73-0.77 mm. LID 0.72-0.74 mm. AOD 0.25-0.26 mm. IAD 0.11-0.11 mm. OAD 0.41-0.49 mm. IOD 0.18-0.21 mm. OOD 0.2-0.22 mm. GW 0.24-0.33 mm. EW 0.32-0.4 mm. BL 5.55-6.48 mm. ML 0.14-0.16 mm. SL 0.3-0.36 mm. FL 4.37-4.63 mm.

Colouration: Clypeus anteriorly black; posteriorly golden green and metallic. Whole clypeus partly iridescent. Supraclypeal area, frons, paraocular area golden green and metallic. Scutum golden green and metallic, partly metallic orange and pink, and can appear reddish. Scutellum golden green and metallic, can be golden, partly metallic orange, pink or blue. Propodeum dorsally golden green and metallic. Metasoma T1 black or nearly so, T2 onwards black to dark green, dark along posterior edges and some iridescent purple.

Sculpturing: Paraocular area some messy striae below antennal sockets and colliculate, longitudinal striae posteriorly and proximally above antennal socket. Frons mostly longitudinal striae and anterior striae messy. Supraclypeal area mostly finely colliculate, rarely some messy striae posteriorly. Clypeus finely colliculate. Vertex punctures fine and close, open and/or sparse, and rarely minute and open. Scutum anteriorly finely colliculate and lineolate; medially and posteriorly finely colliculate. Scutellum punctation close and open. Propodeum dorsally linear pattern present or absent, some posterior transverse striae, weak medial anterior groove and coarsely strigate-rugose; laterally finely colliculate, some striae anteriorly and dorsally and some striae ventrally; posteriorly finely colliculate, transverse striae dorsally, medially and ventrally and proximally and striae originating ventrally and medially almost forms circles with dorsal striae. Pygidial plate open fine punctures medially and few minute sparse punctures.

Morphology: Scape extends to above vertex. Interantennal distance about equal to diameter of socket. Labrum with two medial projections parallel from one another. Clypeus not depressed medially. Area posterior of vertex with strong and close striae. Posterior margin of scutum shape mostly straight.

Comments

Given the very limited geographical and elevational distribution of *H. atritergus* it is likely to be threatened by future climate warming.

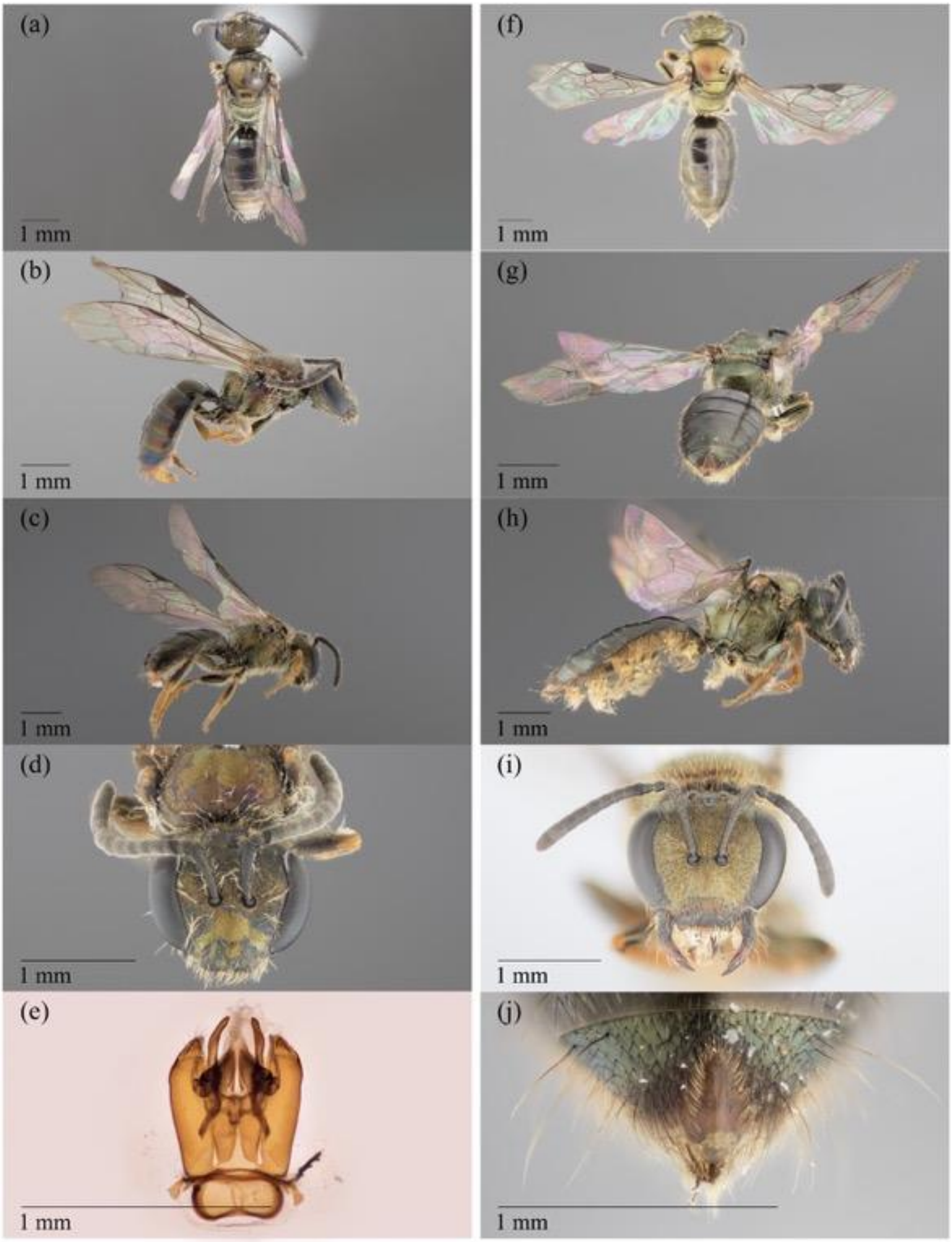

Figure 11. *Homalictus atritergus* **sp. nov.** male (a) dorsal habitus, (b) lateral habitus, (c) dorso posterior, (d) anteriorly frontal face and (e) ventral genitalia. Female (f) dorsal habitus, (g) lateral habitus, (h) dorso posterior, (i) anteriorly frontal face, and (j) pygidial plate.

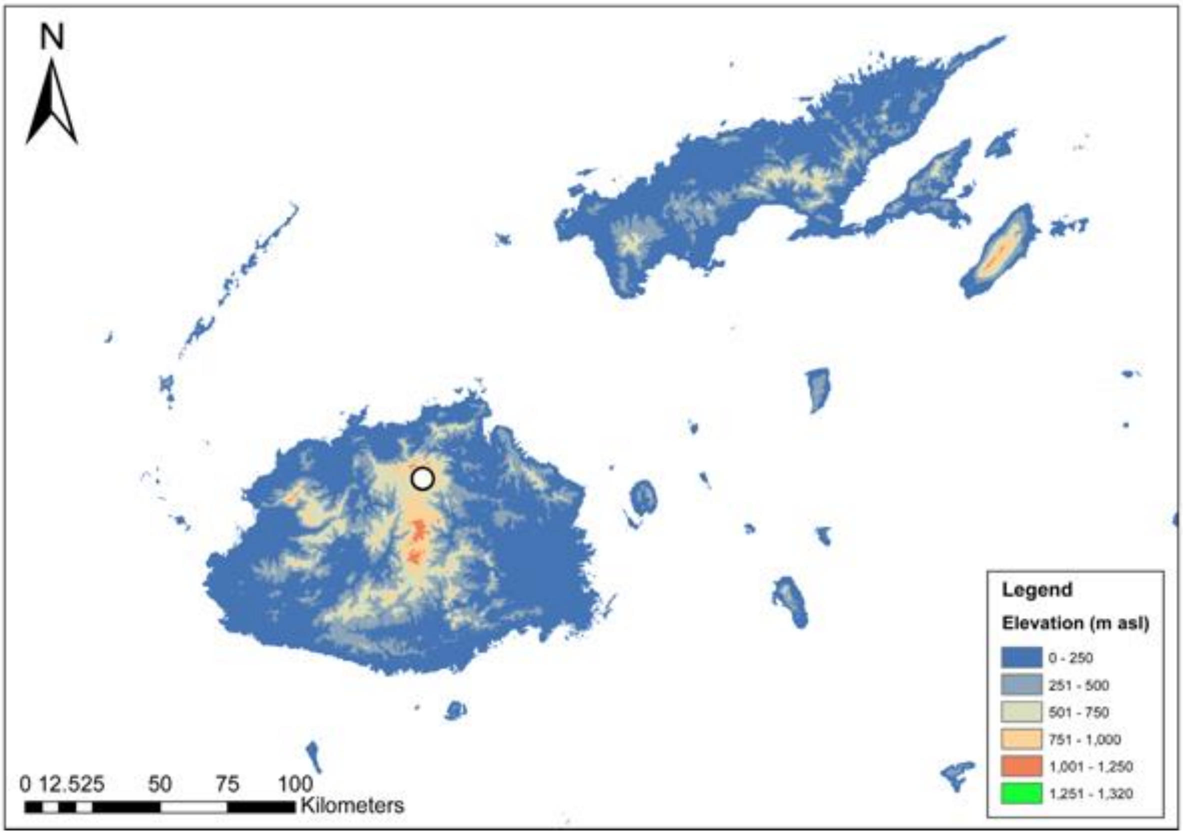

Figure 12. Collection map of *Homalictus atritergus* **sp. nov.** from specimens with identity confirmed by mtDNA COI gene. Sample size is 17.

Distribution

Homalictus atritergus has only been sampled from Mt. Tomanivi on the largest island, Viti Levu (Fig. 12). Collections of *H. atritergus* have only been made between 1,289 m asl and 1,328 m asl, and the latter is the highest elevation in Fiji.

Etymology

T1 of both males and females of *H. atritergus* are black. The name *H. atritergus* is derived from the Latin adjective *atri* meaning ‘dark’ (genitive case of ‘ater’) and the noun *tergus* meaning ‘back’ or ‘rear’.

Homalictus concavus sp. nov.

(Figs 13-14)

Material examined

Holotype ♂: 17FJ170 (SAMA 32-036200), 13/4/17, 1:20 PM, 815 m asl, -16.81945, 179.93845, MI Stevens, Taveuni, edge of the bog from sweeping the tiny white flowers at edge of lake.

Allotype ♀: 17FJ177 (SAMA 32-036201), Taveuni, Fiji, -16.819650, 179.942050, JB Dorey, 14.04.2017, 816 m asl, TV17-JD04, Taveuni, 100 m to edge of forest, wet ground, among stands of cabbage tree-like plants. Several larger plants (trees) with bottle brush-like red flowers. Only a few of these trees were flowering with this tree flowering the most profusely. This tree was 4-5 m high.

Paratypes 2 ♂: AFG006 (SAMA 32-036204) and AFG001 (SAMA 32-036205), 30/8/11, 11:55 AM, 703 m asl, -16.8287, -179.9810, SVC Groom, and 2 ♀, 17FJ182 (SAMA 32-036202), 14/4/17, 11:49 AM, 818 m asl, -16.819267, -179.93862, JB Dorey, edge of the bog from sweeping the tiny white flowers at edge of lake. No bees were caught in the malaise or blue vein at this location, and 17FJ181 (SAMA 32-036203), 14/4/17, 10:47 AM, 816 m asl, -16.81965, -179. 94205, JB Dorey, Taveuni, 100 m from edge of forest, wet ground, among stands of cabbage tree-like plants. Several larger plants (trees) with bottle brush-like red flowers. Only a few of these trees were flowering with this tree flowering the most profusely. This tree was 4-5 m high.

Other material examined

1 ♀: 17FJ171, 13/4/17, 1:20 PM, 815 m asl, -16.81945, 179.93845, MI Stevens, Taveuni, edge of the bog from sweeping the tiny white flowers at edge of lake.

Diagnosis

Males: Supraclypeal area mostly finely colliculate (Fig. 1f-g) and posterior margin of scutum concave (Fig. 13a).

Females: Bee mostly green, posterior margin of scutum concave (Fig. 13f) and propodeum moderately strigate-rugose dorsally (Fig. 13f).

Description

Males:

Measurements: UID 0.69–0.87 mm. LID 0.58–0.69 mm. AOD 0.21–0.24 mm. IAD 0.16–0.19 mm. OAD 0.37–0.45 mm. IOD 0.2–0.25 mm. OOD 0.21–0.27 mm. GW 0.17–0.19 mm. EW 0.25–0.36 mm. ML 0.1–0.17 mm. SL 0.28–0.33 mm. FL 4.13–4.18 mm.

Colouration: Clypeus, supraclypeal area, frons, paraocular area, scutum, scutellum, and propodeum dorsally golden green and metallic. Metasoma T1 can be black or nearly so, T2 onwards green, dark along posterior edges.

Sculpturing: Paraocular area colliculate and some messy striae below antennal sockets, longitudinal striae posteriorly and proximally above antennal socket. Frons mostly longitudinal striae, transverse striae under ocelli and striae messy. Supraclypeal area mostly finely colliculate. Clypeus finely colliculate. Vertex punctures fine, close, and open. Scutum anteriorly finely colliculate and lineolate; medially and posteriorly finely colliculate. Scutellum punctation close and sparse. Propodeum dorsally strong striae, weak medial anterior groove, or coarsely strigate-rugose; laterally fine to moderately colliculate or ventral and anterior striae curve towards each other and can meet; posteriorly finely colliculate, transverse or diagonal striae medially and transverse striae ventrally and proximally with striae almost forming circles with dorsal striae.

Morphology: Scape extends to or below anterior margin of medial ocellus. Interantennal distance greater than diameter of socket. Labrum simple. Clypeus not depressed medially. Area posterior of vertex with strong and close striae. Posterior margin of Scutum shape concave. Gonostylus extends beyond gonocoxite, dorsoapical crest of gonocoxite weak. Gonobase relatively narrow.

Females:

Measurements: UID 0.78–0.79 mm. LID 0.79–0.8 mm. AOD 0.26–0.27 mm. IAD 0.12 mm. OAD 0.43–0.44 mm. IOD 0.19–0.22 mm. OOD 0.23 mm. GW 0.25–0.33 mm. EW 0.34–0.43 mm. BL 5.56–5.61 mm. ML 0.11–0.12 mm. SL 0.33–0.39 mm. FL 4.51–4.7 mm.

Colouration: Clypeus anteriorly black; posteriorly golden green and metallic. Whole clypeus partly iridescent. Supraclypeal area golden green and metallic. Frons golden green and metallic. Paraocular area golden green and metallic. Scutum green and yellow. Scutellum yellow, blue, and green. Propodeum dorsally golden green and metallic. Metasoma T1 black or nearly so, T2 onwards dark green or green, dark along posterior edges.

Sculpturing: Paraocular area colliculate, fine and dense longitudinal striae posteriorly, and proximally above antennal socket with fine striae. Frons mostly fine and dense longitudinal striae. Supraclypeal area mostly finely colliculate. Clypeus finely colliculate. Vertex punctures fine, close, and open. Scutum anteriorly finely colliculate or lineolate; medially and posteriorly finely colliculate. Scutellum punctation close and open. Propodeum dorsally strong striae, strong medial anterior groove and moderately strigate-rugose; laterally finely colliculate, some striae anteriorly, dorsally, and ventrally; posteriorly finely colliculate and striae originating ventrally and medially almost forms circles with dorsal striae. Pygidial plate with few minute sparse punctures.

Morphology: Scape extends to above vertex. Interantennal distance less than or about equal to diameter of socket. Labrum with two medial projections parallel from one another. Clypeus not depressed medially. Area posterior of vertex with strong and close striae. Posterior margin of Scutum shape concave.

Comments

Although *H. concavus* has only been sampled up to 810 m asl, it is possible that it extends higher in elevation as we have not sampled the highest elevation on Taveuni.

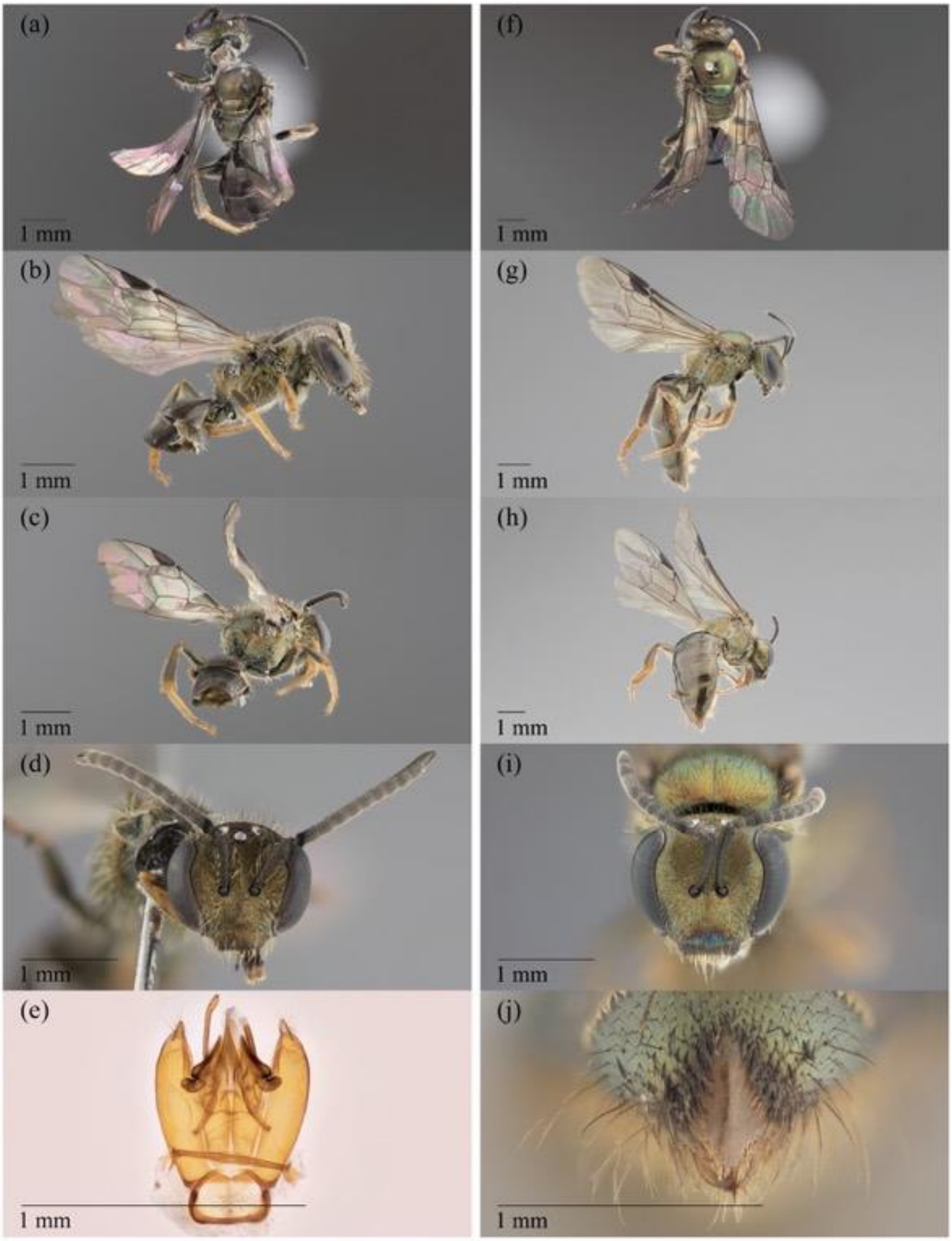

Figure 13. *Homalictus concavus* **sp. nov.** male (a) dorsal habitus, (b) lateral habitus, (c) dorso posterior, (d) anteriorly frontal face and (e) ventral genitalia. Female (f) dorsal habitus, (g) lateral habitus, (h) dorso posterior, (i) anteriorly frontal face, and (j) pygidial plate.

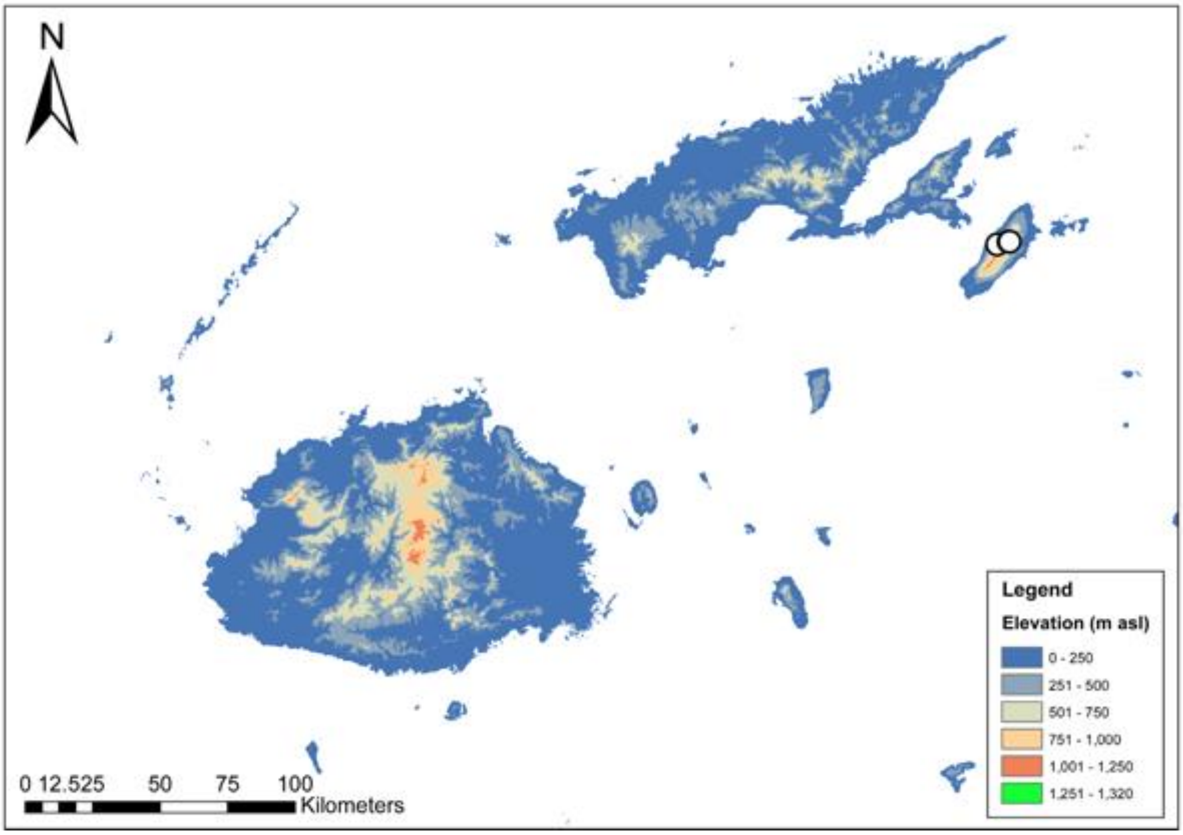

Figure 14. Collection localities of *Homalictus concavus* **sp. nov.** from specimens with identity confirmed by mtDNA COI gene. Sample size is 15.

Distribution

Homalictus concavus has only been sampled from the island of Taveuni (Fig. 14) at elevations between 700 m asl and 810 m asl — Taveuni's highest elevation is 1,241 m asl.

Etymology

The name *concavus* is Latin for 'concave' and refers to the concave posterior scutal margin in both the males and females of this species.

Homalictus groomi sp. nov.

(Figs 15-16)

Material examined

Holotype ♂: yCMR_136 (SAMA 32-036178), 4/5/15, 922 m asl, -17.58268, 177.93645, C Matthews, Viti Levu.

Allotype ♀: ED31_F04 (SAMA 32-036179), 1/4/15, 1,004 m asl, -17.58508, 177.91965, E Deans, Viti Levu.

Paratypes 3 ♂: yCMR52_E06 (SAMA 32-036180), 5/5/15, 889 m asl, -17.57001, 177.95586, C Matthews, yCMR44_E05 (SAMA 32-036181), 5/5/15, 889 m asl, -17.57001, 177.95586, C Matthews, and yCMR41_B05 (SAMA 32-036182), 6/5/15, 923 m asl, -17.58268, 177.93645, C Matthews, and 1 ♀: yCMR27_D03 (SAMA 32-036183), 6/5/15, 923 m asl, -17.58268, 177.93645, C Matthews.

Diagnosis

Males: In combination: Antennal sockets and paraocular area strongly depressed (Fig. 15d) and posterior surface of the propodeum has diagonal striae ventrally and proximally and joins dorsal striae (Fig. 15c). Additionally, male genitalia have a large ridge proximal to the gonostylus (Fig. 15e).

Females: In combination: Bee mostly green, supraclypeal area mostly moderately colliculate (Fig. 1e), and posterior margin of scutum concave (Fig. 15f).

Description

Males:

Measurements: UID 0.65 mm. LID 0.55 mm. AOD 0.2 mm. IAD 0.13 mm. OAD 0.37 mm. IOD 0.17 mm. OOD 0.21 mm. GW 0.15 mm. EW 0.31 mm. BL 4.75 mm. ML 0.13 mm. SL 0.27 mm. FL 2.9 mm.

Colouration: Clypeus, supraclypeal area, frons, paraocular area, scutum, and propodeum dorsally golden green and metallic. Scutellum golden green and metallic or some pink and blue. Metasoma dark green or green and dark green along posterior edges.

Sculpturing: Paraocular area colliculate, some horizontal striae along central margin of compound eyes, longitudinal striae posteriorly and proximally above antennal socket and striae course and messy. Frons mostly longitudinal striae, transverse striae under ocelli, striae messy, and colliculate above antennal sockets. Supraclypeal area mostly moderately colliculate. Clypeus fine and moderate colliculate. Vertex punctures fine, close, and open. Scutum anteriorly moderately colliculate and lineolate; medially finely colliculate; posteriorly finely and moderately fine colliculate. Scutellum punctation open. Propodeum dorsally strong striae, posterior striae triangular, weak medial anterior groove and coarsely strigate-rugose; laterally moderately colliculate and some striae anteriorly and dorsally; posteriorly finely colliculate, striae originating ventrally and medially almost forms circles with dorsal striae and diagonal striae ventrally and proximally.

Morphology: Scape extends to or below anterior margin of medial ocellus. Interantennal distance greater than diameter of socket. Labrum simple. Area posterior of vertex striae strong and close. Region around antennal sockets extending to paraocular area depressed. Posterior margin of scutum shape concave. Gonostylus with strong posterior projection and weaker proximal projection, dorsoapical crest of gonocoxite well developed. Entire genital is smaller and the gonocoxite narrower than in *H. fijiensis*.

Females:

Measurements: UID 0.7 mm. LID 0.66 mm. AOD 0.22 mm. IAD 0.1 mm. OAD 0.42 mm. IOD 0.18 mm. OOD 0.18 mm. GW 0.27 mm. EW 0.32 mm. BL 5.31 mm. ML 0.16 mm. SL 0.29 mm. FL 4.04 mm.

Colouration: Clypeus anteriorly black. Middle and upper clypeus golden and partly iridescent. Supraclypeal area golden, blue and purple. Frons golden and some purple iridescence. Paraocular area golden, golden green and metallic, and some purple iridescence. Scutum and scutellum very dark green, strongly metallic purple and pink, and partly metallic orange. Propodeum dorsally golden green and metallic. Metasoma black, dark green, and some iridescent purple.

Sculpturing: Paraocular area colliculate, some messy striae below antennal sockets, longitudinal striae posteriorly and proximally above antennal socket, and striae course. Frons mostly longitudinal striae. Supraclypeal area mostly moderately colliculate, medial area finely colliculate, or finely colliculate anteriorly. Clypeus finely colliculate. Vertex punctures fine, close and open, and small and open. Scutum anteriorly moderately colliculate and lineolate; medially and posteriorly finely colliculate. Scutellum punctation open. Propodeum dorsally linear pattern, weak medial anterior groove and finely strigate-rugose; laterally finely colliculate, some striae anteriorly, dorsally and ventrally; posteriorly finely colliculate, striae originating ventrally meet those from dorsal side and diagonal striae ventrally and proximally. Pygidial plate with close and fine punctures.

Morphology: Scape extends to posterior margin of medial ocellus. Interantennal distance about equal to diameter of socket. Labrum with two medial projections parallel from one another.

Clypeus not depressed medially. Area posterior of vertex with strong striae and broken. Posterior margin of scutum concave.

Comments

Like *H. hadrander, H. groomi* is found mostly at higher elevations but has also been sampled at a lower elevation site in the southern part of Viti Levu. It is possible that the climate (or some other factor) in this region is similar to climates at higher elevations.

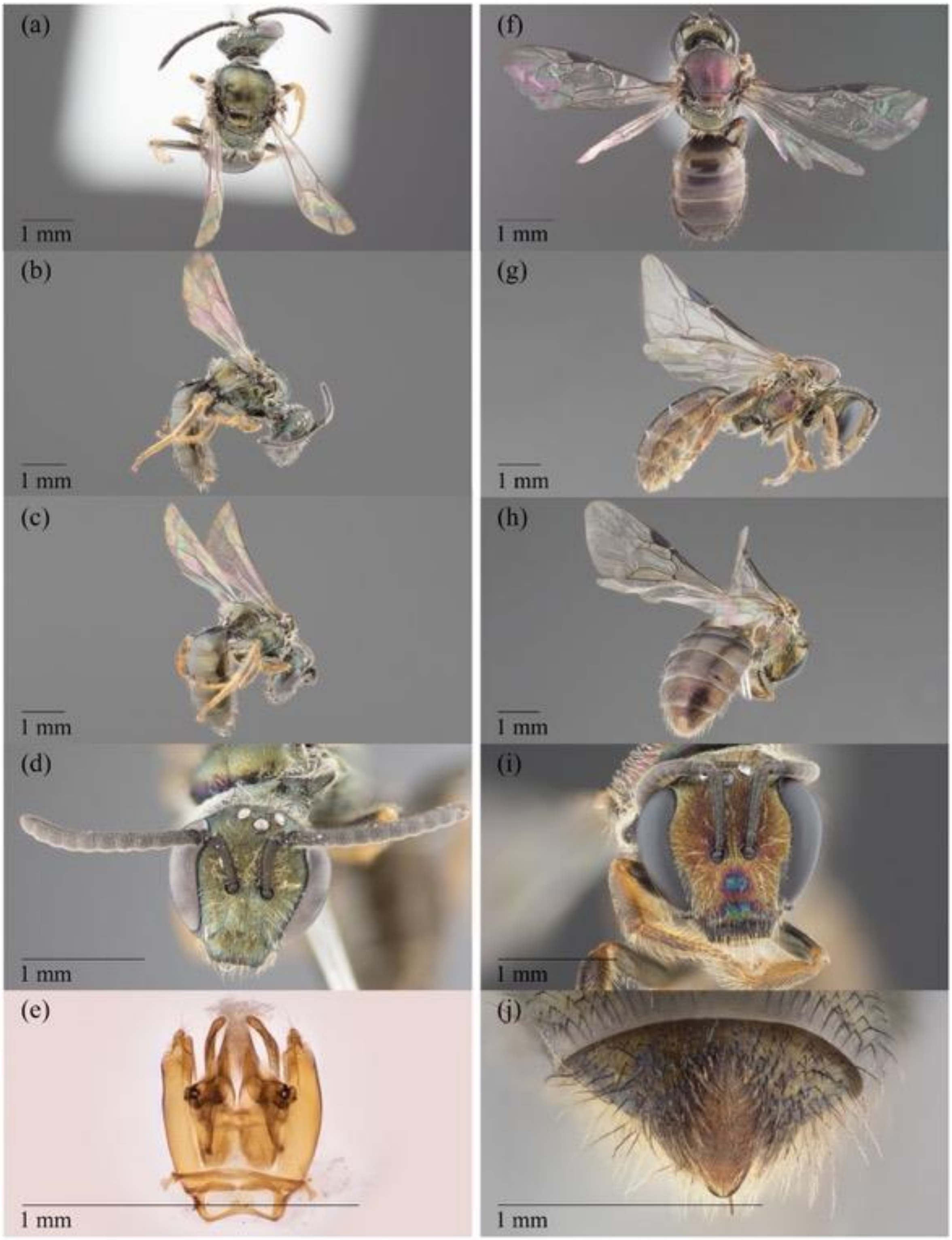

Figure 15. *Homalictus groomi* **sp. nov.** male (a) dorsal habitus, (b) lateral habitus, (c) dorso posterior, (d) anteriorly frontal face and (e) ventral genitalia. Female (f) dorsal habitus, (g) lateral habitus, (h) dorso posterior, (i) anteriorly frontal face, and (j) pygidial plate.

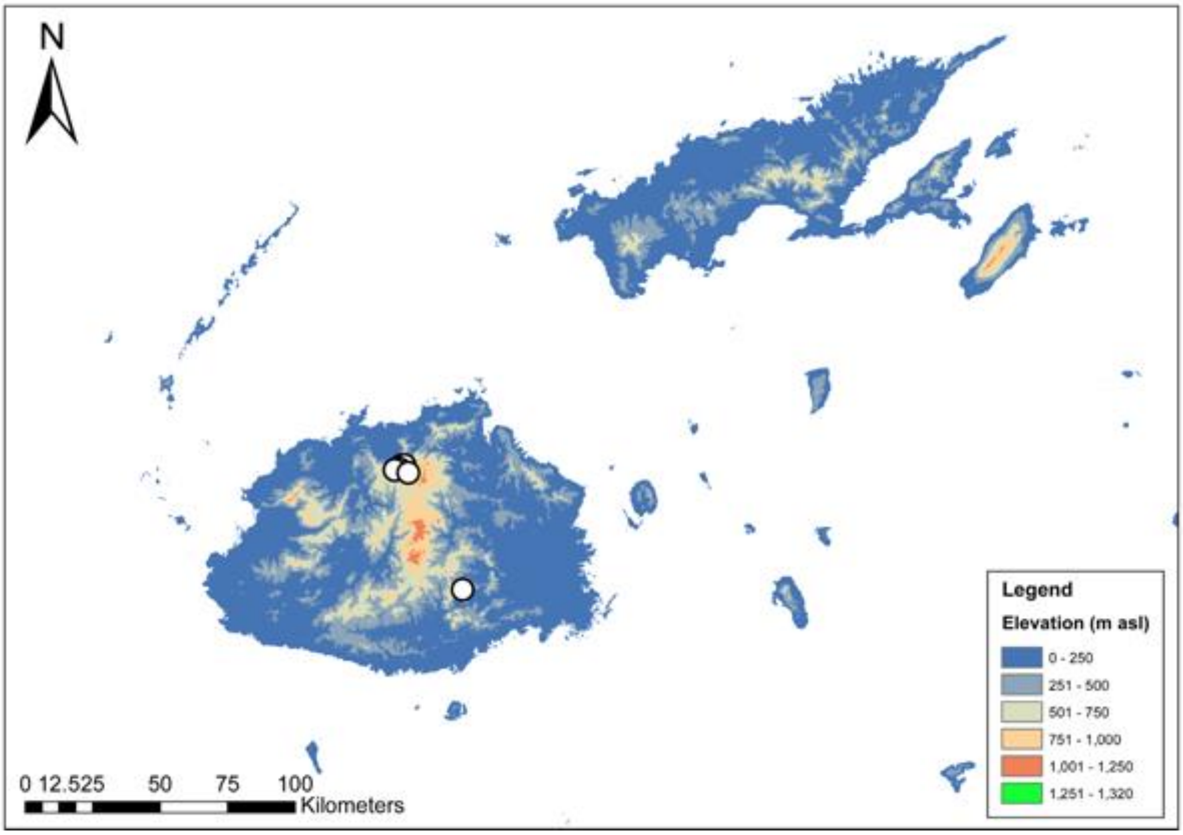

Figure 16. Collection map of *Homalictus groomi* **sp. nov.** from specimens with identity confirmed by mtDNA COI gene. Sample size is 43.

Distribution

Homalictus groomi has mostly been sampled from the central highlands of Viti Levu, near Nadarivatu (Fig. 16). A single specimen has been collected from a remote forested region in the south of Viti Levu at 250 m asl; otherwise, *H. groomi* has been collected between 730 m asl and 1,000 m asl.

Etymology

Homalictus groomi is named after Dr. Scott V. C. Groom who initiated recent studies of Fijian bees and provided the first understandings of their origins and phylogenetics.

Homalictus kaicolo sp. nov.

(Figs 17-18)

Material examined

Holotype ♂: 17FJ197 (SAMA 32-036168), 17/4/17, 1:25 PM, 932 m asl, -17.73810, 178.05539, SA Hammond, Monasavu Rd, roadside sweep.

Allotype ♀: 17FJ94 (SAMA 32-036169), Viti Levu, Fiji, -17.615347, 178. 017228, L, JB Dorey, JB Biddle, RK Schober, 18.04.2017, 1,289 m asl, Mt. Tomanivi — open area along ridge between peaks, sun out, low wind, clear weather grassy open area.

Paratypes 2 ♀: 17FJ205 (SAMA 32-036170) and 17FJ199 (SAMA 32-036171), 17/4/17, 12:43 PM, 872 m asl, -17.73809, 178.05673, MOJ Bazin, caught on *Sphagneticola trilobata*, Monasavu Rd.

Diagnosis

Males*:* In combination: supraclypeal area mostly finely colliculate (Fig 1f-g), posterior margin of scutum about straight, scutum and scutellum mostly golden green and metallic, T1 green and scutellum to forewing length ratio 1:14. Additionally, dorsal subapical crest of gonocoxite is poorly developed, and gonostylus is well developed (Fig. 17e).

Females*:* Striae on dorsal, posterior margin of propodeum forms triangular pattern (Fig. 17f). Supraclypeal area completely finely colliculate, habitus mostly green, scutum and scutellum golden, green or reddish, pygidial plate has few minute sparse punctures or open fine punctures medially, posterior margin of scutum is about straight, scutum and scutellum partly iridescent orange and pink, striae on dorsal, posterior margin of propodeum forms triangular pattern.

Description

Males:

Measurements: UID 0.64 mm. LID 0.54 mm. AOD 0.19 mm. IAD 0.13 mm. OAD 0.33 mm. IOD 0.17 mm. OOD 0.2 mm. GW 0.22 mm. EW 0.29 mm. ML 0.09 mm. SL 0.23 mm. FL 3.8 mm.

Colouration: Upper golden green and metallic. Supraclypeal area golden medially. Frons golden green and metallic. Paraocular area golden green and metallic. Scutum orange or golden green and metallic. Scutellum golden green and metallic. Propodeum dorsally golden green and metallic. Metasoma dark green or green, dark along posterior edges.

Sculpturing: Paraocular area some messy striae below antennal sockets or colliculate, longitudinal striae posteriorly and proximally above antennal socket. Frons mostly longitudinal striae with transverse striae under ocelli. Supraclypeal area mostly finely colliculate. Clypeus finely colliculate. Vertex punctures small, sparse, close, and open. Scutum finely colliculate. Scutellum punctation close and open. Propodeum dorsally no linear pattern and coarsely strigate-rugose; laterally fine to moderately colliculate with some striae anteriorly and dorsally; posteriorly finely colliculate and striae originating ventrally and medially almost forming circles with dorsal striae.

Morphology: Scape extends to or below anterior margin of medial ocellus. Interantennal distance greater than diameter of socket. Labrum simple. Clypeus not depressed medially. Area posterior of vertex with strong and close striae. Posterior margin of scutum shape mostly straight. Gonostylus short and rounded, dorsoapical crest of gonocoxite very weak.

Females:

Measurements: UID 0.72–0.74 mm. LID 0.71–0.73 mm. AOD 0.25–0.27 mm. IAD 0.09–0.1 mm. OAD 0.43–0.47 mm. IOD 0.18–0.18 mm. OOD 0.21–0.22 mm. GW 0.2–0.21 mm. EW 0.31–0.33 mm. BL 4.94–5.18 mm. ML 0.11–0.13 mm. SL 0.28–0.29 mm. FL 4.09–4.13 mm.

Colouration: Clypeus anteriorly black; posteriorly golden green and metallic. Whole clypeus partly iridescent. Supraclypeal area green or golden green and metallic. Frons golden green and metallic. Paraocular area golden green and metallic. Scutum golden green and metallic, partly metallic orange, pink and gold and appears reddish. Scutellum golden green and metallic or golden and partly metallic orange and pink. Propodeum dorsally golden or golden green and metallic. Metasoma T1 black or nearly so, T2 onwards dark green or green, dark along posterior edges with some iridescent purple.

Sculpturing: Paraocular area colliculate, some messy striae below antennal sockets, longitudinal striae posteriorly and proximally above antennal socket. Frons mostly longitudinal striae, anterior striae messy and transverse striae under ocelli. Supraclypeal area mostly finely colliculate. Clypeus finely colliculate. Vertex punctures fine, close, and open. Scutum anteriorly finely colliculate and lineolate; medially and posteriorly finely colliculate. Scutellum punctation close and open. Propodeum dorsally strong striae, posterior striae form consecutive triangular pattern, weak or strong medial anterior groove and coarsely strigate-rugose; laterally finely and moderately colliculate and posteroventral and anterior striae curve towards each other and can meet; posteriorly finely colliculate with striae originating ventrally and medially almost forming circles with dorsal striae. Pygidial plate few minute sparse punctures.

Morphology: Scape extends to above vertex. Interantennal distance about equal to diameter of socket. Labrum has two medial projections parallel from one another. Clypeus not depressed medially. Area posterior of vertex strong and close striae. Posterior margin of scutum shape mostly straight.

Comments

Homalictus kaicolo appears to be a relatively uncommon species in the areas that we sampled.

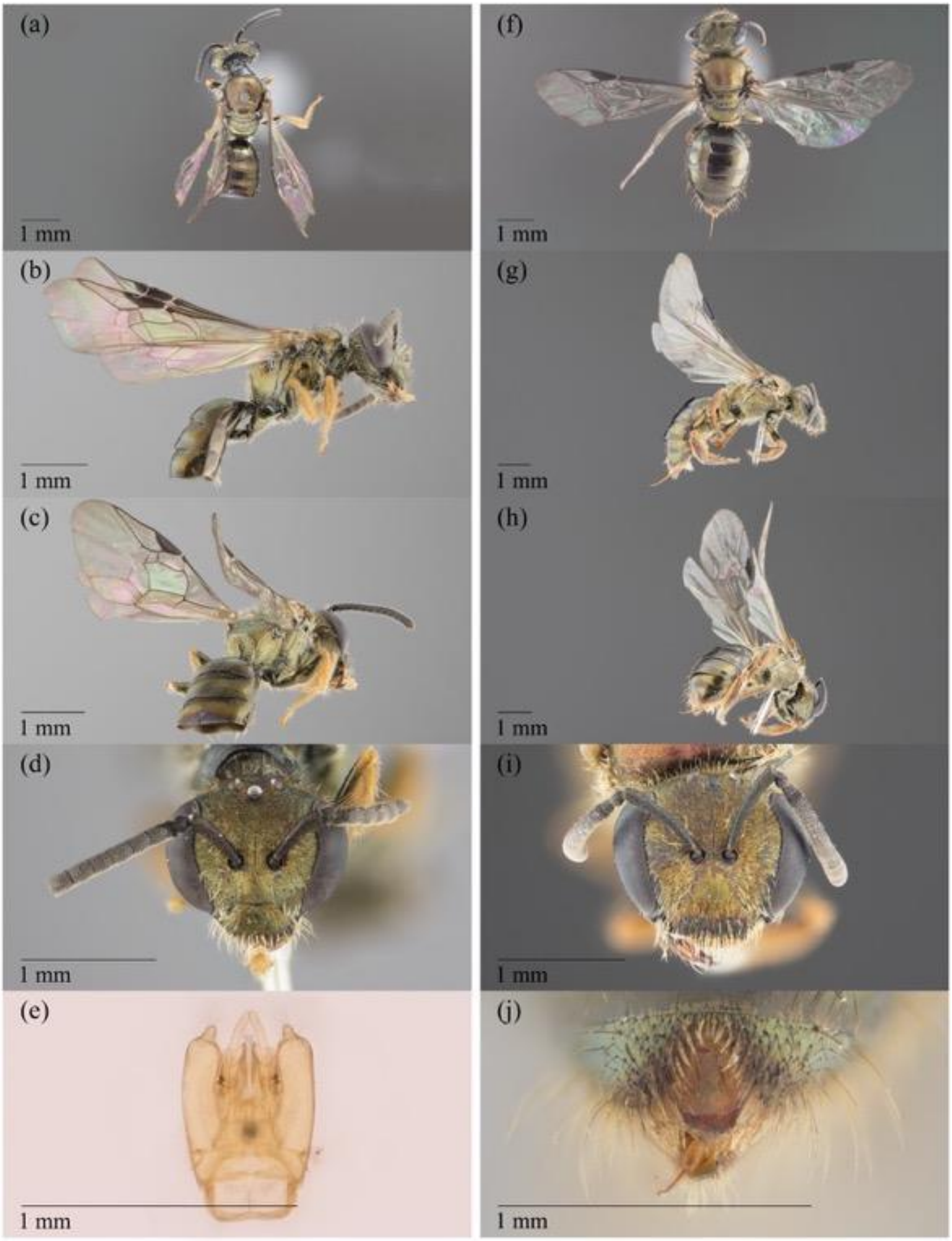

Figure 17. *Homalictus kaicolo* **sp. nov.** male (a) dorsal habitus, (b) lateral habitus, (c) dorso posterior, (d) anteriorly frontal face and (e) ventral genitalia. Female (f) dorsal habitus, (g) lateral habitus, (h) dorso posterior, (i) anteriorly frontal face, and (j) pygidial plate.

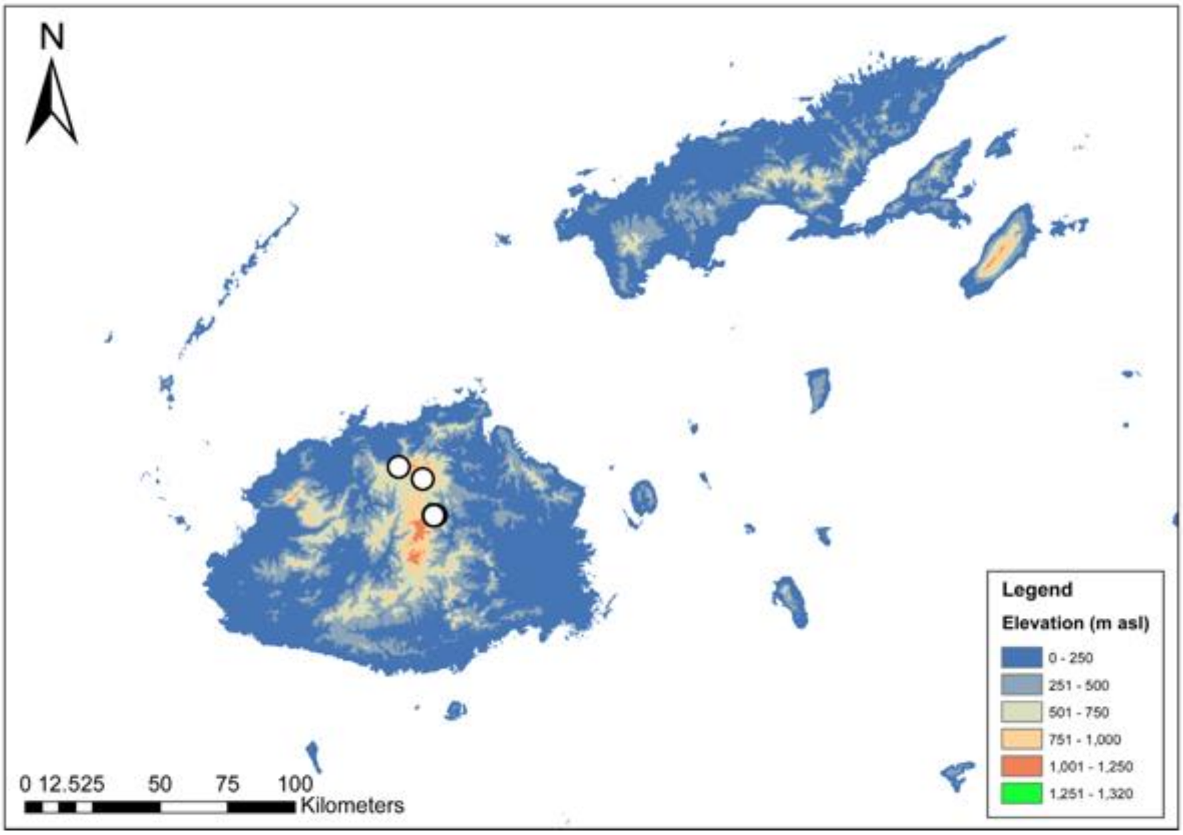

Figure 18. Collection localities of *Homalictus kaicolo* **sp. nov.** from specimens with identity confirmed by mtDNA COI gene. Sample size is 6.

Distribution

Homalictus kaicolo has been sampled from the central highlands of the largest island, Viti Levu (Fig. 18). Collections of *H. kaicolo* have been made between 870 m asl and 1,050 m asl.

Etymology

The name *H. kaicolo* is a noun in apposition derived from the Fijian term “kai colo” (pronounced ky-thow-low) which means “from the hills”. *Homalictus kaicolo* is named so because of its wider-distribution in the highland regions of Viti Levu, between 800 m asl and 1,100 m asl.

Homalictus nadarivatu sp. nov.

(Figs 19-20)

Material examined

Holotype ♂: AFO004 (SAMA 32-036151), Nadarivatu, Fiji, -17.5762, 177.9350, 31.7.2010, SVC Groom, 1,040 m asl, Viti Levu.

Allotype ♀: 17FJ203 (SAMA 32-036152), 21/4/17, 9:40 AM, 842 m asl, -17.73819, 178.06611, AC Grieve, near Monasavu Dam.

Paratypes ♂: AFO049 (SAMA 32-036154), 14/12/11, 10:03 AM, 1,041 m asl, -17.5762, 177.9350, SVC Groom, and ♀: AFO065 (SAMA 32-036153), 14/12/11, 10:03 AM, 1,041 m asl, -17.5762, 177.9350, SVC Groom.

Other material examined

1 ♂: AFO002, 31/7/10, 10:03 AM, 1,040 m asl, -17.5762, 177.9350, SVC Groom, Viti Levu.

Diagnosis

Males: Labrum has two medial projections and can be distinguished from H. terminalis by the many diagonal striae on the frons. Additionally, gonostylus are strongly proximally-directed (Fig. 19e).

Females: In combination: Bee is mostly green, supraclypeal area mostly moderately colliculate (Fig. 1e), scape extends above head and sculpturing on anterior of scutum is colliculate and lineolate.

Description

Males:

Measurements: UID 0.59–0.62 mm. LID 0.5–0.52 mm. AOD 0.17–0.2 mm. IAD 0.12–0.13 mm. OAD 0.28–0.31 mm. IOD 0.16–0.19 mm. OOD 0.18 mm. GW 0.17–0.2 mm. EW 0.26–0.27 mm. ML 0.09–0.1 mm. SL 0.2–0.22 mm. FL 2.99–3.12 mm.

Colouration: Clypeus, supraclypeal area, frons, paraocular area, scutum, scutellum, and propodeum dorsally golden green and metallic.

Sculpturing: Paraocular area fine striae, colliculate along margin of compound eyes. Frons with many diagonal striae and some transverse striae under ocelli. Supraclypeal area mostly moderately colliculate, medial area finely colliculate and quite shiny. Clypeus finely colliculate, quite smooth and shiny. Vertex punctures fine, close, open and/or sparse. Scutum anteriorly moderately colliculate and lineolate; medially finely colliculate, rarely lineolate; posteriorly moderately fine colliculate. Scutellum finely colliculate or almost entirely smooth except for punctation. Scutellum punctation close to sparse. Propodeum dorsally coarsely strigate-rugose or strong striae, striae very sparse, and weak medial anterior groove present; laterally moderately colliculate and posteroventral and anterior striae curve towards each other and can meet; posteriorly finely colliculate and transverse striae ventrally and proximally.

Morphology: Scape extends to posterior margin of medial ocellus or above head. Interantennal distance greater than diameter of socket. Labrum with two medial projections parallel from one another or simple. Clypeus not depressed medially. Area posterior of vertex striae strong and close. Posterior margin of scutum shape mostly straight. Gonostylus directed proximally and well developed, dorsoapical crest of gonocoxite strong with small posterior projection.

Females:

Measurements: UID 0.68 mm. LID 0.63 mm. AOD 0.15 mm. IAD 0.1 mm. OAD 0.36 mm. IOD 0.16 mm. OOD 0.2 mm. GW 0.22 mm. EW 0.29 mm. BL 5.342 mm. ML 0.13 mm. SL 0.24 mm. FL 3.73 mm.

Colouration: Clypeus anteriorly black; posteriorly golden green and metallic. Whole clypeus partly iridescent. Supraclypeal area, frons, paraocular area, scutellum, and propodeum dorsally golden green and metallic. Scutum golden green and metallic, partly metallic orange and pink, and appears reddish. Metasoma dark green or green, dark green along posterior edges.

Sculpturing: Paraocular area striae, some messy striae below antennal sockets, some horizontal striae laterally and colliculate along margin of compound eyes. Frons mostly longitudinal striae, transverse striae under ocelli and colliculate above antennal sockets. Supraclypeal area mostly moderately colliculate, medial area finely colliculate. Clypeus finely colliculate. Vertex punctures fine and open. Scutum anteriorly finely colliculate and lineolate; medially finely and moderately fine colliculate; posteriorly finely colliculate. Scutellum punctation close and open. Propodeum dorsally linear pattern and coarsely strigate-rugose; laterally moderately colliculate and posteroventral and anterior striae curve towards each other and can meet; posteriorly finely colliculate, transverse striae medially and ventrally and proximally. Pygidial plate with close and minute punctures.

Morphology: Scape extends to above vertex. Interantennal distance about equal to diameter of socket. Labrum has two medial projections parallel from one another. Clypeus not depressed medially. Area posterior of vertex with striae strong and close. Posterior margin of Scutum shape mostly straight.

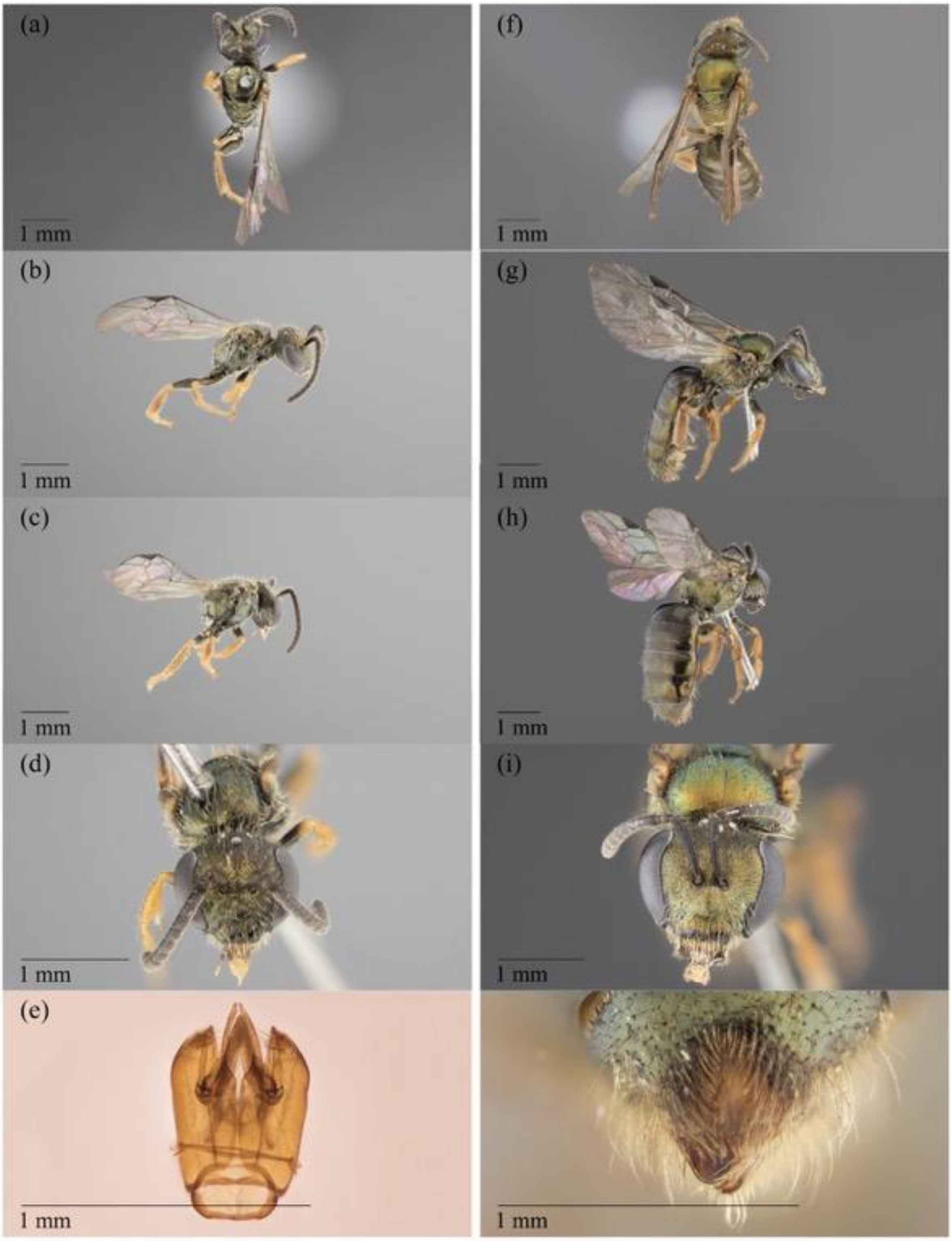

Figure 19. *Homalictus nadarivatu* **sp. nov.** male (a) dorsal habitus, (b) lateral habitus, (c) dorso posterior, (d) anteriorly frontal face and (e) ventral genitalia. Female (f) dorsal habitus, (g) lateral habitus, (h) dorso posterior, (i) anteriorly frontal face, and (j) pygidial plate.

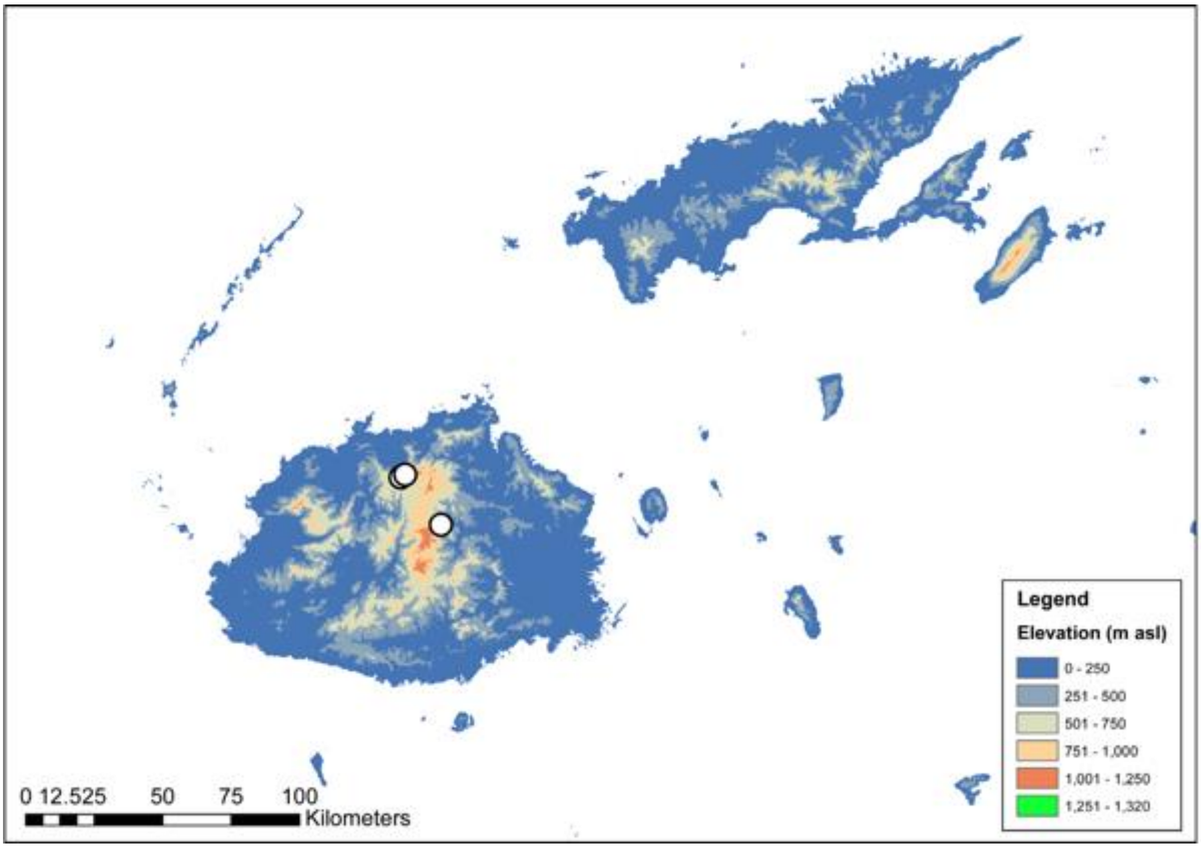

Figure 20. Collection map of *Homalictus nadarivatu* **sp. nov.** from specimens with identity confirmed by mtDNA COI gene. Sample size is 9.

Distribution

Homalictus nadarivatu has mostly been sampled from the Nadarivatu telecom towers, but has also been collected near Monasavu dam (Fig. 20). Collections have been made between 840 m asl and 1,040 m asl.

Etymology

The name *H. nadarivatu* refers to the region that this species was discovered in, Nadarivatu (pronounced Nan-dari-vah-two) on the Fijian island of Viti Levu.

Homalictus ostridorsum sp. nov.

(Figs 21-22)

Material examined

Holotype ♂: 17FJ141 (SAMA 32-036194), 17/4/17, 10:45 AM, 1,328 m asl, -17.614762, 178.018284, JB Biddle, JB Dorey, CS Matthews & RK Schober, peak of Mt. Tomanivi, cleared patch of grass, no flowers, general sweep, sunny, light breeze.

Allotype ♀: 17FJ101 (SAMA 32-036195), Viti Levu, Fiji, -17.615347, 178.017228, Q, JB Dorey, JB Biddle, RK Schober, 18.04.2017, 1,289 m asl, Tomanivi Clade, HG17CM0028, Mt. Tomanivi, open area along ridge between peaks, Sun out, low wind, clear weather grassy open area.

Paratypes 2 ♂: 17FJ110 (SAMA 32-036196) and 17FJ111 (SAMA 32-036197), 18/4/18, 12:31 PM, 1,289 m asl, -17.615347, 178.017228, JB Biddle, JB Dorey & RK Schober, open area along ridge between peaks of Mt. Tomanivi, sun out and low wind, and 2 ♀: 17FJ119 (SAMA 32-036198), 18/4/17, 1:45 PM, 1,303 m asl, -17.616583, 178.016600, JB Biddle, JB Dorey & RK Schober, caught on ridge between peaks but closer to lookout. Clear, sunny and breezy, and 17FJ143 (SAMA 32-036199), 17/4/17, 10:45 AM, 1,328 m asl, -17.614762, 178.018284, JB Biddle, JB Dorey, CS Matthews & RK Schober, cleared patch of grass with no flowers at top of Mt. Tomanivi, sunny and a light breeze. General sweep of grasses and flowers.

Other material examined

1 ♂: 17FJ152, 18/4/17, 2:30 PM, 1,222 m asl, -17.614691, 178.017909, JB Dorey & CS Matthews, open vegetated area flat just before an incline going towards peak, few dead trees sticking up along ridge, swept off grass and plants, stiff breeze, no canopy.

1 ♀: 17FJ131, 17/4/17, 10:45 AM, 1,328 m asl, -17.614762, 178.018284, JB Biddle, JB Dorey, CS Matthews & RK Schober, peak of Mt. Tomanivi, cleared patch of grass, no flowers, general sweep, sunny, light breeze.

Diagnosis

Males: In combination: Supraclypeal area mostly finely colliculate (Fig. 1f-g) and scutum and scutellum mostly golden, purple, blue and/or pink.

Females: In combination: Supraclypeal area mostly finely colliculate (Fig. 1f-g), scutum and scutellum mostly purple, with some orange and green (Fig. 21f), and pygidial plate has close fine punctures (Figs. 2, 21i).

Description

Males:

Measurements: UID 0.67–0.77 mm. LID 0.53–0.59 mm. AOD 0.19–0.28 mm. IAD 0.13–0.15 mm. OAD 0.33–0.37 mm. IOD 0.17–0.0.18 mm. OOD 0.21–0.22 mm. GW 0.17–0.27 mm. EW 0.25–0.35 mm. BL 4.13–4.66 mm. ML 0.09–0.12 mm. SL 0.27–0.33 mm. FL 3.7–4.67 mm.

Colouration: Clypeus, supraclypeal area, paraocular area and propodeum dorsally golden green and metallic. Scutum blue posteriorly, pink and orange medially, golden green and metallic anteriorly and laterally. Scutellum orange, golden and some pink and blue. Metasoma black.

Sculpturing: Paraocular area some horizontal striae along central margin of compound eyes and longitudinal striae, colliculate along margin of compound eyes. Frons many diagonal striae and some transverse striae under ocelli. Supraclypeal area mostly finely colliculate. Clypeus finely colliculate. Vertex punctures small and close. Scutum finely colliculate. Scutellum punctuation open and sparse. Propodeum dorsally coarsely strigate-rugose with strong striae and a strong or weak medial anterior groove; laterally finely colliculate, lineolate and posteroventral and anterior striae curve towards each other and can meet; posteriorly finely colliculate and diagonal striae ventrally and proximally.

Morphology: Scape extends to posterior margin of medial ocellus. Interantennal distance greater than diameter of socket. Labrum simple. Clypeus not depressed medially. Area posterior of vertex with strong striae, striae close, lineolate, and finely colliculate. Posterior margin of Scutum shape mostly straight. Gonostylus moderate, dorsoapical crest of gonocoxite moderate with a small proximal and posterior projection.

Females:

Measurements: UID 0.72–0.89 mm. LID 0.7–0.86 mm. AOD 0.25–0.5 mm. IAD 0.12–0.13 mm. OAD 0.41–0.48 mm. IOD 0.17–0.19 mm. OOD 0.21–0.25 mm. GW 0.25–0.36 mm. EW 0.3–0.34 mm. BL 5.88–6.03 mm. ML 0.14–0.16 mm. SL 0.3–0.35 mm. FL 3.94–4.42 mm.

Colouration: Clypeus anteriorly black; middle iridescent; posteriorly golden green and metallic. Supraclypeal area golden green metallic, orange medially. Frons, paraocular area and Propodeum dorsally golden green and metallic. Scutum mostly purple. Scutellum mostly purple, some orange and green. Metasoma black.

Sculpturing: Paraocular area some horizontal striae along central margin of compound eyes and colliculate, longitudinal striae posteriorly and proximally above antennal socket. Frons mostly longitudinal striae and transverse striae under ocelli. Supraclypeal area mostly finely colliculate. Clypeus finely colliculate. Vertex punctures small and close or fine and sparse. Scutum anteriorly moderately colliculate and lineolate; medially moderately fine colliculate; posteriorly finely colliculate. Scutellum punctation close. Propodeum dorsally strong striae, weak medial anterior groove and coarsely strigate-rugose; laterally finely colliculate and posteroventral and anterior striae curve towards each other and can meet; posteriorly finely colliculate, striae medially and ventrally curve dorsally and then ventrally towards the sides, and medial striae diagonal. Pygidial plate with close and fine punctures.

Morphology: Scape extends to above vertex. Interantennal distance less than or about equal to diameter of socket. Labrum has two medial projections parallel from one another. Clypeus not depressed medially. Area posterior of vertex with strong striae, lineolate and finely colliculate. Posterior margin of scutum shape mostly straight.

Comments

Given the very limited geographical and elevational distribution of *H. ostridorsum*, similar to that of *H. achrostus*, it is also likely to be threatened by future climate warming.

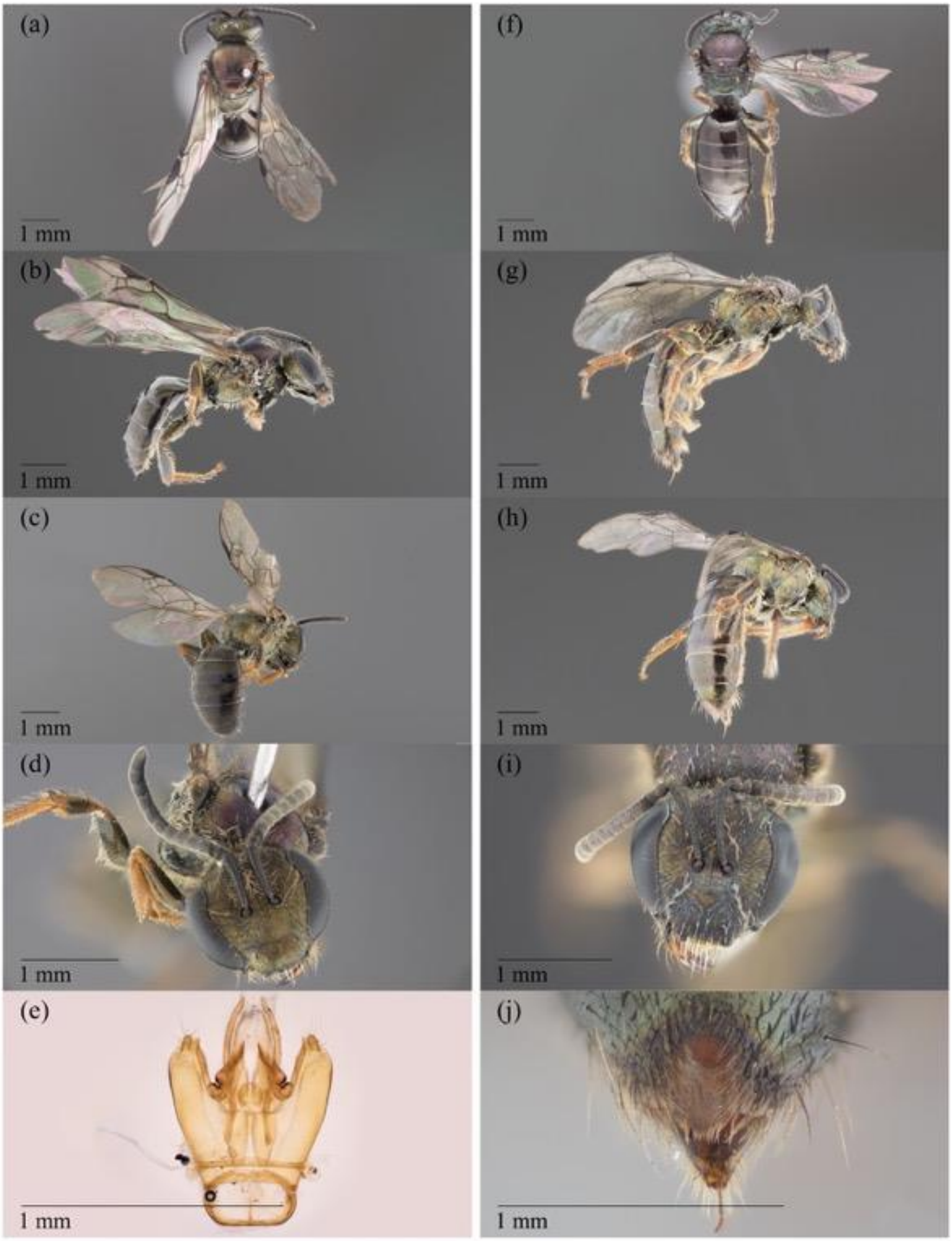

Figure 21. *Homalictus ostridorsum* **sp. nov.** male (a) dorsal habitus, (b) lateral habitus, (c) dorso posterior, (d) anteriorly frontal face and (e) ventral genitalia. Female (f) dorsal habitus, (g) lateral habitus, (h) dorso posterior, (i) anteriorly frontal face, and (j) pygidial plate.

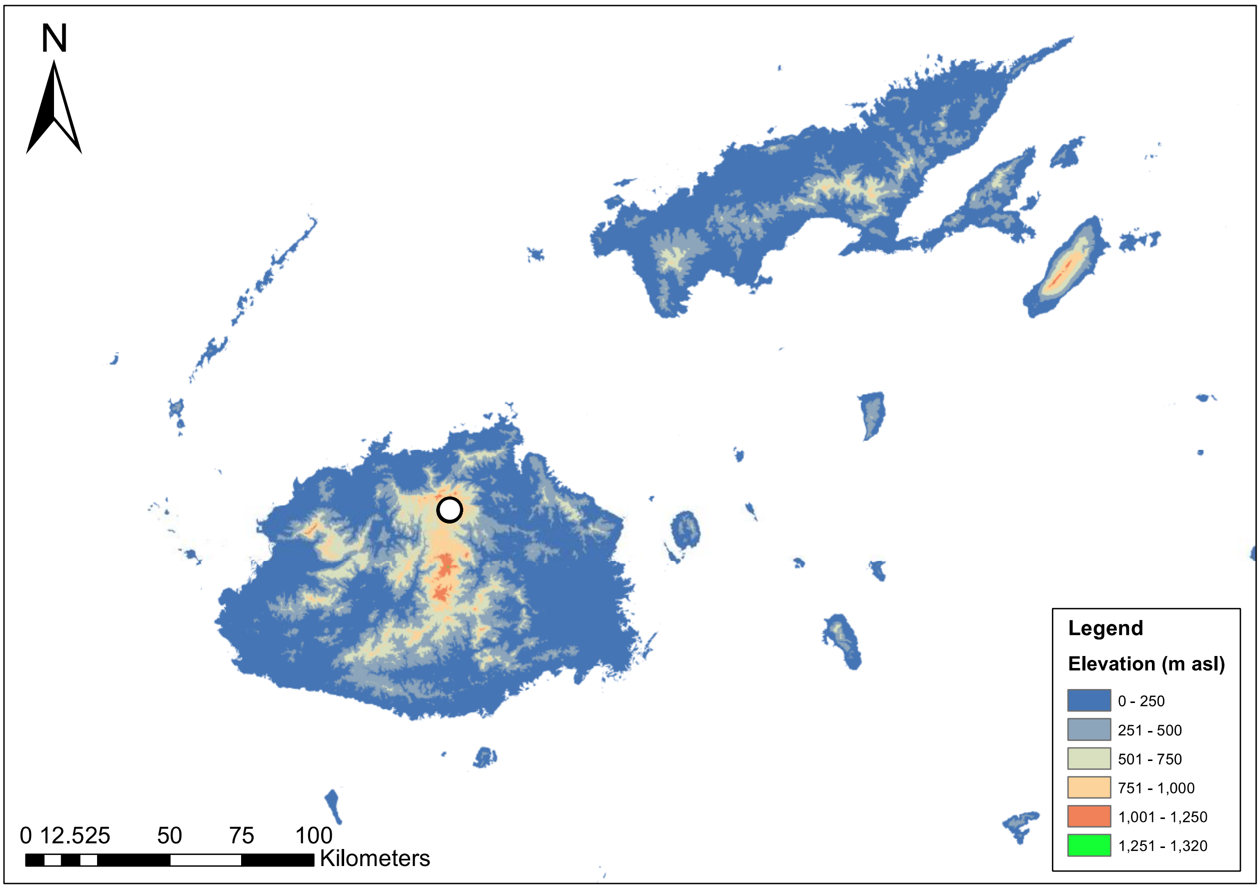

Figure 22. Collection map of *Homalictus ostridorsum* **sp. nov.** from specimens with identity confirmed by mtDNA COI gene. Sample size is 43.

Distribution

Homalictus ostridorsum has only been sampled from Mt. Tomanivi (the highest mountain in Fiji and previously known as Mt. Victoria) on the main island of Viti Levu (Fig. 22). Samples were collected between 1,200 m asl and 1,328 m asl, the latter is the highest elevation of Mt. Tomanivi.

Etymology

Both the males and females of this species have a purple scutum. The name is derived from the Latin *ostrum* meaning ‘purple’ and *dorsus* meaning ‘back’.

Homalictus taveuni sp. nov.

(Figs 23-24)

Material examined

Holotype ♂: ACQ003 (SAMA 32-036163), Taveuni, Fiji, -16.967000, 179.997000, SVC Groom, 01.09.2010, 15 m asl, Clade E, MSAPB164_11_ACQ003.

Allotype ♀: ACQ002 (SAMA 32-036164), Taveuni, Fiji, -16.967, 179.997, 15 m asl, Clade E, SVC Groom, Taveuni.

Paratype ♂: ACQ004 (SAMA 32-036165), 1/9/10, 16 m asl, -16.967, 179.997, SVC Groom.

Diagnosis

Males: In combination: Supraclypeal area mostly finely colliculate (Fig. 1f-g), posterior or margin of scutum about straight (Fig. 23a), scutum, scutellum and supraclypeal area golden green and metallic, and scutellum to forewing length ratio 1:14.

Females: In combination: Supraclypeal area mostly moderately colliculate (Fig. 1e), scape does not extend beyond posterior margin of medial ocellus, propodeum coarsely strigate-rugose (Fig. 1a) and propodeum does not have a medial anterior groove dorsally (Fig. 23f).

Description

Males:

Measurements: UID 0.63 mm. LID 0.46 mm. AOD 0.19 mm. IAD 0.11 mm. OAD 0.32 mm. IOD 0.18 mm. OOD 0.19 mm. GW 0.17 mm. EW 0.29 mm. ML 0.1 mm. SL 0.22 mm. FL 3.14 mm.

Colouration: Clypeus, supraclypeal area, frons, paraocular area, scutum and scutellum golden green and metallic. Propodeum dorsally green. Metasoma dark green or green, dark along posterior edges.

Sculpturing: Paraocular area some messy striae below antennal sockets and colliculate, longitudinal striae posteriorly and proximally above antennal socket. Frons has many diagonal striae and some transverse striae under ocelli. Supraclypeal area mostly finely colliculate. Clypeus finely colliculate. Vertex punctures fine, close, and open. Scutum anteriorly finely colliculate and lineolate; medially finely and moderately fine colliculate; posteriorly finely colliculate. Scutellum punctation open and sparse. Propodeum dorsally strong striae, weak medial anterior groove, and coarsely strigate-rugose; laterally finely colliculate and posteroventral and anterior striae curve towards each other and can meet; posteriorly longitudinal striae ventrally and transverse striae medially.

Morphology: Scape extends to or below anterior margin of medial ocellus. Interantennal distance about equal to diameter of socket. Labrum simple. Clypeus not depressed medially. Area posterior of vertex with striae strong and close. Posterior margin of scutum shape mostly straight. Gonostylus moderate, dorsoapical crest of gonocoxite moderate. Entire genital relatively small.

Females:

Measurements: UID 0.65 mm. LID 0.62 mm. AOD 0.22 mm. IAD 0.9 mm. OAD 0.38 mm. IOD 0.18 mm. OOD 0.165 mm. GW 0.19 mm. EW 0.3 mm. BL 4.51 mm. ML 0.13 mm. SL 0.26 mm. FL 3.61 mm.

Colouration: Clypeus anteriorly black; posteriorly golden green and metallic. Whole clypeus partly iridescent. Supraclypeal area, frons, scutellum, and propodeum dorsally golden green and metallic. Scutum golden green and metallic and partly metallic orange and pink. Metasoma dark green or green, dark green along posterior edges.

Sculpturing: Paraocular area striae, colliculate along margin of compound eyes. Frons mostly longitudinal striae. Supraclypeal area mostly moderately colliculate, medial area finely colliculate. Clypeus finely colliculate. Vertex punctures fine and close. Scutum anteriorly moderately colliculate and lineolate; medially and posteriorly finely colliculate. Scutellum punctation close and open. Propodeum dorsally linear pattern and coarsely strigate-rugose; laterally ventral and anterior striae curve towards each other and can meet; posteriorly finely colliculate and transverse striae ventrally and proximally. Pygidial plate with close minute punctures medially, punctures mostly on posterior half and hairs emerging on ventral 1/3.

Morphology: Scape extends to or below anterior margin of medial ocellus. Interantennal distance about equal to diameter of socket. Labrum with two medial projections parallel from one another. Clypeus not depressed medially. Area posterior of vertex striae strong and close. Posterior margin of scutum shape mostly straight.

Comments

This species has only been found at low elevations and in small numbers at a single site.

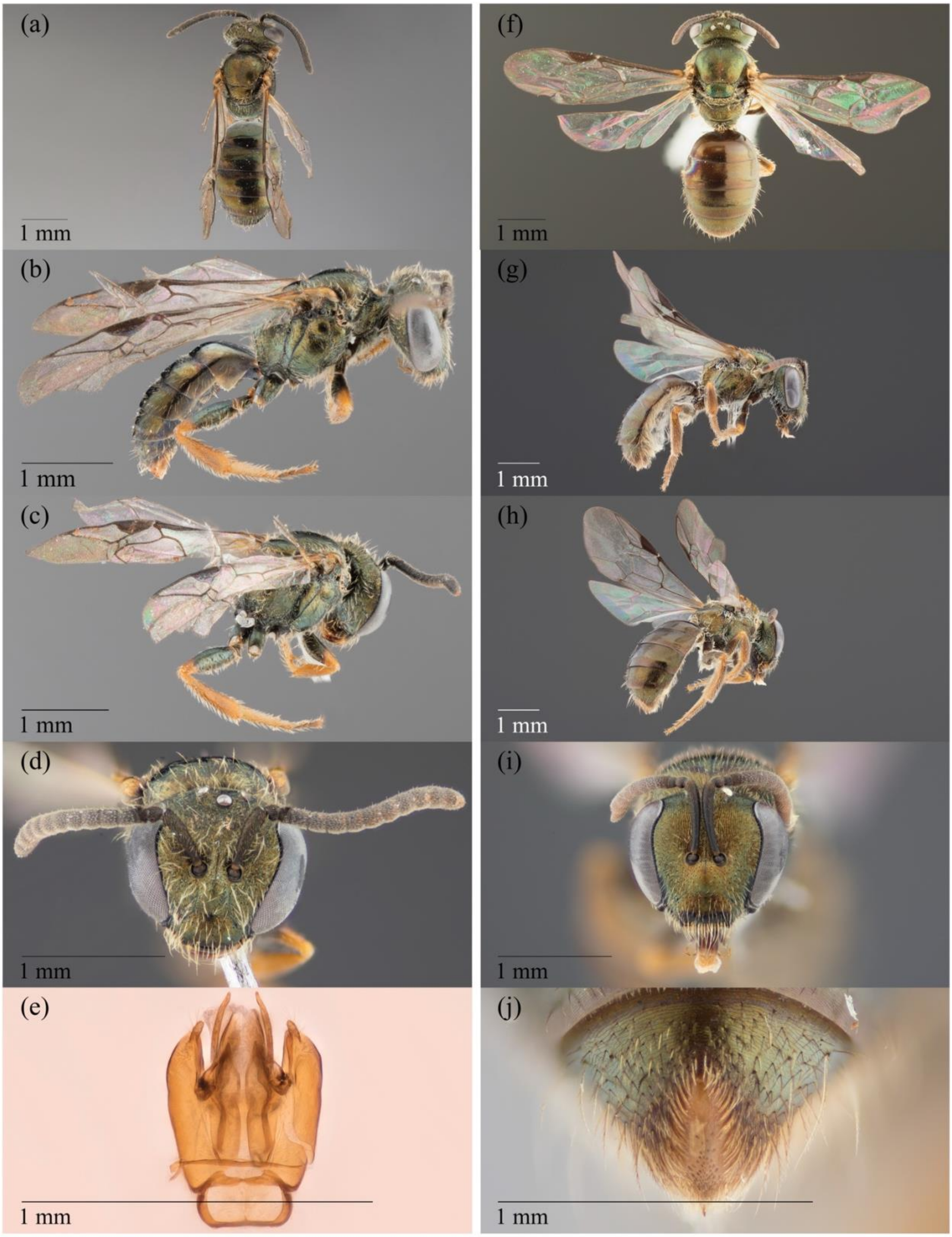

Figure 23. *Homalictus taveuni* **sp. nov.** male (a) dorsal habitus, (b) lateral habitus, (c) dorso posterior, (d) anteriorly frontal face and (e) ventral genitalia. Female (f) dorsal habitus, (g) lateral habitus, (h) dorso posterior, (i) anteriorly frontal face, and (j) pygidial plate.

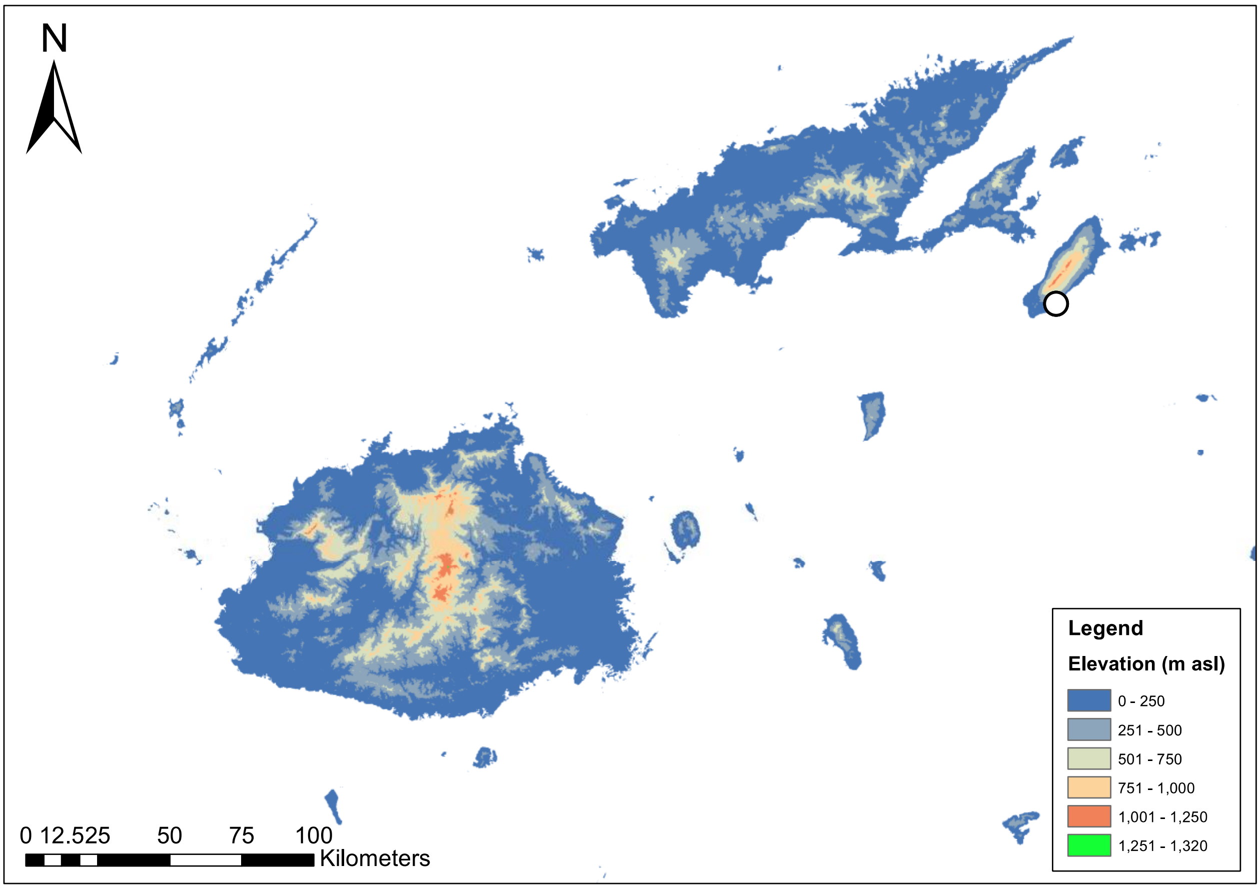

Figure 24. Collection localities of *Homalictus taveuni* **sp. nov.** from specimens with identity confirmed by mtDNA COI gene. Sample size is 3.

Distribution

Homalictus taveuni has only been sampled from the island of Taveuni (Fig. 24). Collections have only been made at 15 m asl.

Etymology

The name *H. taveuni* refers to the island of Taveuni that this species appears to be restricted.

Homalictus terminalis sp. nov.

(Figs 25-26)

Material examined

Holotype ♂: 17FJ48 (SAMA 32-036147), Mt. Batilamu, Fiji, -17.68656, 177.54394, JB Dorey, OK Davies, 27.4.2018, 1,118 m asl, 9:50 AM, RP17OKD0030, sweep netting area around the hut, long grasses and weeds (0.5-2 m high) with minimal flowers. Mostly roosting bees.

Allotype ♀: 17FJ43 (SAMA 32-036148), Mt. Batilamu, Fiji, -17.68656, 177.54394, 1,118 m, sweep netting, JB Dorey, OK Davies, 24.7.17, across the area around the hut, long grasses and weeds (0.5-2 m high) with minimal flowers. Mostly roosting bees.

Paratypes 2 ♀: 17FJ44 (SAMA 32-036149) & 17FJ41 (SAMA 32-036150), 27/4/17, 9:50 AM, 1,118 m asl, -17.68656, 177.54394, JB Dorey & OK Davies, Mt. Batilamu, across the area around the hut, long grasses and weeds (0.5-2 m high) with minimal flowers. Mostly roosting bees.

Other material examined

2 ♀*:* 17FJ50 and 17FJ68, 27/4/17, 9:50 AM, 1,118 m asl, -17.68656, 177.54394, JB Dorey & OK Davies, Mt. Batilamu, across the area around the hut, long grasses and weeds (0.5-2 m high) with minimal flowers. Mostly roosting bees.

Diagnosis

Males: Labrum has two medial projections and can be distinguished from males of *H. nadarivatu* by a lack of many vertical striae on the frons. Dorsal subapical crest of gonocoxite poorly developed and gonostylus laterally flattened (Fig. 25e).

Females: In combination: Bee is mostly green, supraclypeal area is mostly moderately colliculate, scape extends above head and sculpturing on anterior of scutum colliculate but not lineolate.

Description

Males:

Measurements: UID 0.7 mm. LID 0.67 mm. AOD 0.26 mm. IAD 0.1 mm. OAD 0.44 mm. IOD 0.17 mm. OOD 0.2 mm. GW 0.24 mm. EW 0.4 mm. BL: 4.99 mm ML 0.13 mm. SL 0.33 mm. FL 3.85 mm.

Colouration: Whole clypeus partly iridescent, golden green, and metallic. Supraclypeal area, frons, paraocular area, scutellum, and propodeum dorsally golden green and metallic. Scutum partly metallic orange and pink and golden green and metallic. Metasoma T1 is black or nearly so, T2 onwards is green, dark green along posterior edges.

Sculpturing: Paraocular area striae, colliculate along margin of compound eyes. Frons with many diagonal striae, lateral striae under ocelli. Supraclypeal area mostly moderately colliculate, medial area finely colliculate. Clypeus finely colliculate. Vertex punctures very few, small and sparse. Scutum anteriorly finely colliculate and lineolate; medially finely colliculate; posteriorly moderately colliculate and lineolate. Scutellum punctation open and sparse. Propodeum dorsally linear pattern and coarsely strigate-rugose; laterally finely colliculate and posteroventral and anterior striae curve towards each other and can meet; posteriorly finely and moderately colliculate and diagonal striae ventrally and proximally.

Morphology: Scape extends to above vertex. Interantennal distance about equal to diameter of socket. Labrum simple. Clypeus not depressed medially. Area posterior of vertex with strong and close striae. Posterior margin of Scutum shape mostly straight. Gonostylus well developed and flattened laterally, dorsoapical crest of gonocoxite weak. Fovea along anterior and proximal margin of eye absent.

Females:

Measurements: UID 0.6–0.87 mm. LID 0.57–0.84 mm. AOD 0.2–0.3 mm. IAD 0.09–0.1 mm. OAD 0.32–0.49 mm. IOD 0.17–0.21 mm. OOD 0.16–0.25 mm. GW 0.1–0.32 mm. EW 0.11–0.38 mm. BL 4.51–5.56 mm. ML 0.11–0.16 mm. SL 0.25–0.39 mm. FL 3.34–4.18 mm.

Colouration: Clypeus anteriorly black; posteriorly golden green and metallic. Whole clypeus partly iridescent. Supraclypeal area, frons, and paraocular area golden green and metallic or golden. Scutum metallic orange, pink, and golden green. Scutellum golden green and metallic or partly metallic orange and pink. Propodeum dorsally golden green and metallic. Metasoma black, dark green or green, dark green along posterior edges.

Sculpturing: Paraocular area with some horizontal striae laterally and longitudinal striae, colliculate along margin of compound eyes. Frons mostly longitudinal striae. Supraclypeal area mostly moderately colliculate, medial area finely colliculate, rarely finely colliculate anteriorly. Clypeus finely colliculate. Vertex punctures minute open, fine, and close. Scutum anteriorly moderately fine colliculate; medially and posteriorly finely colliculate or moderately fine colliculate. Scutellum punctation close and open. Propodeum dorsally linear pattern, strong striae, weak medial anterior groove and coarsely strigate-rugose; laterally finely colliculate, ventral and anterior striae curve towards each other and can meet, some striae anteriorly and dorsally and some striae ventrally; posteriorly finely colliculate, moderately fine colliculate, transverse striae medially, transverse striae ventrally and proximally and striae originating ventrally and medially almost forms circles with dorsal striae. Pygidial plate with close minute punctures medially.

Morphology: Scape extends to above vertex. Interantennal distance about equal to diameter of socket. Labrum has two medial projections parallel from one another. Clypeus not depressed medially. Area posterior of vertex with strong and close striae. Posterior margin of Scutum shape mostly straight.

Comments

Given the very limited geographical and elevational distribution of *H. terminalis* it is likely to be threatened by climate warming in the future.

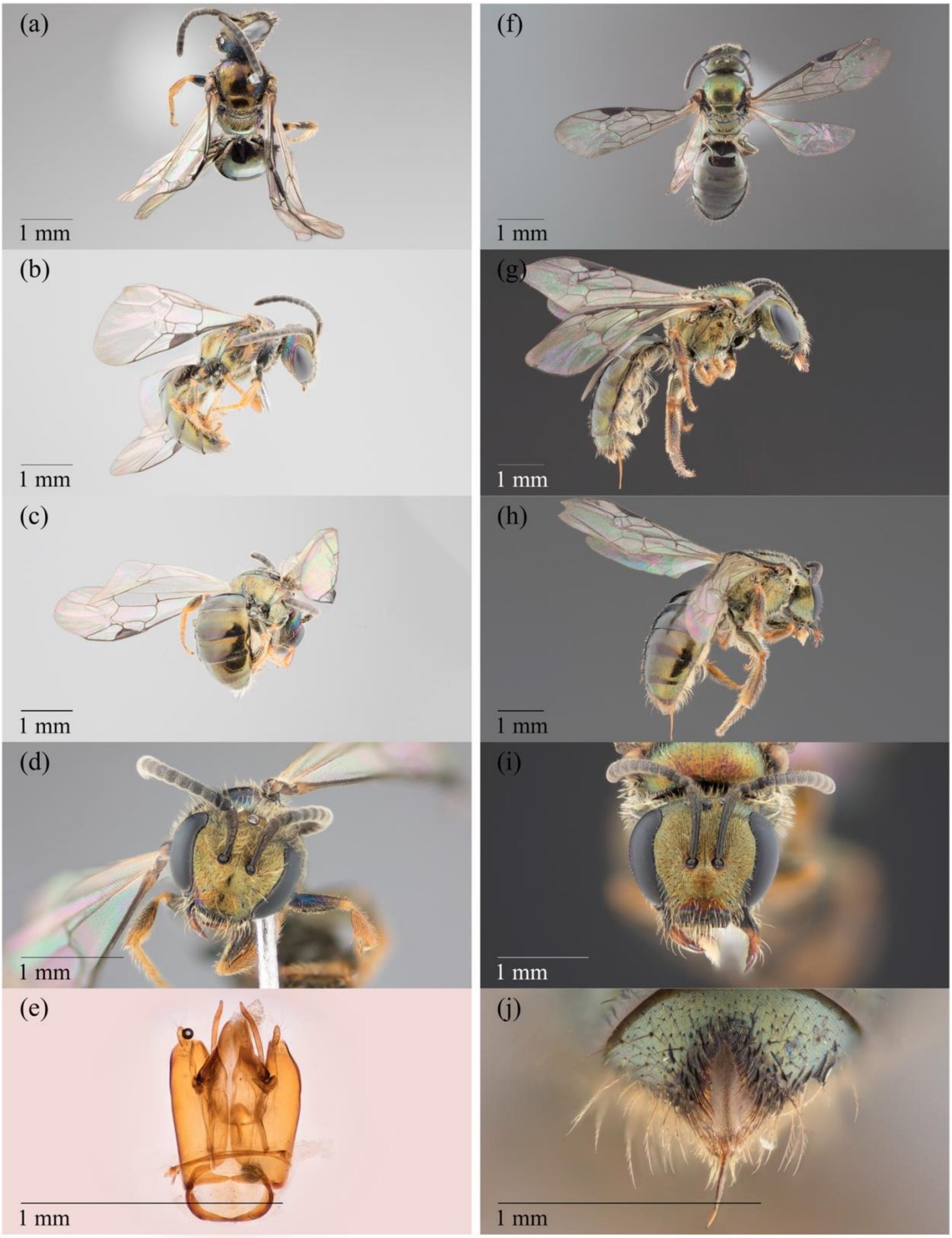

Figure 25. *Homalictus terminalis* **sp. nov.** male (a) dorsal habitus, (b) lateral habitus, (c) dorso posterior, (d) anteriorly frontal face and (e) ventral genitalia. Female (f) dorsal habitus, (g) lateral habitus, (h) dorso posterior, (i) anteriorly frontal face, and (j) pygidial plate.

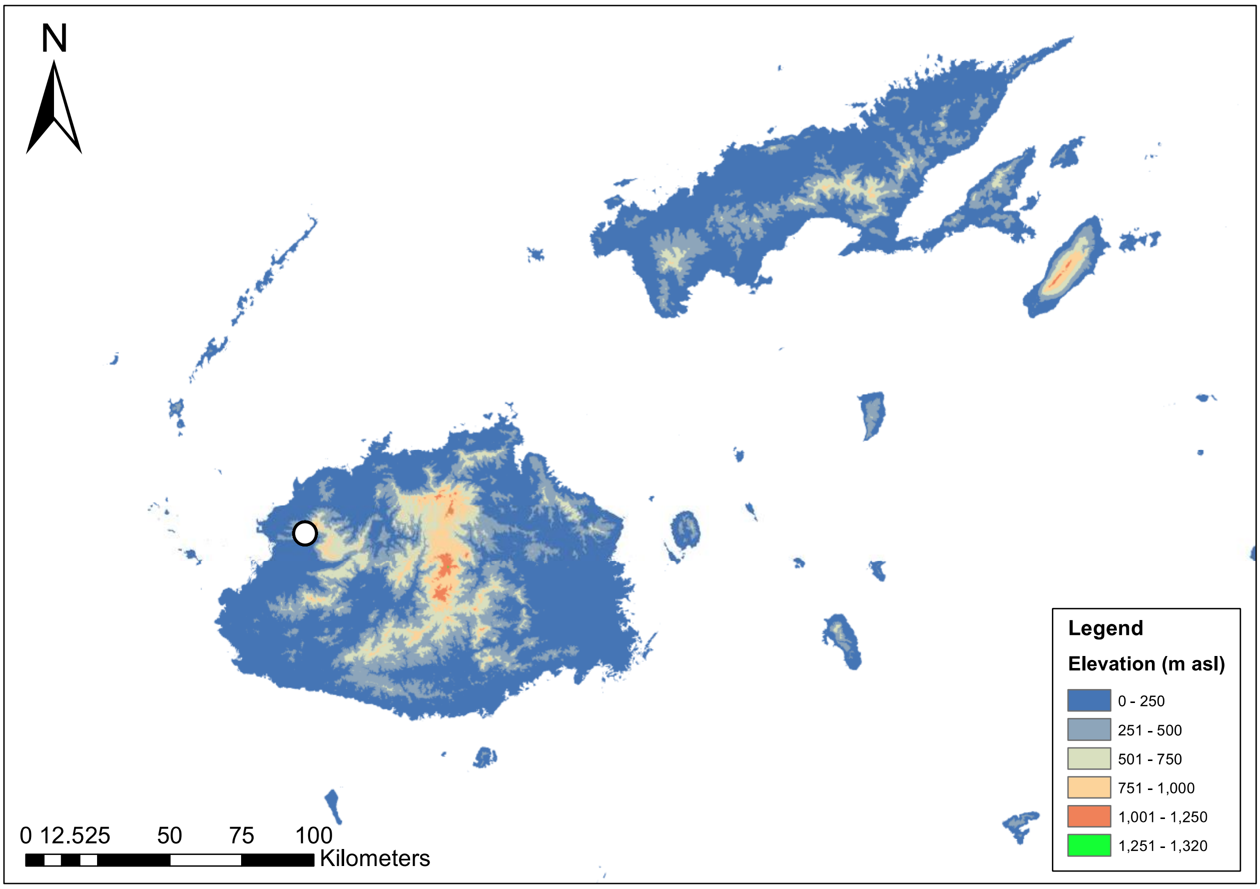

Figure 26. Collection map of *Homalictus terminalis* **sp. nov.** from specimens with identity confirmed by mtDNA COI gene. Sample size is 10.

Distribution

Homalictus terminalis has only been sampled on Mt. Batilamu on the largest island of Viti Levu (Fig. 26). Collections of *H. terminalis* sp. nov. have only been made between 1,100 m asl and 1,118 m asl — the summit of Mt. Batilamu is 1,195 m asl.

Etymology

Homalictus terminalis has only been found within 95 m of the maximum elevation available to it, like numerous other *Homalictus* species in Fiji. The Latin noun *terminalis* means limit or boundary indicating the upper elevational and thermal limit that *H. terminalis* inhabits and could ultimately result in its extinction with global climate warming.

Homalictus tuiwawae sp. nov.

(Figs 27-28)

Material examined

Holotype ♂: 17FJ216 (SAMA 32-036155), Nadarivatu, Fiji, 810 m asl, -17.6185, 177.9787, 18.4.2017, BL Barnden, Nadarivatu Rd, towards telecom tower, caught on 4 petal yellow flower.

Allotype ♀: 17FJ158 (SAMA 32-036156), 19/4/17, 10:35 AM, 865 m asl, -17.609817, 177.979867, JB Biddle, RK Schober, JB Dorey & CS Matthews, caught amongst weeds and grass above kava plantation (cleared and surrounded by forest). Sunny and little to no breeze in clearing.

Paratypes 3 ♂: ED42_D03 (SAMA 32-036157), 28/8/10, 923 m asl, -17.58268, 177.93645, E Deans, ABL002 (SAMA 32-036158), 4/8/10, 12:45 AM, 842 m asl, -17.678, 178.001, SVC Groom, ABL003 (SAMA 32-036159), 4/8/10, 12:45 AM, 842 m asl, -17.678, 178.001, SVC Groom, and 3 ♀: 17FJ80 (SAMA 32-036160), 28/4/17, 11:00 AM, 842 m asl, -17.67782, 177.54044, JB Dorey, Mt. Batilamu, long grass and weeds on the path down near the edge of the forest. Some 'butterfly' suitable flowers. Swept off the trees. Generally, overcast with some sun. Males generally caught around the outside of the compound. ABN001 (SAMA 32-036161), 4/8/10, 1:45 PM, 665 m asl, -17.735, 178.075, SVC Groom, ABO001 (SAMA 32-036162), 4/8/10, 2:02 PM, 357 m asl, 17.727, 178.084, SVC Groom.

Diagnosis

Males: In combination: Supraclypeal area mostly moderately colliculate, frons has many diagonal striae and labrum lacks two medial projections (simple).

Females: In combination: supraclypeal area mostly finely colliculate, scutum golden green and metallic and pygidial plate has a dense line of hairs medially. The latter character is useful to distinguish *H. tuiwawae* from *H. concavus, H. atritergus*, and *H. kaicolo.*

Description

Males:

Measurements: UID 0.61 mm. LID 0.48 mm. AOD 0.19 mm. IAD 0.13 mm. OAD 0.35 mm. IOD 0.15 mm. OOD 0.2 mm. GW 0.22 mm. EW 0.27 mm. BL 3.75 mm. ML 0.11 mm. SL 0.22 mm. FL 3.09 mm.

Colouration: Clypeus, supraclypeal area, frons, paraocular area, scutum, scutellum, and propodeum dorsally golden green and metallic. Metasoma dark green or green, dark green along posterior edges.

Sculpturing: Paraocular area colliculate, longitudinal striae posteriorly and proximally above antennal socket. Frons with many diagonal striae and transverse striae under ocelli. Supraclypeal area mostly moderately colliculate, medial area finely colliculate. Clypeus finely colliculate. Vertex with very few fine and open punctures. Scutum anteriorly moderately colliculate and lineolate; medially and posteriorly moderately fine colliculate. Scutellum punctation close and open. Propodeum dorsally weak medial anterior groove and coarsely strigate-rugose; laterally finely colliculate, some striae anteriorly and dorsally, and some striae ventrally; posteriorly finely colliculate and transverse striae ventrally and proximally.

Morphology: Scape extends to or below anterior margin of medial ocellus. Interantennal distance greater than diameter of socket. Labrum simple. Clypeus not depressed medially. Area posterior of vertex with striae strong and close. Posterior margin of Scutum shape mostly straight. Gonostylus moderate, dorsoapical crest of gonocoxite well developed. Penis valves strongly hooked.

Females:

Measurements: UID 0.63–0.66 mm. LID 0.6–0.64 mm. AOD 0.22–0.23 mm. IAD 0.09–0.1 mm. OAD 0.38–0.42 mm. IOD 0.17–0.18 mm. OOD 0.16–0.2 mm. GW 0.16–0.24 mm. EW 0.27–0.32 mm. BL 4.13–0.49 mm. ML 0.13–0.15 mm. SL 0.25–0.26 mm. FL 3.56–3.61 mm.

Colouration: Clypeus anteriorly black; posteriorly golden green and metallic. Whole clypeus partly iridescent and golden green and metallic. Supraclypeal area, frons and paraocular area golden green and metallic. Scutum golden green and metallic partly metallic orange and pink and can appear reddish. Scutellum golden green and metallic and partly metallic orange and pink. Propodeum dorsally golden green and metallic with some iridescent pink, purple, or blue. Metasoma green, dark green along posterior edges and some iridescent purple.

Sculpturing: Paraocular area striate, colliculate along margin of compound eyes. Frons mostly longitudinal striae, can have transverse striae under ocelli and colliculate above antennal sockets. Supraclypeal area mostly finely colliculate. Clypeus finely colliculate. Vertex punctures fine and open. Scutum anteriorly moderately colliculate and lineolate; medially and posteriorly finely and moderately colliculate. Scutellum punctation close and open. Propodeum dorsally has a linear pattern, some posterior transverse striae and coarsely strigate-rugose; laterally finely colliculate and posteroventral and anterior striae curve towards each other and can meet; posteriorly finely colliculate, transverse striae medially and ventrally and proximally. Pygidial plate with close and fine punctures medially.

Morphology: Scape extends to above vertex. Interantennal distance about equal to diameter of socket. Labrum with two medial projections parallel from one another. clypeus not depressed medially. Area posterior of vertex with strong striae and close. Posterior margin of Scutum shape mostly straight.

Comments

Homalictus tuiwawae is the second most common native bee encountered in Fiji and the most common bee in the highlands.

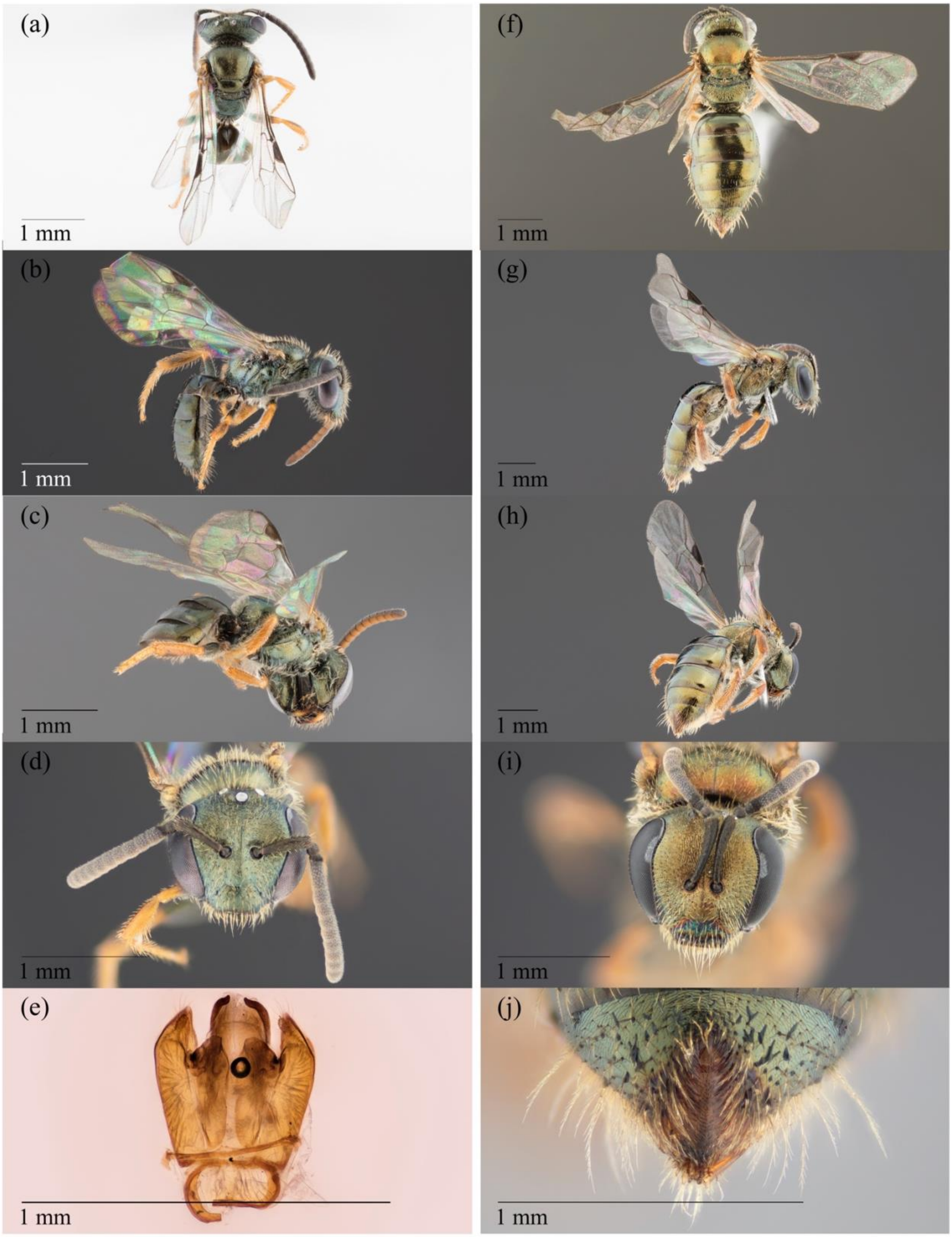

Figure 27. *Homalictus tuiwawae* **sp. nov.** male (a) dorsal habitus, (b) lateral habitus, (c) dorso posterior, (d) anteriorly frontal face and (e) ventral genitalia. Female (f) dorsal habitus, (g) lateral habitus, (h) dorso posterior, (i) anteriorly frontal face, and (j) pygidial plate.

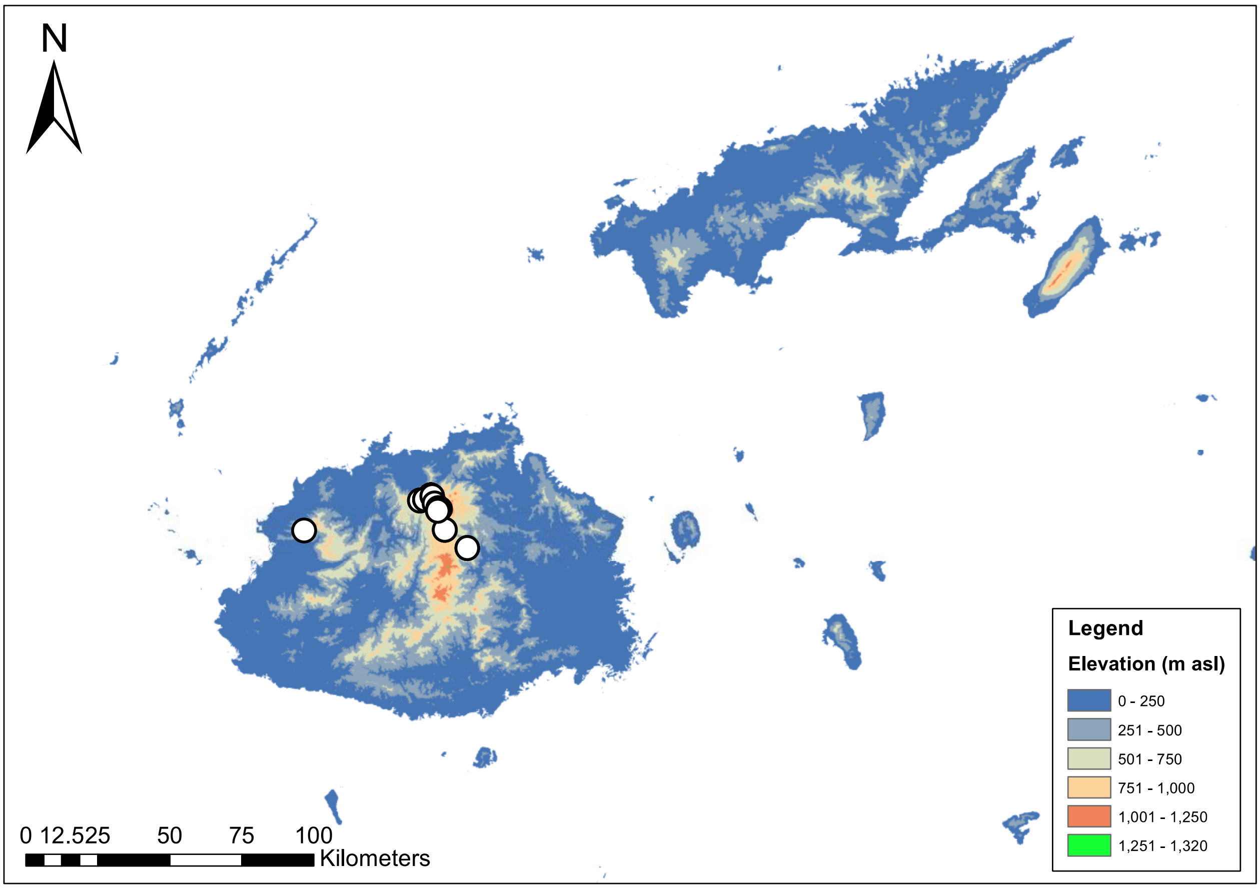

Figure 28. Collection map of *Homalictus tuiwawae* **sp. nov.** from specimens with identity confirmed by mtDNA COI gene. Sample size is 58.

Distribution

Homalictus tuiwawae has a large distribution on the largest island of Viti Levu, ranging from the central highlands to Mt. Batilamu (Fig. 28). Collections of *H. tuiwawae* have been made between 660 m asl and 1,000 m asl.

Etymology

Homalictus tuiwawae is named in recognition of Marika Tuiwawa, the herbarium curator at the Faculty of Science, Technology and Environment at the University of the South Pacific. Marika Tuiwawa has been a key facilitator for past and ongoing bee research in Fiji, contributing greatly to our ecological and behavioural studies, and the discovery of new species in Fiji.

Discussion

With some exceptions (notably *H. hadrander* and *H. achrostus*), most of the Fijian bee species described here are externally very cryptic making species identification challenging. The most reliable morphological character to delineate species for males is the male genitalia and for females often the pygidial plate. Our study of the Fijian *Homalictus* highlights the growing number of studies (e.g., [69-72]) that emphasise the importance of COI barcoding and molecular analysis in conjunction with morphology as a method of species delineation and identification.

Many of the Fijian *Homalictus* appear to be restricted to narrow geographical areas and altitudinal bands, with many species constrained to single mountain tops. These highland regions appear to act as climate refugia for these highland species. From further COI barcoding, we are aware of another 13 potential undescribed Fijian *Homalictus* species [12] but we have not described those species here because we lack representatives for both sexes.

It is likely that other archipelagos with highlands in the tropical Pacific will have a similar hyperdiversity of bees and other tropical invertebrates. Samoa [73], Vanuatu [74], Micronesia [75], Solomon Islands [76], Fiji [65], New Guinea [77], and New Caledonia [41] have all been examined for bee diversity but many of these studies are decades old and are not the result of bee-specific sampling. Additionally, these studies delineate species based on morphology alone, making the identification of cryptic species difficult.

The high number of Fijian *Homalictus* restricted to single highland peaks and near their maximum elevational extent indicates a high risk of numerous species loss under global warming predictions due to their limited ability to track changing climates. It is possible that *H. achrostus* has already gone extinct from its mountain top (Nadarivatu) with six samples collected in 1978 [65], two samples in 2010, and none since then despite extensive sampling in the area. There is a clear need to document and describe these new species in Fiji and the tropics, particularly if many endemic and valuable pollinators are at risk of extinction.

Supporting information

Acknowledgements

We would like to thank Marika Tuiwawa and Alivereti Naikatini for their invaluable assistance with *Homalictus* collection and Fijian field logistics, as well as all the students from Flinders University and University of South Australia who helped collect specimens, particularly Cale Matthews, Justin Biddle, and Rebecca Schober for their help and dedication. We also thank Alejandro Velasco-Castrillón for his support with lab work and DNA sequencing, Mike Lee for his valuable advice on phylogenetic analyses and Olivia Davies for her assistance in the field, data curation, and editorial advice.

Additionally, we would like to thank Ben Parslow for his help in imaging and scoring the traits of the *H. versifrons* type specimen and for editorial advice of this manuscript. David Notton must also be thanked for imaging the type of *H. fijiensis* at the NHMUK and Andrew Bennet at CNC for imaging the type of *H. achrostus* and sending us *H. hadrander* and possible *H. versifrons* material. We would also like to thank Michael Engel of SEMC for imaging the type of *H. hadrander*. Images taken at the NHMUK are ©The Trustees of the Natural History Museum, London, and made available under a Creative Commons License 4.0 (https://creativecommons.org/licenses/by/4.0/). Further thanks go to Jim Boone from the Bishop Museum his help searching for specimens and type material.

Fieldwork was funded by the Australia Pacific Science Foundation and a New Colombo Plan grant (NCPST Fiji 15482) from the Australian Federal Government. Further thanks go to the Playford Memorial Trust for providing funding to James Dorey for the duration of this project.

Supplementary material

Supplementary figures

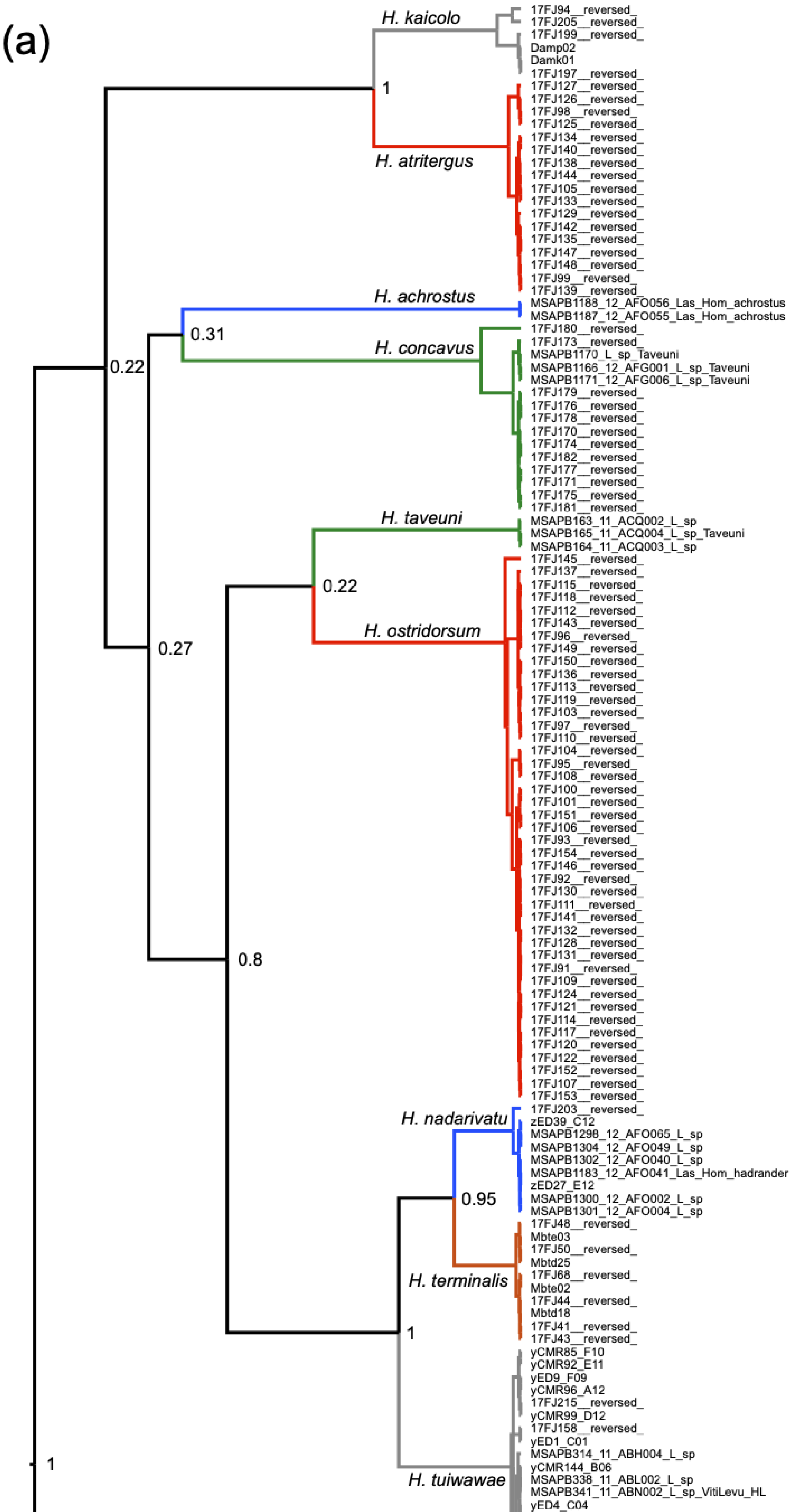

2026

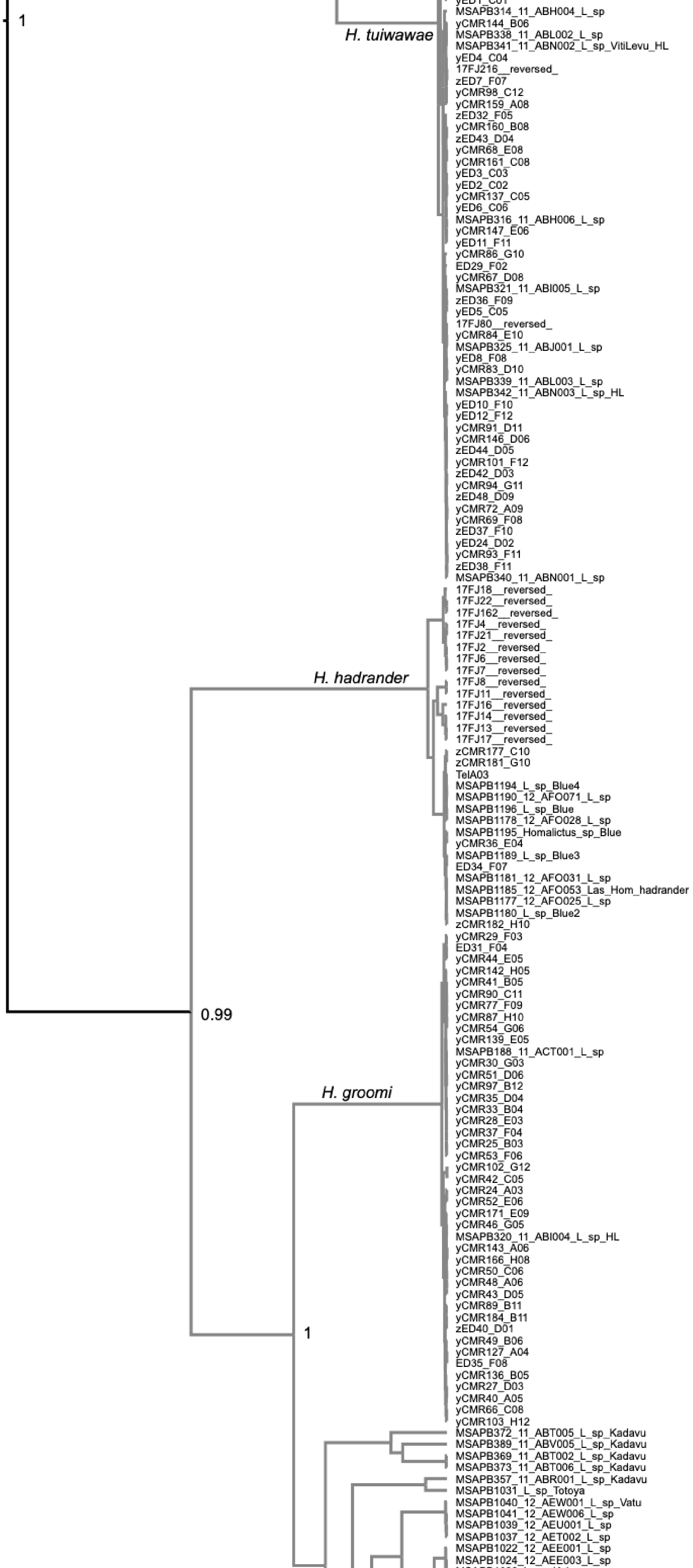
yED1_C01
1
MSAPB314_11_ABH004_L_sp
yCMR144_B06
H. tuiwawae
MSAPB338_11_ABL002_L_sp
MSAPB341_11_ABN002_L_sp_VitiLevu_HL
yED4_C04
17FJ216__reversed_
zED7_F07
yCMR98_C12
yCMR159_A08
zED32_F05
yCMR160_B08
zED43_D04
yCMR68_E08
yCMR161_C08
yED3_C03
yED2_C02
yCMR137_C05
yED6_C06
MSAPB316_11_ABH006_L_sp
yCMR147_E06
yED11_F11
yCMR86_G10
ED29_F02
yCMR67_D08
MSAPB321_11_ABI005_L_sp
zED36_F09
yED5_C05
17FJ80__reversed_
yCMR84_E10
MSAPB325_11_ABJ001_L_sp
yED8_F08
yCMR83_D10
MSAPB339_11_ABL003_L_sp
MSAPB342_11_ABN003_L_sp_HL
yED10_F10
yED12_F12
yCMR91_D11
yCMR146_D06
zED44_D05
yCMR101_F12
zED42_D03
yCMR94_G11
zED48_D09
yCMR72_A09
yCMR69_F08
zED37_F10
yED24_D02
yCMR93_F11
zED38_F11
MSAPB340_11_ABN001_L_sp
17FJ18__reversed_
17FJ22__reversed_
17FJ162__reversed_
17FJ4__reversed_
17FJ21__reversed_
17FJ2__reversed_
17FJ6__reversed_
17FJ7__reversed_
H. hadrander
17FJ8__reversed_
17FJ11__reversed_
17FJ16__reversed_
17FJ14__reversed_
17FJ13__reversed_
17FJ17__reversed_
zCMR177_C10
zCMR181_G10
TelA03
MSAPB1194_L_sp_Blue4
MSAPB1190_12_AFO071_L_sp
MSAPB1196_L_sp_Blue
MSAPB1178_12_AFO028_L_sp
MSAPB1195_Homalictus_sp_Blue
yCMR36_E04
MSAPB1189_L_sp_Blue3
ED34_F07
MSAPB1181_12_AFO031_L_sp
MSAPB1185_12_AFO053_Las_Hom_hadrander
MSAPB1177_12_AFO025_L_sp
MSAPB1180_L_sp_Blue2
zCMR182_H10
yCMR29_F03
ED31_F04
yCMR44_E05
yCMR142_H05
yCMR41_B05
yCMR90_C11
yCMR77_F09
0.99
yCMR87_H10
yCMR54_G06
yCMR139_E05
MSAPB188_11_ACT001_L_sp
yCMR30_G03
yCMR51_D06
yCMR97_B12
H. groomi
yCMR35_D04
yCMR33_B04
yCMR28_E03
yCMR37_F04
yCMR25_B03
yCMR53_F06
yCMR102_G12
yCMR42_C05
yCMR24_A03
yCMR52_E06
yCMR171_E09
yCMR46_G05
MSAPB320_11_ABI004_L_sp_HL
yCMR143_A06
yCMR166_H08
yCMR50_C06
yCMR48_A06
yCMR43_D05
yCMR89_B11
yCMR184_B11
zED40_D01
1
yCMR49_B06
yCMR127_A04
ED35_F08
yCMR136_B05
yCMR27_D03
yCMR40_A05
yCMR66_C08
yCMR103_H12
MSAPB372_11_ABT005_L_sp_Kadavu
MSAPB389_11_ABV005_L_sp_Kadavu
MSAPB369_11_ABT002_L_sp_Kadavu
MSAPB373_11_ABT006_L_sp_Kadavu
MSAPB357_11_ABR001_L_sp_Kadavu
MSAPB1031_L_sp_Totoya
MSAPB1040_12_AEW001_L_sp_Vatu
MSAPB1041_12_AEW006_L_sp
MSAPB1039_12_AEU001_L_sp
MSAPB1037_12_AET002_L_sp
MSAPB1022_12_AEE001_L_sp
MSAPB1024_12_AEE003_L_sp

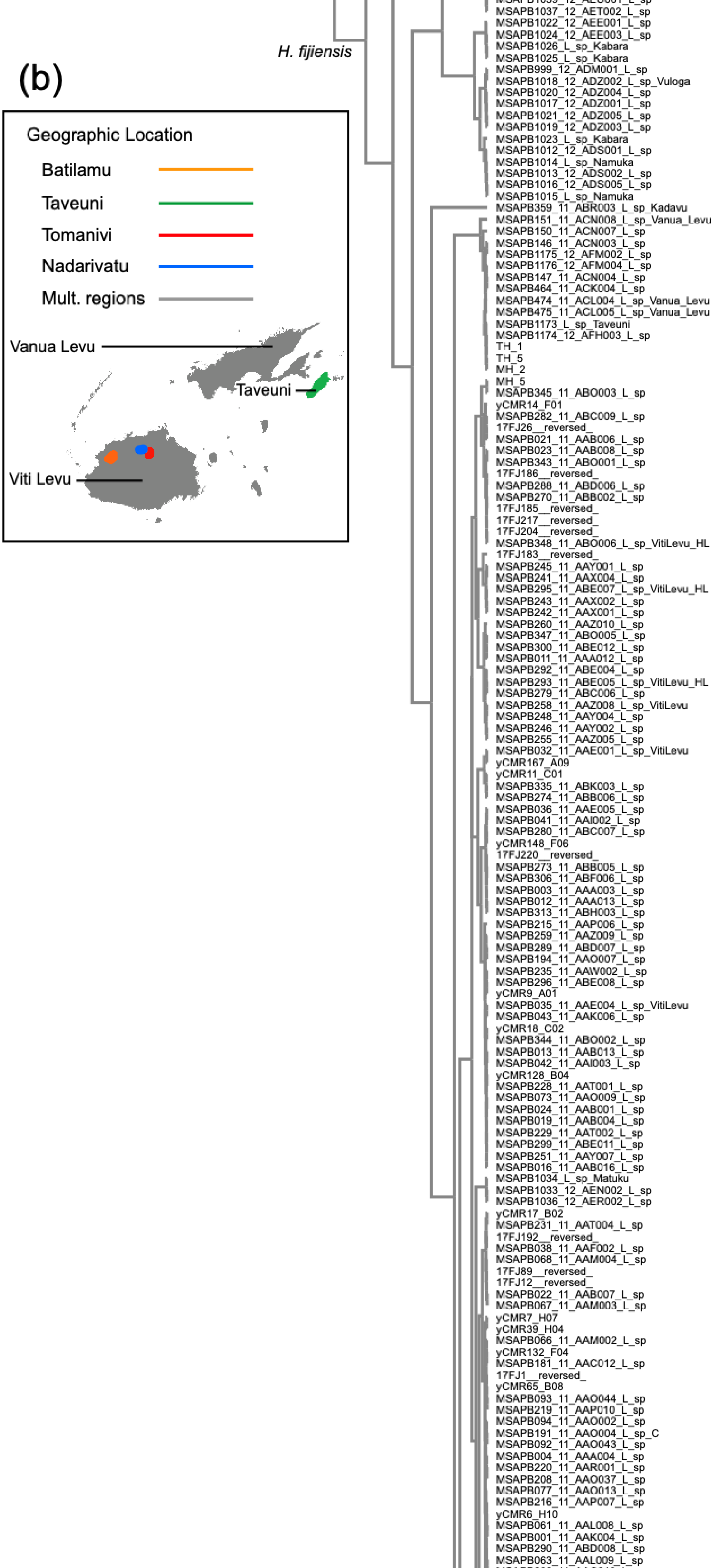
(b)
H. fijiensis
Geographic Location
Batilamu
Taveuni
Tomanivi
Nadarivatu
Mult. regions
Vanua Levu
Taveuni
Viti Levu
MSAPB1037_12_AET002_L_sp
MSAPB1022_12_AEE001_L_sp
MSAPB1024_12_AEE003_L_sp
MSAPB1026_L_sp_Kabara
MSAPB1025_L_sp_Kabara
MSAPB999_12_ADM001_L_sp
MSAPB1018_12_ADZ002_L_sp_Vuloga
MSAPB1020_12_ADZ004_L_sp
MSAPB1017_12_ADZ001_L_sp
MSAPB1021_12_ADZ005_L_sp
MSAPB1019_12_ADZ003_L_sp
MSAPB1023_L_sp_Kabara
MSAPB1012_12_ADS001_L_sp
MSAPB1014_L_sp_Namuka
MSAPB1013_12_ADS002_L_sp
MSAPB1016_12_ADS005_L_sp
MSAPB1015_L_sp_Namuka
MSAPB359_11_ABR003_L_sp_Kadavu
MSAPB151_11_ACN008_L_sp_Vanua_Levu
MSAPB150_11_ACN007_L_sp
MSAPB146_11_ACN003_L_sp
MSAPB1175_12_AFM002_L_sp
MSAPB1176_12_AFM004_L_sp
MSAPB147_11_ACN004_L_sp
MSAPB464_11_ACK004_L_sp
MSAPB474_11_ACL004_L_sp_Vanua_Levu
MSAPB475_11_ACL005_L_sp_Vanua_Levu
MSAPB1173_L_sp_Taveuni
MSAPB1174_12_AFH003_L_sp
TH_1
TH_5
MH_2
MH_5
MSAPB345_11_ABO003_L_sp
yCMR14_F01
MSAPB282_11_ABC009_L_sp
17FJ26__reversed_
MSAPB021_11_AAB006_L_sp
MSAPB023_11_AAB008_L_sp
MSAPB343_11_ABO001_L_sp
17FJ186__reversed_
MSAPB288_11_ABD006_L_sp
MSAPB270_11_ABB002_L_sp
17FJ185__reversed_
17FJ217__reversed_
17FJ204__reversed_
MSAPB348_11_ABO006_L_sp_VitiLevu_HL
17FJ183__reversed_
MSAPB245_11_AAY001_L_sp
MSAPB241_11_AAX004_L_sp
MSAPB295_11_ABE007_L_sp_VitiLevu_HL
MSAPB243_11_AAX002_L_sp
MSAPB242_11_AAX001_L_sp
MSAPB260_11_AAZ010_L_sp
MSAPB347_11_ABO005_L_sp
MSAPB300_11_ABE012_L_sp
MSAPB011_11_AAA012_L_sp
MSAPB292_11_ABE004_L_sp
MSAPB293_11_ABE005_L_sp_VitiLevu_HL
MSAPB279_11_ABC006_L_sp
MSAPB258_11_AAZ008_L_sp_VitiLevu
MSAPB248_11_AAY004_L_sp
MSAPB246_11_AAY002_L_sp
MSAPB255_11_AAZ005_L_sp
MSAPB032_11_AAE001_L_sp_VitiLevu
yCMR167_A09
yCMR11_C01
MSAPB335_11_ABK003_L_sp
MSAPB274_11_ABB006_L_sp
MSAPB036_11_AAE005_L_sp
MSAPB041_11_AAI002_L_sp
MSAPB280_11_ABC007_L_sp
yCMR148_F06
17FJ220__reversed_
MSAPB273_11_ABB005_L_sp
MSAPB306_11_ABF006_L_sp
MSAPB003_11_AAA003_L_sp
MSAPB012_11_AAA013_L_sp
MSAPB313_11_ABH003_L_sp
MSAPB215_11_AAP006_L_sp
MSAPB259_11_AAZ009_L_sp
MSAPB289_11_ABD007_L_sp
MSAPB194_11_AAO007_L_sp
MSAPB235_11_AAW002_L_sp
MSAPB296_11_ABE008_L_sp
yCMR9_A01
MSAPB035_11_AAE004_L_sp_VitiLevu
MSAPB043_11_AAK006_L_sp
yCMR18_C02
MSAPB344_11_ABO002_L_sp
MSAPB013_11_AAB013_L_sp
MSAPB042_11_AAI003_L_sp
yCMR128_B04
MSAPB228_11_AAT001_L_sp
MSAPB073_11_AAO009_L_sp
MSAPB024_11_AAB001_L_sp
MSAPB019_11_AAB004_L_sp
MSAPB229_11_AAT002_L_sp
MSAPB299_11_ABE011_L_sp
MSAPB251_11_AAY007_L_sp
MSAPB016_11_AAB016_L_sp
MSAPB1034_L_sp_Matuku
MSAPB1033_12_AEN002_L_sp
MSAPB1036_12_AER002_L_sp
yCMR17_B02
MSAPB231_11_AAT004_L_sp
17FJ192__reversed_
MSAPB038_11_AAF002_L_sp
MSAPB068_11_AAM004_L_sp
17FJ89__reversed_
17FJ12__reversed_
MSAPB022_11_AAB007_L_sp
MSAPB067_11_AAM003_L_sp
yCMR7_H07
yCMR39_H04
MSAPB066_11_AAM002_L_sp
yCMR132_F04
MSAPB181_11_AAC012_L_sp
17FJ1__reversed_
yCMR65_B08
MSAPB093_11_AAO044_L_sp
MSAPB219_11_AAP010_L_sp
MSAPB094_11_AAO002_L_sp
MSAPB191_11_AAO004_L_sp_C
MSAPB092_11_AAO043_L_sp
MSAPB004_11_AAA004_L_sp
MSAPB220_11_AAR001_L_sp
MSAPB208_11_AAO037_L_sp
MSAPB077_11_AAO013_L_sp
MSAPB216_11_AAP007_L_sp
yCMR6_H10
MSAPB061_11_AAL008_L_sp
MSAPB001_11_AAK004_L_sp
MSAPB290_11_ABD008_L_sp
MSAPB063_11_AAL009_L_sp

2028

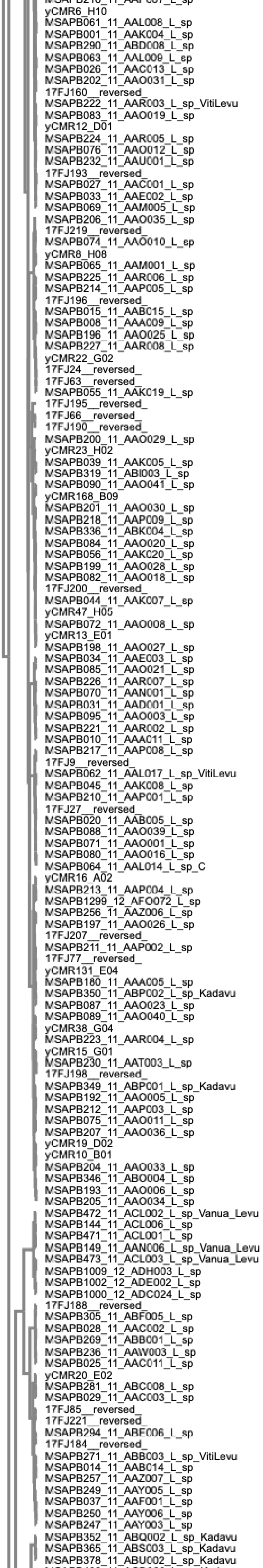

yCMR6_H10
MSAPB061_11_AAL008_L_sp
MSAPB001_11_AAK004_L_sp
MSAPB290_11_ABD008_L_sp
MSAPB063_11_AAL009_L_sp
MSAPB026_11_AAC013_L_sp
MSAPB202_11_AAO031_L_sp
17FJ160__reversed_
MSAPB222_11_AAR003_L_sp_VitiLevu
MSAPB083_11_AAO019_L_sp
yCMR12_D01
MSAPB224_11_AAR005_L_sp
MSAPB076_11_AAO012_L_sp
MSAPB232_11_AAU001_L_sp
17FJ193__reversed_
MSAPB027_11_AAC001_L_sp
MSAPB033_11_AAE002_L_sp
MSAPB069_11_AAM005_L_sp
MSAPB206_11_AAO035_L_sp
17FJ219__reversed_
MSAPB074_11_AAO010_L_sp
yCMR8_H08
MSAPB065_11_AAM001_L_sp
MSAPB225_11_AAR006_L_sp
MSAPB214_11_AAP005_L_sp
17FJ196__reversed_
MSAPB015_11_AAB015_L_sp
MSAPB008_11_AAA009_L_sp
MSAPB196_11_AAO025_L_sp
MSAPB227_11_AAR008_L_sp
yCMR22_G02
17FJ24__reversed_
17FJ63__reversed_
MSAPB055_11_AAK019_L_sp
17FJ195__reversed_
17FJ66__reversed_
17FJ190__reversed_
MSAPB200_11_AAO029_L_sp
yCMR23_H02
MSAPB039_11_AAK005_L_sp
MSAPB319_11_ABI003_L_sp
MSAPB090_11_AAO041_L_sp
yCMR168_B09
MSAPB201_11_AAO030_L_sp
MSAPB218_11_AAP009_L_sp
MSAPB336_11_ABK004_L_sp
MSAPB084_11_AAO020_L_sp
MSAPB056_11_AAK020_L_sp
MSAPB199_11_AAO028_L_sp
MSAPB082_11_AAO018_L_sp
17FJ200__reversed_
MSAPB044_11_AAK007_L_sp
yCMR47_H05
MSAPB072_11_AAO008_L_sp
yCMR13_E01
MSAPB198_11_AAO027_L_sp
MSAPB034_11_AAE003_L_sp
MSAPB085_11_AAO021_L_sp
MSAPB226_11_AAR007_L_sp
MSAPB070_11_AAN001_L_sp
MSAPB031_11_AAD001_L_sp
MSAPB095_11_AAO003_L_sp
MSAPB221_11_AAR002_L_sp
MSAPB010_11_AAA011_L_sp
MSAPB217_11_AAP008_L_sp
17FJ9__reversed_
MSAPB062_11_AAL017_L_sp_VitiLevu
MSAPB045_11_AAK008_L_sp
MSAPB210_11_AAP001_L_sp
17FJ27__reversed_
MSAPB020_11_AAB005_L_sp
MSAPB088_11_AAO039_L_sp
MSAPB071_11_AAO001_L_sp
MSAPB080_11_AAO016_L_sp
MSAPB064_11_AAL014_L_sp_C
yCMR16_A02
MSAPB213_11_AAP004_L_sp
MSAPB1299_12_AFO072_L_sp
MSAPB256_11_AAZ006_L_sp
MSAPB197_11_AAO026_L_sp
17FJ207__reversed_
MSAPB211_11_AAP002_L_sp
17FJ77__reversed_
yCMR131_E04
MSAPB180_11_AAA005_L_sp
MSAPB350_11_ABP002_L_sp_Kadavu
MSAPB087_11_AAO023_L_sp
MSAPB089_11_AAO040_L_sp
yCMR38_G04
MSAPB223_11_AAR004_L_sp
yCMR15_G01
MSAPB230_11_AAT003_L_sp
17FJ198__reversed_
MSAPB349_11_ABP001_L_sp_Kadavu
MSAPB192_11_AAO005_L_sp
MSAPB212_11_AAP003_L_sp
MSAPB075_11_AAO011_L_sp
MSAPB207_11_AAO036_L_sp
yCMR19_D02
yCMR10_B01
MSAPB204_11_AAO033_L_sp
MSAPB346_11_ABO004_L_sp
MSAPB193_11_AAO006_L_sp
MSAPB205_11_AAO034_L_sp
MSAPB472_11_ACL002_L_sp_Vanua_Levu
MSAPB144_11_ACL006_L_sp
MSAPB471_11_ACL001_L_sp
MSAPB149_11_AAN006_L_sp_Vanua_Levu
MSAPB473_11_ACL003_L_sp_Vanua_Levu
MSAPB1009_12_ADH003_L_sp
MSAPB1002_12_ADE002_L_sp
MSAPB1000_12_ADC024_L_sp
17FJ188__reversed_
MSAPB305_11_ABF005_L_sp
MSAPB028_11_AAC002_L_sp
MSAPB269_11_ABB001_L_sp
MSAPB236_11_AAW003_L_sp
MSAPB025_11_AAC011_L_sp
yCMR20_E02
MSAPB281_11_ABC008_L_sp
MSAPB029_11_AAC003_L_sp
17FJ85__reversed_
17FJ221__reversed_
MSAPB294_11_ABE006_L_sp
17FJ184__reversed_
MSAPB271_11_ABB003_L_sp_VitiLevu
MSAPB014_11_AAB014_L_sp
MSAPB257_11_AAZ007_L_sp
MSAPB249_11_AAY005_L_sp
MSAPB037_11_AAF001_L_sp
MSAPB250_11_AAY006_L_sp
MSAPB247_11_AAY003_L_sp
MSAPB352_11_ABQ002_L_sp_Kadavu
MSAPB365_11_ABS003_L_sp_Kadavu
MSAPB378_11_ABU002_L_sp_Kadavu

2029

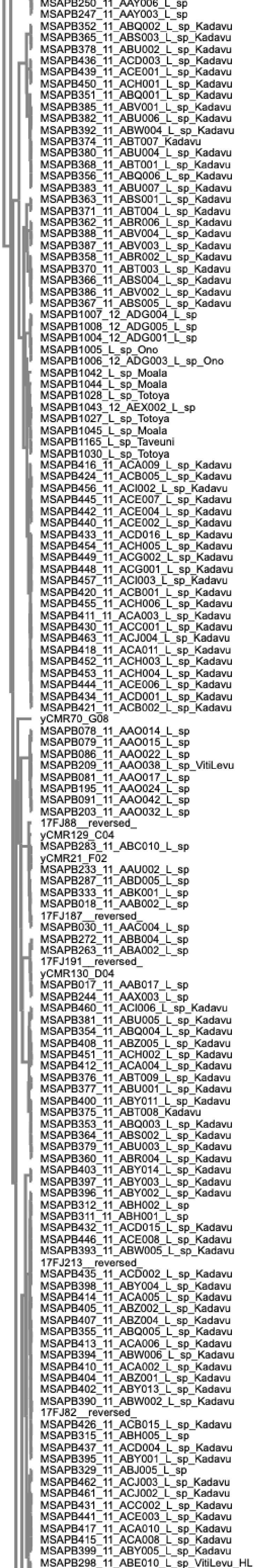
MSAPB250_11_AAY006_L_sp
MSAPB247_11_AAY003_L_sp
MSAPB352_11_ABQ002_L_sp_Kadavu
MSAPB365_11_ABS003_L_sp_Kadavu
MSAPB378_11_ABU002_L_sp_Kadavu
MSAPB436_11_ACD003_L_sp_Kadavu
MSAPB439_11_ACE001_L_sp_Kadavu
MSAPB450_11_ACH001_L_sp_Kadavu
MSAPB351_11_ABQ001_L_sp_Kadavu
MSAPB385_11_ABV001_L_sp_Kadavu
MSAPB382_11_ABU006_L_sp_Kadavu
MSAPB392_11_ABW004_L_sp_Kadavu
MSAPB374_11_ABT007_Kadavu
MSAPB380_11_ABU004_L_sp_Kadavu
MSAPB368_11_ABT001_L_sp_Kadavu
MSAPB356_11_ABQ006_L_sp_Kadavu
MSAPB383_11_ABU007_L_sp_Kadavu
MSAPB363_11_ABS001_L_sp_Kadavu
MSAPB371_11_ABT004_L_sp_Kadavu
MSAPB362_11_ABR006_L_sp_Kadavu
MSAPB388_11_ABV004_L_sp_Kadavu
MSAPB387_11_ABV003_L_sp_Kadavu
MSAPB358_11_ABR002_L_sp_Kadavu
MSAPB370_11_ABT003_L_sp_Kadavu
MSAPB366_11_ABS004_L_sp_Kadavu
MSAPB386_11_ABV002_L_sp_Kadavu
MSAPB367_11_ABS005_L_sp_Kadavu
MSAPB1007_12_ADG004_L_sp
MSAPB1008_12_ADG005_L_sp
MSAPB1004_12_ADG001_L_sp
MSAPB1005_L_sp_Ono
MSAPB1006_12_ADG003_L_sp_Ono
MSAPB1042_L_sp_Moala
MSAPB1044_L_sp_Moala
MSAPB1028_L_sp_Totoya
MSAPB1043_12_AEX002_L_sp
MSAPB1027_L_sp_Totoya
MSAPB1045_L_sp_Moala
MSAPB1165_L_sp_Taveuni
MSAPB1030_L_sp_Totoya
MSAPB416_11_ACA009_L_sp_Kadavu
MSAPB424_11_ACB005_L_sp_Kadavu
MSAPB456_11_ACI002_L_sp_Kadavu
MSAPB445_11_ACE007_L_sp_Kadavu
MSAPB442_11_ACE004_L_sp_Kadavu
MSAPB440_11_ACE002_L_sp_Kadavu
MSAPB433_11_ACD016_L_sp_Kadavu
MSAPB454_11_ACH005_L_sp_Kadavu
MSAPB449_11_ACG002_L_sp_Kadavu
MSAPB448_11_ACG001_L_sp_Kadavu
MSAPB457_11_ACI003_L_sp_Kadavu
MSAPB420_11_ACB001_L_sp_Kadavu
MSAPB455_11_ACH006_L_sp_Kadavu
MSAPB411_11_ACA003_L_sp_Kadavu
MSAPB430_11_ACC001_L_sp_Kadavu
MSAPB463_11_ACJ004_L_sp_Kadavu
MSAPB418_11_ACA011_L_sp_Kadavu
MSAPB452_11_ACH003_L_sp_Kadavu
MSAPB453_11_ACH004_L_sp_Kadavu
MSAPB444_11_ACE006_L_sp_Kadavu
MSAPB434_11_ACD001_L_sp_Kadavu
MSAPB421_11_ACB002_L_sp_Kadavu
yCMR70_G08
MSAPB078_11_AAO014_L_sp
MSAPB079_11_AAO015_L_sp
MSAPB086_11_AAO022_L_sp
MSAPB209_11_AAO038_L_sp_VitiLevu
MSAPB081_11_AAO017_L_sp
MSAPB195_11_AAO024_L_sp
MSAPB091_11_AAO042_L_sp
MSAPB203_11_AAO032_L_sp
17FJ88__reversed_
yCMR129_C04
MSAPB283_11_ABC010_L_sp
yCMR21_F02
MSAPB233_11_AAU002_L_sp
MSAPB287_11_ABD005_L_sp
MSAPB333_11_ABK001_L_sp
MSAPB018_11_AAB002_L_sp
17FJ187__reversed_
MSAPB030_11_AAC004_L_sp
MSAPB272_11_ABB004_L_sp
MSAPB263_11_ABA002_L_sp
17FJ191__reversed_
yCMR130_D04
MSAPB017_11_AAB017_L_sp
MSAPB244_11_AAX003_L_sp
MSAPB460_11_ACI006_L_sp_Kadavu
MSAPB381_11_ABU005_L_sp_Kadavu
MSAPB354_11_ABQ004_L_sp_Kadavu
MSAPB408_11_ABZ005_L_sp_Kadavu
MSAPB451_11_ACH002_L_sp_Kadavu
MSAPB412_11_ACA004_L_sp_Kadavu
MSAPB376_11_ABT009_L_sp_Kadavu
MSAPB377_11_ABU001_L_sp_Kadavu
MSAPB400_11_ABY011_L_sp_Kadavu
MSAPB375_11_ABT008_Kadavu
MSAPB353_11_ABQ003_L_sp_Kadavu
MSAPB364_11_ABS002_L_sp_Kadavu
MSAPB379_11_ABU003_L_sp_Kadavu
MSAPB360_11_ABR004_L_sp_Kadavu
MSAPB403_11_ABY014_L_sp_Kadavu
MSAPB397_11_ABY003_L_sp_Kadavu
MSAPB396_11_ABY002_L_sp_Kadavu
MSAPB312_11_ABH002_L_sp
MSAPB311_11_ABH001_L_sp
MSAPB432_11_ACD015_L_sp_Kadavu
MSAPB446_11_ACE008_L_sp_Kadavu
MSAPB393_11_ABW005_L_sp_Kadavu
17FJ213__reversed_
MSAPB435_11_ACD002_L_sp_Kadavu
MSAPB398_11_ABY004_L_sp_Kadavu
MSAPB414_11_ACA005_L_sp_Kadavu
MSAPB405_11_ABZ002_L_sp_Kadavu
MSAPB407_11_ABZ004_L_sp_Kadavu
MSAPB355_11_ABQ005_L_sp_Kadavu
MSAPB413_11_ACA006_L_sp_Kadavu
MSAPB394_11_ABW006_L_sp_Kadavu
MSAPB410_11_ACA002_L_sp_Kadavu
MSAPB404_11_ABZ001_L_sp_Kadavu
MSAPB402_11_ABY013_L_sp_Kadavu
MSAPB390_11_ABW002_L_sp_Kadavu
17FJ82__reversed_
MSAPB426_11_ACB015_L_sp_Kadavu
MSAPB315_11_ABH005_L_sp
MSAPB437_11_ACD004_L_sp_Kadavu
MSAPB395_11_ABY001_L_sp_Kadavu
MSAPB329_11_ABJ005_L_sp
MSAPB462_11_ACJ003_L_sp_Kadavu
MSAPB461_11_ACJ002_L_sp_Kadavu
MSAPB431_11_ACC002_L_sp_Kadavu
MSAPB441_11_ACE003_L_sp_Kadavu
MSAPB417_11_ACA010_L_sp_Kadavu
MSAPB415_11_ACA008_L_sp_Kadavu
MSAPB399_11_ABY005_L_sp_Kadavu
MSAPB298_11_ABE010_L_sp_VitiLevu_HL

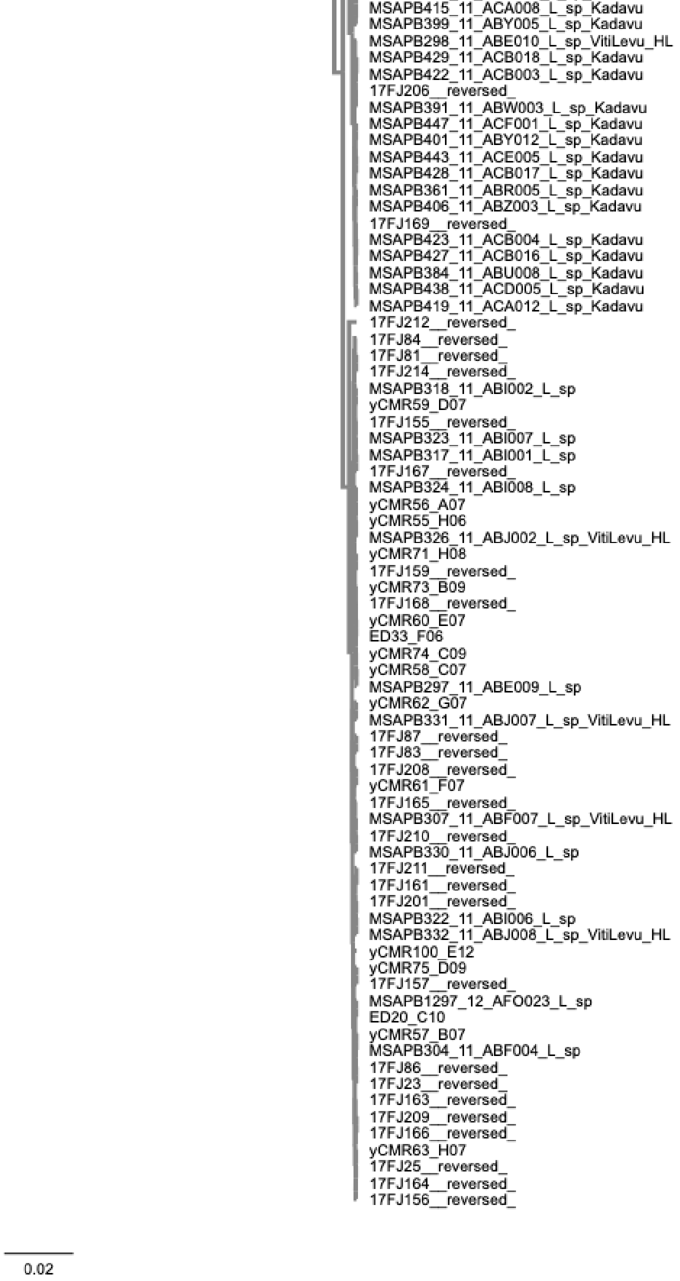

Figure S1: (a) maximum credibility tree of all sequenced Fijian *Homalictus* specimens where branch colour represents (b) geographic location. Numbers show posterior probability at nodes.

Chapter 2: Radiation of tropical island bees and the role of phylogenetic niche conservatism as an important driver of biodiversity

James B. Dorey[a,1], Scott V. C. Groom[b], Elisha H. Freedman[a], Cale S. Matthews[a], Olivia K. Davies[a], Ella J. Deans[a], Celina Rebola[a], Mark I. Stevens[c,d], Michael S. Y. Lee[a,c], and Michael P. Schwarz[a]

[a]*College of Science and Engineering, Flinders University, GPO Box 2100, SA, 5001, Adelaide, Australia*
[b]*School of Agriculture, Food and Wine, The University of Adelaide, Waite Campus, Urrbrae, SA, 5064, Adelaide, Australia*
[c]*Biological and Earth Sciences, South Australian Museum, GPO Box 234, SA, 5001, Adelaide, Australia*
[d]*School of Pharmacy and Medical Sciences, University of South Australia, SA, 5001, Adelaide, Australia*
[1]*To whom correspondence may be addressed. Email: jbdorey@me.com*

Published in Proceedings B (https://doi.org/10.1098/rspb.2020.0045).

Abstract

Island biogeography explores how biodiversity in island ecosystems arises and is maintained. The topographical complexity of islands can drive speciation by providing a diversity of niches that promote adaptive radiation and speciation. However, recent studies have argued that phylogenetic niche conservatism, combined with topographical complexity and climate change, could also promote speciation if populations are episodically fragmented into climate refugia that enable allopatric speciation. Adaptive radiation and phylogenetic niche conservatism therefore both predict that topographical complexity should encourage speciation, but they differ strongly in their inferred mechanisms. Using genetic (mitochondrial DNA — mtDNA — and single-nucleotide polymorphism — SNP) and morphological data, we show high species diversity (22 species) in an endemic clade of Fijian *Homalictus* bees, with most species restricted to highlands and frequently exhibiting narrow geographical ranges. Our results indicate that elevational niches have been conserved across most speciation events, contradicting expectations from an adaptive radiation model but concordant with phylogenetic niche conservatism. Climate cycles, topographical complexity, and niche conservatism could interact to shape island biodiversity. We argue that phylogenetic niche conservatism is an important driver of tropical island bee biodiversity but that this phylogenetic inertia also leads to major extinction risks for tropical ectotherms under future warming climates.

Keywords

Evolution, climate change, allopatric, tropical ectotherms, thermal specialist, adaptive radiation

Introduction

At its heart, evolutionary biology attempts to explain how new species arise and evolve to occupy a myriad of niches. A predominant paradigm in evolution is that species arise from adaptive radiation into new niche spaces, with gene flow between the new and ancestral populations subsequently inhibited, eventually leading to speciation [78-81]. Phylogenetic niche conservatism provides an alternative, whereby the inability of a lineage to adapt to new or changing environments promotes speciation when populations become isolated [82-84]. This model is particularly relevant to lineages with narrow climatic niches, especially those that are spatially fragmented across existing landscapes or constrained to isolated refugia during climate extremes, promoting allopatric speciation [84].

Distinct shifts in climate since the beginning of the Quaternary enable the relative roles of adaptive radiation versus phylogenetic niche conservatism to be explored as instigators of speciation. A key issue in assessing the role of phylogenetic niche conservatism for climate-driven speciation is that continental species may alter their latitudinal distributions in response to climate [83], rather than only elevation. Depending on continental geography, such latitudinal shifts can lead to population fragmentation or range expansion [85]. However, terrestrial biota of isolated islands and archipelagos have limited opportunities for latitudinal shifts, restricting responses to shifts in elevation [86].

Island biogeography therefore provides an opportunity to compare adaptive radiation and phylogenetic niche conservatism as drivers of speciation, in a system where changes in elevational range are not confounded by other (e.g., latitudinal) shifts. The ‘taxon cycle’ provided an initial paradigm for how speciation within islands could be explained by adaptive radiation. Using Fijian ants as a model system, Wilson [87] argued that colonizing ant species were more likely suited to coastal habitats that reflect their origin, with subsequent speciation driven by niche expansion into inland and highland ecosystems. Early data and some subsequent ant studies from South Pacific islands support this adaptive radiation model [87,88].

However, no compelling empirical studies have indicated that speciation in island taxa has been driven by niche conservatism and past climate cycles, forcing lineages into fragmented elevational refugia (though sea level changes have been implicated [89]). Any such studies would require islands with substantial variation in topography [19]. Topographic complexity has been associated with *in situ* speciation in island biogeography models. However, this has often been attributed to adaptive responses to an increased number of possible microclimatic niches rather than effects of climate cycles on lineages with narrow thermal tolerances [88,90]. Discriminating between these adaptive and non-adaptive mechanisms is possible empirically if phylogenetic histories are sufficiently resolved.

There are also theoretical reasons to expect that any non-adaptive responses to climate change might be larger in the tropics compared to temperate or boreal regions. Tropical ectotherms are expected to be less tolerant of changing climates because they have evolved in environments that experience much lower thermal variation [91,92]. For example, tropical *Drosophila* species demonstrate lower genetic variation in cold and desiccation traits than do temperate species [93]. More broadly, ‘Rapoport’s Rule’ is the observation that species tend to have more narrow latitudinal ranges when their overall distribution is closer to the equator, interpreted as indicating that lower exposure to climate variation selects for narrower climatic tolerances [93,94].

One way to explore phylogenetic niche conservatism is to infer how traits have evolved over phylogenetic trees. Retention of ancestral climatic niches across speciation events, when alternative niches are presumably available, would support a phylogenetic niche conservatism model. On the other hand, gradual extensions of niche range by daughter species would suggest adaptive radiation. Bayesian phylogenetic methods allow ancestral traits and their rates of evolution to be inferred [95,96] using constant-rate and relaxed Brownian motion (‘random walk’) models of evolutionary change [97]. For example, it is possible to examine whether trait changes are concentrated at the base of a tree, which would suggest early adaptive radiation. When applied to climatic niches, these issues are important for understanding how past climates have influenced biodiversity and when asking how well species will adapt, or not, to changing climates.

Fiji is a tropical archipelago in the Pacific Ocean, consisting of several hundred islands of varying ages and sizes. Three of these islands first emerged during the Oligocene and exhibit substantial ranges in elevation up to 1,324 m. Endemic bee species of the genus *Homalictus* (Halictidae) arose from a single dispersal event into Fiji during the Quaternary [32]. *Homalictus* species are generally communal ground-nesting species and often generalist pollinators, yet little has been published on their habits [40]. Most Fijian *Homalictus* species forage on both weedy and native plants, indicating polylectic diets, while *H. fijiensis* is a super-generalist pollinator [98]. Until recently only four Fijian species were known, but genetic and morphological studies indicate a much more speciose clade (25), with many species only recorded from high elevations [99]. Here we combine molecular phylogenetic analyses and elevation distribution data, which reveal at least 22 candidate species (independent lineages) and demonstrate how elevational niches have evolved since the Quaternary colonization of Fiji. We further highlight that such phylogenetic signals could indicate climate-related extinction risks.

Results

Data from COI sequences (630 bp) for 764 specimens, and consilience with morphology and single nucleotide polymorphism (SNP) data (8,381 filtered SNP loci) for 94 specimens indicate the existence of 22 *Homalictus* species in our samples (Figs 1 and 2). The maximum credibility all-sample tree from *BEAST* [60] for COI indicates that more distal nodes tend to have higher posterior probability support than more basal nodes (Fig. S1). Some poorly-resolved clades have slightly different relationships across analyses, due largely to stochastic sampling of tree topologies. Complete concordance between currently described species [99], the highly supported SNP-based phylogenetic tree for five species where SNP data were available, and the COI-based all-sample tree for all 22 species in our study suggests that COI sequences are able to recover species trees (Fig. 2; Fig. S3 and supplementary results).

Eighteen of 22 Fijian bee species had a median elevation of over 800 m asl and only four species had median elevations from below 800 m asl (Fig. 2b). Most species have very narrow elevational bands with only four species having an elevational range greater than 500 m (*H. fijiensis*, *H. hadrander*, *H. groomi*, and *H.* sp. O) and these form a monophyletic group (Fig. 2a). Fourteen species were only recovered from single mountain peaks (Fig. 2).

Multiple regression analyses indicate that sampling effort (measured as the number of DNA sequences obtained for each elevational band) had a relatively small and only marginally significant effect on the number of species detected ($\beta = 0.536$, $t = 3.213$, $P = 0.049$). Elevation had a much larger and clearly significant impact ($\beta = 0.925$, $t = 5.540$, $P = 0.012$). We can therefore conclude that species' distributions are strongly tied to elevation, and that this is not solely an artefact of differing sampling efforts across different elevations.

To test for mode of evolution, elevational shifts were optimized on a species-level phylogeny using *BayesTraits* version 3.0 [96] under a range of models (e.g., early burst or punctuated changes). We tested if changes in elevation were phylogenetically conserved (λ), associated with speciation events (κ), or relatively constant through time (δ), as indicated respectively by tree transformation parameters. When $\lambda = 0$ it indicates that a trait is evolving among species completely independently of phylogeny, while $\lambda = 1$ indicates that trait evolution is entirely explained by phylogeny. Our λ estimate was 0.37 (95% highest posterior density (HPD) = 7.79×10^{-5}, 0.86) for median elevation and 0.59 (95% HPD = 0.14, 0.99) for minimum elevation (Table 1; Fig. S2), indicating moderate to strong trait correlations with phylogenetic history. Values of κ stretch or compress individual phylogenetic branch lengths: when $\kappa = 0$ trait evolution is independent of branch length (change occurs at nodes suggesting punctuated evolution), $\kappa > 0$ indicates trait change is associated with branch length (trait change occurs along branches, rather than concentrated at speciation nodes). Our κ estimate was 1.21 (95% HPD = 0.09, 2.99) for median elevation and 0.98 (95% HPD = $3.37\text{x}10^{-4}$, 1.91) for minimum elevation (Table 1; Fig. S2), indicating that elevational changes are strongly associated with branch lengths, and not concordant with a punctuated model of evolution, where elevational changes should instead be associated with speciation events. Delta scales the length of basal vs terminal branches: $\delta < 1$ stretches basal branches and $\delta > 1$ stretches terminal branches (i.e., the rate of trait evolution varies with distance from the phylogenetic root). Our δ estimate was 2.18 (95% HPD = 1.17, 3.00) for median elevation and 1.95 (95% HPD = 0.489, 2.99) for minimum elevation (Table 1; Fig. S2) providing no evidence for an early-burst model of change, but is instead consistent with approximately constant rates across time. The inferred median and minimum elevations for the most recent common ancestor of Fijian *Homalictus* were 828 m asl (95% HPD = 636, 1020) and 687 m asl (95% HPD = 451, 947), respectively (Table 1). The strong phylogenetic signal, strong correlation between change and branch length, and lack of early burst changes all indicate that a Brownian motion model is appropriate.

To trace the evolution of elevational range across the full phylogeny, and incorporate phylogenetic uncertainty in our inferences of niche evolution, we traced elevation across all post-burnin trees sampled in the COI all-sample analysis (see above), using *BEAST* 1.10. The actual elevation of each sequenced specimen was used, and modelled using standard and relaxed Brownian motion models [100]; both gave very similar results but the latter fitted the data better (Bayes Factor score >1000) and is presented in Fig. 1. Other deviations from Brownian motion — such as punctuated and early burst evolution — were not indicated (see *BayesTraits* above). From our *BEAST* analysis, the inferred ancestral elevation of the most recent common ancestor of Fijian *Homalictus* was 896 m asl (Fig. 1), highly consistent with the *BayesTraits* results above. Most (17-18) speciation events have involved no major elevational transitions, and there were only 3-4 speciation events that involved transitions from highland to lowland habitats in one of two daughter species (*H. fijiensis, H. taveuni, H*. sp. I, and O; the clade including *H. fijiensis, H. groomi,* and *H*. sp. O could represent one or two elevational transitions) (Fig. 2).

Discussion

The COI, SNP, and morphological data considered together indicate that the 22 major clades we have identified here comprise valid biological species (Fig. S3). Our phylogeny of 22 species entails 21 speciation events, with branch transformation parameters λ, κ, and δ providing support for a niche conservation model of speciation over adaptive radiation (Table 1; Fig. S2). The low frequency of elevational shifts (three or four elevational transitions from 21 speciation events) suggests that adaptive radiation, at least in terms of climatic niche shifts, has not been a major driver or correlate of speciation (Fig. 2). The clade containing *H. fijiensis*, *H. hadrander*, *H. groomi*, and *H.* sp. O likely has a more eurythermic common ancestor compared to its sister clade (*H*. sp. N) due to its wider elevational range. Eurythermy could be an important trait allowing lowland insular species to persist during cooler glacial periods. Trait reconstructions indicate that the common ancestor of *Homalictus* in Fiji occupied an elevation that would roughly correspond to between 800 and 900 m asl in today's climate (Fig. 1).

Extensive anthropogenic habitat destruction in many lowland regions since human habitation of Fiji ~3.5 kya [101] is unlikely to have caused reductions in lowland *Homalictus* species diversity for several reasons. Firstly, lowland rainforest (under 600 m asl) makes up 78% of all natural forests, with upland (601-800 m asl) and montane rainforest (over 801 m asl) accounting for only 8% and 4%, respectively [102]. Secondly, a generalist diet in Fijian *Homalictus* enables the use of introduced and weedy plants that may have been brought to Fiji by the earliest human settlers and up until current times [98]. Finally, nesting preference for bare or sparsely-vegetated ground indicates likely resilience of these bees to habitat clearing.

Climate conditions associated with specific elevations in Fiji today are likely to have been different over past climate cycles [19,103]. Groom, *et al.* [32] estimated a crown age for Fijian *Homalictus* in the mid-to-late Pleistocene, but that may well be an underestimate since those analyses did not incorporate many of the recently discovered species. Regardless, *Homalictus* lineages in Fiji will have experienced multiple glacial-interglacial cycles such that thermal niches associated with highlands in the current climate are likely to have episodically extended to lower elevations in the past [104-106]. However, past climates would also have included warming maxima similar to the current time [104-106]. Narrow thermal tolerances and poor adaptive capabilities of some tropical ectotherms [92,94], the topographical complexity of Fiji, and Quaternary climate cycles could act synergistically. These synergies could produce repeated cycles of population admixture and isolation as species moved into lower elevations during glacial maxima, and retreated to highland refugia during interglacial periods, such as the present [82]. In this sense, phylogenetic niche conservatism combined with climate cycles could have driven repeated cycles of allopatry and speciation [82].

It is possible that speciation by both niche conservatism and by adaptive radiation occur concurrently and could act synergistically. Isolation initiated by climatic niche conservatism could subsequently be promoted by differential adaptations to other local conditions [107] in addition to genetic drift. Despite such potential interactions, our results clearly indicate widespread phylogenetic niche conservatism for elevational niches. This contrasts with studies on Fijian ants where initial colonization by lowland, coastal-adapted species was followed by gradual adaptive expansion into higher inland elevations [87,88,108]. Instead, our results for the Fijian bees support a very different model where ancestral niches are retained and speciation arises by geographical fragmentation of this niche space, promoting allopatry.

The same climatic factors that could drive tropical ectotherm speciation [82,83,107] could also determine extinction risks with globally changing climates. For example, a narrow climatic tolerance means that tropical ectotherms are expected to be particularly vulnerable to changing climates [92,109,110]. Many lineages have altered their distributions in the direction locally expected with climate change and 41% of species that have been examined have responded to recent mild (0.6˚C) global warming [111]. Mountaintop species are predicted to be particularly vulnerable to climate change because of their limited ability to disperse in response to warming climates [112]. There is a global trend of declining distributions amongst montane species as their lower elevational extents shift towards mountain peaks [113]. Several studies indicate that some species are already nearing their elevational limits [99,114-116].

Tropical ectotherm taxa that have demonstrated strong elevational tracking with past climate cycles are at risk from globally warming climates as elevational shifts in distribution are associated with a reduction or loss of viable habitat [112,115,117]. Local extinctions of some highland taxa due to elevational tracking of climate have already been recorded [112,115,117], and one Fijian *Homalictus* species (*H. achrostus*) is suspected to be verging on extinction or be functionally extinct [99]. The generality of niche conservatism-driven speciation across various taxonomic groups in the tropics is an important and pressing area of future research. While islands provide a simplified system to examine these patterns, similar patterns might be found in montane continental systems where niche conservatism might result in speciation as lineages track climate latitude and altitude simultaneously. Such investigations will have important implications for our understanding of how biodiversity arises and will inform us about broad-scale climate extinction risks.

Our data and the arguments above, combined with narrow climatic envelopes of many tropical ectotherms [92,118,119], shows the potential importance of the niche conservatism model of speciation, as a contrast to the adaptive radiation model. Indeed, if Darwin had studied these Fijian bees instead of Galapagos finches, he might have come to rather different conclusions about the origin of species. Our results advance fundamental questions of island biogeography [120], and have three important implications for understanding the role of climate cycles in island and tropical biodiversity. First, they support the notion that speciation events resulting in the rich biodiversity of tropical ecosystems might be driven, at least in part, by niche conservatism as well as adaptive radiation. Second, they suggest that topographical complexity and climate cycles might strongly interact to shape island biodiversity. Finally, our inferred elevational niche conservatism suggests widespread yet clade-specific extinction risks for tropical invertebrates for warmer and more variable future climates. This indicates a need to explore evolutionary limits to thermal adaptation when assessing susceptibility of tropical insular ecosystems to future climates.

Materials and Methods

Sample locations and collection methods

Collections throughout Fiji were made between 2010 and 2017 from multiple localities including the main islands of Viti Levu, Vanua Levu, Kadavu, and Taveuni, as well as multiple small islands in the Lau group (Fig. S5). Sampling of specimens at each location was not biased towards particular species because, for these very small bees, only *H. achrostus* could be easily identified in the field due to its distinctive coloration; all other species required microscopy or DNA sequencing for species identification.

Samples were collected from 3 m to 1,324 m asl (highest elevation of Fiji) by sweep netting both native and introduced plants, and from nesting aggregations along roadsides. For each collection site, latitude, longitude, and elevation were recorded using a Garmin 550 (Garmin Ltd., USA); latitude and longitude were then checked against satellite images (Google Earth) to confirm accuracy. Once collected, bees were immediately transferred into vials containing 98% ethanol. Vials were kept cool at ~5˚C and ethanol was replaced within a week of collection to reduce DNA degradation.

Maps of Fiji were produced in *ArcMap* [66] and a digital elevation model (DEM) of the archipelago was provided by Fiji Lands Information System (FLIS).

Sampling bias and elevational species richness

It was not possible to evenly sample bees across all geographical and elevational regions of Fiji because physical access to many regions was restricted by terrain and lack of roads. Access constraints could therefore affect sampling effort and this, in turn, could influence ability to recover true species richness in different elevational bands. Here, we quantize sampling effort as the number of DNA sequences obtained for different elevations, categorized into 200 m asl bands. Because specimens were only identified to species levels after DNA sequencing, the number of obtained sequences represents sampling effort. We examined whether this sampling effort may have influenced our estimates of species richness using multiple regression, where the number of detected species was the dependent variable and the number of sequences (sampling effort) and elevational band were the independent variables. The relative importance of sampling effort and elevation band for detected species richness can then be explored by regression β values and their statistical significance.

DNA extraction and sequencing

Tissue samples for DNA extraction were obtained by removing a single hind leg from each of the 764 specimens. For all samples obtained after 2014, DNA extraction and PCR amplification was completed at the South Australian Regional Facility for Molecular Ecology and Evolution (SARFMEE). DNA extraction and PCR amplification of COI prior to the 2014 samples was completed at the Canadian Centre for DNA Barcoding (CCDB) at the Biodiversity Institute of Ontario [32] and amplification used the universal primer pair LepF1 and LepR2 [32,50]. Extractions at SARFMEE followed protocols described by [52] with the subsequent DNA eluted into 75 µL of TLE buffer. PCR amplification of the 710 bp fragment of the DNA (COI) was completed using the primers LCO1490 (forward) and HCO2198 (reverse). The 25 µL PCR reactions comprised the following reagents: Sterile H2O (15.9 µL), MRT buffer (5 µL), 1 µL (5 µM) of LCO1490, 1 µL (5 µM) of HCO2198, Immolase Taq (0.1 µL), and DNA from specimen (2 µL). The thermocycling regime comprised of one cycle at 94˚C for 10 minutes, then five cycles at 94˚C for 60 seconds, 46˚C for 90 seconds, 72˚C for 75 seconds, followed by 35 cycles at 94˚C for 60 seconds, 51˚C for 90 seconds, 72˚C for 75 seconds, followed by 72˚C for 10 minutes, and then 25˚C for 2 minutes.

Sequences were checked against the NCBI BLAST database to screen for non-target DNA. Forward and reverse sequences were aligned and chromatograms visually checked before creating final consensus sequences in *Geneious* version 10.2.2 [53]. Initial alignments were trimmed to 630 bp to avoid any problems associated with missing data.

Phylogenetic, elevational and species analyses

The full COI alignment consisted of 630 bp for 764 specimens. *PartitionFinder* version 2 was employed using BIC and a greedy algorithm to find the best partition schemes and DNA substitution models from widely-used (i.e., *MrBayes*) models [121-123]. The first and second codon positions were combined into a single partition with an HKY+I substitution model. A GTR substitution model was applied to third codon position. The *BEAST* file and parameters for phylogenetic analyses were set using *BEAUti* version 1.8.4 [56]. Because of the small numbers of substitutions on each branch, a strict clock was used to avoid overparameterization. To infer changes in elevation across the tree we included elevation as a continuous trait using a strict or relaxed Brownian motion model (confirmed as adequate given our λ, κ, and δ estimates; Table 1). Phylogenetic analyses were implemented in *BEAST* version 1.10 [60] with 200 million iterations sampled every 50,000th iteration. Resulting log files were analyzed in *Tracer* version 1.6 [61] and a burnin of $2.5\text{x}10^7$ iterations was employed, which was always after stationarity had been achieved. Maximum clade credibility trees and posterior probability support values were obtained using *TreeAnnotator* Version 1.8.4 [56]. Each run was performed four times for each analysis to ensure consistent results and stationarity. Post-burnin log and tree files for each run were then combined using *LogCombiner* version 2.5.2 [124] for the final analysis.

To infer the evolutionary mode and phylogenetic signal in the elevation data, we used *BayesTraits* version 3.0 [96]. The tree-transformation models employed in *BayesTraits* assume that each terminal taxon is a species, hence we repeated the *BEAST* analysis using only one DNA sample from each species, and elevation data as either the median or minimum for all samples of that species. The (reduced) *BEAST* analysis used 100 million iterations, sampling every 50,000th iteration; stationarity and burnin was checked as above. The resulting consensus tree was run in *BayesTraits* using the median and the minimum elevational value for each terminal taxon to estimate λ (degree of phylogenetic signal), κ (degree of punctuated evolution), and δ (degree of early burst, adaptive radiation). The model of best fit for each estimate was chosen using Akaike's Information Criterion with 100 bootstrap replicates in *Tracer* [125]. Analyses in *BayesTraits* used 500 million iterations sampled every 50,000th iteration. Each run was performed four times for each model at each elevation to ensure consistent results. *BayesTraits* log files for each run were then combined using *LogCombiner* version 2.5.2 [124] for the final analysis.

We attempted to co-estimate phylogeny and elevational niche evolution, but these analyses repeatedly failed to converge. Thus, to infer elevational changes across the full phylogeny, we mapped elevation across all post-burnin trees sampled in the full COI analysis. This was done using *BEAST*, under a standard rate-constant Brownian motion model, as well as a rate-variable Brownian motion model, which assumes rates vary across branches according to an uncorrelated relaxed clock [100]. Stationarity and burnin were confirmed as above. Both models gave very similar ancestral state reconstructions, but the latter model fitted better and is shown in Fig. 1.

Genetic analyses of bee clades were explored using *Arlequin* version 3.11 [126]. For each species with multiple haplotypes and a sample size of more than 10 specimens we calculated haplotype diversity (h) and pairwise F_{ST} values.

SNP quality filtering and analyses

The thorax and front legs were taken from 19 individuals from *H. fijiensis, H. tuiwawae, H. ostridorsum, H. groomi,* and *H.* sp. *S,* respectively. To perform Restriction-site Associated DNA sequencing (RAD seq), the solid state method Diversity Arrays Technology (DArT) was used [127]. The restriction enzymes used were a combination of PstI and HpaII enzymes. Only female specimens were used to avoid the impact of male haploidy on SNP diversity. Post filtering, missing data was capped at 1.16%.

A total of 62,426 SNP loci were called across all species. Using the *R* package *DArTR* version 1.0.5 low quality loci were removed at a threshold of 0.85% removing loci with 15% or more missing values [128], leading to retention of 8,381 SNP loci. The neighbour joining tree (Fig. S4) was made using the *R* package *ape* with the ‘nj’ function [129].

Once SNP data were filtered they were subjected to a discriminant analysis of principal components (DAPC) using the DAPC procedure [130] in the *Adegenet* package in R [131]. The DAPC was used to identify the number of genetic clusters within the SNP data and the relationship between these clusters. DAPC uses synthetic variables constructed as linear combinations from the original alleles, showing the largest between group variations and lowest within group variation. Discriminant analysis also provides membership probabilities of each individual to the different clusters. Our DAPC followed protocols outlined by Jombart [130].

Morphological data

To determine if major mitochondrial clades corresponded to biological species we examined multiple morphological traits. Internal male genitalic traits have been used as major species diagnostic characters for *Homalictus* species in the southwest Pacific [65,99] and these were examined for 12 species in this study where male specimens were available, along with external female morphology [99]. For the remaining species, only female external morphology was compared with COI and SNP phylogenies.

Supporting information

Acknowledgments

We would like to thank Marika Tuiwawa and Alivereti Naikatini, for their invaluable assistance with Fijian field logistics, as well as all the students from Flinders University who assisted in field work. We also thank Alejandro Velasco-Castrillón for his support with lab work and DNA sequencing. Final thanks goes to the Fiji Lands Information System (FLIS) for providing the digital elevation model that was used to produce our maps.

Author Contributions

JBD, MIS, and MPS conceived the study and developed the experimental design; JBD, EHF, CSM, SVCG, EJD, CR, OKD, MIS, and MPS performed the fieldwork; JBD, CR, and OKD edited sequence data and elevation and geographical records; JBD, MSYL, EHF, and CSM carried out the analyses with advice from MIS and MPS; JBD wrote the manuscript and prepared the figures, with editorial advice from SVCG, OKD, MIS, MSYL, and MPS; all authors gave final approval for publication.

Funding

Project and personal funding was provided by the Australian and Pacific Science Foundation, New Colombo Plan program, Flinders University, The South Australian Museum, and Playford Trust Scholarships to JBD and OKD.

Competing interests

The authors declare no competing interests.

Data accessibility

Collection and GenBank accession data for *Homalictus* specimens are provided in electronic supplementary, additional data table S2. The alignments, SNP data, *BEAST* and *BayesTraits* executables are deposited in Dryad and can be accessed at https://doi.org/10.5061/dryad.80gb5mknf.

Tables

Table 1. Results from *BayesTraits* analyses estimating different parameters for both median or minimum elevation for each clade. The parameters estimated are lambda (λ), kappa (κ), delta (δ), and alpha (α), where λ, κ, and δ represent standard estimates of character change across a phylogeny and α is the inferred ancestral elevational state at the root node. Values chosen to be the best fit by Akaike's information criterion with 100 bootstrap replicates are shown in bold.

Elevation	**Parameter**	**λ (95% HPD lower, upper)**	**K (95% HPD lower, upper)**	**∂ (95% HPD lower, upper)**	**α (95% HPD lower, upper)**
Median	λ	**0.37 (7.79x10^{-5}, 0.86)**			852 (546, 1143)
	K		1.15 (0.06, 2.19)		835 (383, 1276)
	∂			**2.18 (1.17, 3.00)**	832 (709, 1044)
	λ and K	0.36 (4.10x10^{-7}, 0.85)	**1.21 (0.09, 2.99)**		852 (569, 1138)
	λ and ∂	0.40 (3.18x10^{-5}, 0.90)		1.84 (0.52, 3.00)	**828 (636, 1020)**
Minimum	λ	**0.59 (0.14, 0.99)**			710 (326, 1080)
	K		0.89 (1.69x10^{-5}, 1.80)		713 (254, 1184)
	∂			**1.95 (0.89, 2.99)**	675 (491, 883)
	λ and K	0.59 (0.13, 1.00)	**0.98 (3.37 x10^{-4}, 1.91)**		707 (350, 1076)
	λ and ∂	0.59 (0.12, 1.00)		1.70 (0.47, 2.97)	**687 (451, 947)**

Figure captions

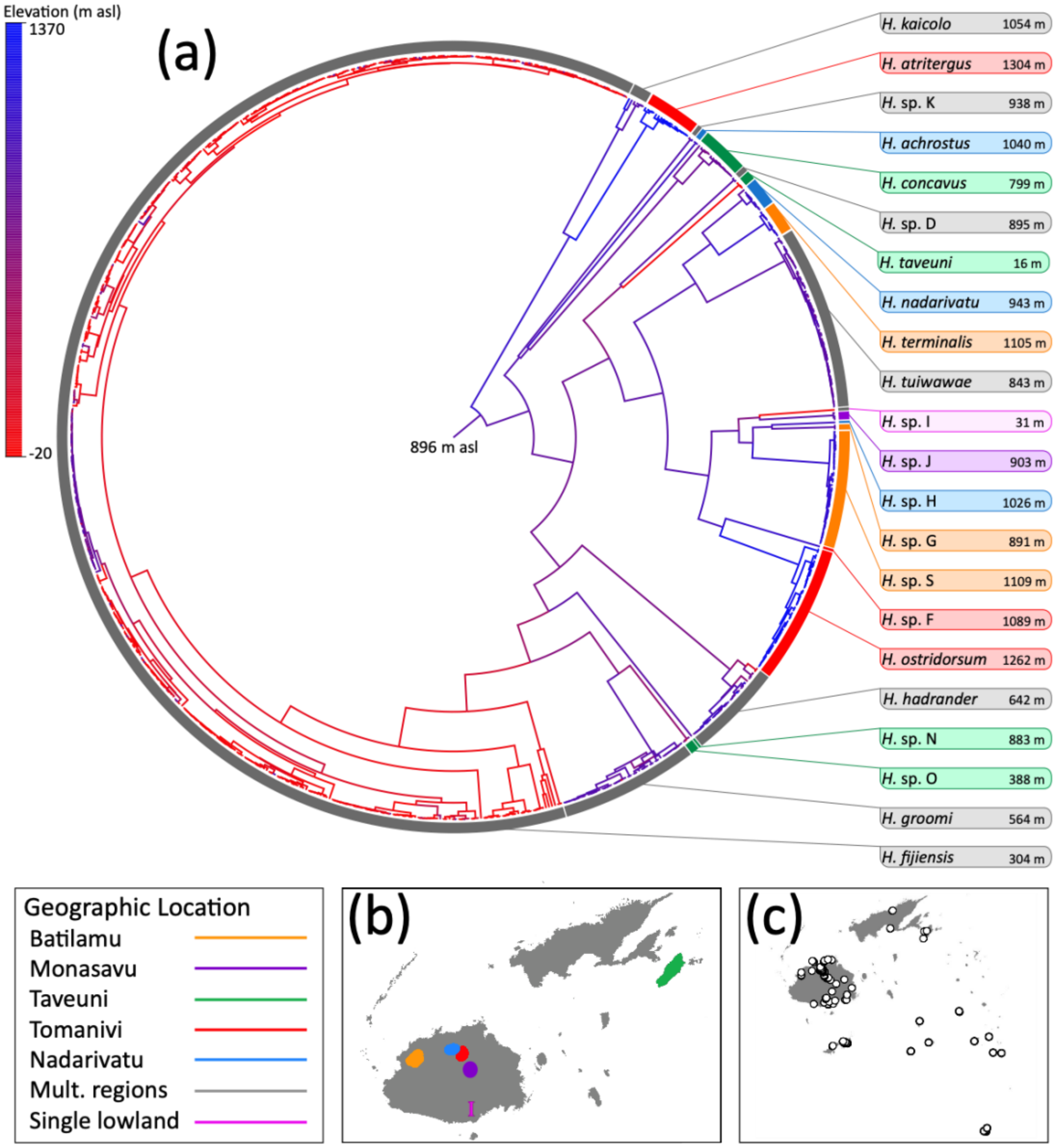

Figure 1. (a) Maximum credibility tree from Bayesian phylogenetic analysis of Fijian *Homalictus* based on analysis of the COI gene showing inferred elevation along branches (meters above sea level), where blue branches are higher elevation than red branches. Species are indicated in boxes, where colour refers to geographic location. (b) Map insets show coloured geographic locations of clades, with an “I” to show the location of *Homalictus* sp. I and (c) all the *Homalictus* collection sites across the Fijian archipelago.

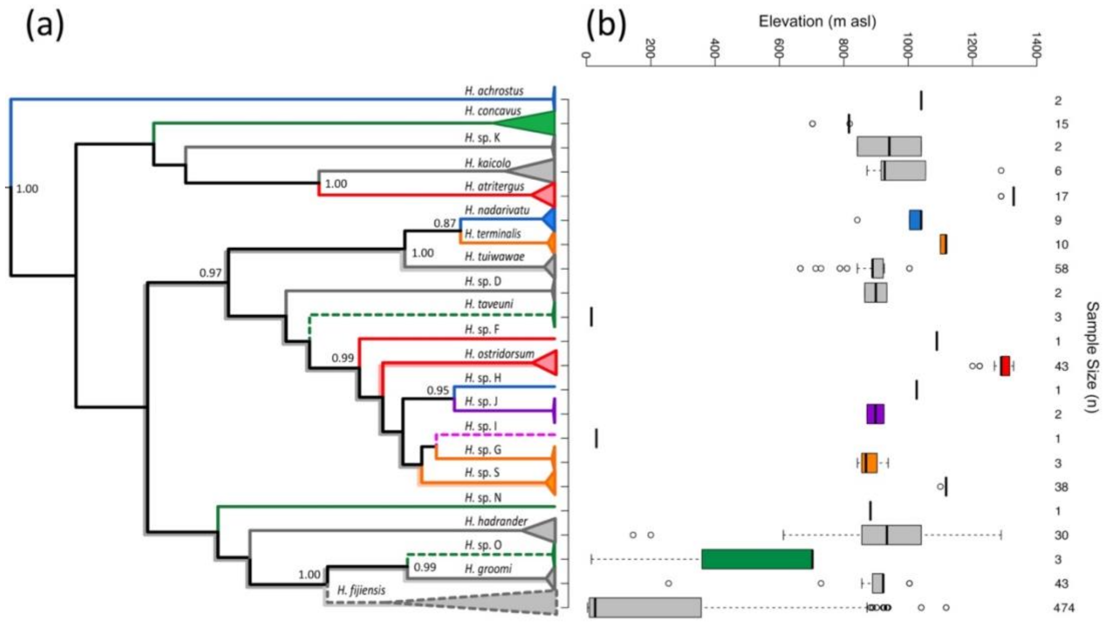

Figure 2. (a) A COI phylogenetic tree of the Fijian *Homalictus* clades coloured by geographic location where terminal triangle depth indicates branch depth for that species and (b) a box plot of elevation in meters above sea level (m asl) and sample size. Hashed tree branches indicate clades with a median elevation below 800 m asl and shadowed branches indicate SNP tree topology. Branch and boxplot colour refer to geographic location in Fig. 1b. Node values indicate posterior probability where it exceeds 0.85. The approximate maximum elevation the sampled highland regions are as follows: Mt. Batilamu (1,110 m asl), eastern Monasavu dam (1087 m asl), Mt. Tomanivi (1,324 m asl), De Voux's peak, Taveuni (1,195 m asl), and Mt. Nadarivatu (1054 m asl).

Supplementary material

Supplementary results

The filtered SNPs developed from five mitochondrial clades confirmed five clear species. Our SNP neighbor-joining tree confirms the presence of five distinct species and matches the topology of our mitochondrial tree with 100% bootstrap support at each node (Fig. S3). These findings are corroborated by our discriminant analysis of principal components, which strongly inferred five clusters within our SNP data (Fig. S4). While some species are not well differentiated by some individual principal components, they are all very strongly differentiated by a combination of component scores, indicating that species identified by COI sequences are also strongly supported by genome-wide SNP data (Fig. S4). All F_{ST} values are significant ($p > 0.001$) and ranged between 0.90 and 0.98 (Table S1). Among population variation explain 92.4% of variation with a fixation index of 0.92. We therefore have high confidence that the species identified by COI sequences, morphology, and SNP data represent genuine species.

Supplementary tables

Table S1. Population pairwise F_{ST} values for the Fijian *Homalictus* species with multiple haplotypes and a sample size of greater than 10. Among population variation explain 92.4% of variation with a fixation index of 0.924. All F_{ST} values are significant ($p > 0.001$).

Species	*H. hadrander*	*H. concavus*	*H. ostridorsum*	*H. atritergus*	*H.* sp. S	*H. fijiensis*
H. hadrander	-					
H. concavus	0.950	-				
H. ostridorsum	0.950	0.958	-			
H. atritergus	0.953	0.945	0.960	-		
H. sp. S	0.975	0.982	0.947	0.983	-	
H. fijiensis	0.897	0.925	0.909	0.927	0.916	-

Supplementary figures

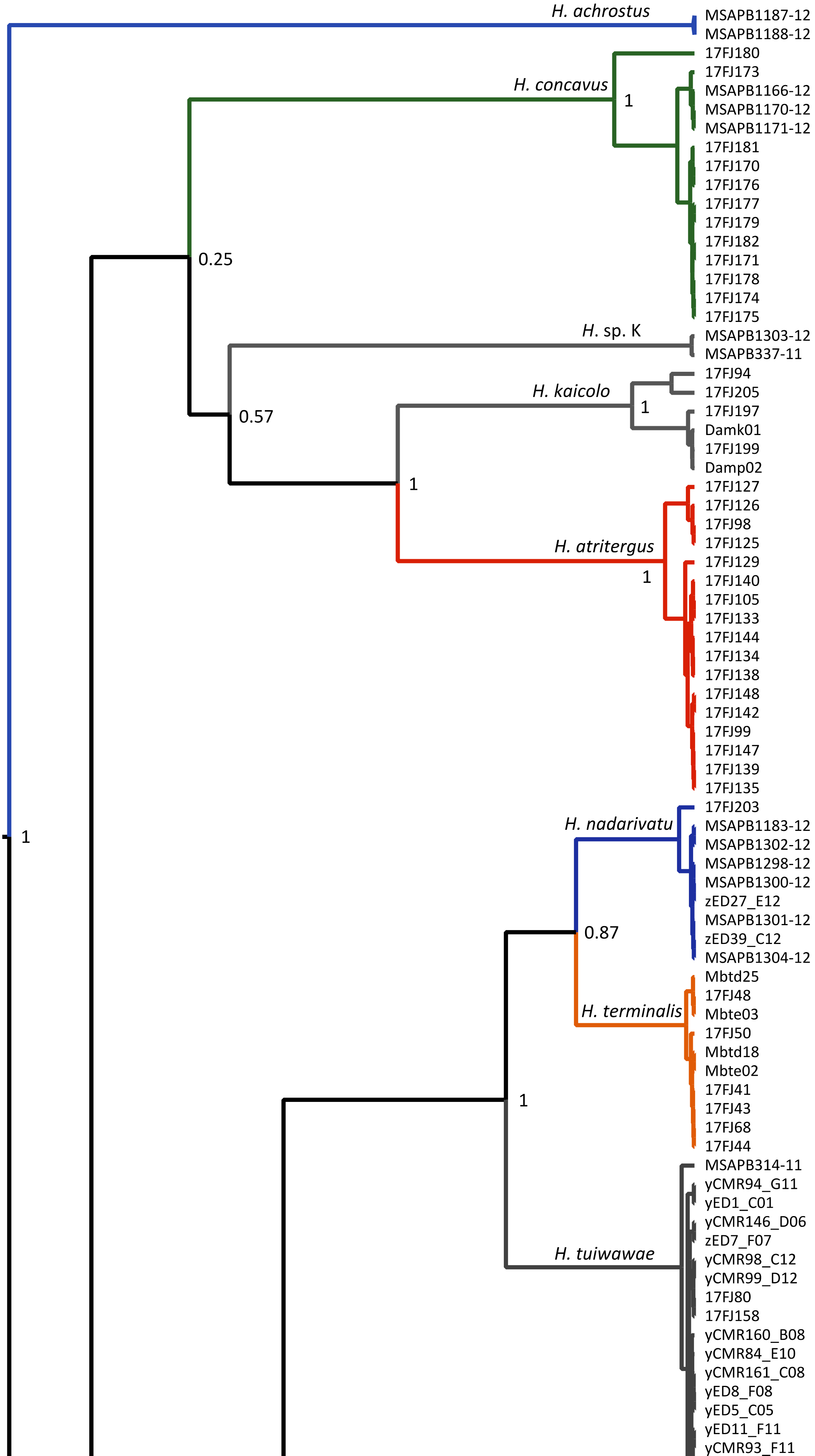

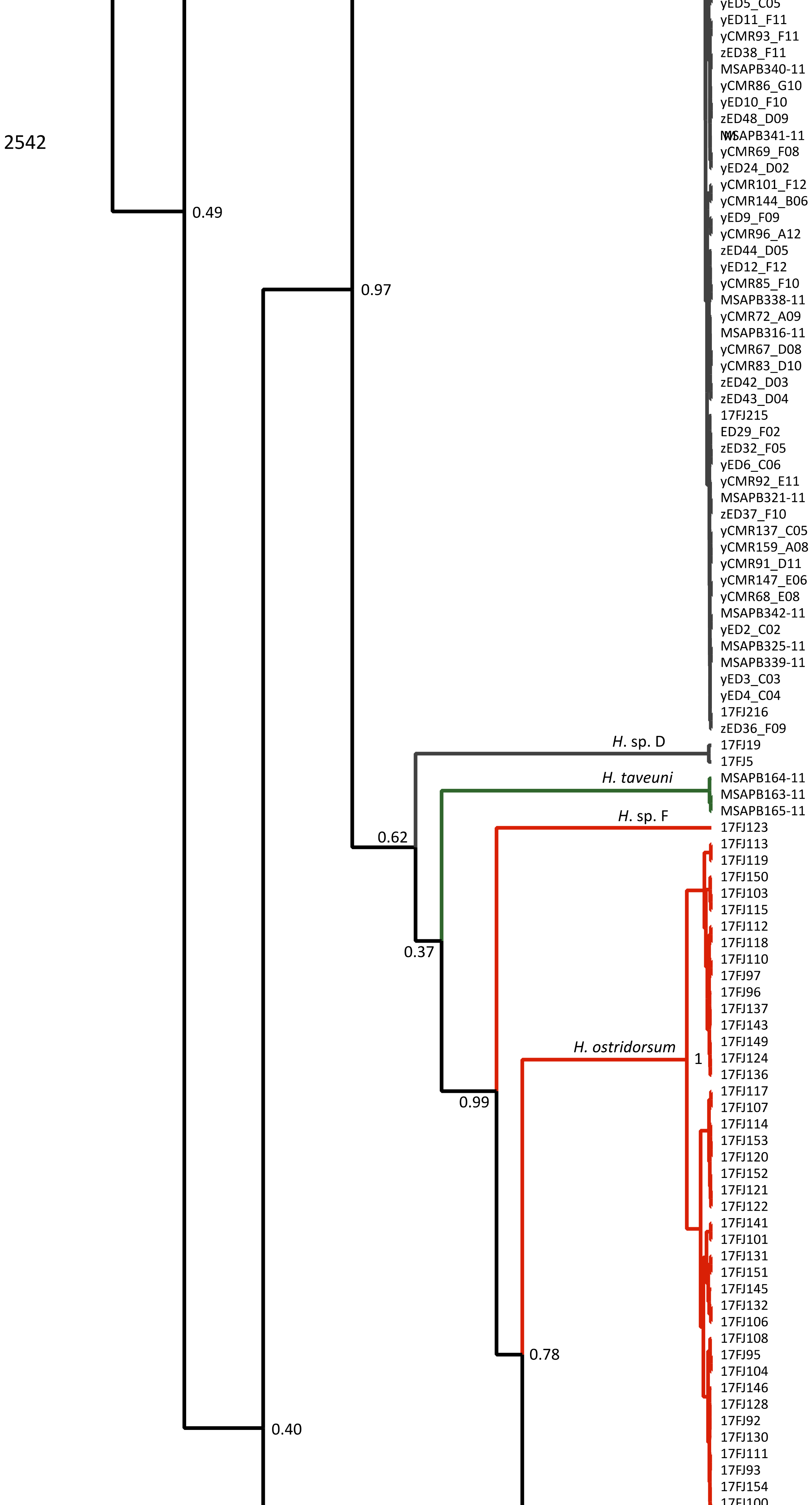
2542
yED5_C05
yED11_F11
yCMR93_F11
zED38_F11
MSAPB340-11
yCMR86_G10
yED10_F10
zED48_D09
MSAPB341-11
yCMR69_F08
yED24_D02
yCMR101_F12
yCMR144_B06
yED9_F09
yCMR96_A12
zED44_D05
yED12_F12
yCMR85_F10
MSAPB338-11
yCMR72_A09
MSAPB316-11
yCMR67_D08
yCMR83_D10
zED42_D03
zED43_D04
17FJ215
ED29_F02
zED32_F05
yED6_C06
yCMR92_E11
MSAPB321-11
zED37_F10
yCMR137_C05
yCMR159_A08
yCMR91_D11
yCMR147_E06
yCMR68_E08
MSAPB342-11
yED2_C02
MSAPB325-11
MSAPB339-11
yED3_C03
yED4_C04
17FJ216
zED36_F09
H. sp. D
17FJ19
17FJ5
H. taveuni
MSAPB164-11
MSAPB163-11
MSAPB165-11
H. sp. F
17FJ123
17FJ113
17FJ119
17FJ150
17FJ103
17FJ115
17FJ112
17FJ118
17FJ110
17FJ97
17FJ96
17FJ137
17FJ143
17FJ149
H. ostridorsum
1
17FJ124
17FJ136
17FJ117
17FJ107
17FJ114
17FJ153
17FJ120
17FJ152
17FJ121
17FJ122
17FJ141
17FJ101
17FJ131
17FJ151
17FJ145
17FJ132
17FJ106
17FJ108
17FJ95
17FJ104
17FJ146
17FJ128
17FJ92
17FJ130
17FJ111
17FJ93
17FJ154
17FJ100
0.49
0.97
0.62
0.37
0.99
0.78
0.40

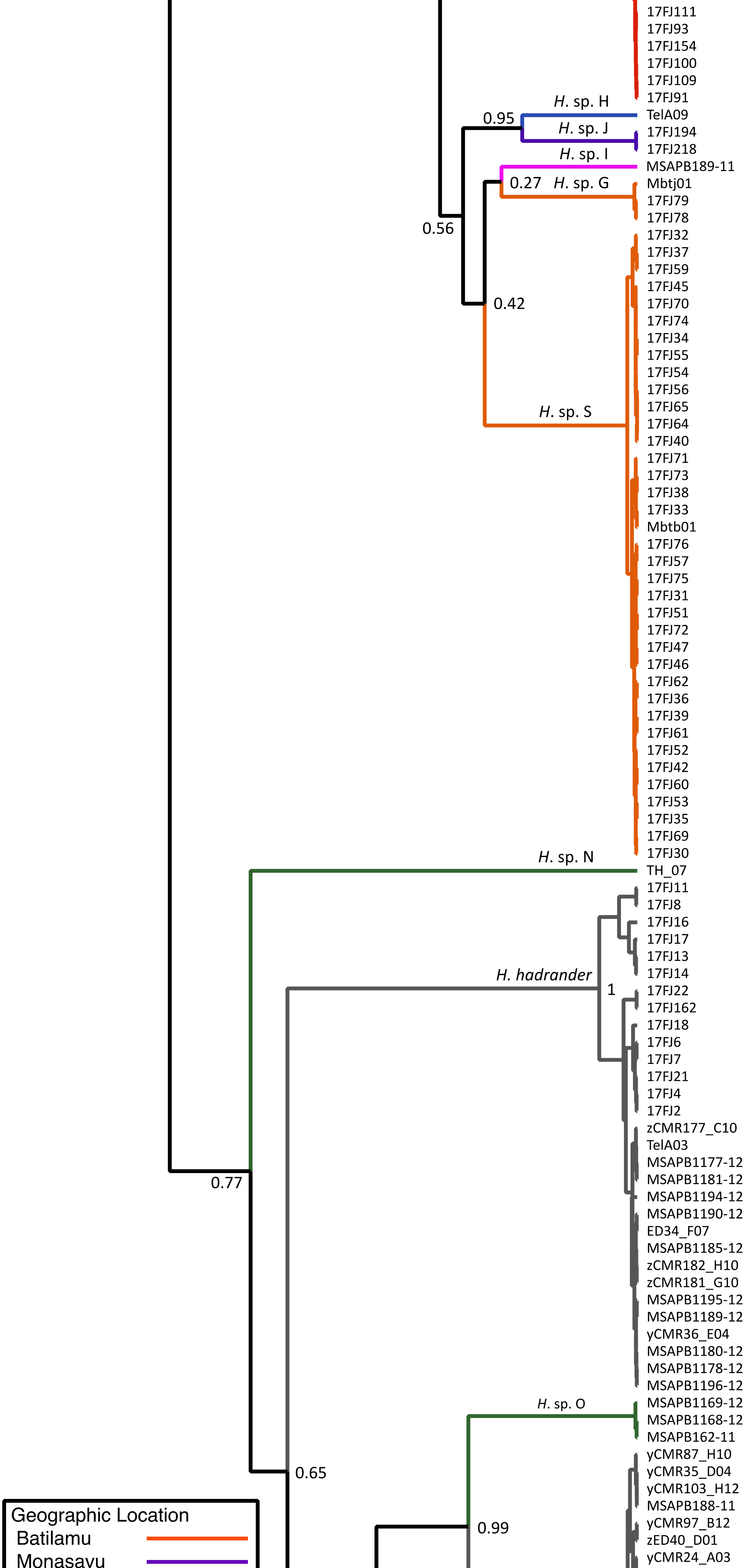
17FJ111
17FJ93
17FJ154
17FJ100
17FJ109
17FJ91
H. sp. H
0.95
TelA09
H. sp. J
17FJ194
17FJ218
H. sp. I
MSAPB189-11
0.27
H. sp. G
Mbtj01
17FJ79
17FJ78
0.56
17FJ32
17FJ37
17FJ59
17FJ45
0.42
17FJ70
17FJ74
17FJ34
17FJ55
17FJ54
17FJ56
17FJ65
H. sp. S
17FJ64
17FJ40
17FJ71
17FJ73
17FJ38
17FJ33
Mbtb01
17FJ76
17FJ57
17FJ75
17FJ31
17FJ51
17FJ72
17FJ47
17FJ46
17FJ62
17FJ36
17FJ39
17FJ61
17FJ52
17FJ42
17FJ60
17FJ53
17FJ35
17FJ69
17FJ30
H. sp. N
TH_07
17FJ11
17FJ8
17FJ16
17FJ17
17FJ13
H. hadrander
17FJ14
1
17FJ22
17FJ162
17FJ18
17FJ6
17FJ7
17FJ21
17FJ4
17FJ2
zCMR177_C10
TelA03
MSAPB1177-12
0.77
MSAPB1181-12
MSAPB1194-12
MSAPB1190-12
ED34_F07
MSAPB1185-12
zCMR182_H10
zCMR181_G10
MSAPB1195-12
MSAPB1189-12
yCMR36_E04
MSAPB1180-12
MSAPB1178-12
MSAPB1196-12
H. sp. O
MSAPB1169-12
MSAPB1168-12
MSAPB162-11
yCMR87_H10
0.65
yCMR35_D04
yCMR103_H12
Geographic Location
MSAPB188-11
Batilamu
0.99
yCMR97_B12
zED40_D01
Monasavu
yCMR24_A03

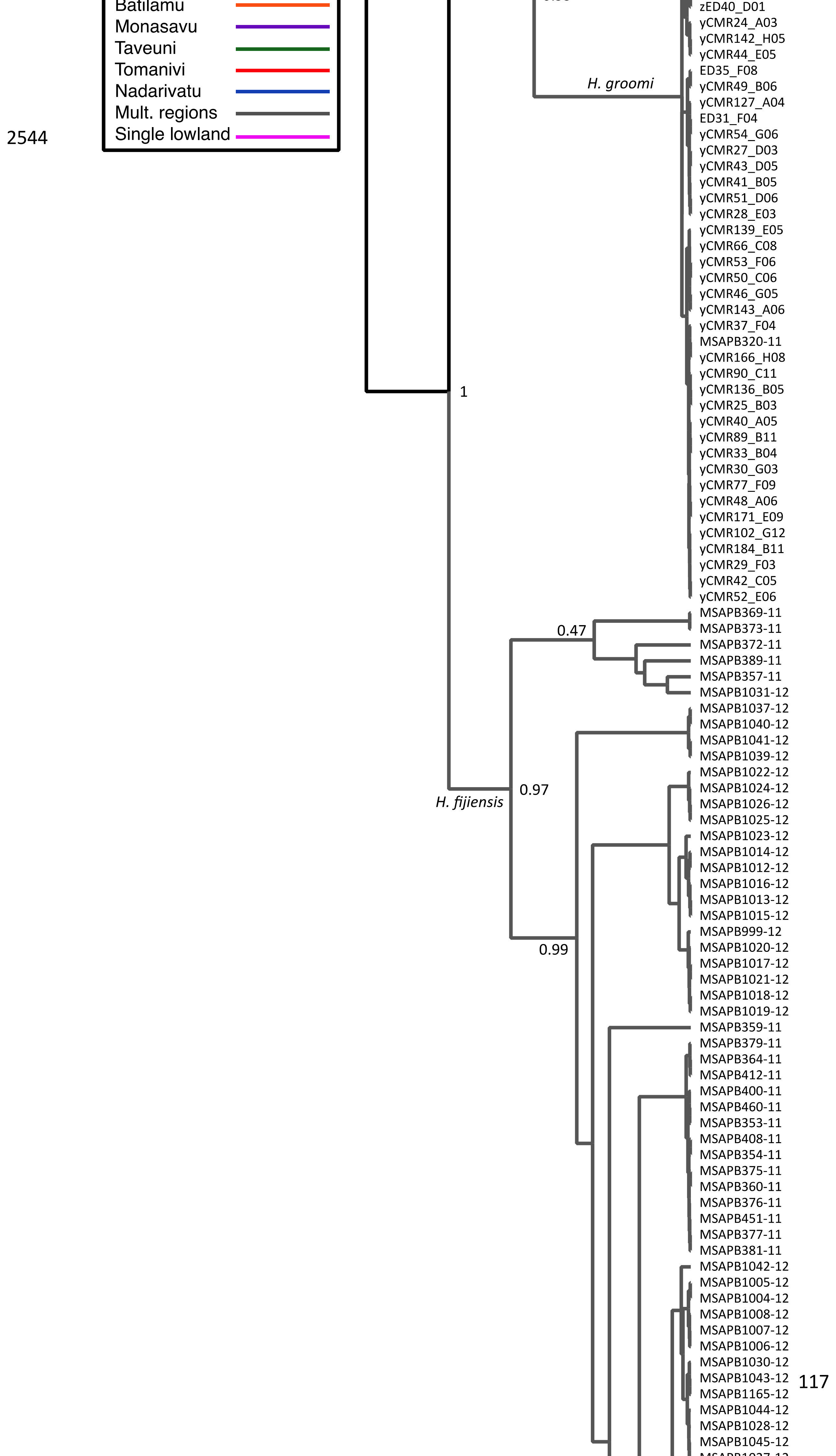
Batilamu
Monasavu
Taveuni
Tomanivi
Nadarivatu
Mult. regions
Single lowland
2544
1
H. groomi
H. fijiensis
0.47
0.97
0.99
117
zED40_D01
yCMR24_A03
yCMR142_H05
yCMR44_E05
ED35_F08
yCMR49_B06
yCMR127_A04
ED31_F04
yCMR54_G06
yCMR27_D03
yCMR43_D05
yCMR41_B05
yCMR51_D06
yCMR28_E03
yCMR139_E05
yCMR66_C08
yCMR53_F06
yCMR50_C06
yCMR46_G05
yCMR143_A06
yCMR37_F04
MSAPB320-11
yCMR166_H08
yCMR90_C11
yCMR136_B05
yCMR25_B03
yCMR40_A05
yCMR89_B11
yCMR33_B04
yCMR30_G03
yCMR77_F09
yCMR48_A06
yCMR171_E09
yCMR102_G12
yCMR184_B11
yCMR29_F03
yCMR42_C05
yCMR52_E06
MSAPB369-11
MSAPB373-11
MSAPB372-11
MSAPB389-11
MSAPB357-11
MSAPB1031-12
MSAPB1037-12
MSAPB1040-12
MSAPB1041-12
MSAPB1039-12
MSAPB1022-12
MSAPB1024-12
MSAPB1026-12
MSAPB1025-12
MSAPB1023-12
MSAPB1014-12
MSAPB1012-12
MSAPB1016-12
MSAPB1013-12
MSAPB1015-12
MSAPB999-12
MSAPB1020-12
MSAPB1017-12
MSAPB1021-12
MSAPB1018-12
MSAPB1019-12
MSAPB359-11
MSAPB379-11
MSAPB364-11
MSAPB412-11
MSAPB400-11
MSAPB460-11
MSAPB353-11
MSAPB408-11
MSAPB354-11
MSAPB375-11
MSAPB360-11
MSAPB376-11
MSAPB451-11
MSAPB377-11
MSAPB381-11
MSAPB1042-12
MSAPB1005-12
MSAPB1004-12
MSAPB1008-12
MSAPB1007-12
MSAPB1006-12
MSAPB1030-12
MSAPB1043-12
MSAPB1165-12
MSAPB1044-12
MSAPB1028-12
MSAPB1045-12


2545
MSAPB1044-12
MSAPB1028-12
MSAPB1045-12
MSAPB1027-12
MSAPB380-11
MSAPB352-11
MSAPB367-11
MSAPB363-11
MSAPB362-11
MSAPB382-11
MSAPB378-11
MSAPB365-11
MSAPB356-11
MSAPB368-11
MSAPB385-11
MSAPB370-11
MSAPB366-11
MSAPB351-11
MSAPB374-11
MSAPB387-11
MSAPB388-11
MSAPB386-11
MSAPB383-11
MSAPB358-11
MSAPB392-11
MSAPB444-11
MSAPB411-11
MSAPB450-11
MSAPB439-11
MSAPB440-11
MSAPB434-11
MSAPB442-11
MSAPB433-11
MSAPB448-11
MSAPB463-11
MSAPB454-11
MSAPB420-11
MSAPB418-11
MSAPB436-11
MSAPB456-11
MSAPB416-11
MSAPB455-11
MSAPB457-11
MSAPB452-11
MSAPB424-11
MSAPB430-11
MSAPB421-11
MSAPB453-11
MSAPB449-11
MSAPB445-11
MSAPB298-11
MSAPB413-11
17FJ206
MSAPB407-11
MSAPB447-11
MSAPB397-11
MSAPB395-11
MSAPB405-11
17FJ213
MSAPB432-11
MSAPB384-11
MSAPB435-11
MSAPB401-11
MSAPB423-11
MSAPB462-11
MSAPB426-11
MSAPB390-11
MSAPB429-11
MSAPB437-11
MSAPB427-11
MSAPB441-11
MSAPB311-11
MSAPB394-11
MSAPB461-11
MSAPB446-11
MSAPB355-11
MSAPB422-11
MSAPB329-11
MSAPB414-11
MSAPB312-11
MSAPB438-11
MSAPB396-11
MSAPB419-11
MSAPB371-11
17FJ169
MSAPB398-11
MSAPB443-11
MSAPB361-11
MSAPB406-11
MSAPB415-11
MSAPB315-11
MSAPB393-11

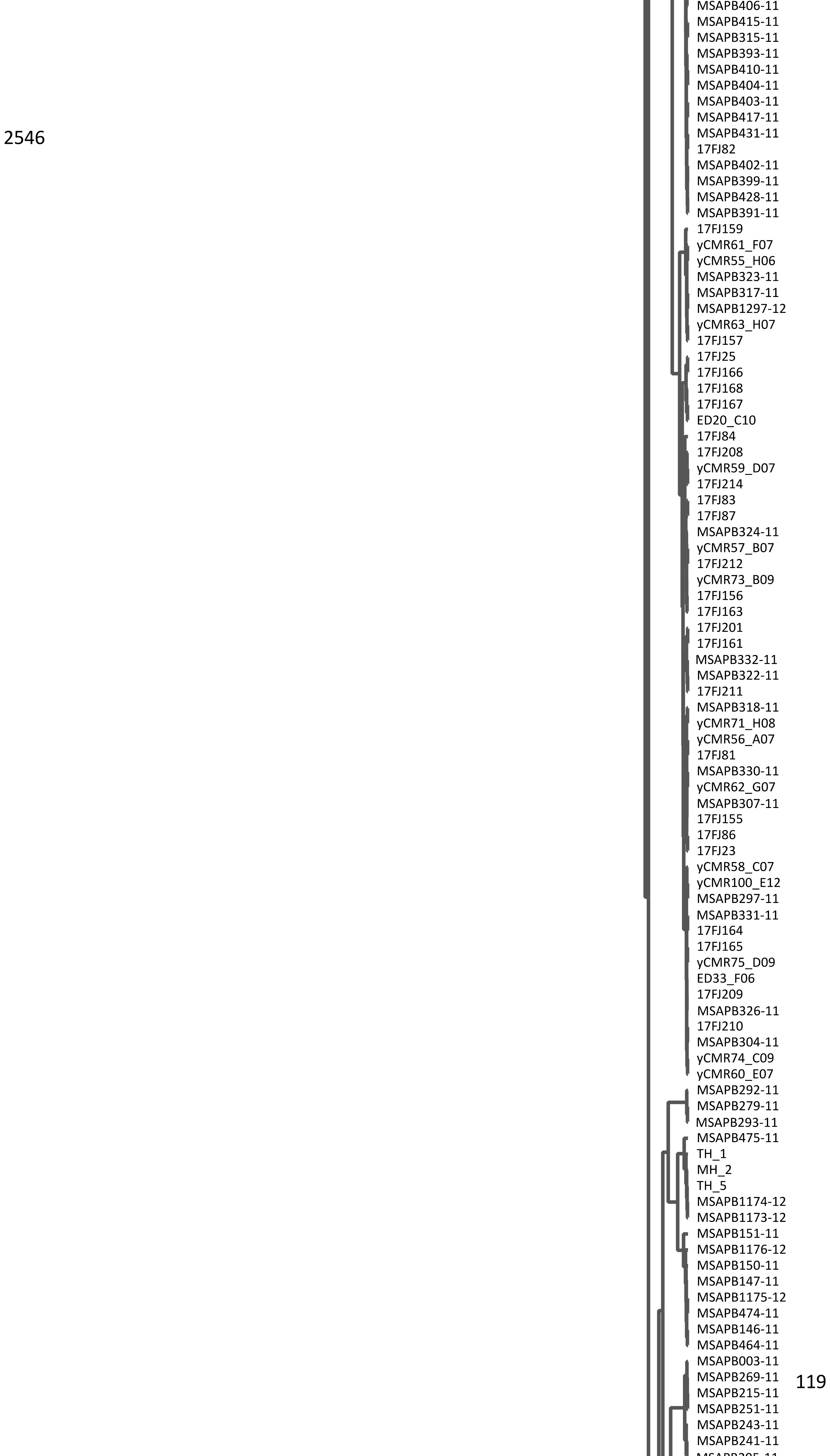
2546
MSAPB406-11
MSAPB415-11
MSAPB315-11
MSAPB393-11
MSAPB410-11
MSAPB404-11
MSAPB403-11
MSAPB417-11
MSAPB431-11
17FJ82
MSAPB402-11
MSAPB399-11
MSAPB428-11
MSAPB391-11
17FJ159
yCMR61_F07
yCMR55_H06
MSAPB323-11
MSAPB317-11
MSAPB1297-12
yCMR63_H07
17FJ157
17FJ25
17FJ166
17FJ168
17FJ167
ED20_C10
17FJ84
17FJ208
yCMR59_D07
17FJ214
17FJ83
17FJ87
MSAPB324-11
yCMR57_B07
17FJ212
yCMR73_B09
17FJ156
17FJ163
17FJ201
17FJ161
MSAPB332-11
MSAPB322-11
17FJ211
MSAPB318-11
yCMR71_H08
yCMR56_A07
17FJ81
MSAPB330-11
yCMR62_G07
MSAPB307-11
17FJ155
17FJ86
17FJ23
yCMR58_C07
yCMR100_E12
MSAPB297-11
MSAPB331-11
17FJ164
17FJ165
yCMR75_D09
ED33_F06
17FJ209
MSAPB326-11
17FJ210
MSAPB304-11
yCMR74_C09
yCMR60_E07
MSAPB292-11
MSAPB279-11
MSAPB293-11
MSAPB475-11
TH_1
MH_2
TH_5
MSAPB1174-12
MSAPB1173-12
MSAPB151-11
MSAPB1176-12
MSAPB150-11
MSAPB147-11
MSAPB1175-12
MSAPB474-11
MSAPB146-11
MSAPB464-11
MSAPB003-11
MSAPB269-11
119
MSAPB215-11
MSAPB251-11
MSAPB243-11
MSAPB241-11

2547

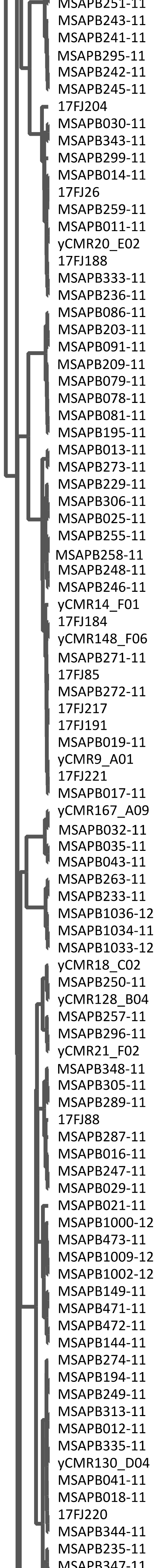
MSAPB251-11
MSAPB243-11
MSAPB241-11
MSAPB295-11
MSAPB242-11
MSAPB245-11
17FJ204
MSAPB030-11
MSAPB343-11
MSAPB299-11
MSAPB014-11
17FJ26
MSAPB259-11
MSAPB011-11
yCMR20_E02
17FJ188
MSAPB333-11
MSAPB236-11
MSAPB086-11
MSAPB203-11
MSAPB091-11
MSAPB209-11
MSAPB079-11
MSAPB078-11
MSAPB081-11
MSAPB195-11
MSAPB013-11
MSAPB273-11
MSAPB229-11
MSAPB306-11
MSAPB025-11
MSAPB255-11
MSAPB258-11
MSAPB248-11
MSAPB246-11
yCMR14_F01
17FJ184
yCMR148_F06
MSAPB271-11
17FJ85
MSAPB272-11
17FJ217
17FJ191
MSAPB019-11
yCMR9_A01
17FJ221
MSAPB017-11
yCMR167_A09
MSAPB032-11
MSAPB035-11
MSAPB043-11
MSAPB263-11
MSAPB233-11
MSAPB1036-12
MSAPB1034-11
MSAPB1033-12
yCMR18_C02
MSAPB250-11
yCMR128_B04
MSAPB257-11
MSAPB296-11
yCMR21_F02
MSAPB348-11
MSAPB305-11
MSAPB289-11
17FJ88
MSAPB287-11
MSAPB016-11
MSAPB247-11
MSAPB029-11
MSAPB021-11
MSAPB1000-12
MSAPB473-11
MSAPB1009-12
MSAPB1002-12
MSAPB149-11
MSAPB471-11
MSAPB472-11
MSAPB144-11
MSAPB274-11
MSAPB194-11
MSAPB249-11
MSAPB313-11
MSAPB012-11
MSAPB335-11
yCMR130_D04
MSAPB041-11
MSAPB018-11
17FJ220
MSAPB344-11
MSAPB235-11
MSAPB347-11

2548


MSAPB018-11
17FJ220
MSAPB344-11
MSAPB235-11
MSAPB347-11
yCMR11_C01
MSAPB280-11
MH_5
MSAPB036-11
17FJ187
MSAPB288-11
MSAPB300-11
17FJ186
MSAPB270-11
MSAPB028-11
MSAPB345-11
MSAPB282-11
MSAPB260-11
MSAPB281-11
MSAPB294-11
MSAPB023-11
MSAPB037-11
MSAPB228-11
MSAPB024-11
MSAPB073-11
yCMR129_C04
17FJ185
17FJ183
MSAPB042-11
MSAPB283-11
MSAPB244-11
yCMR70_G08
MSAPB087-11
MSAPB204-11
MSAPB067-11
MSAPB214-11
17FJ193
MSAPB220-11
MSAPB208-11
MSAPB336-11
MSAPB063-11
MSAPB068-11
MSAPB031-11
MSAPB227-11
MSAPB077-11
17FJ9
17FJ63
MSAPB045-11
MSAPB062-11
yCMR13_E01
MSAPB181-11
MSAPB290-11
MSAPB201-11
MSAPB061-11
MSAPB197-11
yCMR7_H07
yCMR39_H04
yCMR6_H10
17FJ192
MSAPB210-11
MSAPB226-11
MSAPB084-11
MSAPB055-11
yCMR17_B02
MSAPB180-11
MSAPB015-11
MSAPB222-11
yCMR23_H02
MSAPB218-11
MSAPB225-11
MSAPB232-11
17FJ200
MSAPB205-11
MSAPB082-11
MSAPB346-11
MSAPB200-11
yCMR132_F04
MSAPB064-11
17FJ190
yCMR8_H08
17FJ24
17FJ219
17FJ27
yCMR168_B09
yCMR10_B01
yCMR65_B08
yCMR16_A02
MSAPB319-11
MSAPB223-11
MSAPB070-11
MSAPB083-11
MSAPB192-11


MSAPB070-11
MSAPB083-11
MSAPB192-11
MSAPB207-11
MSAPB349-11
yCMR38_G04
17FJ89
17FJ1
MSAPB066-11
17FJ66
yCMR131_E04
MSAPB231-11
MSAPB026-11
MSAPB256-11
MSAPB093-11
MSAPB221-11
MSAPB039-11
MSAPB071-11
MSAPB074-11
17FJ160
MSAPB224-11
MSAPB090-11
MSAPB350-11
MSAPB004-11
MSAPB089-11
MSAPB213-11
MSAPB075-11
MSAPB080-11
MSAPB022-11
MSAPB010-11
MSAPB085-11
MSAPB217-11
MSAPB065-11
MSAPB056-11
MSAPB206-11
MSAPB069-11
MSAPB1299-12
MSAPB001-11
yCMR15_G01
MSAPB211-11
MSAPB219-11
MSAPB033-11
MSAPB072-11
MSAPB027-11
yCMR22_G02
MSAPB020-11
yCMR19_D02
MSAPB212-11
17FJ196
MSAPB193-11
MSAPB198-11
MSAPB044-11
MSAPB092-11
MSAPB191-11
MSAPB094-11
yCMR47_H05
MSAPB038-11
MSAPB008-11
MSAPB230-11
MSAPB199-11
MSAPB034-11
MSAPB202-11
17FJ77
MSAPB216-11
MSAPB076-11
yCMR12_D01
MSAPB196-11
17FJ207
MSAPB088-11
17FJ12
17FJ198
MSAPB095-11
17FJ195
0.0070

Figure S1. Maximum credibility tree from Bayesian phylogenetic analysis of Fijian *Homalictus* based on analysis of the COI gene showing posterior probabilities at nodes. Branch color represents geographic extent.

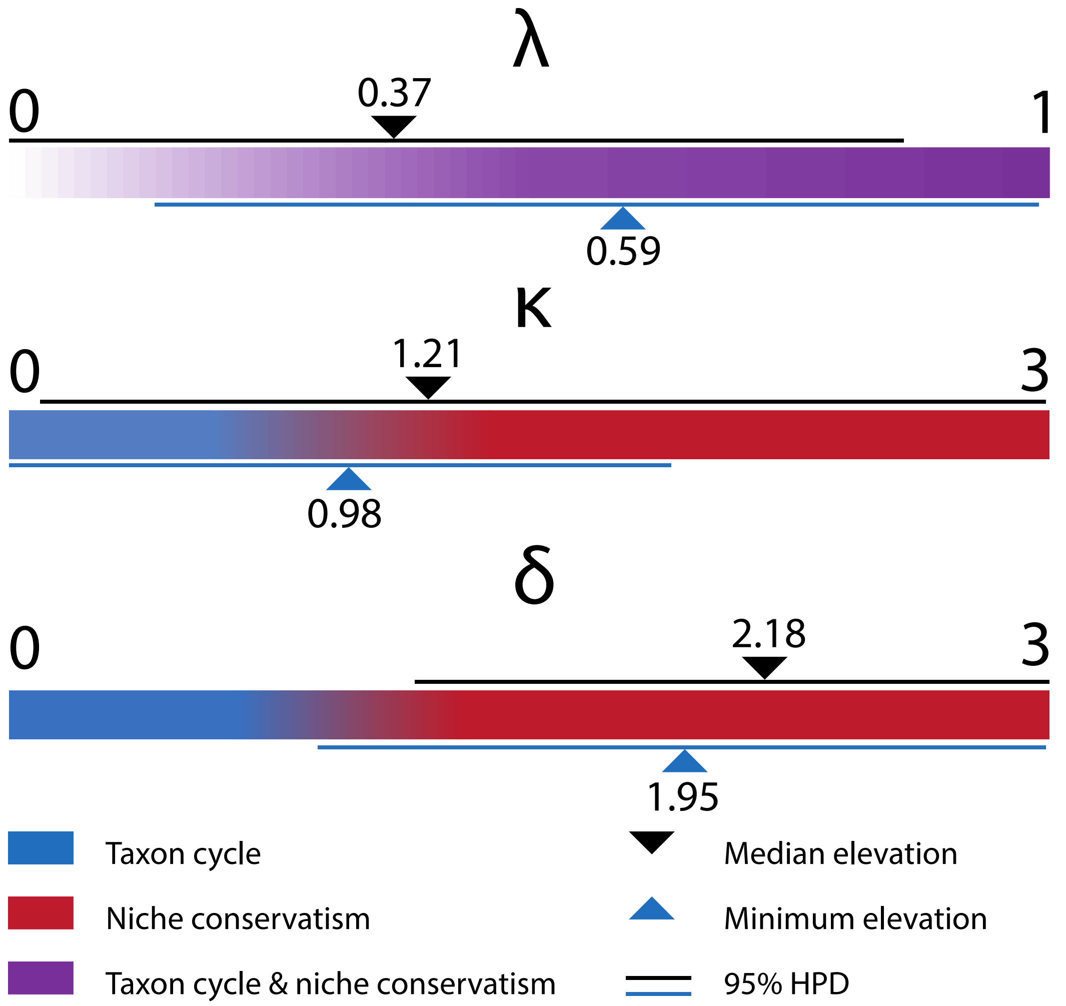

Figure S2. Mean values of branch transformation parameters λ, κ, and δ for median (black triangles) and minimum (blue triangles) elevations. Solid black and blue bars indicate 95% highest posterior densities (HPD) for median and minimum elevations, respectively. Parameter values are indicated along the bar showing the minimum and maximum possible values for each factor and whether it supports the taxon cycle (blue), niche conservatism (red) or both (purple).

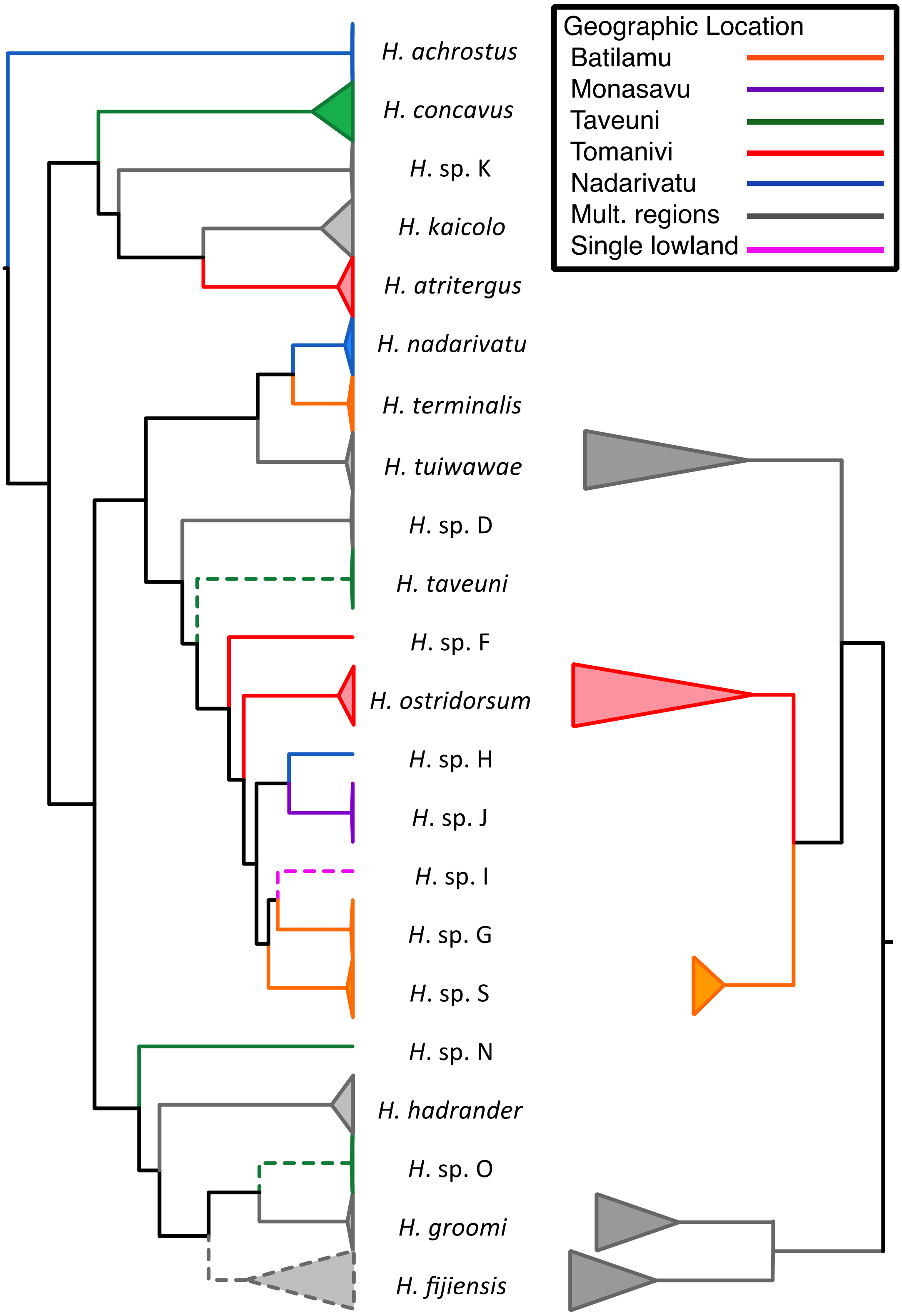

Figure S3. Cophylogeny comparing our COI maximum credibility tree and our 5-species SNP-based phylogenetic tree showing congruent topology. Branch colors represent geographic extent.

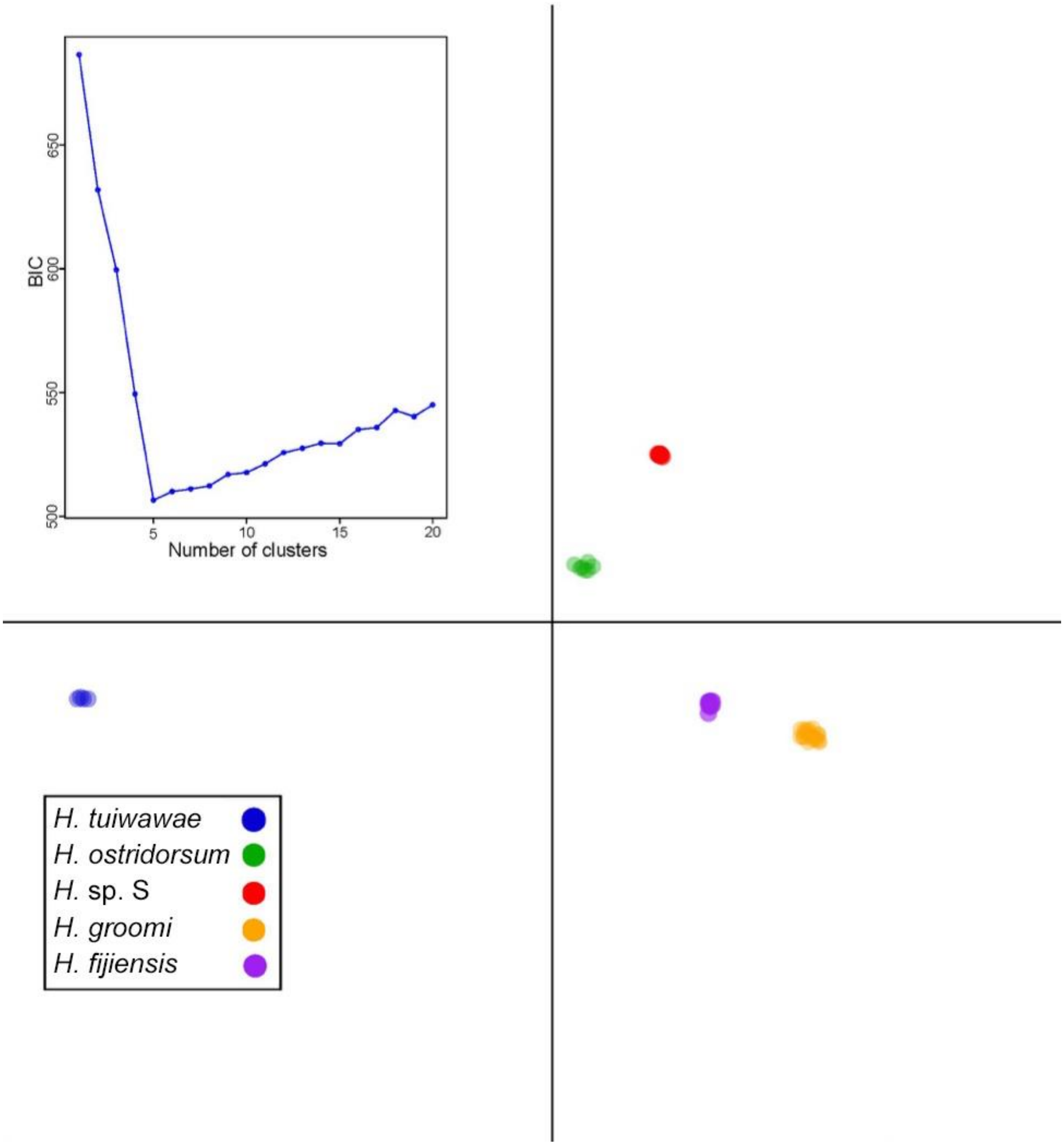

Figure S4. Discriminant analysis of principal components for the SNP data showing the clustering of each species. Inset graph showing the Bayesian information criterion (BIC) values for each inferred clustering level, with the lowest inferred BIC being the preferred number of clusters.

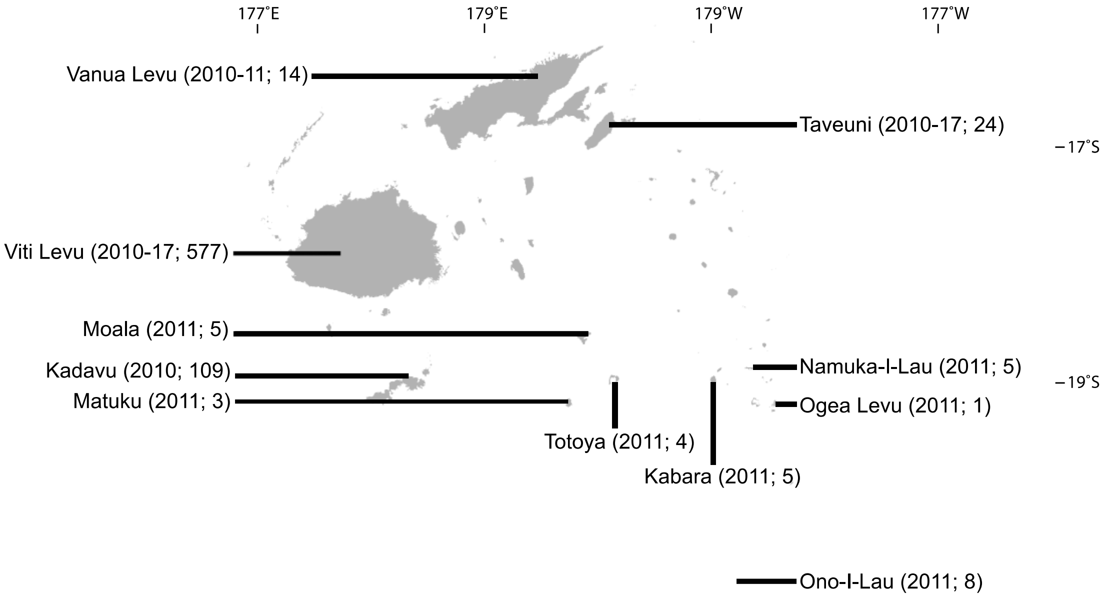

Figure S5. The Fijian islands that were sampled. Parentheses indicate the period in which they were sampled followed by the number of sequences from each island.

Chapter 3: Holocene population expansion of a tropical bee coincides with early human colonisation of Fiji rather than climate change

James B. Dorey[a,b,1], Scott V.C. Groom[c], Alejandro Velasco-Castrillón[b], Mark I. Stevens[b,d], Michael S.Y. Lee[a,b], and Michael P. Schwarz[a]

[a] *College of Science and Engineering, Flinders University, SA 5001, Adelaide, Australia*
[b] *Biological and Earth Sciences, South Australian Museum, SA 5000, Australia*
[c] *School of Agriculture, Food and Wine, The University of Adelaide, Waite Campus Urrbrae, Adelaide, SA 5064, Australia*
[d] *School of Biological Sciences, University of Adelaide, SA 5005, Australia*
[1]Corresponding author email: jbdorey@me.com

Published in Molecular Ecology (https://doi.org/10.1111/mec.16034).

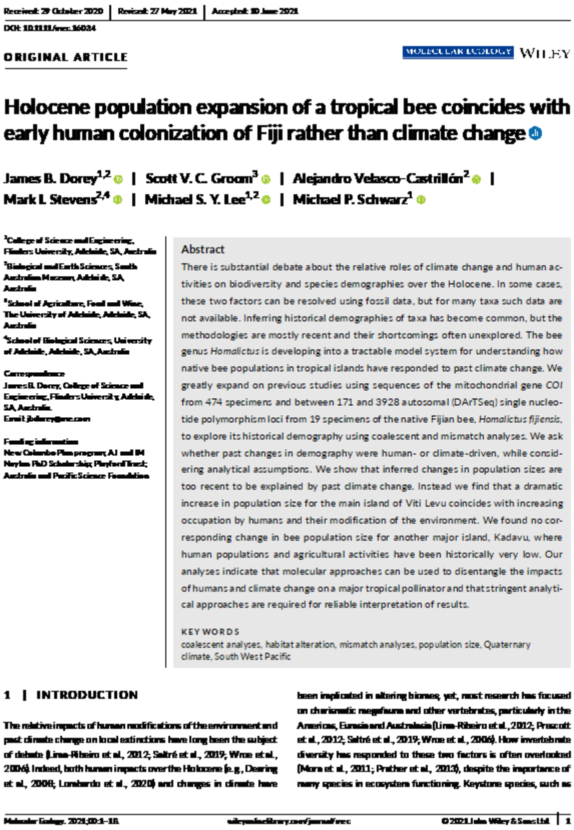

Received: 29 October 2020 | Revised: 27 May 2021 | Accepted: 10 June 2021
DOI: 10.1111/mec.16034

ORIGINAL ARTICLE

MOLECULAR ECOLOGY WILEY

Holocene population expansion of a tropical bee coincides with early human colonization of Fiji rather than climate change

James B. Dorey[1,2] | Scott V. C. Groom[3] | Alejandro Velasco-Castrillón[2] | Mark I. Stevens[2,4] | Michael S. Y. Lee[1,2] | Michael P. Schwarz[1]

[1]College of Science and Engineering, Flinders University, Adelaide, SA, Australia
[2]Biological and Earth Sciences, South Australian Museum, Adelaide, SA, Australia
[3]School of Agriculture, Food and Wine, The University of Adelaide, Adelaide, SA, Australia
[4]School of Biological Sciences, University of Adelaide, Adelaide, SA, Australia

Correspondence
James B. Dorey, College of Science and Engineering, Flinders University, Adelaide, SA, Australia.
Email: jbdorey@me.com

Funding information
New Colombo Plan program; AJ and IM Naylon PhD Scholarship; Playford Trust; Australia and Pacific Science Foundation

Abstract

There is substantial debate about the relative roles of climate change and human activities on biodiversity and species demographies over the Holocene. In some cases, these two factors can be resolved using fossil data, but for many taxa such data are not available. Inferring historical demographies of taxa has become common, but the methodologies are mostly recent and their shortcomings often unexplored. The bee genus *Homalictus* is developing into a tractable model system for understanding how native bee populations in tropical islands have responded to past climate change. We greatly expand on previous studies using sequences of the mitochondrial gene *COI* from 474 specimens and between 171 and 3928 autosomal (DArTSeq) single nucleotide polymorphism loci from 19 specimens of the native Fijian bee, *Homalictus fijiensis*, to explore its historical demography using coalescent and mismatch analyses. We ask whether past changes in demography were human- or climate-driven, while considering analytical assumptions. We show that inferred changes in population sizes are too recent to be explained by past climate change. Instead we find that a dramatic increase in population size for the main island of Viti Levu coincides with increasing occupation by humans and their modification of the environment. We found no corresponding change in bee population size for another major island, Kadavu, where human populations and agricultural activities have been historically very low. Our analyses indicate that molecular approaches can be used to disentangle the impacts of humans and climate change on a major tropical pollinator and that stringent analytical approaches are required for reliable interpretation of results.

KEY WORDS
coalescent analyses, habitat alteration, mismatch analyses, population size, Quaternary climate, South West Pacific

1 | INTRODUCTION

The relative impacts of human modifications of the environment and past climate change on local extinctions have long been the subject of debate (Lima-Ribeiro et al., 2012; Saltré et al., 2019; Wroe et al., 2006). Indeed, both human impacts over the Holocene (e.g., Dearing et al., 2008; Lombardo et al., 2020) and changes in climate have been implicated in altering biomes; yet, most research has focused on charismatic megafauna and other vertebrates, particularly in the Americas, Eurasia and Australasia (Lima-Ribeiro et al., 2012; Prescott et al., 2012; Saltré et al., 2019; Wroe et al., 2006). How invertebrate diversity has responded to these two factors is often overlooked (Mora et al., 2011; Prather et al., 2013), despite the importance of many species in ecosystem functioning. Keystone species, such as

Abstract

There is substantial debate about the relative roles of climate change and human activities on biodiversity and species demographies over the Holocene. In some cases, these two factors can be resolved using fossil data, but for many taxa such data are not available. Inferring historical demographies of taxa has become common, but the methodologies are mostly recent and their shortcomings often unexplored. The bee genus *Homalictus* is developing into a tractable model system for understanding how native bee populations in tropical islands have responded to past climate change. We greatly expand on previous studies using sequences of the mitochondrial gene COI from 474 specimens and between 171 and 3,928 autosomal (DArTSeq) SNP loci from 19 specimens of the native Fijian bee, *Homalictus fijiensis* (Perkins & Cheesman, 1928), to explore its historical demography using coalescent and mismatch analyses. We ask whether past changes in demography were human- or climate-driven, while considering analytical assumptions. We show that inferred changes in population sizes are too recent to be explained by past climate change. Instead we find that a dramatic increase in population size for the main island of Viti Levu coincides with increasing occupation by humans and their modification of the environment. We found no corresponding change in bee population size for another major island, Kadavu, where human populations and agricultural activities have been historically very low. Our analyses indicate that molecular approaches can be used to disentangle the impacts of humans and climate change on a major tropical pollinator and that stringent analytical approaches are required for reliable interpretation of results.

Keywords

Coalescent analyses, population size, Quaternary climate, South West Pacific, mismatch analyses, habitat alteration

Introduction

The relative impacts of human modifications of the environment and past climate change on local extinctions have long been the subject of debate [20-22]. Indeed, both human impacts over the Holocene — e.g., Lombardo, *et al.* [23] and Dearing, *et al.* [24] — and changes in climate have been implicated in altering biomes; yet, most research has focussed on charismatic megafauna and other vertebrates, particularly in the Americas, Eurasia and Australasia [20-22,132]. How invertebrate diversity has responded to these two factors is often overlooked [133,134], despite the importance of many species in ecosystem functioning. Keystone species, such as pollinators, can influence ecosystem functioning in major ways and so identifying the factors that affect their abundance and diversity is critical. Determining how these factors have shaped past demographic shifts will be important for anticipating their impacts on future scenarios.

In many regions (e.g., the Americas, Eurasia, and Australia), climate change during the Quaternary coincided with the migration of humans and their modification of the environment — e.g., through hunting, agriculture, and fire [135]. Disentangling how both climate and humans have shaped ecosystem responses is understandably challenging, typically requiring fine-scale interrogation of the fossil record [20,22]. However, many invertebrate groups, including those with key roles in ecosystem function, have a poor Holocene fossil record. Biases in the fossil record can be taxonomic and geographical and caused by: (i) the specific environmental and biotic requirements for preservation and (ii) the discovery and publication by researchers [136-138].

In taxa with limited fossil records, coalescent analyses of genetic markers from extant populations can enable us to overcome such shortcomings and provide insight into past demographic changes [60]. This approach uses the expected time, in generations, for different alleles to have derived from a single gene sequence via mutational steps and genetic drift. However, there are two major caveats that arise for these kinds of analyses: (i) firstly, they require genetic markers that are not heavily biased by selection and (ii) they need to be able to distinguish between ‘local’ and ‘global’ changes in demography [54]. For example, in species that occupy regions with large latitudinal extents, such as continents, the effects of climate- or human-mediated disturbance on regional population sizes could be masked by the ability of species to shift their ranges latitudinally [83,86]. But when dispersal is largely precluded by substantial oceanic barriers, as in many islands, demographic responses to changing climates can be assessed without these confounding distributional shifts. However, elevational shifts are still possible and can be strongly phylogenetically structured [139]. Additionally, the short generation times of many tropical invertebrates (i.e., more mutations/year), coupled with the tractability of insular systems, make tropical island invertebrates ideal model organisms for investigating relatively recent past demographies [14-16,47].

Multiple studies have posited that tropical ectotherms such as insects should have narrow thermal tolerances and might be particularly susceptible to climate variation [91,92]. As the tropics are less thermally variable than temperate and boreal regions [91,92], it is thought that species evolving in tropical climates would possess relatively narrow thermal niches. This is indirectly supported by ‘Rapoport’s Rule’, where species distributions tend to become latitudinally narrower as their range approaches the equator [93,94,139,140]. The impact of both historical and future climate change may then be expected to be greater in tropical ectotherms than in taxa of higher latitudes — e.g., Kellermann, *et al.* [93].

Fiji is a tropical archipelago that began subaerial emergence in the late Eocene, mostly through volcanic activity, with the main island of Viti Levu emerging in the Oligocene [141]. The next largest islands, Vanua Levu, Taveuni, and Kadavu became subaerial in the late Miocene and Pliocene, followed by a large number of smaller islands [141]. The earliest records of humans in Fiji comprise Lapita pottery fragments dated to about 3 kya [25-27], with subsequent migration through the Lau islands to Tonga and then Samoa within a relatively short window between 2.95 and 2.75 kya [27]. Sediment and ash layers in estuarine deposits from Viti Levu could indicate terrestrial impacts of the Lapita people shortly after their arrival [142], but with little evidence that they substantially occupied inland regions [143]. A second wave of human occupation of Fiji commenced approximately 2.5 kya, with changes in mobility, intensified land use and inland settlement [27]. Archaeological studies suggest that movement of humans into highland regions began about 2.1 kya [144].

The earliest evidence of slash-and-burn agriculture on Viti Levu is from up to 1.8 kya [25]. Dense charcoal sediments on Viti Levu coincide with early Lapita settlement (~3 kya); however, it is uncertain if this indicates slash-and-burn agriculture or natural processes [142].

A single ground-nesting bee genus, *Homalictus*, has been shown to represent the entire endemic bee fauna of Fiji [11,32,47]. Following a single colonisation event during the Pleistocene, insular diversification has led to at least 22 species; and only one species, *H. fijiensis* (Perkins & Cheesman, 1928), is common in lowland regions (< 800 m asl; metres above sea-level) [99,139]. Bayesian analyses of speciation patterns and elevational niches have indicated a high degree of phylogenetic inertia for most Fijian *Homalictus* species that limits their ability to adjust their elevational ranges [139]. Using Bayesian skyline plot analyses, Groom, *et al.* [32] argued that *H. fijiensis* populations had increased dramatically since the last glacial maximum and this was likely due to a warming climate and not human occupation. However, that study was undertaken at a time when the species diversity of *Homalictus* in Fiji was very poorly understood and likely combined multiple *Homalictus* cryptic species, which confounds Bayesian skyline plot interpretations [54]. Additionally, the super-generalist behaviour of *H. fijiensis* and its nesting preference for open, sunny areas might interact in a positive manner with anthropogenic clearing and floral introductions [145]. Much more stringent analyses are therefore required to infer historical changes in population demography, especially if the relative impacts of humans and climate change are to be distinguished.

Here we use mismatch and coalescent analyses of a much-expanded dataset to investigate the past demographic changes of *H. fijiensis* and assess whether human modification of the environment, historical climate change, or a combination of the two, could have driven population changes. To examine the findings of Groom, *et al.* [32], we test if: (i) the effective population size (*Ne*) of *H. fijiensis* on Viti Levu and Kadavu increased in the recent past (assessed using mismatch and coalescence analyses), and (ii) the timing of this increase coincided with warming climates following the end of the last glacial maxima and not human occupation of Fiji (assessed using coalescence analyses).

Methods

Sampling sites and methods

Collections were made throughout Fiji between 2010 and 2017 from multiple localities but with the greatest number of samples from the largest island of Viti Levu (n = 309) and then the island of Kadavu (n = 109) (Table S1). Samples were collected from 3 to 1,328 m asl by sweep netting both native and introduced plants, and from nesting aggregations along roadsides. For each collection site, latitude, longitude, and elevation were recorded using GPS devices (primarily using a Garmin 550). Once collected, bees were immediately transferred into individual vials of ≥98% ethanol. Vials were kept at ~5˚C and ethanol was replaced within a week of collection to lessen DNA degradation.

Geographic information systems

In order to explore whether patterns in historical demography were related to subaerial land mass over time, we used bathymetric maps to examine how subaerial landmass and connectivity have changed since the last glacial maximum. Bathymetric data were downloaded in *R* version 3.6.2 using the package *marmap* version 1.0.4 [146]. The *marmap* package was also used to produce maps and calculate subaerial landmasses presently and at the last glacial maximum.

COI data generation

We subjected a subset of COI data from a previous study [147] to different analyses to answer novel hypotheses about past population demography of a single species, rather than relationships between many species. Tissue samples for DNA extraction were obtained by removing a single hind leg from each specimen. Samples prior to 2015 were sequenced at the Canadian Centre for DNA Barcoding (CCDB) at the Biodiversity Institute of Ontario [32]. For these samples DNA amplification used the universal primer pair LepF1 and LepR2 [32,50]. For all other samples DNA extractions and PCR amplifications were completed at the South Australian Regional Facility for Molecular Ecology and Evolution (SARFMEE) and DNA sequencing and purification carried out at Macrogen Inc. (Korea). DNA extractions at SARFMEE were performed using a Gentra Puregene® DNA Purification kit (Gentra Systems Inc.) according to the manufacturer’s protocol. PCRs amplified a 710 bp fragment of the mtDNA (COI) gene using the primers LCO1490 (forward) and HCO2198 (reverse). The 25 µL PCR reactions comprised the following reagents: Sterile H_2O (15.9 µL), MRT buffer (5 µL), 1 µL (5 µM) of LCO1490, 1 µL (5 µM) of HCO2198, Immolase Taq (0.1 µL) and mtDNA from specimen (2 µL). The thermocycling regime comprised of one cycle at 94˚C for 10 minutes, then five cycles at 94˚C for 60 seconds, 46˚C for 90 seconds, 72˚C for 75 seconds, followed by 35 cycles at 94˚C for 60 seconds, 51˚C for 90 seconds, 72˚C for 75 seconds, followed by 72˚C for 10 minutes, and then 25˚C for 2 minutes.

Sequences were checked against the NCBI database using BLAST (blastn and blastx) to screen for non-*Homalictus* DNA. Forward and reverse sequences of each *H. fijiensis* specimen were aligned and checked for stop codons and/or nucleotide assignment errors using chromatograms examined with *Geneious* version 10.2.2 [53]. Any sequences with one or more base pairs that could not be reliably determined were excluded from the dataset. The *H. fijiensis* alignment was trimmed to 630 bp to remove primers and avoid spurious results that could arise from missing data in mismatch and Bayesian skyline coalescence analyses [54,55]. A total of 474 *H. fijiensis* sequences were analysed from across the entire Fijian archipelago including 309 sequences from the largest island of Viti Levu.

SNP data generation

We subjected the raw SNP data from a previous study [147] to more rigorous filtering and analyses that resulted in substantially changed subsets of the initial dataset that are more relevant to the present questions. The thorax and front legs were taken from 19 Viti Levu females from each of five species: *H. fijiensis, H. tuiwawae, H. ostridorsum, H. groomi,* and *H*. sp. *S* [99,139]. We used the solid-state method Diversity Arrays Technology in Canberra, Australia (DArTseq™) [127] to perform restriction site-associated DNA sequencing. DArTseq combines complexity reduction with a next generation sequencing platform in a conceptually-similar method to double digest RADseq [148]. The restriction enzymes PstI and Hpall were used.

A total of 62,426 SNP loci were called across all five sequenced species. We used the *R* package *DArTR* version 1.3.4 [128] to filter our data. The original SNP dataset was filtered to only include *H. fijiensis*. Monomorphic (non-variable) sites were then removed, leaving 7,719 loci. We then filtered these data to remove all missing data (4,046 loci remaining), for repeatability (percentage of scores that are repeated in the technical replicate dataset; 3,928 loci remaining) and to remove secondaries (multiple linked SNPs per fragment; 3,768 loci remaining). Genome-wide SNPs can suffer from large numbers of linked loci and this linkage can break assumptions of independence for many analyses, and bias results [149]. Hence, we analysed a wide variety of linkage disequilibrium (LD) filtering criteria. We filtered for linkage, removing loci with r^2 values below 0.9, 0.7, and 0.2, retaining 1,811, 1,646, and 171 loci, respectively. Linked loci were removed sequentially in order of most- to least-linked connections to retain loci that might otherwise be removed (Script S1). We used the latter five filtering levels in analyses.

Haplotype analyses of COI data

A minimum-spanning network [150] of our complete COI dataset was created using *PopART* version 1.7 [151]. *Geneious* version 10.2.2 [53] was used to examine unique haplotypes and amino acid sequences.

Mismatch analyses of COI data

Mismatch analyses, and extended Bayesian skyline plots (EBSPs), make several assumptions about the data provided, including that: (i) a random sample is drawn from the population, (ii) the population is panmictic, and (iii) largely neutral markers were used [54]. To examine panmixia, we used *Arlequin* version 3.11 [126] to examine pairwise F_{ST} values of COI haplotypes between all islands and combined island datasets that were not significantly different ($p > 0.05$). We then carried out mismatch analyses to explore whether past demographic changes could be explained by population expansion towards the present, graphing observed pairwise nucleotide differences with those expected under a recent population expansion, with 2,000 simulations used to generate an expected distribution of nucleotide differences. A unimodal distribution in a mismatch graph can be consistent with a sudden population expansion, whilst multimodal distributions can suggest past population bottlenecks or demographic structure [152].

Extended Bayesian skyline plots (EBSP) of COI data

We employed *PartitionFinder* version 2.1 [122] to determine the most appropriate model of molecular evolution for all COI datasets. Because the existence of population structure violates assumptions of panmixia [153] our all-islands dataset was not used in our final demographic Bayesian analyses. For the island groups with sample sizes >50 (see Appendix) — Viti Levu and Kadavu — we used extended Bayesian skyline plots of COI data sets in *BEAST* version 2.6.3 [56,124] to infer changes in historical demography. We restricted demographic EBSP analyses to the third codon position, where most synonymous mutations occur [154]. We applied a strict molecular clock and the best-fit *PartitionFinder 2* model, an HKY and an HKY+Γ substitution model for the Viti Levu and Kadavu populations, respectively. Four independent runs for each analysis were performed, to confirm stationarity. For the Viti Levu population, each run consisted of 4 chains with heating, carried out for 300 million iterations, resampling every 30,000th iteration using the *BEAST* package *CoupledMCMC* version 1.0.2 [155]. Multiple chains were required to properly sample across multiple possible optima in phylospace. For the Kadavu population, we used single chains with 500 million iterations sampled every 100,000th iteration. The log files from each run were examined in *Tracer* version 1.7.1 [156] and a burnin of 10% was used, which was always after stationarity had been achieved (effective sample sizes all exceeding 200). Log and tree files were combined using *LogCombiner* version 2.5.0 [157]. The EBSP log files were analysed with the *plotEBSP* script in *R* version 3.5 [157].

The estimated mutation rate of 1.09×10^{-7} per site per generation, based on only the 3rd codon position from the whole mitogenome of *Caenorhabditis elegans* [158] was applied to all of our EBSP plots to infer an approximate time scale in generation units. This directly-estimated mutation rate is appropriate for inferring recent demographic changes and is broadly consistent with other empirical values [159,160]. The AT bias of *C. elegans* (70.3% from 21 *C. elegans* COI sequences; BOLD [161]) is similar to that of our *H. fijiensis* COI fragment (74% from 474 *H. fijiensis* COI sequences). We converted the EBSP time scale from generations to chronological time by assuming four *Homalictus* generations per year, following Groom, *et al.* [47]. However, we also explored the effects of assuming three or five generations per year, which is analytically equivalent to assuming a faster or slower per-generation mutation rate.

For our reconstruction of island ancestral states, we analysed all three codon positions using within-island unique COI sequences and the *BEAST 2* package *CoupledMCMC* with eight chains and an EBSP tree prior. Four independent runs were performed, to confirm stationarity. We used two outgroup species — *H. groomi* and *H.* sp. O. The molecular data were allocated to a single partition to which we applied a single HKY+I substitution model and an uncorrelated relaxed clock model. "Island" was included in the analysis as a discrete trait given a symmetric change model and a strict clock (more complex models prevented this partition from converging). Each run was 100 million iterations, resampling every 20,000th iteration. Log files were examined in *Tracer* and a burnin of 10% was used. The maximum clade credibility tree as well as posterior support values were produced in *TreeAnnotator* version 2.6.3 [124] using median node heights. The tree was visualised in *FigTree* version 1.4.4 [162].

Extended Bayesian skyline plots and *Ne* using SNP data

We employed *PartitionFinder 2* to determine the most appropriate model of molecular evolution for each SNP dataset corresponding to the different levels of linkage filtering. For our SNP datasets, we ran EBSP analyses in *BEAST 2* using the following models: for our $LD_{R2=0.2}$ we used a K80 model, for $LD_{R2=0.7}$ and $LD_{R2=0.9}$ we used HKY+Γ, and for the remaining datasets (without and with secondaries — multiple SNPs on a single fragment — included) we used a GTR+Γ model. We used a relaxed log normal clock for all SNP EBSP analyses [100]. All runs except for that with secondaries were executed for 100 million iterations, sampling every 50,000th iteration, and were repeated four times to confirm convergence in EBSP results. For the run that kept secondaries, four heated-chain runs were carried out for 100 million iterations, resampling every 10,000th iteration using the *BEAST* package *CoupledMCMC*. The log files from each run were examined in *Tracer* and then combined using *LogCombiner* with a burnin of 20%, which was always after stationarity had been achieved (effective sample sizes all exceeding 200). The EBSP log files were analysed using *plotEBSP* [157].

Supplementary methods summary

We examined haplotype sample sizes required for robust demographic inference, using rarefaction analysis in *EstimateS* version 9.1.0 [163] (see Appendix). We also undertook nested sampling (*NS* package in *BEAST 2*) and used *DIYABC-RF* version

1.0.12 in *R* [164,165] to explicitly compare alternative possible demographic patterns (see Appendix).

Results

Geographic information systems

During the last glacial maximum, global sea-levels were approximately 120 m lower than today [19]. Using bathymetric data we can infer that many islands that are separate today might have been joined at the last glacial maximum (Fig. 1b). The removal or reduction of inter-island barriers could have made dispersal and inter-island colonisation achievable. Additionally, the subaerial landmass of the Fijian archipelago was potentially 2.6 times greater at the last glacial maximum ~26 kya and 2.2 times greater ~11.5 kya (see EBSP results below) than it is today (~21,000 km^2 today compared to ~56,000 km^2 at the last glacial maximum and ~47,000 km^2 ~11.5 kya; Fig. 1b). Hence, most of the reduction in subaerial landmass has occurred in the last 11,500 years (Fig. 1).

Haplotype analyses of COI data

In total, we found 67 haplotypes among the 474 all-islands specimens (Fig. 1). Of the 67 haplotypes, 16 each entailed eight unique amino acid sequences, two of which might have evolved convergently (Fig. 1a). From the Viti Levu population (n = 309 specimens) there were 27 haplotypes and these entailed only two amino acid sequence changes (Fig. 1a). The Kadavu sample (n = 109) consisted of 18 haplotypes and three amino acid differences (Fig. 1a). The smaller island groups in Fiji's south-west include 18 haplotypes, many of which tended to cluster near the Kadavu or Viti Levu haplotypes (Fig. 1). The other two large islands of Vanua Levu and Taveuni had a total of seven haplotypes, clustered with Viti Levu haplotypes (Fig. 1). However, sample sizes for all islands other than Viti Levu and Kadavu are low (Table S1). When restricted to 3rd codon positions we found 60 haplotypes across all islands, 24 haplotypes for the Viti Levu population and 17 haplotypes for the Kadavu population.

Mismatch analyses of COI data

From our *Arlequin* analyses the islands pairs of Fulqana and Ogea, Totoya and Moala, as well as Vanua Levu and Taveuni had non-significant population pairwise F_{ST}

values ($p > 0.05$) and were therefore combined (Table S2). Only Viti Levu and Kadavu had large sample sizes ($n \geq 50$; see Appendix) and are included in our main mismatch analyses results (Fig. 2, S1; Table 1, S1).

Mismatch analyses suggested that the sequences from the Viti Levu population are consistent with a recent population expansion, approximating the null model (Fig. 2). The Viti Levu population of *H. fijiensis* had a significant negative Tajima's D ($D = -1.81$, $p = 0.006$) and Fu's *Fs* ($Fs = -18.54$, $p = 0.0005$) (Table 1) [166]. The Kadavu population differs from the simulated frequencies and does not indicate a sudden population expansion (Fig. 2). Tajima's D and Fu's *Fs* for this population were non-significant (Table 1). Mismatch diagrams from the other islands also showed deviations from simulated values (Fig. S1), however sample sizes might be too small to draw reliable conclusions — e.g., López-Uribe, *et al.* [167].

Extended Bayesian skyline plots of COI data

Our COI analyses indicate that the *H. fijiensis* population on Viti Levu started expanding as long ago as ~3 kya, with a sharper increase beginning about ~2 kya (Fig. 3a). Prior to ~3 kya there were not enough inferred coalescent events to reliably interpret demographic patterns (Fig. S2c). During this time, the median *Ne* increased by a factor of eight (oldest $Ne \approx 0.01$ and present-day $Ne \approx 0.08$; Fig. 3; Table 2). Our COI analyses also indicate that the early *Ne* of the Viti Levu population was about a third that of Kadavu ($Ne \approx 0.03$) until ~1 kya — after the onset of slash and burn agriculture. Present-day absolute *Ne* values of ~734,000 for Viti Levu and ~275,000 for Kadavu are likely to be under-estimates; on Viti Levu *H. fijiensis* can be found in great abundance [65,99] (Table 2). The Kadavu population, in contrast to that on Viti Levu, shows no indication of population change in the last ~11,500 years for which demography can be inferred (Figs 3b and S2g-i). At about 11.5 kya, sea-level might have been ~50 m below current levels, yet temperatures were possibly similar to what they are today (Fig. 3). Assuming fewer (3) or more (5) annual generations, respectively, increases these ages by 33% or decreases them by 20% (Fig. S3).

Ancestral state reconstruction in *BEAST 2* provides most support for a Kadavu origin of *H. fijiensis*. Posterior probability support for the ancestral state of this node is low (PP = 0.35), but much larger than the next highest (Moala & Totoya; PP = 0.22) (Fig.

S4). Most of the deeper branches belong to the smaller south-eastern islands (Fig. 1b), with many nodes indicating dispersals from Kadavu (Fig. S4). The larger islands of Viti Levu, Taveuni, and Vanua Levu appear in a shallower clade, with Kadavu at its basal node (Fig. S4).

Extended Bayesian skyline plots and *Ne* using SNP data

All of our SNP EBSP analyses indicated broadly similar patterns of population expansion on Viti Levu. This is consistent with our COI results and indicates resilience of the retrieved patterns to SNP linkage filtering (Fig. 4). The biggest differences between the results of the datasets were (i) the length of the X-axes which ranged from ~0.1 (for no LD filtering) to 0.2 (for LD-filtered datasets) mutations/site and (ii) a variation in range of the median size of the increase in *Ne* (a ~2 times increase for $LD_{R2=0.2}$ when compared to the other levels of filtering; Fig. 4). Our median *Ne* values increased by a factor of between 154 to 327, depending on filtering level (Fig. 4; Table 2).

Supplementary results summary

We found that a minimum sample size of ~50 captured most haplotype variation (see Appendix). Our nested sampling and *DIYABC-RF* analyses broadly supported our primary demographic results (see Appendix).

Discussion

Groom, *et al.* [32] argued that Fijian *Homalictus* populations expanded strongly after the last glacial maximum and linked this to a warming climate and not human occupation. However, that study did not distinguish *H. fijiensis* from cryptic species, unrecognized at the time, that recent studies now allow us to overcome [99,139]. In addition, we also consider the effects of population genetic structure, and ensure that genetic markers include mostly synonymous substitutions, both of which are important for coalescent analyses of historical demography [54]. We now consider the results of our analyses and how these might correspond to the effects of climate change and human impacts on the ecology of Fijian native bees.

Haplotype and population genetic analyses of COI data

Our F_{ST} values and haplotype network analysis indicated significant population genetic structure among the different island groups (Fig. 1 and Table S2); not unusual for tropical island bees [90]. Interestingly, the Kadavu population harbours greater nucleotide diversity ($\pi = 3.15$; Table 1) than the Viti Levu population ($\pi = 1.53$; Table 1) despite Viti Levu being ~25 times larger in geographical size (642 km^2 for Kadavu and 10,388 km^2 for Viti Levu) (Fig. 1). Additionally, Kadavu haplotypes appeared to be intermediate between those from Viti Levu and the smaller islands in the south east, whereas haplotypes from the major islands of Vanua Levu and Taveuni are more connected to Viti Levu (Fig. 1). These northern islands are largest by far and appear to connect Kadavu (by least geographic distance) with the rest of the archipelago, particularly during the last glacial maximum. We might therefore expect these islands to harbour the most diversity and link the archipelago (Fig. 1). Hence the observed patterns seem counter-intuitive because the far greater size of Viti Levu should make the loss of genetic diversity through drift less frequent, and the gain in diversity through mutation more frequent. This contrasts with previous studies that suggest positive relationships between genetic diversity and island area [168-170]. There are three broad possibilities for this unusual finding: (i) the Kadavu population is older than the Viti Levu population and haplotype diversity on Viti Levu reflects accumulation of mutations subsequent to a relatively recent founder effect following extirpation (Fig. 5a); (ii) as above, except the Viti Levu population expanded from a local haplotype following a population bottleneck (Fig. 5b); or (iii) haplotype diversity on Viti Levu reflects an event that reduced mitochondrial diversity, such as a mitochondrial sweep, that did not occur on Kadavu (Fig. 5c).

Past demographies on Viti Levu and Kadavu

Mismatch analyses. In contrast to the Kadavu population, we found significantly negative Fu's *F*s [171] and Tajima's D [172] values for the Viti Levu population (Table 1). These values indicate an excess of rare alleles and low-frequency polymorphism, which could imply a recent population expansion (possibly following a founder event or bottleneck) [166,173]. Additionally, the Viti Levu mismatch diagram matched that expected under a sudden population increase (Fig. 2a), while the Kadavu mismatch showed a strong deviation from this expected pattern (Fig. 2b). While these parameters were originally designed to detect departures from neutrality [171,172], they can also be used for demographic inferences. In our case, because we chose the markers most likely to be neutral, our results should reflect changes in past demography.

Extended Bayesian skyline plot analyses using COI data. Our EBSP analyses of COI sequences concord with mismatch analyses, and additionally allow us to estimate how changes in effective mitochondrial population size have varied through time (Fig. 3a). These analyses indicated a substantial increase in *H. fijiensis* population size for Viti Levu (starting ~3 kya), but little or no increase for Kadavu (over ~11,500 years). A sudden recent population expansion could also explain the lower nucleotide diversity (π) on Viti Levu as such haplotypes should be more-similar than if populations had been stable with mutations accumulating over a longer time period, as on Kadavu (Fig. 5). The Viti Levu analyses suggested an increase in population sizes beginning approximately 3 kya and accelerating from about 2 kya (Fig. 3a). While our COI-based mismatch and EBSP analyses used the same sequence data sets, they differ in analytical approaches. Concordance of results from the above approaches suggests that the Viti Levu and Kadavu populations have indeed differed in their mitochondrial demographic history.

Ancestral state reconstruction indicated that *H. fijiensis* originated, or at least maintained the oldest lineages, on Kadavu and that there have been many dispersals from Kadavu to other islands (Fig. S4). The analysis also suggests strong geographic structure with many older lineages found on the smaller south-eastern islands (Figs 1 and S4). The large northern islands — Viti Levu, Taveuni and Vanua Levu — all appear to form a more-recent lineage (Fig. S4). This is congruent with an older Kadavu population and more-recent Kadavu-derived Viti Levu diversification. The occurrence of Matuku and Ono-i-Lau haplotypes amongst the northern island lineage is unusual and might represent a more-recent, and potentially human-mediated, dispersal; however, this requires more data to determine and is beyond the scope of our hypotheses.

Extended Bayesian skyline plots using SNP data. Our EBSP analyses of SNP loci for the Viti Levu samples concord with our analyses of COI data by also indicating major population expansion towards the present (Fig. 4). Combined with the above results, these data support possibility i above (Fig. 5a); the Viti Levu population expansion likely followed a founding event from the older Kadavu population, perhaps after extirpation on Viti Levu. Extirpation or haplotype replacement of *H. fijiensis* on Viti Levu could conceivably be explained by competition from the massive highland *Homalictus* diversity on the large and topographically-complex northern islands [99,139] as they moved into lowland regions combined with cooler and potentially less-favourable conditions during the last glacial maximum.

Our COI and SNP analyses diverged in the estimated magnitude of *Ne* increase. Our COI analyses indicated an eight-fold increase in *Ne,* while our SNP data predicted increases of between 154 and 327 times (Figs 3 and 4; Table 2). The upper estimate of 327 ($LD_{R2 = 0.2}$) far-exceeded the next highest value of 180 times increase ($LD_{R2=0.9}$). This might be expected as linkage disequilibrium can decrease contemporary *Ne* estimates [174]. Estimates of *Ne* from mitochondrial data might also be expected to be about one third that of haplo-diploid autosomal DNA [175]. Yet, because our SNP data contains many more informative sites, we might expect it to provide a better estimation of past demographic patterns than our COI data.

We do not attempt to date our SNP-inferred demographic changes because dating SNP phylogenies based on mutation rates is not yet common practice with robust protocols and we cannot justify the assumptions behind the use of such methods for our data set — e.g., [176]. Additionally, we lack SNP data for the Kadavu population and so we could not examine if genomic patterns matched the stable past demography shown by our COI analyses (Fig. 3). However, we are unaware of a population genetic scenario that would leave mtDNA *Ne* unchanged following a large autosomal *Ne* increase.

The possible causes of population expansion on Viti Levu could be: (i) changing climate, (ii) human modification of the environment, or (iii) both (Figs 2 and 3). Whatever the driver is, it apparently did not act on the Kadavu population (Figs 2, 3 and S2).

Potential drivers of demographies

Sea-levels and subaerial landmass. Changes in sea-level and subaerial landmass might be expected to impact past demographies of species [120]. Global sea-levels began to rise ~26 kya and continued to rise in a major way until ~5 kya [177]. Hence, we might expect to see a decline in bee population sizes in that time if landmass was a key driver of demography. Our GIS analyses indicated that the Fijian islands were larger by a factor of ~2.6 (26 kya when sea-levels were ~120 m lower than today), ~2.2 (11.5 kya when sea levels were ~50 m below current levels), and better-connected (Fig. 1). The largest Fijian islands, the northern islands of Viti Levu, Vanua Levu, and Taveuni, were better connected and larger than they are today (Fig. 1). Similarly, Kadavu was larger in size than it is today and was somewhat less isolated from the other islands (Fig. 1). Although our inferred timeframes do not entirely overlap with that time period, the Kadavu EBSP extends back ~11.5 kya to when sea-levels were ~50 m below current levels and shows no sign of population decrease [177] (Fig. 3). Consequently, sea-level change is unlikely to be a major driver for our inferred changes in *H. fijiensis* demography on Viti Levu.

Mean sea-surface temperatures. Although global mean temperatures have varied considerably since the last glacial maximum, there has been little substantial change over the last 11,500 years, with a cooling trend over that time [178] (Fig. 3). Similar to sea-levels and landmass, changes in sea-surface temperatures (as a proxy for air temperature) are unlikely to have driven demographic patterns in *H. fijiensis* over the past 11,500 years (Fig. 3).

Human occupation of Fiji. Human occupation of Fiji is thought to have begun ~3 kya. Substantial modification of non-coastal regions began ~2.5 kya, with movement into inland highland regions by ~2.1 kya, and the earliest evidence of slash-and-burn agriculture starting shortly thereafter at ~1.8 kya [25-27]. Clearing of vegetation and alteration of the landscape by humans might have been beneficial for *H. fijiensis* populations for two reasons. Firstly, *H. fijiensis* is a ground-nesting bee that requires open and sunny nesting areas [99]. Secondly, *H. fijiensis* is a super-generalist pollinator, capable of using native, invasive and Aboriginally-introduced resources from a broader floral range in Fiji than even the archetypal super-generalist pollinator, the European honeybee (*Apis mellifera* Linnaeus, 1758) [98,145]. Both of these life-history traits are likely to enable *H. fijiensis* to benefit from the disturbed and weedy habitats that might be associated with land-use intensification or slash and burn agriculture. Importantly, our inferred increases in the population size of *H. fijiensis* coincide with human-mediated changes in landscape use and do not coincide with changes in climate. This pattern remains plausible if assuming three, four or five generations per year; all of which are possible as suggested by Groom, *et al.* [47] (Fig. S3).

In contrast to Viti Levu, the mismatch and demographic analyses for the Kadavu *H. fijiensis* population shows essentially no demographic change in at least the past 11,500 years for which demographic patterns can be inferred (Figs 2 and 3). Although Kadavu, and its surrounding islands, are relatively large in size (642 km^2) it differs strongly from Viti Levu in terms of both landscapes and human occupation. Over 78% of Kadavu has steep slopes of above 18°, and a surrounding reef that is often in close proximity to the shore, making it a far less hospitable location for human occupation than Viti Levu [179]. Volcanic activity since early human colonisation [180] could have also impeded population and development resulting in reduced landscape modification by humans. The vegetation on Kadavu remains relatively intact, while Viti Levu has been heavily cleared in the distant and recent past [25,102]. Hence, stable population sizes of *H. fijiensis* on Kadavu might reflect the differing amounts of clearing between Viti Levu and Kadavu, with Kadavu almost acting as a control for human-modification of the environment.

Conclusions

The considerations and arguments above can be summarized by several key points, namely:

(i) There is substantial population genetic structure between multiple islands or island groups based on the mitochondrial gene COI, indicating a lack of panmixis for *H. fijiensis* across the Fijian archipelago. This structure precludes the use of coalescent and mismatch analyses that combine different island samples.

(ii) When mismatch and coalescence analyses are restricted to the two islands (Viti Levu and Kadavu) where COI sequence sample sizes are substantial ($n > 50$), we found significant differences in inferred patterns of historical demography. The Viti Levu population showed strong signs of population expansion towards the present (supports hypothesis i), but Kadavu exhibited stasis in population size over the past 11,500 years for which demographies could be inferred (falsifies hypothesis i).

(iii) Analyses of genome-wide SNP data for Viti Levu specimens show that the recent population expansion inferred from mitochondrial sequences implies an increase in actual population size, rather than a mitochondrial sweep (supports hypothesis i).

(iv) Our dated COI demographic reconstruction indicates population expansion that correlates with the arrival of the Lapita people and the following intensification of land-use on Viti Levu, and not changing climates (falsifies hypothesis ii).

(v) We found no evidence of demographic change in the past 11,500 years on Kadavu, despite changing climates during this time (falsifies hypothesis ii). Similarly, there is no evidence for human-mediated demographic changes on Kadavu during this time — likely due to low-levels of human modification of the environment.

We accept hypothesis i — increasing *Ne* in the recent past — for Viti Levu but reject it for Kadavu. We reject hypothesis ii — effective populations size changes mediated by past climate change — on both islands and provide support for a human-mediated hypothesis on Viti Levu. However, we do note that *H. fijiensis* appears to be less resilient to changing climates than the alien bee species *Braunsapis puangensis* (Cockerell, 1929) and *Ceratina dentipes* Friese, 1914 [182]. Additionally, our demographic analyses do not include past major changes in sea surface temperature (Fig. 3); given the narrow thermal tolerance of tropical ectotherms [91,92] and the results of da Silva*, et al.* [182], our results do not suggest that *H. fijiensis* is resilient to changing climates. However, *H. fijiensis* does appear to be more eurythermic (tolerates a broader temperature range) than most other Fijian *Homalictus* species [139].

Our data demonstrate that invertebrates, particularly multivoltine species, can be used to determine very recent demographic patterns. Few other empirical studies have achieved this using terrestrial invertebrates. López-Uribe, *et al.* [167] was able to use demographic analyses to infer a geographic co-expansion of the squash bee, *Peponapis pruinose* (Say, 1837), with the cultivation of its host plants from ~5 kya.

Similarly, Silva, *et al.* [184] found a very recent (300-400 years ago) expansion of the pest soybean looper moth, *Chrysodeixis includens*, that was perhaps related to human colonisation and agriculture. Some other studies have examined past demography using Bayesian methods with variable results, but most infer older and often climate-related demographies (e.g., López-Uribe, *et al.* [167] and references therein). However, some studies might violate assumptions of panmixia and marker neutrality. Importantly, we show that past demographies of invertebrates can also be used to contrast human-driven and climate-driven disturbance. Tropical insular invertebrate taxa are likely to be ideal in both respects. In turn, such analyses could be used to infer changes in invertebrate-associated taxa. For example, it might be possible to infer declines in megafauna by examining the past demography of associated taxa (e.g., ticks, mites or dung beetles).

Supporting information

Acknowledgments

We thank Marika Tuiwawa and Alivereti Naikatini, for their invaluable assistance with Fijian field logistics, and Flinders University students who helped collect specimens in 2015-2017, particularly Cale Matthews, Justin Biddle, and Rebecca Schober for their dedication to highland collections in 2017. Additional thanks go to the bodies who funded this research, including: the Australia and Pacific Science Foundation, the Australian Department of Foreign Affairs and Trade (via the New Colombo Plan program), the Playford Trust (PhD scholarship), and Flinders University (AJ and IM Naylon PhD Scholarship). This work was completed under permit number 1755-11.

Author Contributions

JBD conceived the study; JBD, MSYL, and MPS developed the research design; JBD, SVCG, MIS, and MPS undertook field work; AVC completed all laboratory work; JBD, MSYL, and MPS completed analyses; JBD, MPS, and SVCG wrote the manuscript; JBD created figures and tables; all authors gave their final approval for publication.

Competing interests

The authors declare no competing interests

Data accessibility

This study is based on previously published data, the raw versions of which can be found on Dryad [147]. New run-files will be uploaded to Dryad upon acceptance of the manuscript.

Tables

Table 1. COI sample size (*n*), number of polymorphic sites (S), nucleotide diversity (π), Tajima's D and Fu's *F*s with *p*-values in parentheses for the Fijian islands Kadavu and Viti Levu. Significant values are bolded. A significant negative Tajima's D indicates an excess of low-frequency polymorphisms comparative to expectations; significant positive Tajima's D values indicate lower amounts of low and high frequency polymorphisms [166]. A significant negative Fu's *Fs* indicates an excess of alleles, as predicted for genetic hitchhiking or population expansion; while significant positive values indicate allele deficiency as expected for recent population bottlenecks [166].

Islands	***n***	**S**	π	**Tajima's D (*p*-value)**	**Fu's *Fs* (*p*-value)**
Kadavu	109	25	3.15	-0.99 (0.159)	-3.56 (0.130)
Viti Levu	309	29	1.53	**-1.81 (0.006)**	**-18.54 (0.00005)**

Table 2. The median effective population size (*Ne*) values for each extended Bayesian skyline plot analysis along with the data used (mitochondrial COI or autosomal SNPs). Values are the initial *Ne* (oldest value), final *Ne* (present-day value) and the factor of increase from initial to final (Figures 3 and 4). Parentheses indicate absolute female *Ne* (in thousands) for COI data, where mutation rates have been applied.

Analysis	**Data Used**	**Initial *Ne***	**Final *Ne***	**Increase factor**
Viti Levu	COI	0.01 (92 k)	0.08 (734 k)	8
Kadavu	COI	0.03 (275 k)	0.03 (275 k)	1
Viti Levu, $\text{LD}_{\text{R2 = 0.2}}$	SNP	0.03	9.8	327
Viti Levu, $\text{LD}_{\text{R2 = 0.7}}$	SNP	0.03	5.16	172
Viti Levu, $\text{LD}_{\text{R2 = 0.9}}$	SNP	0.03	5.39	180
Viti Levu, no secondaries	SNP	0.02	3.27	164
Viti Levu, with secondaries	SNP	0.02	3.08	154

Figures

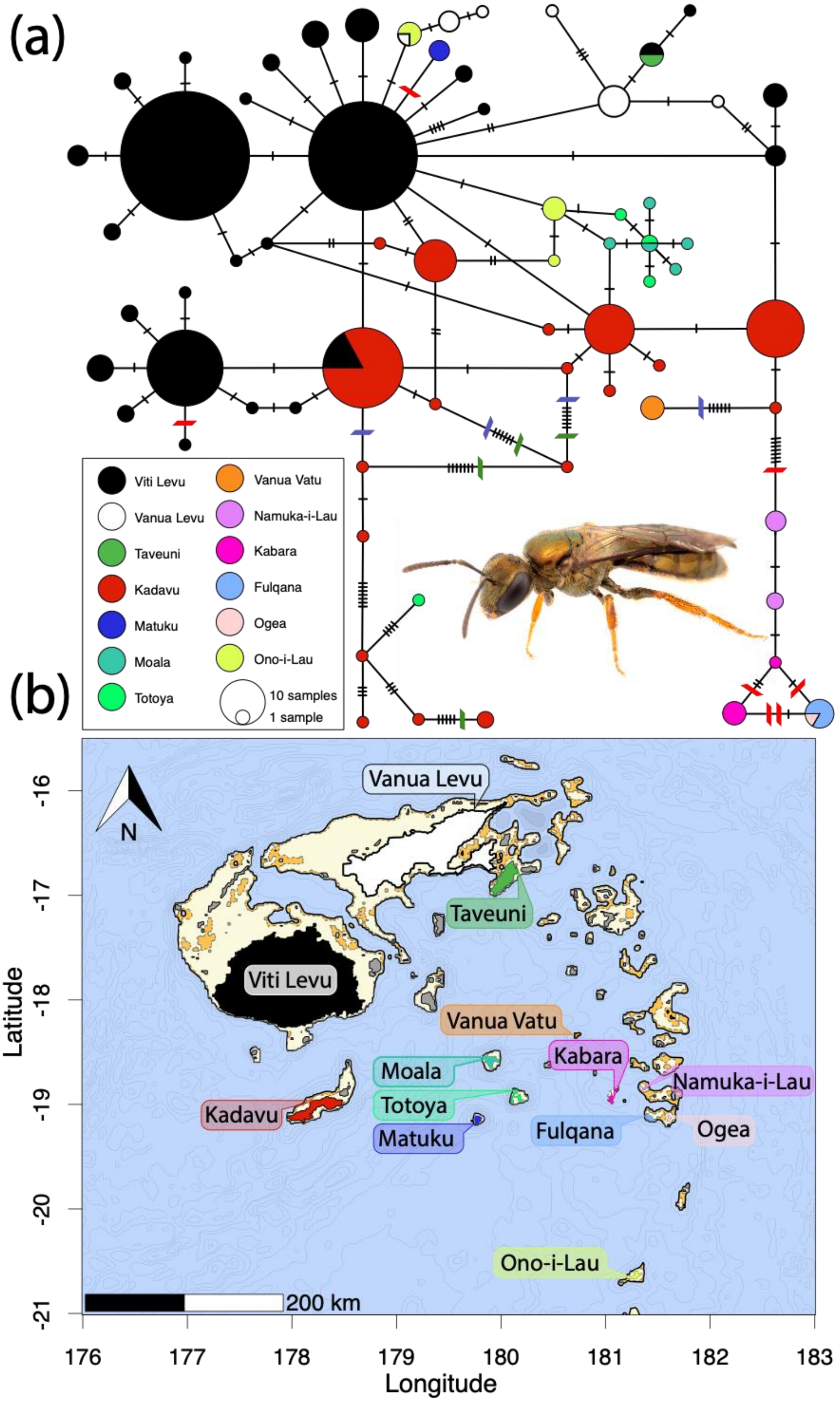

Figure 1. (a) a COI haplotype network of *Homalictus fijiensis* (using all codons) coloured by (b) island in the Fijian archipelago. Simple hatch-marks represent nucleotide changes. Red hatch-marks represent various amino acid changes and green and blue hatch-marks represent

amino acid changes from Ile (ATT) to Val (GTT) at positions 85 and 469 respectively. Bee is a female *H. fijiensis*. Pale yellow shading with dashed grey lines on the (b) map indicates approximate subaerial landmass when sea-level was 50 m below current levels (~11.5 kya) and orange shading and with solid black lines indicates when sea-level was 120 m below current levels (~26 kya) [19,177]. The large northern islands are (black) Viti Levu, (white) Vanua Levu, and (dark green) Taveuni. The smaller south eastern islands are (dark blue) Matuku, (blue-green) Moala, (light green) Totoya, (orange) Vanua Vatu, (pale pink) Namuka-i-Lau, (dark pink) Kabara, (light blue) Fulqana, (salmon) Ogea, and (yellow) Ono-i-Lau.

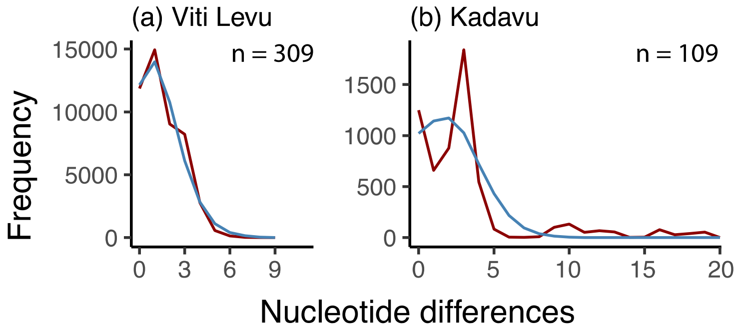

Figure 2. (red) Observed and (blue) simulated pairwise haplotype frequencies based on COI haplotypes (630 bp) of *Homalictus fijiensis* from Fijian islands where n ≥50.

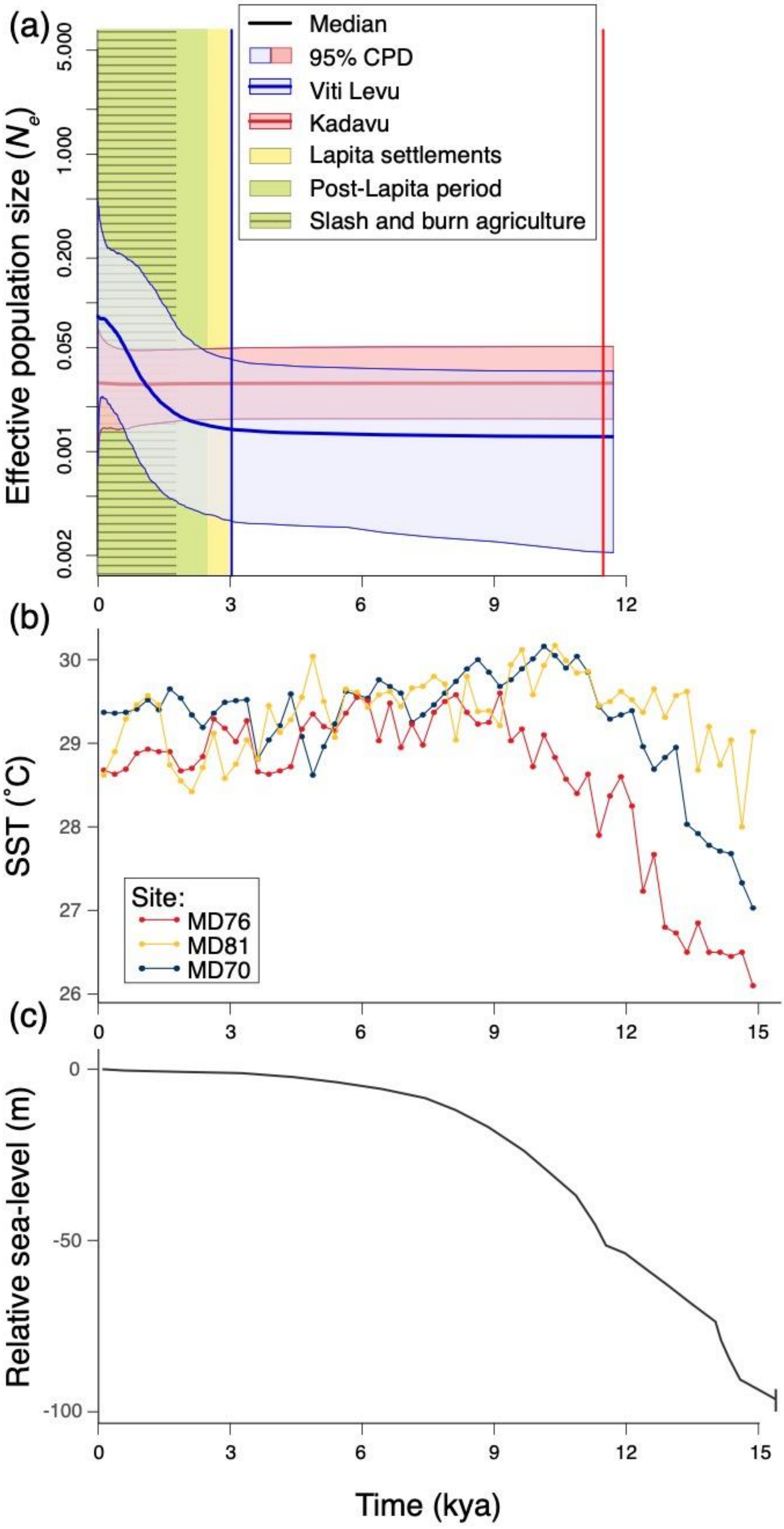

Figure 3. An (a) extended Bayesian skyline plot using the third codon position of COI for *Homalictus fijiensis* on (purple) Viti Levu and (red) Kadavu. The y-axis indicates effective

population size (*Ne*) on a $\log_{10}$ scale. The dark solid lines indicate the median *Ne*s and the light shading indicates the 95% CPDs. The vertical column shading indicates (yellow; ~3 kya) first evidence of the Lapita, (green; ~2.5 kya) first evidence of the post-Lapita period and (horizontal hashing; 1.8 kya) first evidence of slash and burn agriculture on Viti Levu [25,27]. The red and purple vertical lines in a indicate the points beyond which demography should not be interpreted for Viti Levu and Kadavu, respectively, based on Fig. S2c. Full extended Bayesian skyline plot output plots are available in Fig. S2. The (b) mean sea surface temperature (SST; ˚C) for three sites, (red) MD76, (yellow) MD81, and (blue) MD70, in the West Pacific based off data from [178]. And (c) relative sea-level (meters) in Barbados where the line indicates the ICE-5G (VM2) model fit [185]. All panels share their x-axis scale — time in thousands of years ago (kya) — which extends from the left (present) to the right (12 or 15 kya).

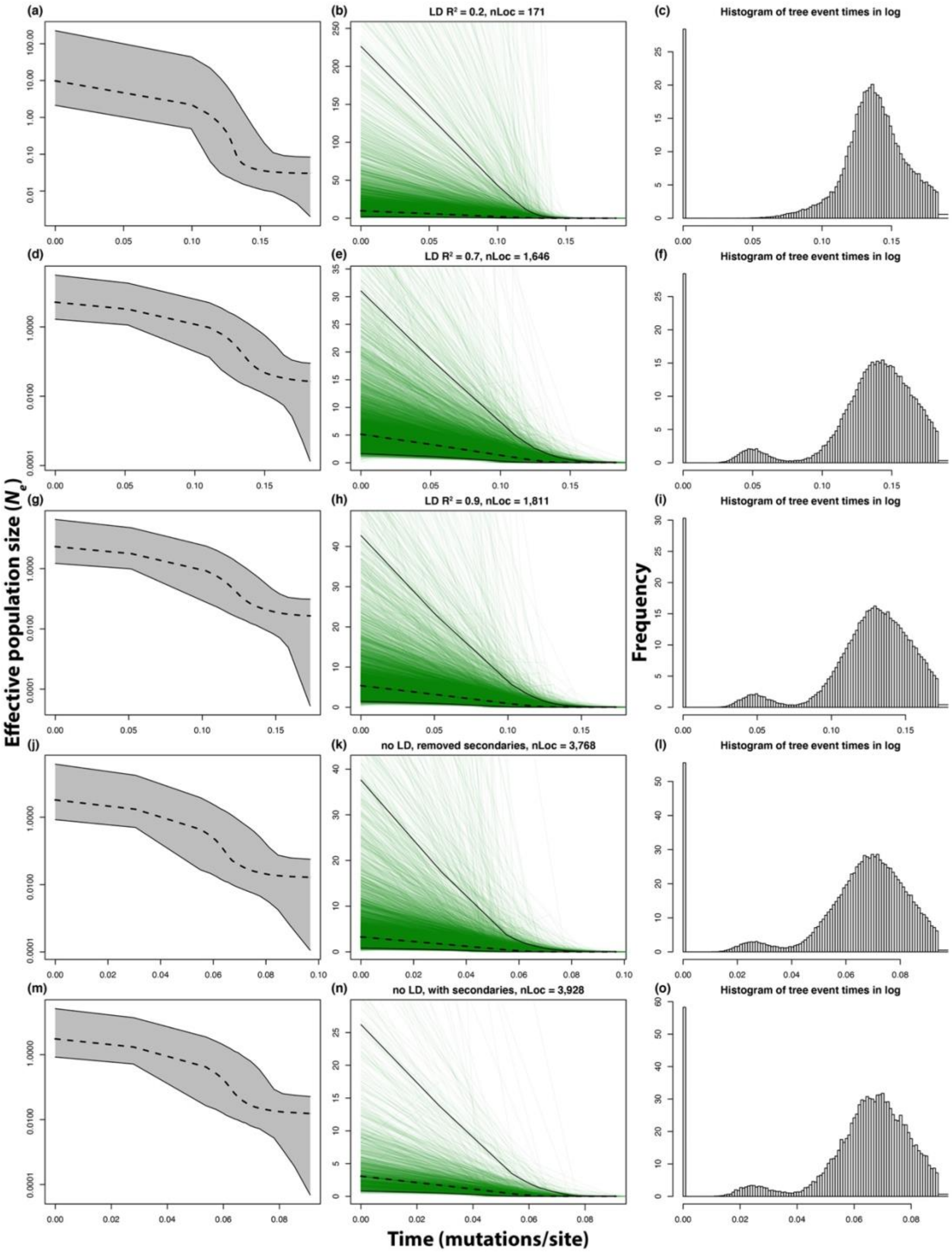

Figure 4. Results from extended Bayesian skyline plots of *Homalictus fijiensis* using SNP data from Viti Levu with several levels of filtering. In order of strongest to weakest filtering: (a-c) $R^2 = 0.2$ resulting in 171 loci, (d-f) $R^2 = 0.7$ resulting in 1,646 loci, (g-i) $R^2 = 0.9$ resulting in 1,811 loci, (j-k) no linkage filtering and removed secondary loci resulting in 3,768 loci, and (m-o) no linkage filtering and kept secondary loci resulting in 3,928 loci. Leftmost and central figures show median (dotted lines) and 95% CPDs (solid lines), while the central figures also show the actual sampled population distributions. Rightmost figures

indicate counts of tree (coalescence) events through time. The y-axes of the leftmost column indicates effective population size (*Ne*) on a $\log_{10}$ scale, while the middle column has *Ne* on a linear scale (see main text). The y-axes of the rightmost column indicates frequency.

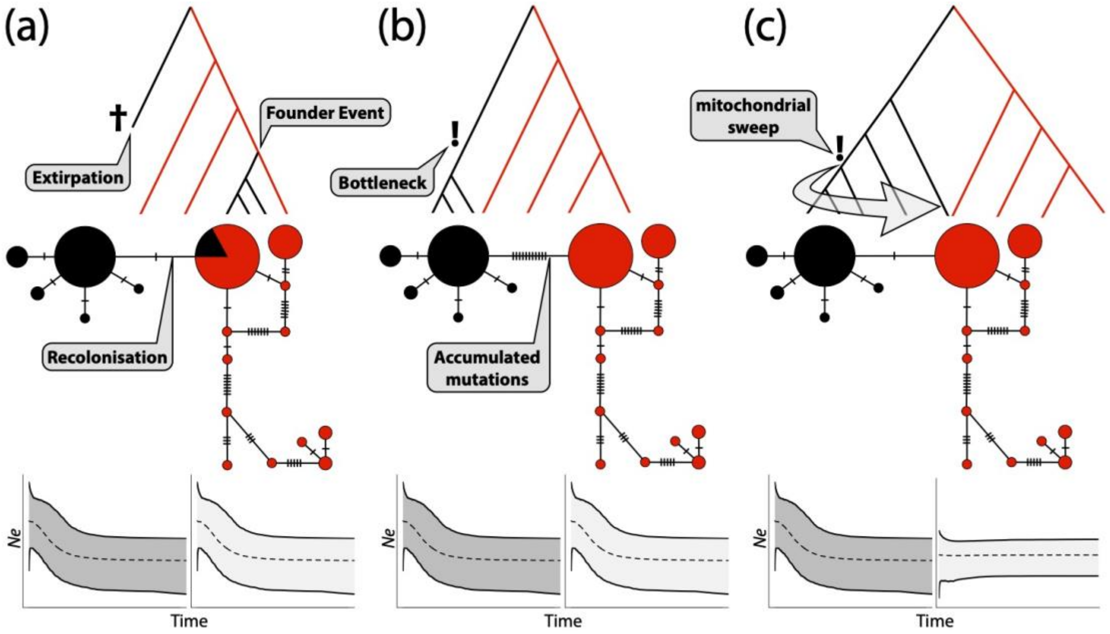

Figure 5. Diagrammatic examples based loosely on our data of the (top row) three scenarios of actual phylogenetic events that could explain the patterns observed and the evidence required to distinguish between them; (middle row) haplotype networks and (bottom row) past demography of (dark grey) COI data and (light grey) SNP data. Possibility A could be explained by: (a) Extirpation (†) or COI haplotype replacement on Viti Levu followed by a founder event (recolonisation) from Kadavu as typified by a highly similar COI haplotypes and increasing COI and SNP effective population sizes (*Ne*). Or (b) a genuine population bottleneck (!) that would be exemplified by highly dissimilar COI haplotypes between the islands and increasing COI and SNP *Ne*. Possibility (c) could be explained by a mitochondrial sweep (! and arrow) as typified by an inferred *Ne* increase in the COI past demography and stable *Ne* in the SNP past demography.

Supplementary material

Appendix

Estimating sample sizes needed for historical demography analyses

A key issue in our demographic analyses concerns the sample sizes needed to conduct meaningful coalescent analyses for historical demography. Very generally, smaller sample sizes lead to wider confidence limits in any estimated parameters.

Bayesian Skyline Plots (BSP), Extended Bayesian Skyline Plots (EBSP), and mismatch analyses all rely on assumptions that assayed samples capture enough (and unbiased) genetic variation for coalescent-based analyses to enable reasonable inferences. For haplotype data, such as mtDNA sequences, these analyses depend on both the number of haplotypes as well as their relative frequencies. Both measurements will be subject to sample size.

We can think of the number of distinct haplotypes as akin to 'species richness' in ecological studies, and the evenness in the frequencies of haplotypes as akin to relative species abundances. These two features are captured in ecological studies that use diversity indices. Perhaps the most widely deployed diversity index used in such studies is Shannon's diversity index, which is calculated as:

$$H' = -\sum_{i=1}^{R} p_i \ln p_i$$

Where, in our case, p_i is the proportion of individuals having haplotype i and R is the number of distinct haplotypes.

For both Viti Levu and Kadavu samples, we counted the number of individuals assayed for each unique haplotype. These counts were then used in rarefaction analyses using the *EstimateS* software package version 9.1.0 for Macintosh [163]. We calculated Shannon's diversity index as a function of each addition of a randomly sampled individual (sampled without replacement) with 10,000 randomizations for each individual entry. Standard deviations for each Shannon's diversity index were calculated for each entry step.

Resulting analyses for Shannon's diversity index are given in Fig. S5a (Viti Levu) and Fig. S5b (Kadavu) where we had sample sizes of 309 and 109 individuals, respectively. Both plots indicate a steep rise in the estimated index up until about 50 sampled haplotypes, after which slopes tend to plateau. It is clear in both these plots that sample sizes less than ~30-50 would fail to capture a substantial amount of total diversity, but that larger sample sizes would only increase estimate diversity in successively smaller increments.

Whilst sample sizes for Viti Levu and Kadavu were quite large, all other Fijian islands had sample sizes ≤ 16. If those islands held similar haplotype diversity to either Viti Levu or

Kadavu, our sample sizes would grossly under-estimate that diversity. Since we cannot *a priori* discount such possibilities, coalescent analyses of those smaller island samples could be very misleading and are hence omitted.

Additional comparison of demographic patterns

BEAST analyses

We additionally analysed demographic patterns using different tree models in *BEAST* version 2.6.3 [124]. For our COI data from Viti Levu and Kadavu as well as our SNP data from Viti Levu, we used an exponential positive, negative and constant (growth rate = 0) tree model. We then compared these models using the *NS* (nested sampling) package in *BEAST 2* [125].

These results provide support for: (i) constant population size on Kadavu, (ii) negative population growth on Viti Levu using COI data, and (iii) positive population growth on Viti Levu using SNP data (Table S3). The Viti Levu analysis using COI data differs from our EBSP analysis. This is likely due to the more-complex demographic pattern uncovered using the EBSP — constant population size followed by sudden growth nearer to the present (Fig. 3a) — that cannot be recovered when using a simple exponential growth tree model.

In comparison, our EBSP models show that there is a probability of ~0.94 that the Viti Levu population size has increased, regardless of the clock model employed (Fig. S6).

DIYABC-RF analysis

Our additional *BEAST 2* analyses did not distinguishing between demographic models using our Viti Levu COI data well. To better address this issue we undertook additional analyses using explicit model comparisons in the program *DIYABC-RF* (do-it-yourself approximate Bayesian computations using Random Forests machine learning) [164,165]. We examined four discrete scenarios of demographic patterns between Viti Levu and Kadavu, using Vanua Vatu as an outgroup (Fig. S7a).

- Scenario 1: Dispersal from Kadavu to Viti Levu. Founder effect on Viti Levu followed by expansion.
- Scenario 2: Dispersal from Viti Levu to Kadavu then population expansion on Viti Levu.
- Scenario 3: Dispersal from Viti Levu to Kadavu, no change in population size.
- Scenario 4: Dispersal from Kadavu to Viti Levu, no change in population size.

We split the COI fragment into first, second, and third codon positions and applied an HKY+I substitution model to the first and an HKY substitution model to the second and third. We used broad uniform distributions for all effective population size (*Ne*) and time priors. We restricted *Ne* priors — Ne1 < Ne3 < Ne8 — and time priors — t1 < t2 < t3. We ran 100,000 simulated datasets (~25,000 per scenario) and considered 80,000 of these in each Random Forest training set. We then created five noise variables and ran 10,000 Random Forest trees.

Scenario two received the most votes (7,292/10,000 votes; posterior probability: 0.89) and is hence considered the most-likely of the four models (Fig. S7). This result agrees with our COI EBSP from Viti Levu in that there was population increase. In contrast to our previous results, this scenario does not support a Kadavu origin. However, the analysis does not include all islands and we still consider our *BEAST 2* analyses to be more accurate in this regard.

Supplementary tables

All data supplementary tables can be downloaded from the Molecular Ecology website at https://onlinelibrary.wiley.com/action/downloadSupplement?doi=10.1111%2Fmec.16034&file=mec16034-sup-0008-TableS1-S3.xlsx

Table S1. Various statistics including sample size, nucleotide diversity (π), Tajima's D and Fu's *F*s with p-values indicated for the Fijian islands sampled. Significant values are bolded. A significant negative Tajima's D indicates an excess of low-frequency polymorphisms comparative to expectations; significant positive Tajima's D values indicate lower amounts of low and high frequency polymorphisms [166]. A significant negative Fu's *Fs* indicates an excess of alleles, as predicted for genetic hitchhiking or population expansion; while significant positive values indicate allele deficiency as expected for recent population bottlenecks [166].

Table S2. Population pairwise F_{ST} values between island groups with *p*-values in parentheses. All values are significant ($p \leq 0.05$).

Table S3. The results of the nested sampling tree model comparisons of the Kadavu COI, Viti Levu COI, and Viti Levu SNP demographic reconstructions for *Homalictus fijiensis*. All analyses used an exponential growth model with a uniform distribution that was fixed at zero (constant), positive (>0) or negative (<0). The marginal likelihood values that were best-supported are in bold and standard deviations are provided. The respective final growth rates are also given for each analysis.

Run	Analysis	Marginal likelihood	SD	Growth rate end
Kadavu	Constant	**-579.56**	1.41	NA
Kadavu	Positive	-596.7	1.45	51.17
Kadavu	Negative	-584.29	1.46	-38.61
Viti Levu COI	Constant	-944.2	2.21	NA
Viti Levu COI	Positive	-942.12	2.22	3.031
Viti Levu COI	Negative	**-937.34**	2.32	-30.52
Viti Levu SNP	Constant	-13690.69	1.1	NA
Viti Levu SNP	Positive	**-13663.15**	0.9	69.67
Viti Levu SNP	Negative	-13691.52	1.07	-0.75

Supplementary figures

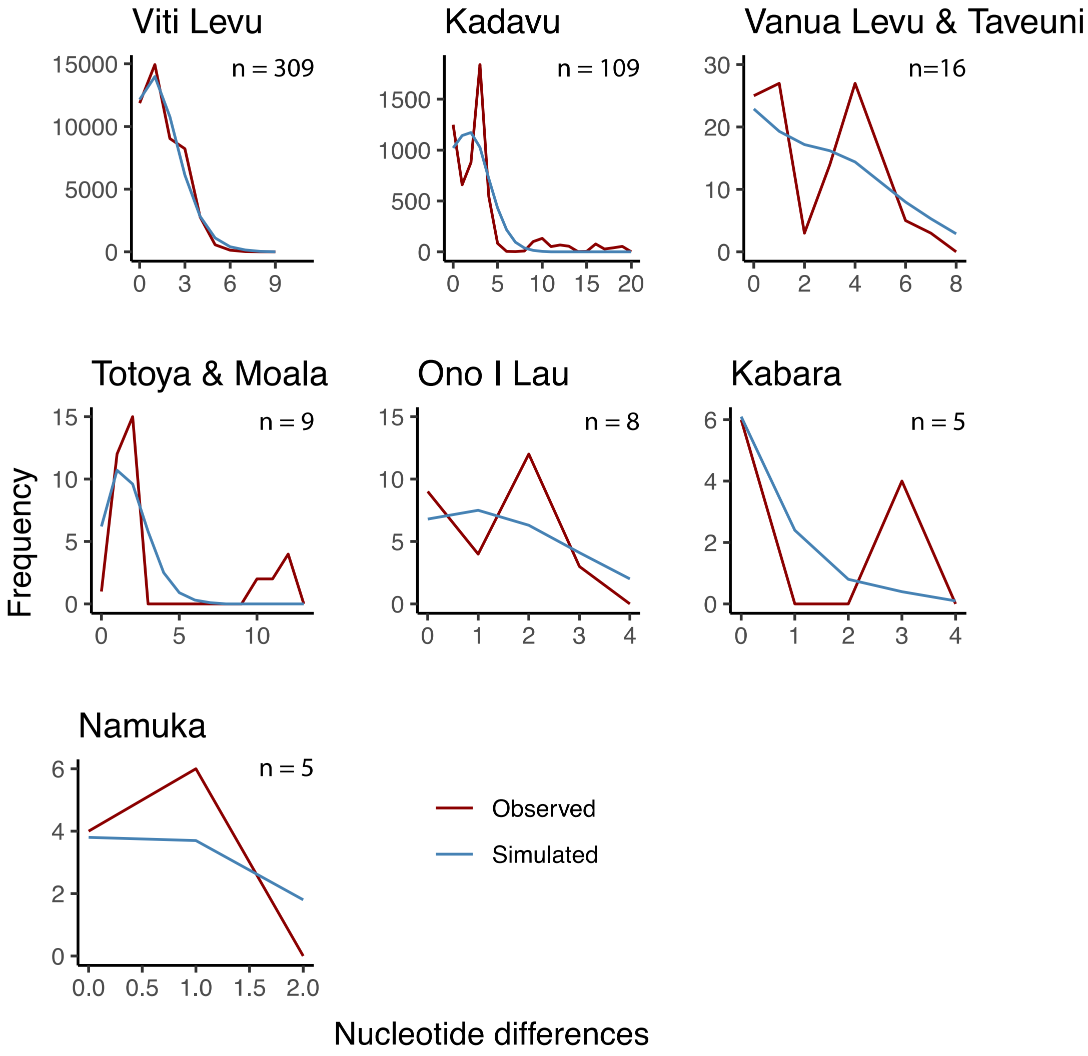

Figure S1. (red) Observed and (blue) simulated pairwise haplotype frequencies based on COI haplotypes (630 bp) of *Homalictus fijiensis* from Fijian islands where there were multiple haplotypes. Note: X-axes vary greatly.

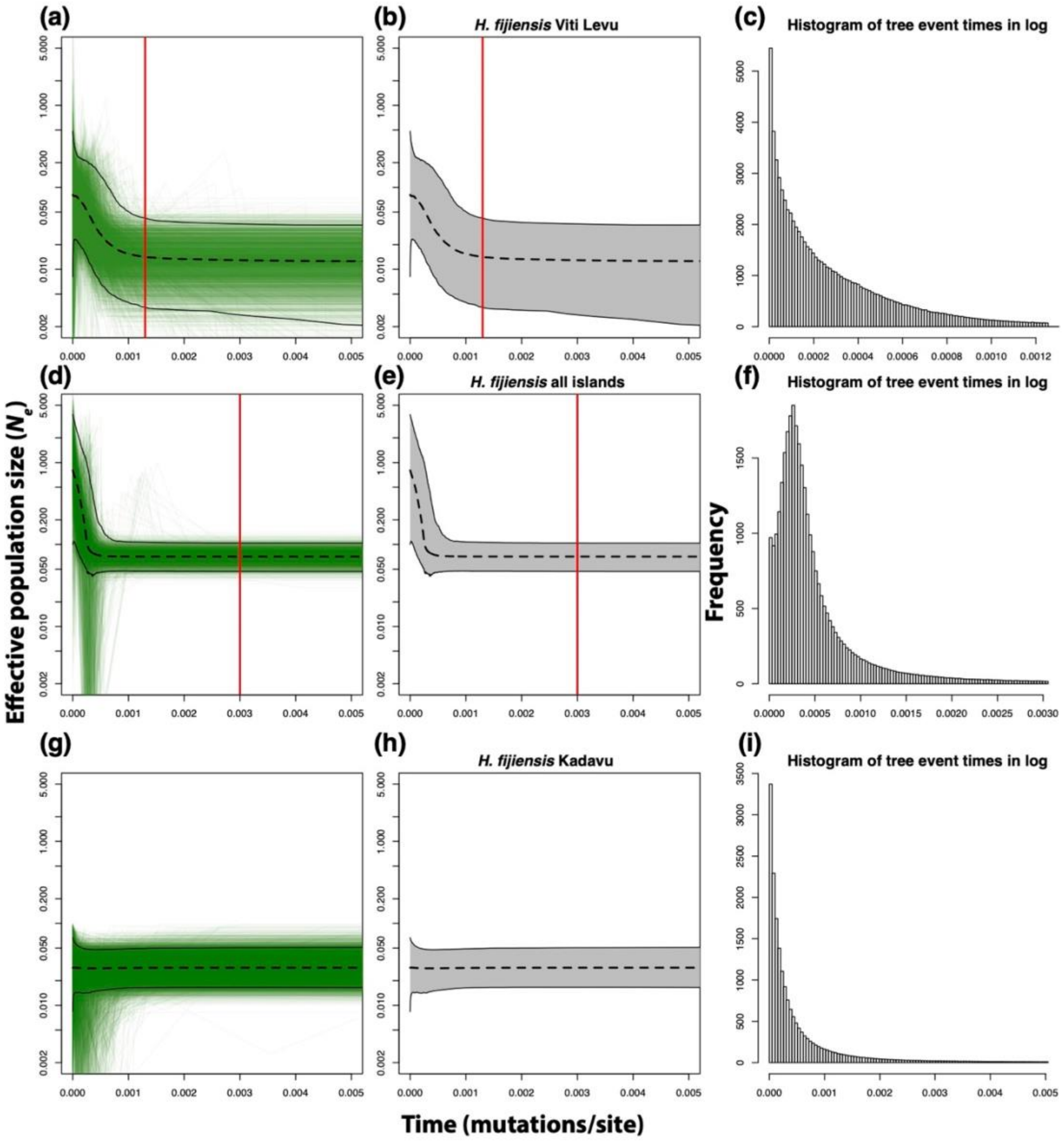

Figure S2. Results from extended Bayesian skyline plots of *Homalictus fijiensis* from (a-c) Viti Levu, (d-f) all islands, and (g-i) Kadavu. Analyses used only the third codon of the COI gene. Leftmost and central figures show median (dotted lines) and 95% CPDs (solid lines), while the leftmost figures also show the actual sampled population distributions. Rightmost figures indicate counts of tree (coalescence) events through time. The red line in a, b, d, and e indicates the point beyond which demography should not be interpreted, based on c and f. Both axes of the leftmost and central figures are identical to improve interpretation. The y-axes of the leftmost two columns indicate effective population size (*Ne*) on a $\log_{10}$ scale. The y-axes of the rightmost column indicates frequency.

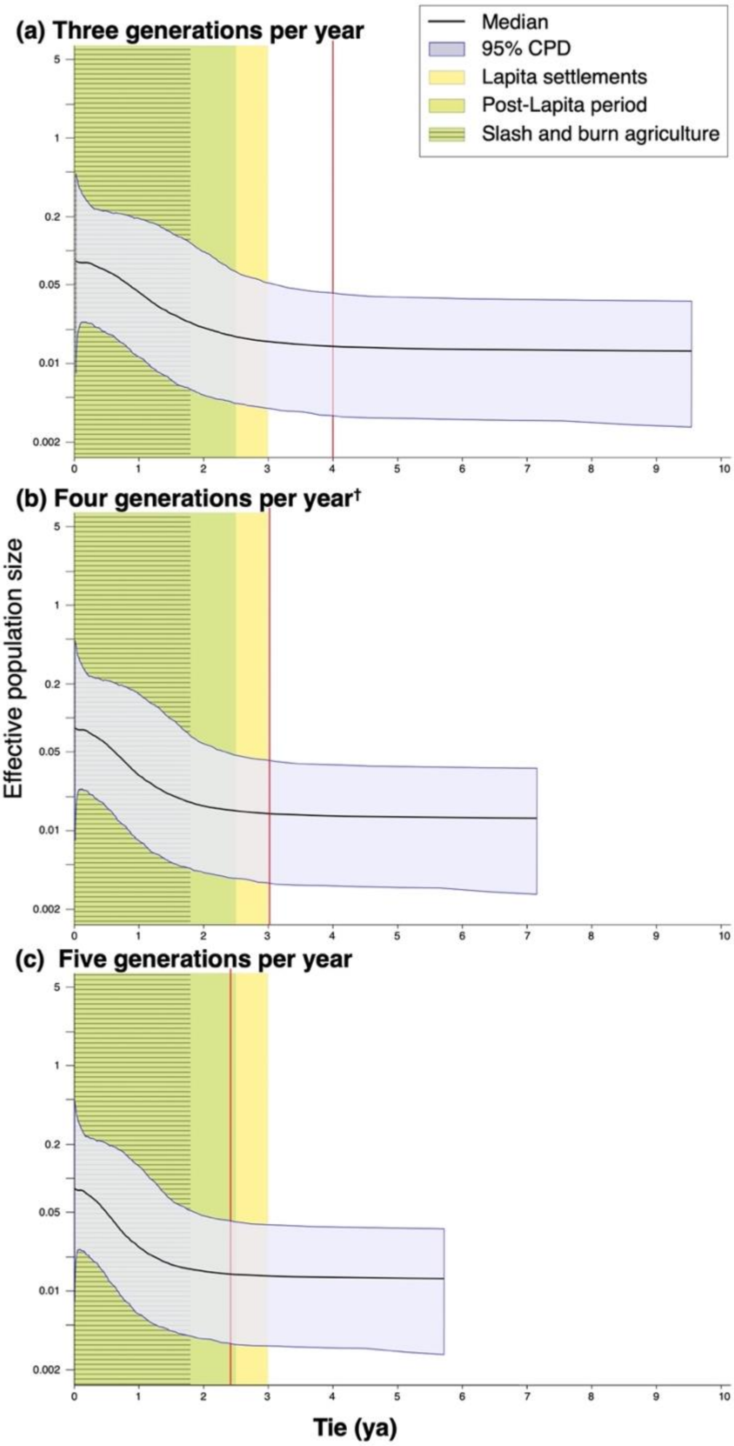

Figure S3. Extended Bayesian skyline plots using 3rd codon only COI data of *Homalictus fijiensis* assuming (a) three generations per year, (b) four generations per year, and (c) five generations per year. The solid black lines indicate the median effective population sizes (*Ne*) and the purple shading indicates the 95% CPDs. The shading indicates (yellow; ~3 kya) first evidence of the Lapita, (green; ~2.5 kya) first evidence of the post-Lapita period and (horizontal hashing; 1.8 kya) first evidence of slash and burn agriculture on Viti Levu [25,27]. The red line in a indicates the point beyond which demography should not be interpreted, based on Fig. S2c. The y-axes indicate *Ne* on a $\log_{10}$ scale. Full extended Bayesian skyline plot output plots are available in Fig. S2. The plot shown in Fig. 3 is indicated by †.

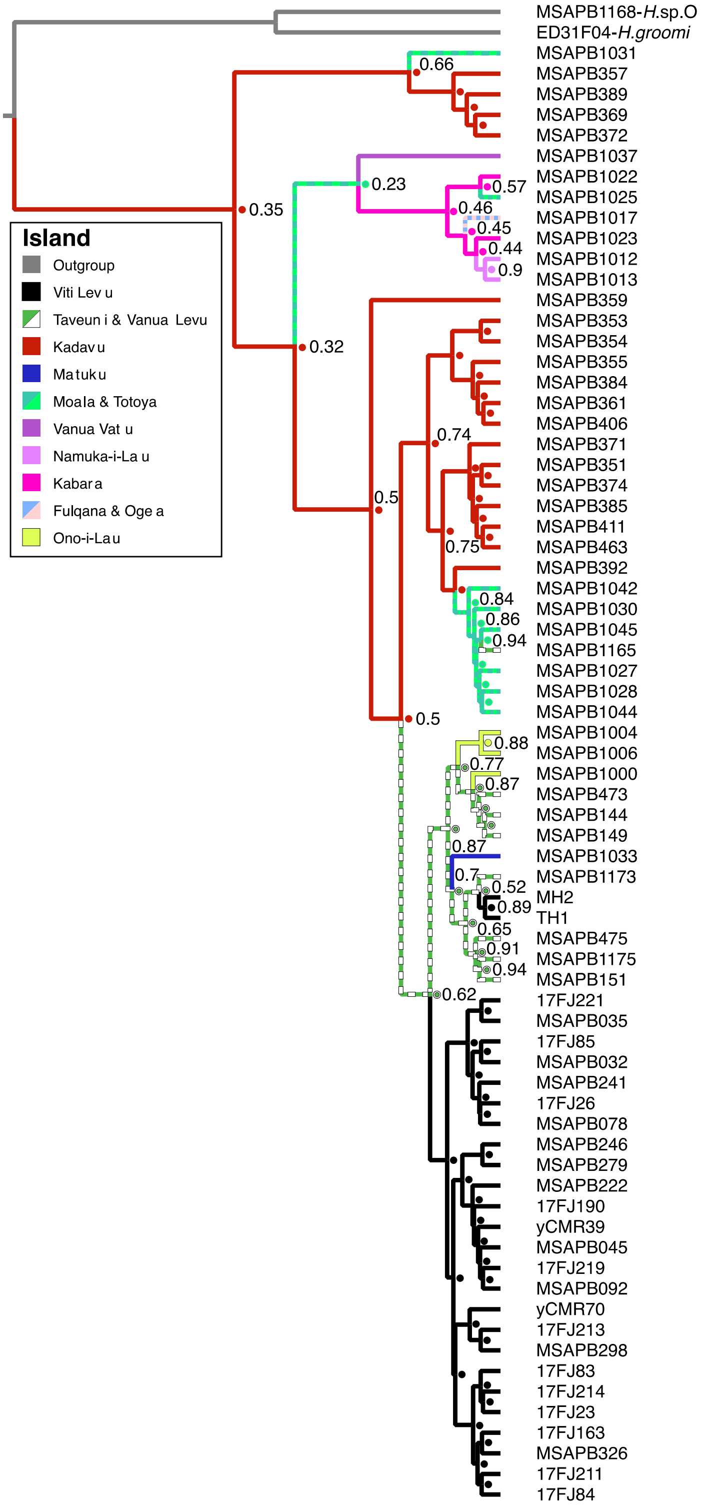

Figure S4 Ancestral state reconstruction of *Homalictus fijiensis* islands using an EBSP tree model and *H. groomi* and *H.* sp. O as outgroups. Branch and node (indicated by circles) colours indicate island location as marked in the legend; colours match Fig. 1. The posterior probabilities (PP) for ancestral state nodes where PP < 0.95 are indicated on the tree. Where F_{ST} values have indicated that island populations cannot be distinguished, they have been combined and both colours are shown along branches and in the legend.

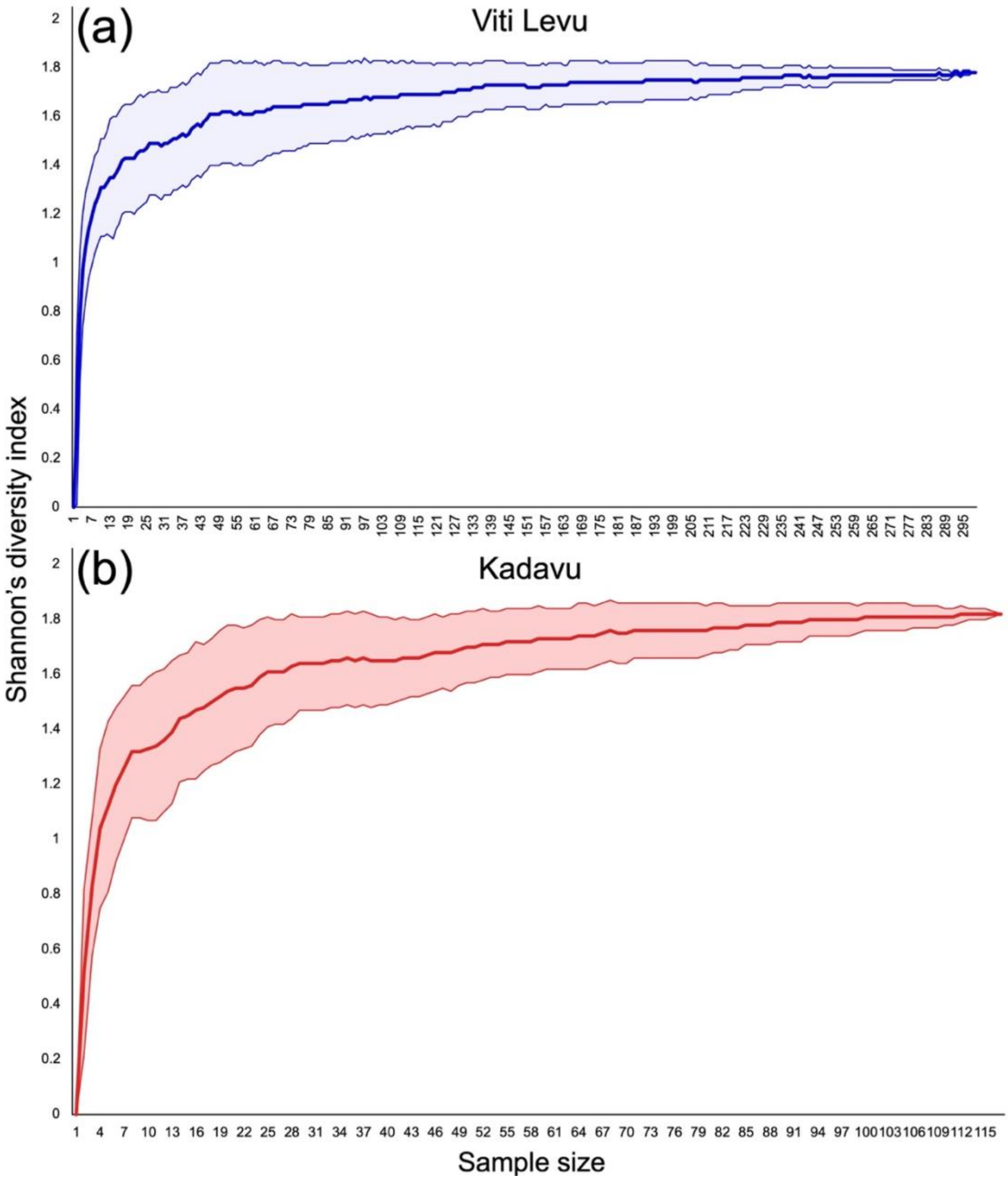

Figure S5. The Shannon's diversity index of *Homalictus fijiensis* haplotypes over sample size for (a) Viti Levu and (b) Kadavu.

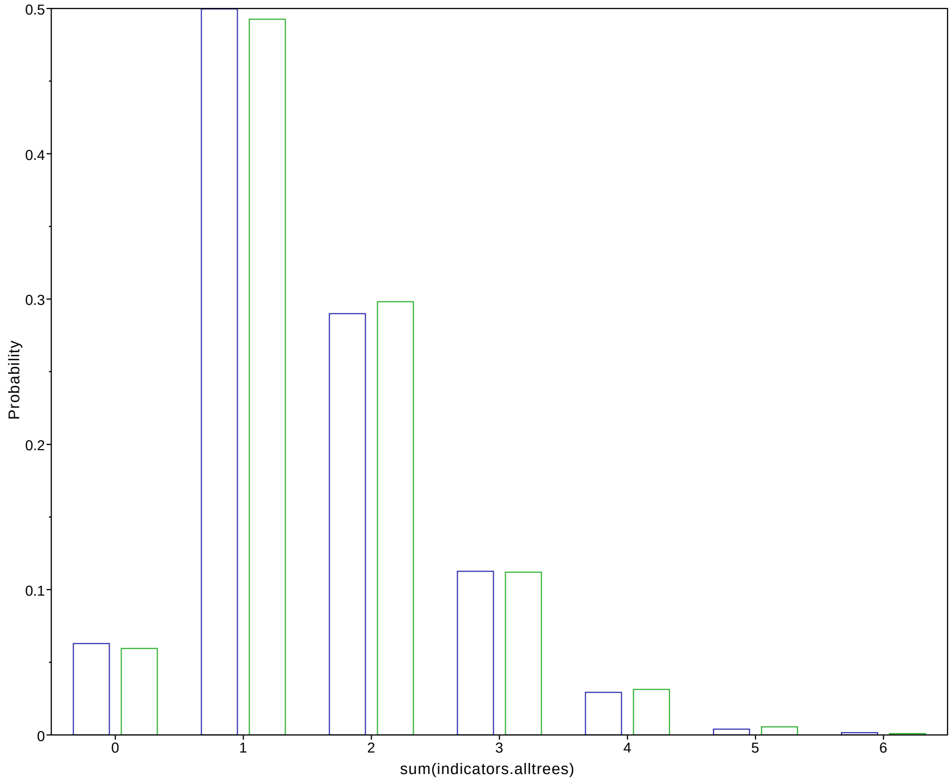

Figure S6. A histogram showing the probability of each indicators.alltrees bin (where number of population changes of >0 indicate population growth). The bars show the model using a (purple) strict clock or (green) uncorrelated relaxed clock model. Log files were analysed using *Tracer* version 1.7.1 [156].

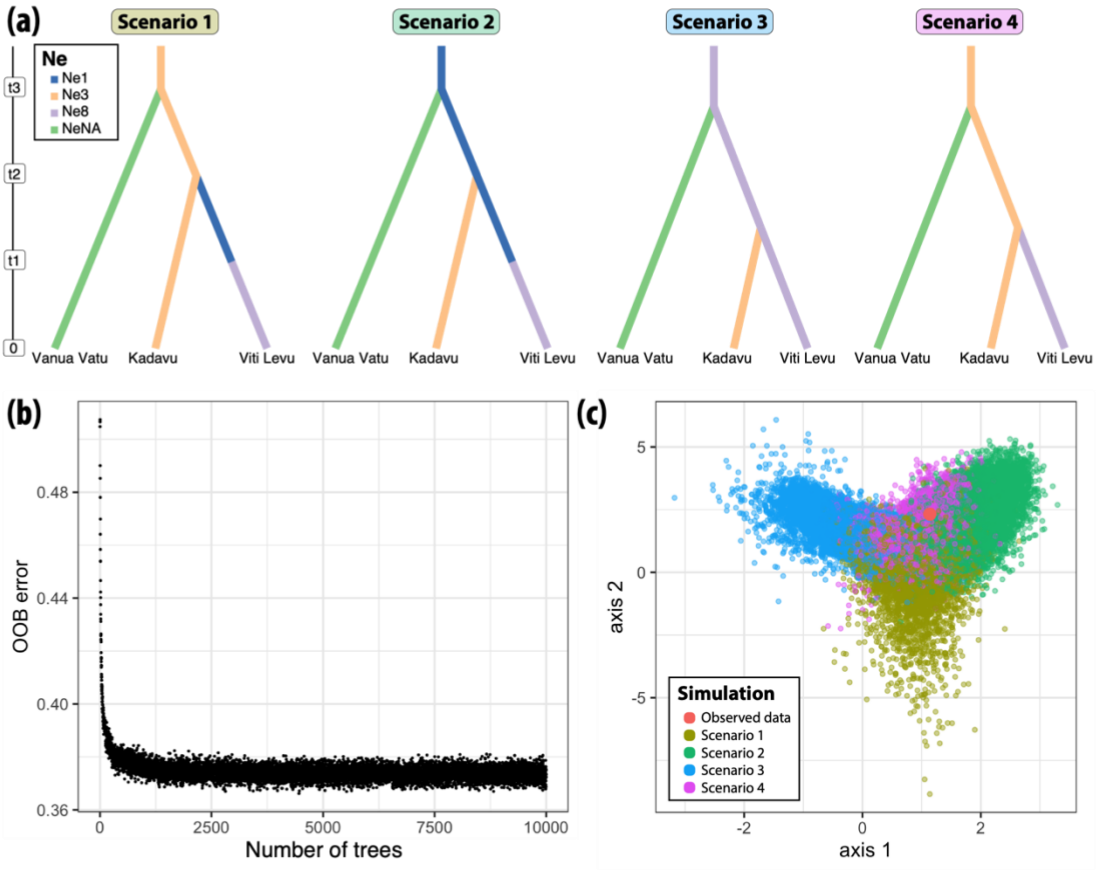

Figure S7: (a) Scenarios one through four that were analysed in *DIYABC-RF*. Branch colour in (a) indicates effective population size (*Ne*) prior. (b) The evolution of predictive power over the number of trees in the forest. (c) The linear discriminant (LDA) analysis of the training datasets on the first two axes. Scenario 1 (gold; 355 votes), scenario 2 (green; 7,292 votes), scenario 3 (blue; 42 votes), and scenario 4 (purple; 2,311 votes) are indicated by coloured dots. The red data point indicates the location of the observed data.

Chapter 4: Missing for almost 100 years: the rare and potentially threatened bee, *Pharohylaeus lactiferus* (Hymenoptera, Colletidae)

James B. Dorey[a,b]

[a]*College of Science and Engineering, Flinders University, GPO Box 2100, SA, 5001, Adelaide, Australia.*
[b]*Terrestrial Invertebrates, South Australian Museum, GPO Box 234, SA, 5001, Adelaide, Australia.*

Published in the Journal of Hymenoptera Research (https://doi.org/10.3897/jhr.81.59365).

Reproduced with permission from the journal.

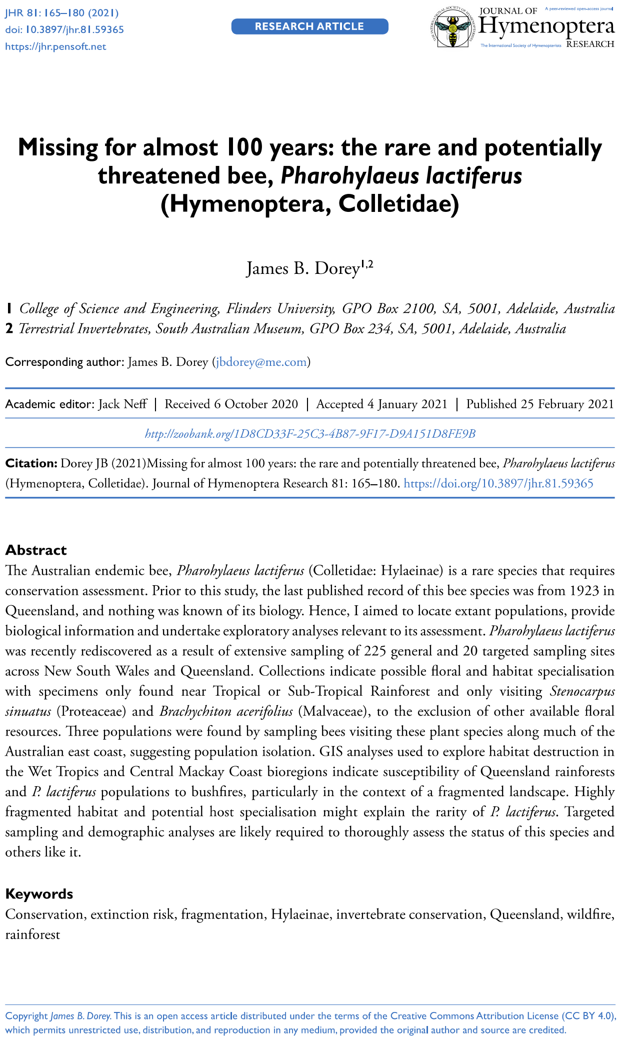

JHR 81: 165–180 (2021)
doi: 10.3897/jhr.81.59365
https://jhr.pensoft.net

RESEARCH ARTICLE

JOURNAL OF Hymenoptera RESEARCH
A peer-reviewed open-access journal
The International Society of Hymenopterists

Missing for almost 100 years: the rare and potentially threatened bee, *Pharohylaeus lactiferus* (Hymenoptera, Colletidae)

James B. Dorey[1,2]

1 *College of Science and Engineering, Flinders University, GPO Box 2100, SA, 5001, Adelaide, Australia*
2 *Terrestrial Invertebrates, South Australian Museum, GPO Box 234, SA, 5001, Adelaide, Australia*

Corresponding author: James B. Dorey (jbdorey@me.com)

Academic editor: Jack Neff | Received 6 October 2020 | Accepted 4 January 2021 | Published 25 February 2021

http://zoobank.org/1D8CD33F-25C3-4B87-9F17-D9A151D8FE9B

Citation: Dorey JB (2021)Missing for almost 100 years: the rare and potentially threatened bee, *Pharohylaeus lactiferus* (Hymenoptera, Colletidae). Journal of Hymenoptera Research 81: 165–180. https://doi.org/10.3897/jhr.81.59365

Abstract

The Australian endemic bee, *Pharohylaeus lactiferus* (Colletidae: Hylaeinae) is a rare species that requires conservation assessment. Prior to this study, the last published record of this bee species was from 1923 in Queensland, and nothing was known of its biology. Hence, I aimed to locate extant populations, provide biological information and undertake exploratory analyses relevant to its assessment. *Pharohylaeus lactiferus* was recently rediscovered as a result of extensive sampling of 225 general and 20 targeted sampling sites across New South Wales and Queensland. Collections indicate possible floral and habitat specialisation with specimens only found near Tropical or Sub-Tropical Rainforest and only visiting *Stenocarpus sinuatus* (Proteaceae) and *Brachychiton acerifolius* (Malvaceae), to the exclusion of other available floral resources. Three populations were found by sampling bees visiting these plant species along much of the Australian east coast, suggesting population isolation. GIS analyses used to explore habitat destruction in the Wet Tropics and Central Mackay Coast bioregions indicate susceptibility of Queensland rainforests and *P. lactiferus* populations to bushfires, particularly in the context of a fragmented landscape. Highly fragmented habitat and potential host specialisation might explain the rarity of *P. lactiferus*. Targeted sampling and demographic analyses are likely required to thoroughly assess the status of this species and others like it.

Keywords
Conservation, extinction risk, fragmentation, Hylaeinae, invertebrate conservation, Queensland, wildfire, rainforest

Abstract

The Australian endemic bee, *Pharohylaeus lactiferus* (Colletidae: Hylaeinae) is a rare species that requires conservation assessment. Prior to this study, the last published record of this bee species was from 1923 in Queensland, and nothing was known of its biology. Hence, I aimed to locate extant populations, provide biological information and undertake exploratory analyses relevant to its conservation assessment. *Pharohylaeus lactiferus* was recently rediscovered as a result of extensive sampling of 225 general and 20 targeted sampling sites across New South Wales and Queensland. Collections indicate possible floral and habitat specialisation with specimens only found near Tropical or Sub-Tropical Rainforest and only visiting *Stenocarpus sinuatus* (Proteaceae) and *Brachychiton acerifolius* (Malvaceae), to the exclusion of other available floral resources. Three populations were found by sampling bees visiting these plant species along much of the Australian east coast, suggesting population isolation. GIS analyses used to explore habitat destruction in the Wet Tropics and Central Mackay Coast bioregions indicate susceptibility of Queensland rainforests and *P. lactiferus* populations to bushfires, particularly in the context of a fragmented landscape. Highly fragmented habitat and potential host specialisation might explain the rarity of *P. lactiferus*. Targeted sampling and demographic analyses are likely required to thoroughly assess the status of this species and others like it.

Keywords

Hylaeinae, Queensland, conservation, wildfire, extinction risk, invertebrate conservation, fragmentation, rainforest

Introduction

The greatest threats to ecosystems and species worldwide are habitat loss, fragmentation, and degradation [186]. Australia has already cleared over 40% of its forests and woodlands since European colonisation, leaving much of the remainder fragmented and degraded [187]. The vast majority of clearing has occurred on freehold and leasehold land and for animal agriculture [188]. In particular, Queensland is a contemporary land-clearing hotspot and is responsible for more than half of all land-clearing in Australia over the past four decades [188]. It is a failing of state and federal government policy and regulation that land clearing in Queensland continues at rates that should be of concern both nationally and internationally [189].

Despite the ecological importance of Australian native bees, we know very little about their biology [10] or conservation status. North Queensland hosts high species richness, endemism [190-192], and several bee genera that are found nowhere else in Australia [40,193]. These restricted bee genera include: *Ctenoplectra* Kirby (Apidae: Apinae), *Nomada* Scopoli (Apidae: Nomadinae), *Mellitidia* Guérin-Méneville (Halictidae: Nomiinae), *Reepenia* Friese (Halictidae: Nomiinae), *Patellapis* Friese (Halictidae: Halictinae), and *Pharohylaeus* Michener (Colletidae: Hylaeinae).

Pharohylaeus has only two described species: *P. papuaensis* Hirashima & Roberts in Papua New Guinea and *P. lactiferus* (Cockerell) in Australia [63,195]. Both species are relatively large (9-11 mm), robust, mostly black with distinctive white facial and body markings, and have the first three tergal segments enlarged and enclosing the others. The former is known only from two females which were collected on *Syzygium aqueum* (Burm.f.) Alston (Myrtaceae) in 1982 [195]. No published records of *P. lactiferus* have been made since the third of January 1923, when three males were collected in the Atherton Tablelands; in May of 1900 a male and a female were collected in Mackay while another female was collected in Kuranda prior to 1910 [63,194]. However, the collection localities of these specimens are imprecise and no biological data were recorded.

Due to the dearth of biological information on *P. lactiferus* prior to this study, I aimed to locate extant populations and contribute biological information as part of a broader bee survey. Because of this, much of what follows are exploratory analyses of the potential risks for *P. lactiferus* and suggestions for future research. Hence, I undertook a series of post-hoc analyses in order to provide insights into the biology, ecology, and potential extinction risks associated with *P. lactiferus*. I provide insights into the circumstances of the rediscovery of *P. lactiferus* and what is now known of its floral and habitat associations. I also explore spatial data relating to *P. lactiferus* (vegetation association, potential fire risks, and occurrences) and my sampling methods (for potential biases). The possible floral and habitat specialisation along with the rarity of *P. lactiferus* raises concerns about its conservation status. I further highlight the need for preservation of remnant vegetation and better arthropod-diversity monitoring, particularly for at-risk and phylogenetically important species.

Methods

Sample locations and methods

I undertook general collections in parts of Queensland and New South Wales in a variety of habitats with most collections made across two sampling periods from December to February 2018-19 and November to December of 2019 (summer). I chose sampling sites by the presence of flowering vegetation on the side of roads and trails. I caught specimens by sweep-netting (up to 13 m from the ground using an 11 m Lito net) off flowering plants, vegetation or potential bee-nesting sites. After collection, I transferred specimens to 99% ethanol and stored them at ~2˚C. For each collection event I recorded latitude, longitude, and elevation in metres above sea level (m asl) and later checked these to ensure accuracy. I estimated the number of bees for each vial while in the field. Other data that I collected included date, time, collector, sampling effort (in minutes), sampling notes, and where possible, flower species visited and the resource that I used to identify that plant. I undertook general collections between 0525 and 2200 (Table S1). I did not keep any plant vouchers. I identified *Pharohylaeus* using the keys by Houston [63] and Smith [193].

I used two initial collection events of *P. lactiferus* to inform targeted sampling (see results). However, I undertook general collections and observations at every site where I found *P. lactiferus* in an attempt to find additional associated plant species. I chose targeted sampling sites haphazardly as target plant species were encountered, generally on the side of roads or hiking trails. I undertook observations of the target plant species, *Stenocarpus sinuatus* (Loudon) Endl. (Proteaceae) and *Brachychiton acerifolius* (A.Cunn. ex G.Don) F.Muell.

(Malvaceae), for a minimum of five minutes (maximum of 67 minutes) for each collection event (Table S1). Where I increased sampling time, I did so to collect *P. lactiferus* specimens and to determine their distribution or activity times. I did not undertake a systematic temporal sampling regime; however, I made targeted collections throughout the day (between 0730 and 1751; Table S1).

Representative materials are stored at the South Australian Museum (SAMA 32-37949, SAMA 32-37950, SAMA 32-40838, SAMA 32-40846, SAMA 32-40847, SAMA 32-40848, and SAMA 32-40849).

Data sources and terminology

Historic bee records. I sourced general bee collection data for Australian bioregions from the Atlas of Living Australia [196] and overlaid them with Australian bioregion data using *QGIS* version 3.8 [197]. I analysed all data using *R* version 3.6.1 [198] and produced plots using the *R* packages *graphics* and *ggplot2* [199]. Because I sampled flowering plants as I encountered them, I also examined potential collection biases (Appendix).

Geographic information system data. I sourced current and pre-European National Vegetation Information System maps from the National Mapping Division [200,201], which defines 85 Major Vegetation Subgroups for Australia (e.g., Tropical or Sub-Tropical Rainforests (TSTRs); Major Vegetation Subgroup 2). NMD [200] compiled pre-European maps using the best-available data collected at varying scales, on varying dates, and by several organisations. I sourced Interim Biogeographic Regionalisation for Australia maps from the Department of Environment and Energy [202], which defines 89 large and distinct bioregions (e.g., the Wet Tropics and Central Mackay Coast).

Results

Sampling

Of the ~3,585 bee specimens that I collected in Queensland over 3,446 sampling-minutes, I collected 694 (19%) in the Wet Tropics and 153 (4%) in the Central Mackay Coast bioregions (Fig. S3; Table S3). In the adjacent bioregions of Cape York Peninsula, Einasleigh Uplands, and the Brigalow Belt North, I collected 260 (7%), 453 (13%), and 271 (8%) bee specimens, respectively (Fig. S3). In New South Wales, I collected 2,141 bee specimens over

2,441 sampling-minutes (Table S3). In total I sampled 225 general collection sites; 130 in Queensland and 95 in New South Wales (Table S3).

Following my initial collection of a *P. lactiferus* female on foliage adjacent to Hallorans Hill Conservation Park, Queensland (Atherton; Wet Tropics), I intensified my sampling of flowering plants around the park for a period of three days between the 3rd and 5th of February 2019 (Fig. 1). Subsequently, I collected five males patrolling the flowers of an ~8 m high *S. sinuatus* tree (flowering times range from February to June [203,204]). *Pharohylaeus lactiferus* males patrolled all flowers (5-8 m high). I undertook further sampling of *S. sinuatus* (and other plants) in nearby rainforest patches between the 5th and 19th of February 2019 but I did not collect any further *P. lactiferus* during this period (Fig. 1).

I resampled Hallorans Hill Conservation Park on the 13th of November 2019 and collected *P. lactiferus* foraging on *B. acerifolius* (flowers November to January [205]). I then undertook further sampling on *B. acerifolius* in Queensland and New South Wales between the 13th and 28th of November (Fig. S3). From these collections, I collected four (2♂2♀) *P. lactiferus* near Hallorans Hill Conservation park on *B. acerifolius*. In Kuranda (Wet Tropics) and Eungella (Central Mackay Coast), I collected five (4♂1♀) and seven (3♂4♀) specimens, respectively, on *B. acerifolius* (Fig. 1).

From the sites where I successfully collected *P. lactiferus*, I sampled most plant species that were flowering at the time (and with flowers at or below ~13 m). The plants on which I collected bees — other than *P. lactiferus* — at these sites included: *Alpinia* sp. (Zingiberaceae), Asteraceae sp., *Callicarpa pedunculata* R.Br. (Lamiaceae), *Duranta repens* L. (Verbenaceae), *Leptospermum* sp. (Myrtaceae), *Melicope rubra* (Lauterb. & K.Schum.) T.G.Hartley (Rutaceae), *Parsonsia straminea* (R.Br.) F.Muell. (Apocynaceae), *Senna*. sp. (Fabaceae), *Solanum seaforthianum* Andrews (Solanaceae), and *Syzygium* sp. (Myrtaceae) (Table S3). I only identified plants on which I caught bee specimens; thus, this represents a subset of those examined.

I undertook a total of 42 observation events on either *S. sinuatus* or *B. acerifolius.* Ten of my observation events resulted in *P. lactiferus* collections across three sites and 32 of my observation events returned no *P. lactiferus* across 20 sites (Fig. 1). I was only successful in collecting *P. lactiferus* between 351 and 877 m asl and only at three sites in the Atherton, Kuranda, and Eungella regions of Queensland (Fig. 1; Table S1). Successful collections were made between 0855 and 1637 (Table S1). Of the 20 sites examined, 15 were within 1 km of TSTRs and 12 were within 213 m (Table S1). According to Beck, *et al.* [206]'s Köppen-Geiger climate classification map, *P. lactiferus* occurs in both tropical and sub-tropical climates.

Historic collection data

Historic bee records. The Atlas of Living Australia has a total of 2,198 bee records for the Wet Tropics and 584 for the Central Mackay Coast. Of these records, 637 (29%) in the Wet Tropics and 250 (43%) in the Central Mackay Coast do not include year of collection. Of the records that included year of collection, the Atlas of Living Australia only had 11 of 1,561 and 15 of 334 records that pre-dated 1924 for the Wet Tropics and Central Mackay Coast, respectively (Fig. 2).

Supplementary results summary

I caught significantly more *P. lactiferus* and other bees and spent more time sampling near TSTRs (Appendix; Fig. S4). However, the sum of sampling time was not significantly correlated with the number of *P. lactiferus* caught, suggesting some resilience of data interpretation to bias (Appendix; Fig. S4). *Pharohylaeus lactiferus* was only collected within 213 m of TSTR (Appendix). Tropical or Sub-Tropical Rainforests have undergone habitat destruction and fragmentation since European colonisation and are susceptible to fire (Appendix). In New South Wales and Queensland, most *B. acerifolius* and *S. sinuatus* records are occur in rainforests.

Discussion

Despite my extensive non-targeted and targeted sampling as well as bee collection records on the Atlas of Living Australia, *P. lactiferus* records remain rare. Apparent habitat specialisation to TSTRs and few associated floral taxa (*S. sinuatus* and *B. acerifolius*) might explain the rarity of *P. lactiferus*. However, in many cases I found *P. lactiferus* difficult to catch due to the height of the associated plant species (of the trees that I sampled, flowers were between 1 m and 13 m high) and the bees' quick flight (Appendix). It is possible that *P. lactiferus* is a naturally rare species that is not threatened. But, why at least two early collectors sampled *P. lactiferus* on three separate occasions prior to 1924 [63] and no published records have been made in the years since, despite a greater sampling effort (Fig. 2), is both unclear and of concern.

The occurrence of host plant species could limit suitable habitat for *P. lactiferus*. For example, the persistence of a *P. lactiferus* population in any one rainforest could require several host plant species to provide food throughout their activity period. From current and historical collections, we know that *P. lactiferus* is active at least between November and May. This could indicate a long flight period, bivoltinism or, like many other tropical bee species (e.g., ALA [196] and Dorey, *et al.* [99]), activity could be year-round. Additionally, as many hylaeines nest in preformed holes [40,207], *P. lactiferus* might require very specific nesting substrates [208]. Nesting substrate could further be limited to certain plant species, and by certain stem-borers that pre-excavate potential nests [40,209]. Habitat destruction and fragmentation might also limit the persistence of the required species in fragments (Appendix). These factors might be particularly relevant to *P. lactiferus*, which was only found within ~200 m of TSTR, suggesting a low foraging and dispersal distance (Appendix).

That bees use *S. sinuatus* and *B. acerifolius* might be unexpected for two primary reasons. Firstly, both plant species exhibit a pollination syndrome that is associated with birds (e.g., they are bright red) [210-212]. Bee vision is shifted towards ultraviolet wavelengths and they are thought to not perceive red wavelengths [213]; although, this is not always the case [214] and insect visual perception is complex [215]. It is possible that the flowers of *S. sinuatus* and *B. acerifolius* have ultraviolet, or similar, markings or produce olfactory cues that attract bees. That at least ten bee species across eight genera were foraging on *B. acerifolius* could indicate that this plant is not exclusively bird-pollinated (Table S1). Hylaeinae bees were the primary visitors of *B. acerifolius* during observations (Table S1) which could indicate phylogenetically conserved traits that allow the use of flowers that exhibit bird-pollination syndromes (e.g., pollen specialisation or red-shifted vision). Secondly, Guymer [205] reported that *B. acerifolius* lacks nectaries. While I did not observe bees inside flowers due to the height of trees, I did observe bees ‘drinking’ from flowers of the related *B. populneus* (Schott & Endl.) R.Br., which Guymer [205] also reports as lacking nectaries. Melittologists might avoid sampling plants that exhibit bird-pollination syndromes and this could bias their collections. The foraging preferences of *P. lactiferus* require further study, likely with a particular focus on plants exhibiting bird-pollination syndromes (e.g., *Alloxylon pinnatum*

(Maiden & Betche) P.H.Weston & Crisp, *Castanospermun australe* A.Cunn. ex Mudie, or *Erythrina vespertilio* Benth.) or even on canopy-flowering plants in general [216].

In the bioregions that *P. lactiferus* has been found, this major vegetation subgroup has undergone habitat destruction and fragmentation since European colonisation (Appendix) [187]. Although Queensland's Wet Tropics have largely been protected from clearing in contemporary times, like much of the state, habitat fragmentation remains a major conservation concern [217]. Additionally, three of four rainforest vegetation types (including TSTR) burnt every year between 1988 and 2020 (for which data are available; Appendix). While there was no significant change over time in the area of rainforest burnt during that period, the 2019-20 bushfire season burnt a greater area than in any year prior for each rainforest type (Appendix).

To monitor and assess the conservation status of each species we require an understanding of their biology and targeted sampling. Data deficiency for rare species raises concerns that other rare or specialist species could become extinct before being discovered, leaving no opportunity to conserve those taxa. We must increase biomonitoring, particularly of diverse invertebrate fauna to assess and protect such taxa worldwide. Additionally, increasing institutional investment to digitise collections would vastly increase the research utility of online databases and potentially allow us to differentiate rare from threatened taxa.

Future research should aim to increase our understanding of the biology, ecology, and population genetics of *P. lactiferus*. This work could use targeted seasonal sampling throughout the year at sites where *P. lactiferus* is known to occur, providing insights into phenology and host plants. Future studies could also use trap-nests at various heights from the ground and targeted searches to uncover nesting requirements and inform conservation management [216,218]. These data, along with an expanded *a priori* sampling regime, should allow accurate implementation of species distribution models to uncover other potential populations or translocation sites. To determine if *P. lactiferus* is threatened (undergone population declines in the recent past) or simply rare (stable population in the recent past), genetic data could be used to examine past demographies. Additionally, genetic data for each population could allow examination of population isolation. Such research will be invaluable to assess the conservation status of *P. lactiferus* and provide an exemplar for the assessment of other poorly-studied and threatened bee taxa.

Conclusions

Despite extensive sampling undertaken during this study and from publicly available records, *P. lactiferus* remains poorly collected and little is known of its biology. *Pharohylaeus lactiferus* has only been collected on two plant species (*S. sinuatus* and *B. acerifolius*), to the exclusion of other available resources. Thus far, only males have been collected on *S. sinuatus*. These collections might indicate floral specialisation, potentially on plants that exhibit bird-pollination syndromes.

Many of the analyses undertaken here are exploratory and this must be considered when making conclusions. However, it is important for likely issues to be raised in order to inform future research and conservation efforts. To these ends, I make the following remarks. *Pharohylaeus lactiferus* could be a floral- and habitat-specialist bee. The absence of *P. lactiferus* collections since 1923, despite far-greater sampling effort prior to this study, raises concerns about its conservation status. Habitat destruction and fragmentation might have acted synergistically with the floral- and habitat-specialisation of *P. lactiferus* to explain its rarity. However, collection habits of melittologist (e.g., possible avoidance of plants with bird-pollination syndromes) and the height of known associated plants might make possible declines difficult to confirm. Regardless, known populations of *P. lactiferus* remain rare and susceptible to habitat destruction (e.g., from changed land use or stochastic events such as fires; Appendix).

Supporting information

Acknowledgements

I would like to thank Olivia K. Davies, Michael P. Schwarz, and Mark I. Stevens for proofing early versions of the manuscript. I further thank Lori Lach, Jack Neff, Terry Houston, and four anonymous reviewers for their insightful comments on the manuscript that led to its improvement. I would also like to thank Erinn P. Fagan-Jeffries and Peter Rühr for their company during field work. I would finally like to thank the funders of this research (Holsworth Wildlife Research Endowment, Playford Trust PhD Scholarship, and the AJ and IM Naylon PhD Scholarship) that support and promote the research of many young scientists. This work was carried out under the Queensland national parks research permit number PTU18-001277-1 and the New South Wales National Parks & Wildlife Service scientific licence number SL102137.

Funding

The field work on which these observations were collected was funded by the Holsworth Wildlife Research Endowment, Playford Trust PhD Scholarship, and the AJ and IM Naylon PhD Scholarship to JBD. Funders had no involvement in the design, implementation, analysis, or writing of this article.

Competing interests

I declare no conflicts of interest.

Data accessibility

Data are made available in supplementary tables and materials.

Figures

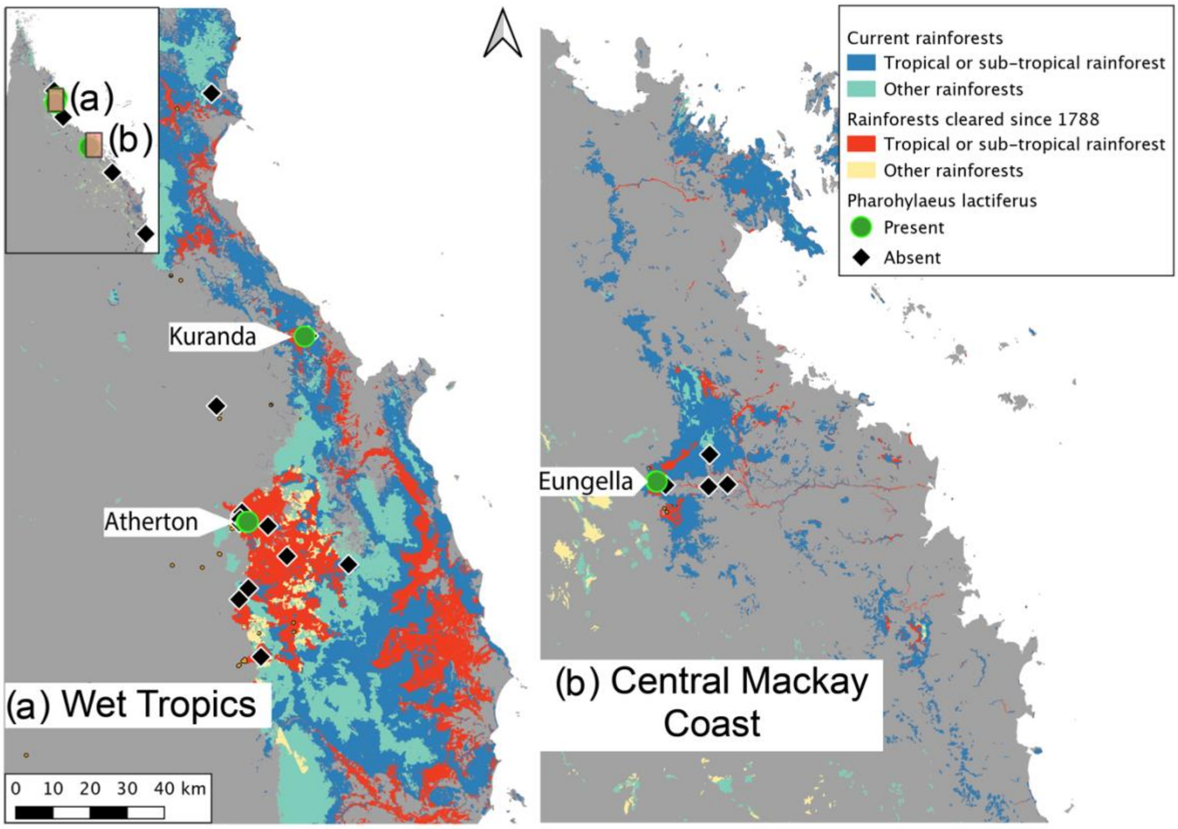

Figure 1. (blues) Current rainforests and (reds) rainforests cleared since European arrival (1788) in the (a) Wet Tropics and the (b) Central Mackay Coast [200,201]. Black markers indicate flowering *Stenocarpus sinuatus* or *Brachychiton acerifolius*, sites where no *Pharohylaeus lactiferus* were detected (Kuranda, Hallorans Hill C.P. (Atherton), and Eungella) and green markers indicate those where they were present. Inset shows QLD and northern NSW as well as sample locations.

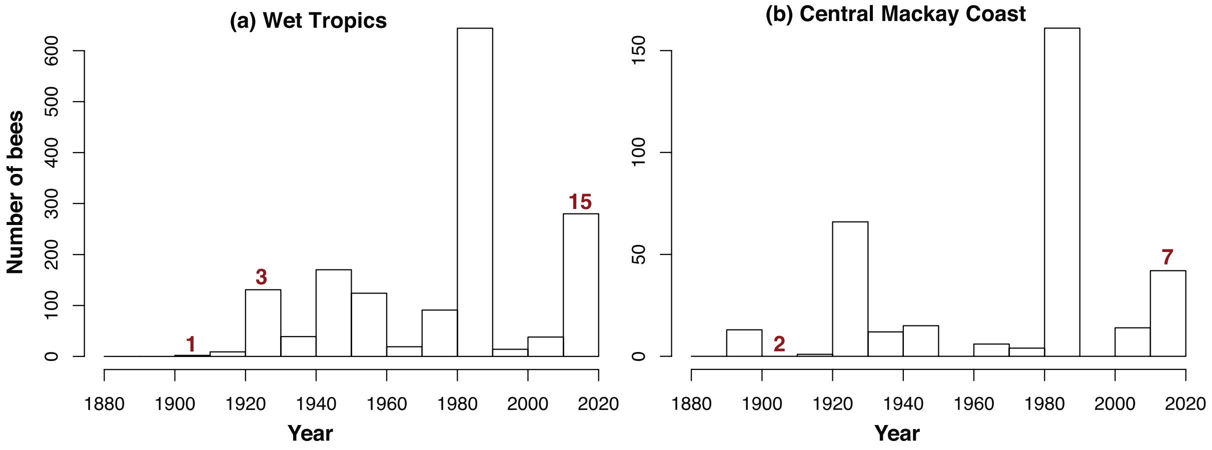

Figure 2. The number of bee specimens recorded on ALA for the (a) Wet Tropics and (b) Central Mackay Coast bioregions in ten-year intervals. Numbers above bars indicate *Pharohylaeus lactiferus* specimen collections.

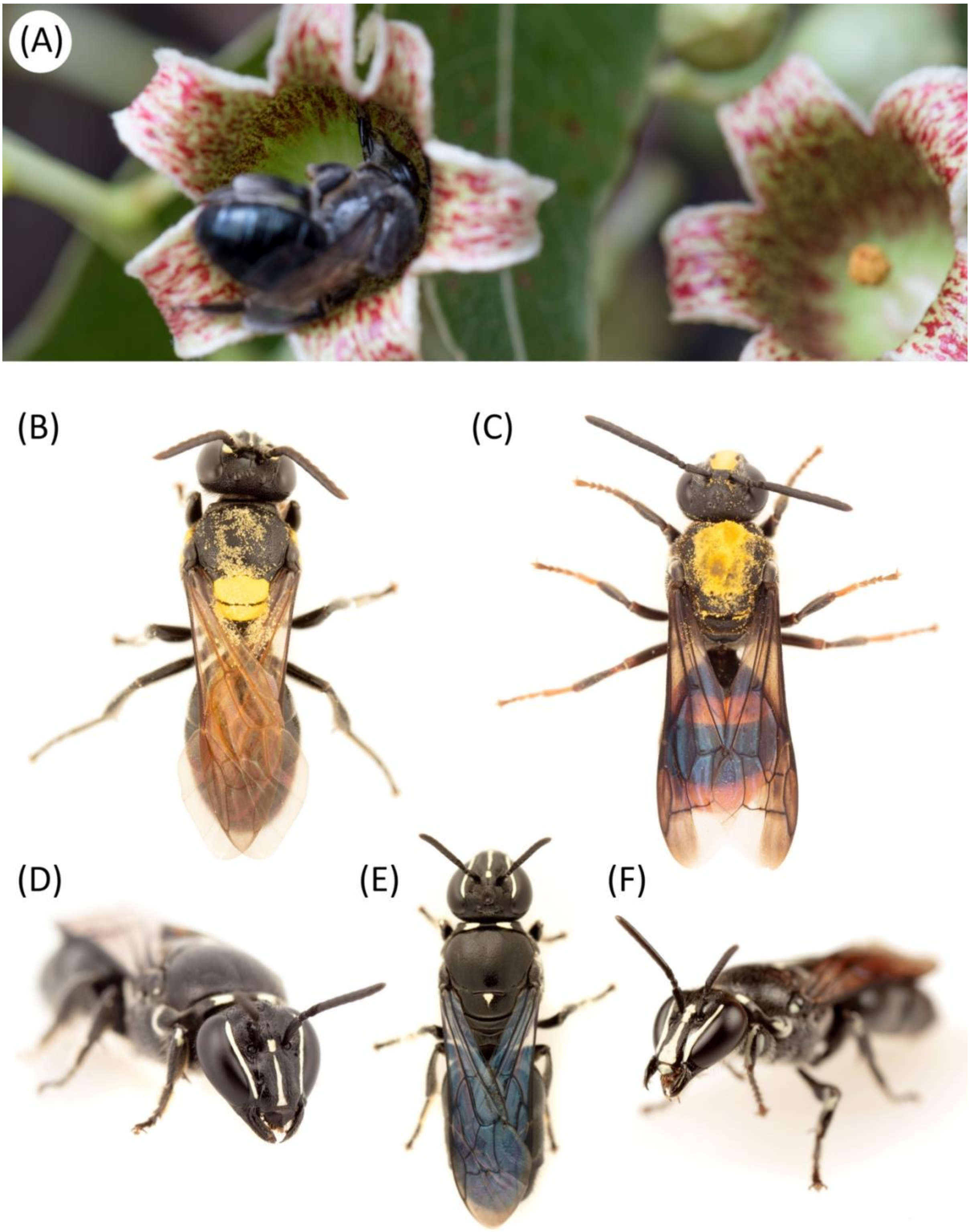

Figure 3. (a) A *Leioproctus* sp. foraging on *Brachychiton populneus*. Pollen shown on the mesosomas of (b) *Meroglossa itamuca* (Cockerell, 1910) and (c) *Hyleoides concinna* (Fabricius, 1775) males after the bees foraged on *B. acerifolius*. An (d) oblique and (e) dorsal photo of a female, and an (f) oblique photo of a male *P. lactiferus*. Hylaeinae swallow pollen instead of carrying it in scopae and are often disparaged as pollinators for this reason (e.g.,

Keys, *et al.* [221] and Ballantyne, *et al.* [222]). However, the hylaeines that commonly visited *B. acerifolius* often had large amounts of pollen dorsally (e.g., b, c, and *P. lactiferus*) on their mesosomas suggesting that they are efficient pollinators of these plants. Scale bar indicates 5 mm for (b). Photos are not to scale.

Supplementary material

Appendix

Bee flight observations: *Pharohylaeus lactiferus* is ~11 mm long; smaller than the *Hyleoides* Smith, 1853 (~15 mm) and generally larger than the *Meroglossa* Smith, 1853 or *Hylaeus* Fabricius, 1793 (<7 mm) species that were also commonly found foraging on *B. acerifolius*. All of these hylaeines are relatively robust and darkly coloured bees but, *Hyleoides* species could be often identified on the wing by their colour (orange and black warning colouration), and when alighted by their wasp-like stance. The flight patterns of all three bee groups were similar — quick and controlled (can be distinguish from the less-common bee visitors such as *Apis mellifera* Linnaeus, 1758, *Lasioglossum* sp. Curtis, 1833, *Megachile* sp. Latreille, 1802, and *Tetragonula* sp. Moure, 1961 species), with males of at least *P. lactiferus* quickly patrolling flowers and rarely alighting.

Collection bias analysis: To examine potential collection biases, I analysed geographical data in several ways. Firstly, all collection buffers were overlaid with the National Vegetation Information System major vegetation subgroups in Queensland and New South Wales. For each site, the sum of bees collected and sampling time were counted towards each major vegetation subgroup in the 500 m buffer (Table S4). These data were used to examine the cumulative number of bees, cumulative sampling time, and total area for each major vegetation subgroup. The number of bees, sample time, and number of *P. lactiferus* were summed in bins of 10 km distances from TSTRs. Because most data occurred in the first bin, this was repeated with bin widths of 200 m and a maximum distance from TSTRs of 10 km (i.e., the first 10 km bin). For each of these distances, the sum number of *P. lactiferus* was plotted against the sum of sampling time in those bins. A two-sided Spearman's rank correlation was implemented using the *R* package *stats* to analyse the correlation between each of these variables.

For analyses using both the full dataset and the 10 km dataset there were significant and negative correlations between the sum of bees caught (full: $p = 1\text{x}10^{-15}$, rho = -0.69; 10 km: $p = 0.001$, rho = 0.47; Fig. S4a and e), sum of sample time (full: $p = 7\text{x}10^{-11}$, rho = -0.59; 10 km: $p = 2\text{x}10^{-4}$, rho = 0.51; Fig. S4b and f), and, for at least the 10 km dataset, sum of *P. lactiferus* (full: $p = 0.09$, rho = -0.17; 10 km: $p = 0.02$, rho = 0.34; Fig. Fig. S4c and g). In contrast, there were no significant correlations between the sum of *P. lactiferus* and sampling time (full: $p = 0.16$, rho = 0.23; 10 km: $p = 0.31$, rho = -0.17) (Fig. S4d and h). Larger absolute values of rho indicate a stronger correlation and the sign indicates direction (i.e., negative values of rho indicate a negative relationship). The cumulative number of bees and sampling time as well as the area sampled in each major vegetation subgroup from this study generally do not match the total proportions from NSW and QLD (Fig. S5). This reflects a lack of *a priori* site choice in the study design.

My sampling was biased, with significantly fewer bees caught and less time spent sampling moving further away from TSTRs (Fig. S4). There were significantly more *P. lactiferus* caught near TSTRs (Fig. S4). Additionally, the number of bees that I caught, time that I spent sampling, and area that I sampled did not match the relative areas of each major vegetation subgroup in New South Wales and Queensland (Fig. S5). However, sampling time and the number of *P. lactiferus* caught were not significantly correlated (Fig. S4). Additionally, the aim of this research was to rediscover and provide the first biological information on *P. lactiferus* and to suggest the further research that needs to be completed to assess and ensure its protection.

Geographical information systems: I sourced National vegetation information system major vegetation subgroup maps from Geoscience Australia [200,201] and Australian bioregion data from DEE [202]. I obtained Queensland burn scar data from 1988 to 2016 from the DSITI [223] and 2019-20 bushfire data from the DAWE [224]. I undertook GIS analyses using *QGIS* version 3.8 [197]. I calculated fragmentation indices using *LecoS* version 3.0.0 [225]. I analysed Bushfire data using a two-sided Spearman's rank correlation as implemented in the *R stats* package to examine correlation between year and area burnt. I defined collection and observation sites by discrete, non-contiguous 500 m buffers around collection points: where buffers overlapped I counted them as a single site (Table S3).

The furthest from TSTR that I collected *P. lactiferus* was 213 m. However, I made this collection in a contiguous wooded and urban habitat and so that distance might be an over-estimate. I made most other successful collections within 65 m of TSTRs (Table S1). For this reason, I analysed the changes in this habitat type for the Wet Tropics and Central Mackay Coast between 1788 and 2018. It is possible that *P. lactiferus* also inhabits other vegetation types that I did not analysed. The most likely additional habitat types are warm temperate rainforest and dry rainforest or vine thickets; both of which are found in the region.

Tropical or Sub-Tropical Rainforest decreased in overall area by 33% in the Wet Tropics tropical. Tropical or Sub-Tropical Rainforest decreased in overall area by 11% in the Central Mackay Coast tropical (Table S5). The number of patches increased and mean patch area decreased for both the Wet Tropics (14% increase in number of patches, and 39% decrease in area) and the Central Mackay Coast (9% increase in number of patches, and 17% decrease in area) (Table S5). The smallest patch that I collected *P. lactiferus* near was Hallorans Hill Conservation Park, which was just 0.09 km^2 in area.

To determine the amount of rainforest that has burned, I overlaid Queensland burn scar data from 1988 to 2016 and the 2019-20 bushfire season with national vegetation information system 5.1 data [201,226]. Two-sided Spearman's rank correlation regressions found no significant change in area burned by year for any rainforest type (major vegetation subgroups one, two, six, and 62). However, I found that all vegetation types, except for major vegetation subgroup one (cool temperate rainforest) have burned every year for which records exist (Fig. S6). Additionally, all rainforests types burned more in the 2019/20 fire season than any previous year; however, these data include fires from July 2019 to May 2020, while the Queensland burn scar dataset runs from January to December [223,224]. On average, 2.2% (μ = 226 km^2, standard deviation = 124 km^2) of TSTR (major vegetation subgroup 2) burned each year between 1988 and 2020 in Queensland (Fig. S6).

Tropical or Sub-Tropical Rainforest in Queensland have experienced habitat destruction and fragmentation since European arrival (Fig. 1). For both the Wet Tropics and Central Mackay Coast, the overall area and mean patch areas were reduced and the number of patches have increased (Table S5). The Wet Tropics had the largest decrease in overall area, with 33% of area lost compared to 11% in the Central Mackay Coast. The number of patches increased by 14% and 9% for the Wet Tropics and Central Mackay Coast, respectively. While the decrease in mean patch area was greater at 39% and 17% for Wet Tropics and Central Mackay Coast, respectively. Mean patch area for each (1.71 km^2 and 1.82 km^2, respectively) was still much larger than the area of Hallorans Hill Conservation Park (0.09 km^2). Hence, habitat destruction and fragmentation alone are unlikely to cause the rarity of *P. lactiferus*. Regardless, habitat fragmentation and destruction, however small, decreases the ability of populations to colonize new fragments [227]. For example, bushfires burnt an average of 226 km^2 of TSTR every year between 1988 and 2020 (Fig. S6). The 2019-20 fire season burnt more rainforest in each major vegetation subgroup than any year before (Fig. S6). Additionally, Eungella National Park experienced severe fires in late 2018 (burning close to the Eungella *P. lactiferus* collection site [228]; however, no data have been made available for the 2017 or 2018 fire seasons). Hence, *P. lactiferus* habitat patches are at risk of destruction by fire, and fires might also increase with changing climates [229].

Historic associated plant records: Because the two known associated plant species, *B. acerifolius* (2,396 individuals total) and *S. sinuatus* (1,456 individuals total), are easily identifiable, I used all records on the Atlas of Living Australia for New South Wales and Queensland (their natural range [205]). Additionally, because these species are commonly cultivated, I focus on records in natural major vegetation subgroups, however total values are reported in Table S2 and shown in Figs S1 and S2. I obtained plant occurrence data from the Atlas of Living Australia [230,231] and overlaid them with New South Wales and Queensland National Vegetation Information System data using *QGIS*.

Over 50% of New South Wales and Queensland records that were found in natural regions occurred in rainforests (Table S2). In New South Wales 28% and 4% of *B. acerifolius* and *S. sinuatus* records occurred in TSTR (Major Vegetation Subgroup 2), respectively (Table S2). In Queensland, 38% and 39% of *B. acerifolius* and *S. sinuatus* records occurred in TSTR, respectively (Table S2). Warm temperate rainforest (major vegetation subgroup 6) accounted for 28% and 78% of all natural *B. acerifolius* and *S. sinuatus* records, respectively (Fig. S1; Table S2). Older records of *B. acerifolius* and *S. sinuatus* tended to occur in natural areas, and most recent records occurred in cleared or non-native habitats (Fig. S2). Compared to New South Wales plant records, Queensland records (where *P. lactiferus* has been found) that occurred in cleared or non-native habitats tended to be older (Fig. S2). These older records could represent natural habitats that have been subsequently cleared.

Supplementary tables

All data tables can be downloaded from the Journal of Hymenoptera Research website at https://jhr.pensoft.net/article/59365/download/suppl/32/

Table S1. Collection data and notes for both successful and unsuccessful searches for *Pharohylaeus lactiferus* in QLD and north-east NSW, Australia.

Table S2. Atlas of Living Australia data for *Brachychiton acerifolius* and *Stenocarpus sinuatus* by major vegetation subgroup (MVS) number in New South Wales and Queensland. Green highlighted rows indicate rainforest major vegetation subgroups.

Table S3. Collection data from New South Wales and Queensland.

Table S4. Major vegetation subgroup (MVS) data including MVS number, MVS name. Measurements include total MVS area (km^2) and proportions, and sampled MVS area (km^2) and proportions. Sum of the number of bees, sample time, and the total area of NSW and QLD for each MVS are also included.

Table S5. Summary of the calculated fragmentation statistics for the two bioregions, the Wet Tropics and Central Mackay Coast.

Supplementary figures

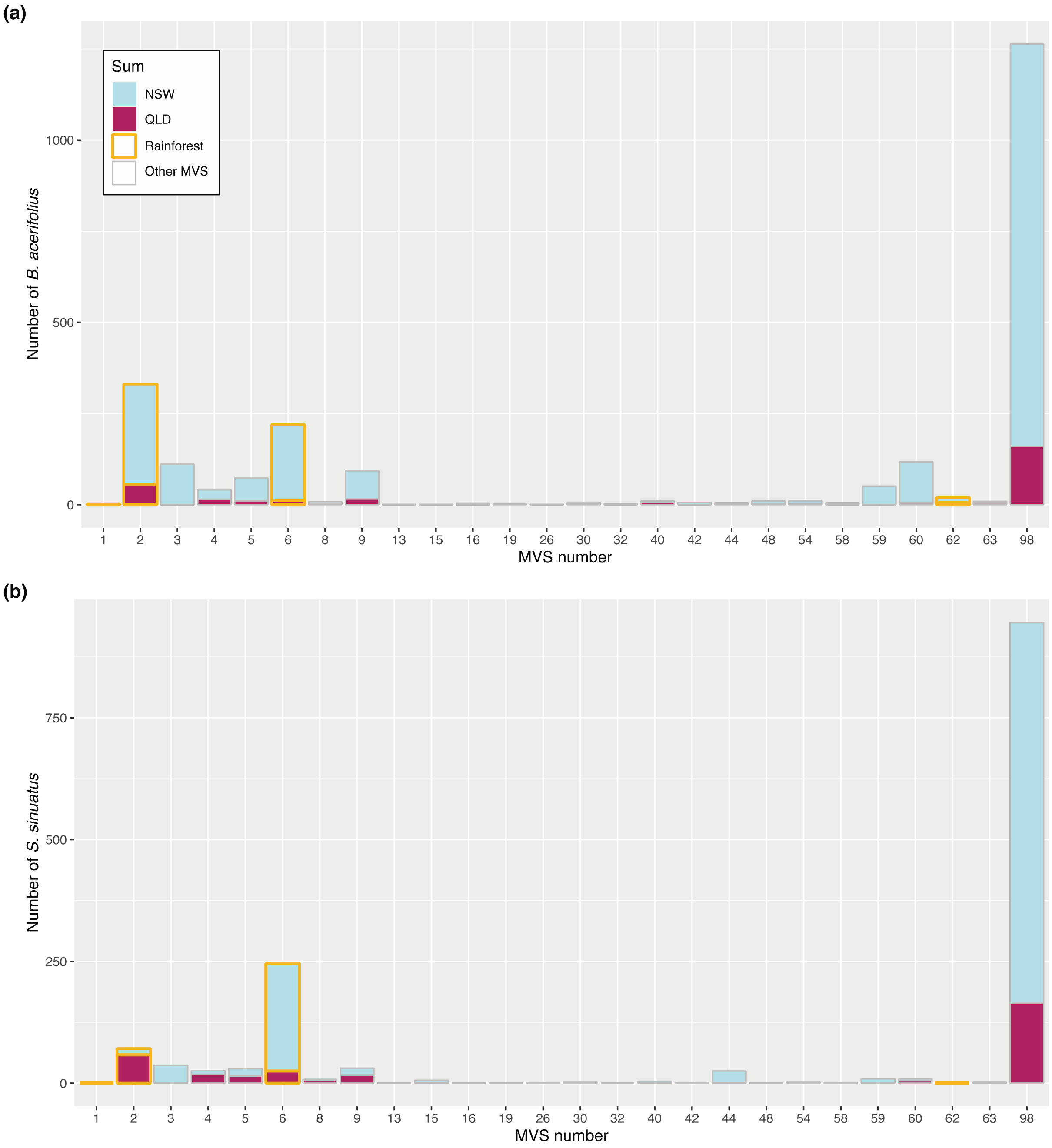

Figure S1. The number of (a) *Brachychiton acerifolius* and (b) *Stenocarpus sinuatus* in New South Wales (NSW; blue) and Queensland (QLD; maroon) by each major vegetation subgroup (MVS). Orange highlights indicate rainforests. Major vegetation subgroups are as follows: 1 (Cool temperate rainforest), 2 (Tropical or Sub-Tropical Rainforest), 3 (*Eucalyptus* (+/- tall) open forest with a dense broad-leaved and/or tree-fern understorey (wet sclerophyll)), 4 (*Eucalyptus* open forests with a shrubby understorey), 5 (*Eucalyptus* open forests with a grassy understorey), 6 (Warm temperate rainforest), 8 (*Eucalyptus* woodlands with a shrubby understorey), 9 (*Eucalyptus* woodlands with a tussock grass understorey), 13

(Brigalow (*Acacia harpophylla*) forests and woodlands), 15 (*Melaleuca* open forests and woodlands), 16 (Other forests and woodlands), 19 (*Eucalyptus* low open woodlands with tussock grass), 26 (*Casuarina* and *Allocasuarina* forests and woodlands), 30 (Heathlands), 32 (Other shrublands), 40 (Mangroves), 42 (Naturally bare, sand, rock, claypan, mudflat), 44 (Freshwater, dams, lakes, lagoons or aquatic plants), 48 (*Eucalyptus* open woodlands with a grassy understorey), 54 (*Eucalyptus* tall open forest with a fine-leaved shrubby understorey), 58 (*Leptospermum* forests and woodlands), 59 (*Eucalyptus* woodlands with ferns, herbs, sedges, rushes or wet tussock grassland), 60 (*Eucalyptus* tall open forests and open forests with ferns, herbs, sedges, rushes or wet tussock grasses), 62 (Dry rainforest or vine thickets), 63 (Sedgelands, rushs or reeds), and 98 (Cleared, non-native vegetation, buildings).

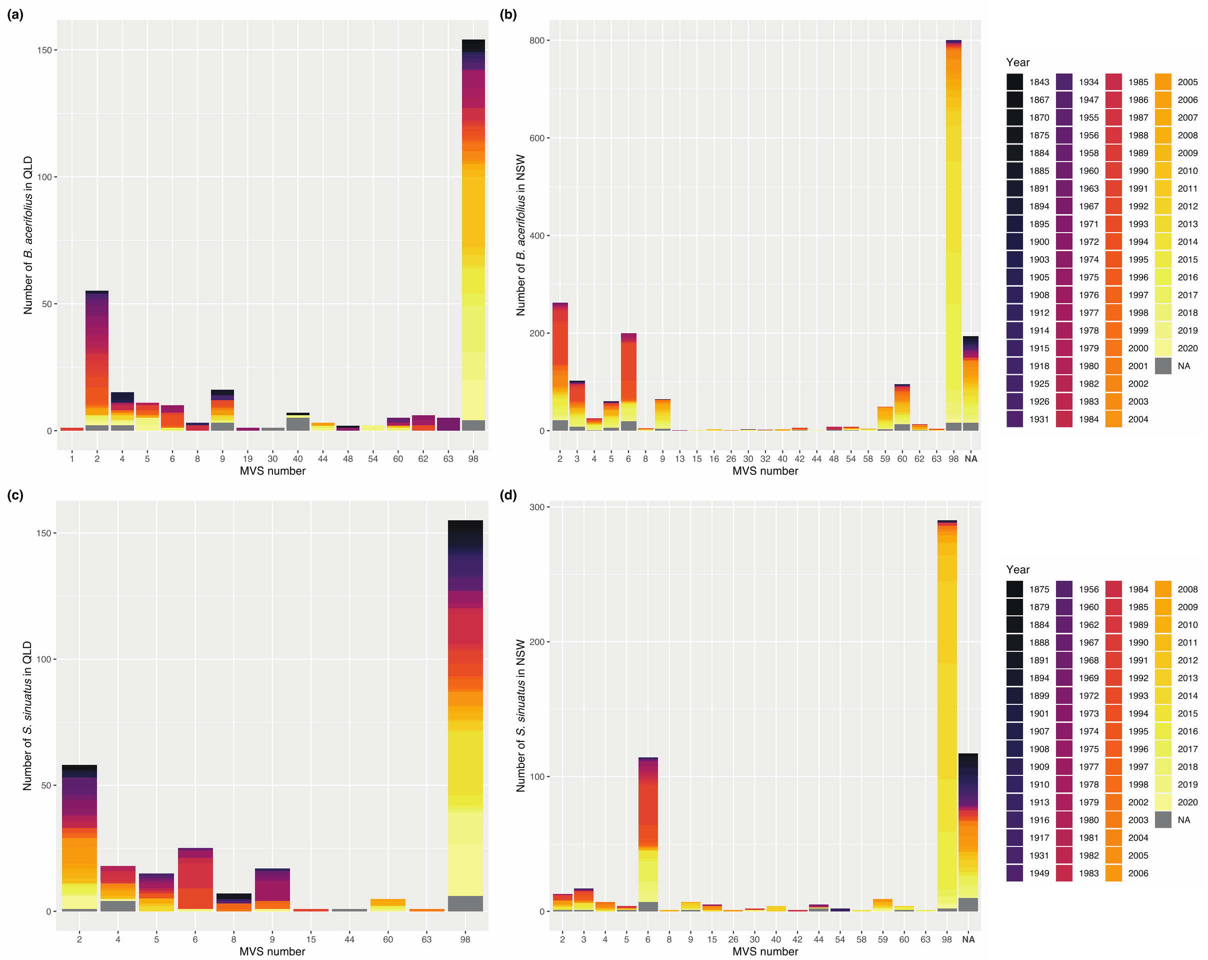

Figure S2. The number of (a & b) *Brachychiton acerifolius* and (c & d) *Stenocarpus sinuatus* in New South Wales (NSW; blue) and Queensland (QLD; maroon) by each major vegetation subgroup (MVS). Colours indicates year of record with darker colours indicating older records. Major vegetation subgroups are as follows: 1 (Cool temperate rainforest), 2 (Tropical or Sub-Tropical Rainforest), 3 (*Eucalyptus* (+/- tall) open forest with a dense broad-leaved and/or tree-fern understorey (wet sclerophyll)), 4 (*Eucalyptus* open forests with a shrubby understorey), 5 (*Eucalyptus* open forests with a grassy understorey), 6 (Warm temperate rainforest), 8 (*Eucalyptus* woodlands with a shrubby understorey), 9 (*Eucalyptus* woodlands with a tussock grass understorey), 13 (Brigalow (*Acacia harpophylla*) forests and woodlands), 15 (*Melaleuca* open forests and woodlands), 16 (Other forests and woodlands), 19 (*Eucalyptus* low open woodlands with tussock grass), 26 (*Casuarina* and *Allocasuarina* forests and woodlands), 30 (Heathlands), 32 (Other shrublands), 40 (Mangroves), 42 (Naturally bare, sand, rock, claypan, mudflat), 44 (Freshwater, dams, lakes, lagoons or aquatic plants), 48 (*Eucalyptus* open woodlands with a grassy understorey), 54 (*Eucalyptus* tall open forest with a fine-leaved shrubby understorey), 58 (*Leptospermum* forests and woodlands), 59 (*Eucalyptus* woodlands with ferns, herbs, sedges, rushes or wet tussock grassland), 60 (*Eucalyptus* tall open forests and open forests with ferns, herbs, sedges, rushes or wet tussock grasses), 62 (Dry rainforest or vine thickets), 63 (Sedgelands, rushs or reeds), and 98 (Cleared, non-native vegetation, buildings).

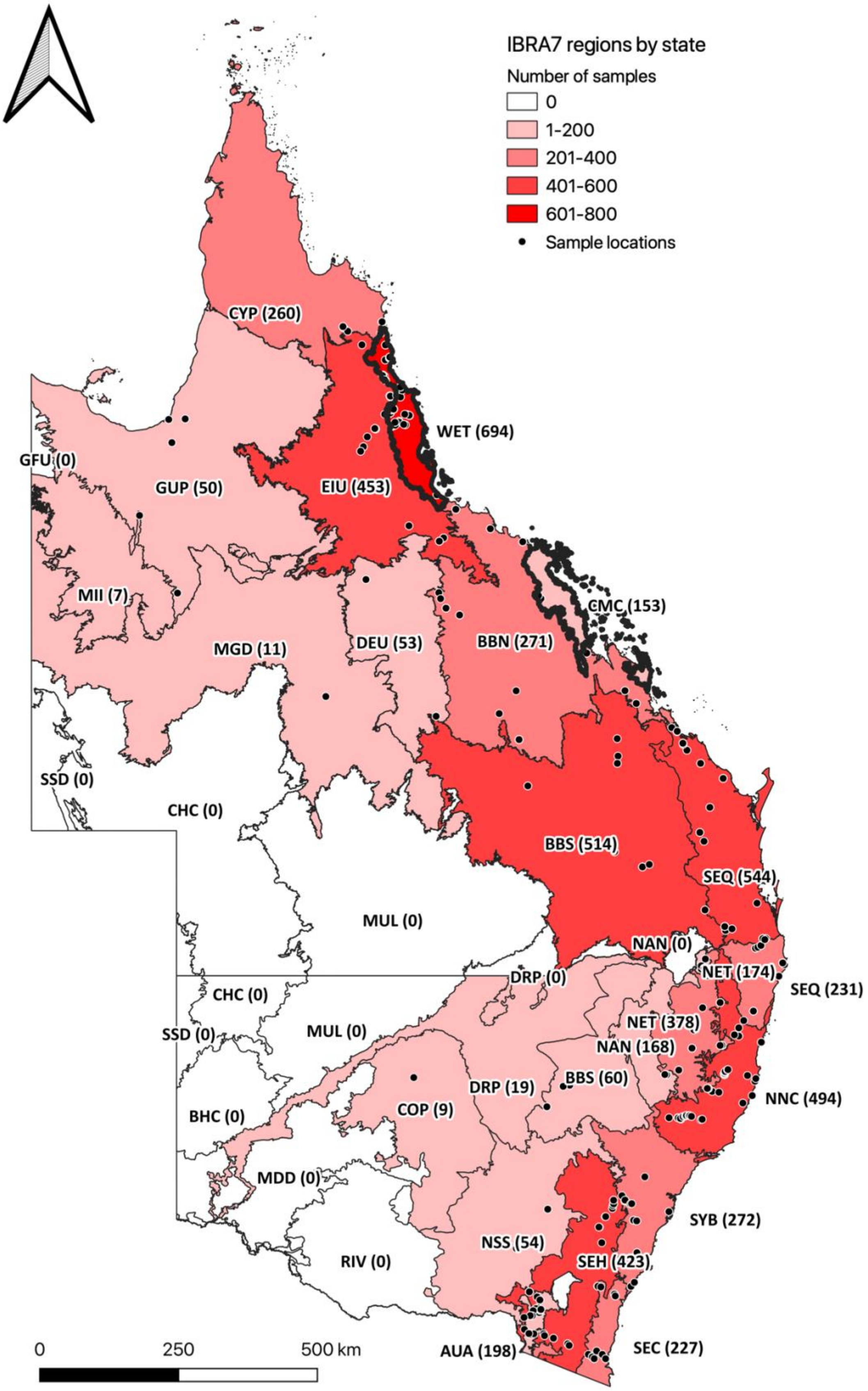
IBRA7 regions by state
Number of samples
☐ 0
1-200
201-400
401-600
601-800
● Sample locations
CYP (260)
WET (694)
GFU (0)
GUP (50)
EIU (453)
MII (7)
CMC (153)
MGD (11)
DEU (53)
BBN (271)
SSD (0)
CHC (0)
BBS (514)
SEQ (544)
MUL (0)
NAN (0)
DRP (0)
NET (174)
SEQ (231)
CHC (0)
SSD (0)
MUL (0)
NET (378)
NAN (168)
BBS (60)
DRP (19)
NNC (494)
BHC (0)
COP (9)
MDD (0)
SYB (272)
NSS (54)
SEH (423)
RIV (0)
AUA (198)
SEC (227)
0
250
500 km

Figure S3. Heatmap of bee collections by Australian bioregion with the focus bioregions bolded. Points indicate the location of bee samples. Bioregion codes are: Australian Alps (AUA), Brigalow Belt South (BBS), Broken Hill Complex (BHC), Channel Country (CHC), Cobar Peneplain (COP), Darling Riverine Plains (DRP), Murray Darling Depression (MDD), Mulga Lands (MUL), Nandewar (NAN), New England Tablelands (NET), NSW North Coast (NNC), NSW South Western Slopes (NSS), Riverina (RIV), South East Corner (SEC), South Eastern Highlands (SEH), South Eastern Queensland (SEQ), Simpson Strzelecki Dunefields (SSD), Sydney Basin (SYB), Brigalow Belt North (BBN), Brigalow Belt South (BBS), Channel Country (CHC), **Central Mackay Coast (CMC)**, Cape York Peninsula (CYP), Desert Uplands (DEU), Darling Riverine Plains (DRP), Einasleigh Uplands (EIU), Gulf Fall and Uplands (GFU), Gulf Plains (GUP), Mitchell Grass Downs (MGD), Mount Isa Inlier (MII), Mulga Lands (MUL), Nandewar (NAN), New England Tablelands (NET), South Eastern Queensland (SEQ), and **Wet Tropics (WET)**.

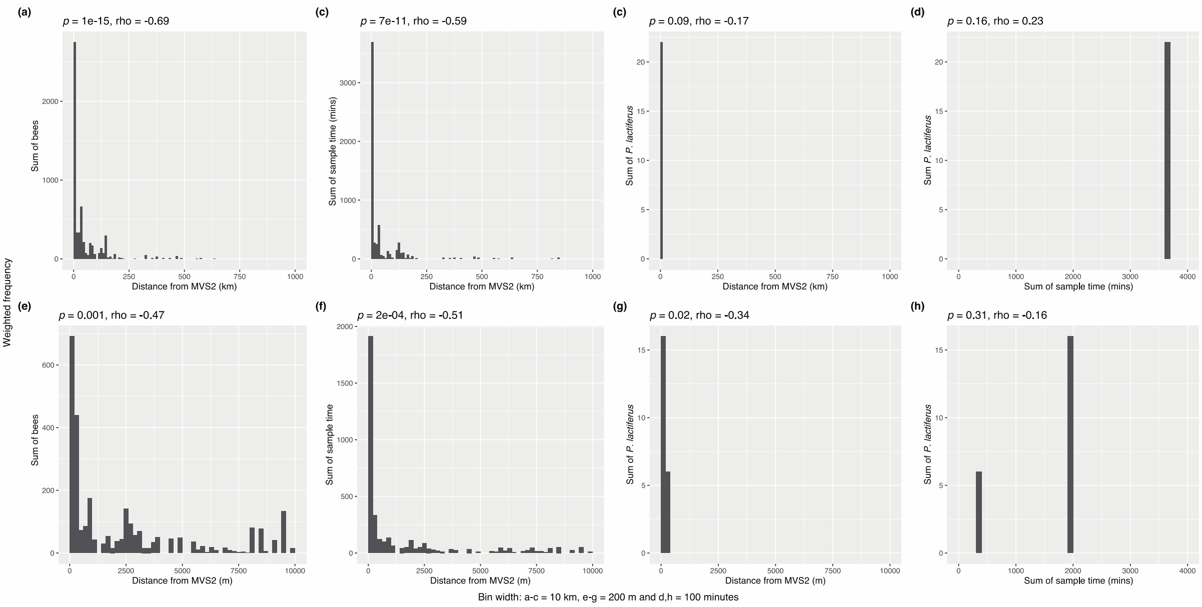

Bin width: a-c = 10 km, e-g = 200 m and d,h = 100 minutes

Figure S4. The sum of (a) number of bees, (b) sample time (mins), and (c) *P. lactiferus* by distance from major vegetations subgroup (MVS) 2 — Tropical or Sub-Tropical Rainforest — in 10 km bins. The sum of (e) number of bees, (f) sample time (mins), and (g) *P. lactiferus* by distance from MVS 2 in the first 10 km bin of a, b and c split in 200 m bins. The sum of *P. lactiferus* in (d) 10 km bins and (h) 200 m bins over sampling time (mins) where bin width is 100 minutes. The *p* and rho values are from a two-sided Spearman's rank correlation test, where the sign of rho indicates the direction and the absolute value indicates strength of relationship (H_0 = zero, maximum strength = one).

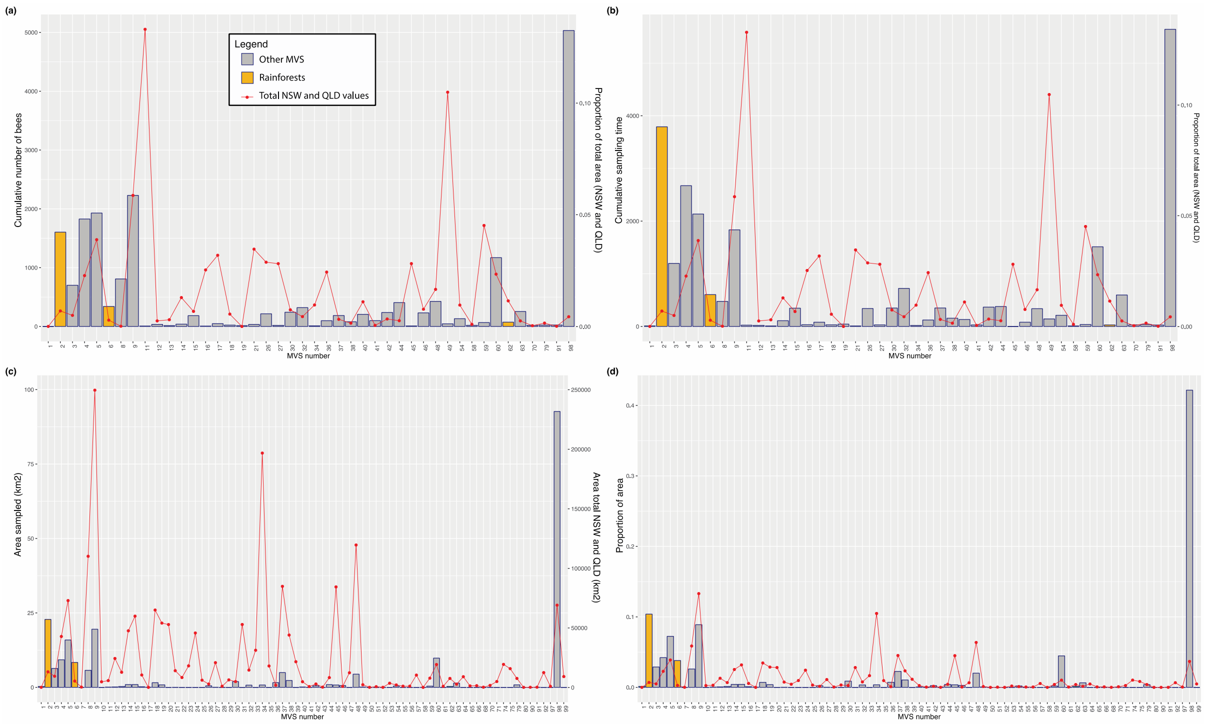

Figure S5. Bars show the cumulative (a) number of insects and (b) sampling time by the major vegetation subgroups (MVS) that were sampled in New South Wales (NSW) and Queensland (QLD) (left-most Y-axes). Red points and lines indicate the proportion of the total area of NSW and QLD for each MVS (rightmost Y-axes). The (c) area sampled in this study (leftmost Y-axes and bars; km^2) and total area in NSW and QLD (rightmost Y-axes and points with lines; km^2) and (d) the proportion of area sampled in this study (bars) and the proportion of the total area in NSW and QLD (points with lines) by all MVS in both states. Orange bars indicate rainforest habitat and grey indicate all other types. Major vegetation subgroups are as follows: 1 (Cool temperate rainforest), 2 (Tropical or Sub-Tropical Rainforest), 3 (*Eucalyptus* (+/- tall) open forest with a dense broad-leaved and/or tree-fern understorey (wet sclerophyll)), 4 (*Eucalyptus* open forests with a shrubby understorey), 5 (*Eucalyptus* open forests with a grassy understorey), 6 (Warm temperate rainforest), 7 (Tropical *Eucalyptus* open forests and woodlands with a tall annual grassy understorey), 8 (*Eucalyptus* woodlands with a shrubby understorey), 9 (*Eucalyptus* woodlands with a tussock grass understorey), 10 (*Eucalyptus* woodlands with a hummock grass understorey), 11 (Tropical mixed spp forests and woodlands), 12 (Callitris forests and woodlands), 13 (Brigalow (*Acacia harpophylla*) forests and woodlands), 14 (Other *Acacia* forests and woodlands), 15 (*Melaleuca* open forests and woodlands), 16 (Other forests and woodlands), 17 (Boulders/rock with algae, lichen or scattered plants, or alpine fjaeldmarks), 18

(*Eucalyptus* low open woodlands with hummock grass), 19 (*Eucalyptus* low open woodlands with tussock grass), 20 (Mulga (*Acacia aneura*) woodlands +/- tussock grass +/- forbs), 21 (Other *Acacia* tall open shrublands and [tall] shrublands), 22 (*Acacia* (+/- low) open woodlands and shrublands with chenopods), 23 (*Acacia* (+/- low) open woodlands and shrublands with hummock grass), 24 (*Acacia* (+/- low) open woodlands and shrublands +/- tussock grass), 25 (*Acacia* (+/- low) open woodlands and sparse shrublands with a shrubby understorey), 26 (*Casuarina* and *Allocasuarina* forests and woodlands), 27 (Mallee with hummock grass), 28 (Low closed forest or tall closed shrublands (including *Acacia*, *Melaleuca* and *Banksia*)), 29 (Mallee with a dense shrubby understorey), 30 (Heathlands), 31 (Saltbush and bluebush shrublands), 32 (Other shrublands), 33 (Hummock grasslands), 34 (Mitchell grass (*Astrebla*) tussock grasslands), 35 (Blue grass (*Dicanthium*) and tall bunch grass (*Vitiveria* syn: *Chrysopogon*) tussock grasslands), 36 (Temperate tussock grasslands), 37 (Other tussock grasslands), 38 (Wet tussock grassland with herbs, sedges or rushes, herblands or ferns), 39 (Mixed chenopod, samphire +/- forbs), 40 (Mangroves), 41 (Saline or brackish sedgelands or grasslands), 42 (Naturally bare, sand, rock, claypan, mudflat), 43 (Salt lakes and lagoons), 44 (Freshwater, dams, lakes, lagoons or aquatic plants), 45 (Mulga (*Acacia aneura*) open woodlands and sparse shrublands +/- tussock grass), 46 (Sea, estuaries (includes seagrass)), 47 (*Eucalyptus* open woodlands with shrubby understorey), 48 (*Eucalyptus* open woodlands with a grassy understorey), 49 (*Melaleuca* shrublands and open shrublands), 50 (*Banksia* woodlands), 51 (Mulga (*Acacia aneura*) woodlands and shrublands with hummock grass), 52 (Mulga (*Acacia aneura*) open woodlands and sparse shrublands with hummock grass), 53 (*Eucalyptus* low open woodlands with a shrubby understorey), 54 (*Eucalyptus* tall open forest with a fine-leaved shrubby understorey), 55 (Mallee with an open shrubby understorey), 56 (*Eucalyptus* (+/- low) open woodlands with a chenopod or samphire understorey), 57 (Lignum shrublands and wetlands), 58 (*Leptospermum* forests and woodlands), 59 (*Eucalyptus* woodlands with ferns, herbs, sedges, rushes or wet tussock grassland), 60 (*Eucalyptus* tall open forests and open forests with ferns, herbs, sedges, rushes or wet tussock grasses), 61 (Mallee with a tussock grass understorey), 62 (Dry rainforest or vine thickets), 63 (Sedgelands, rushs or reeds), 64 (Other grasslands), 65 (*Eucalyptus* woodlands with a chenopod or samphire understorey), 66 (Open mallee woodlands and sparse mallee shrublands with a hummock grass understorey), 68 (Open mallee woodlands and sparse mallee shrublands with an open shrubby understorey), 70 (Callitris open woodlands), 71 (*Casuarina* and *Allocasuarina* open woodlands with a tussock grass understorey), 74 (*Casuarina* and *Allocasuarina* open woodlands with a shrubby understorey), 75 (*Melaleuca* open woodlands), 79 (Other open Woodlands), 80 (Other sparse shrublands and sparse heathlands), 90 (Regrowth or modified forests and woodlands), 91 (Regrowth or modified shrublands), 92 (Regrowth or modified graminoids), 97 (Unclassified native vegetation), 98 (Cleared, non-native vegetation, buildings), and 99 (Unknown/No data).

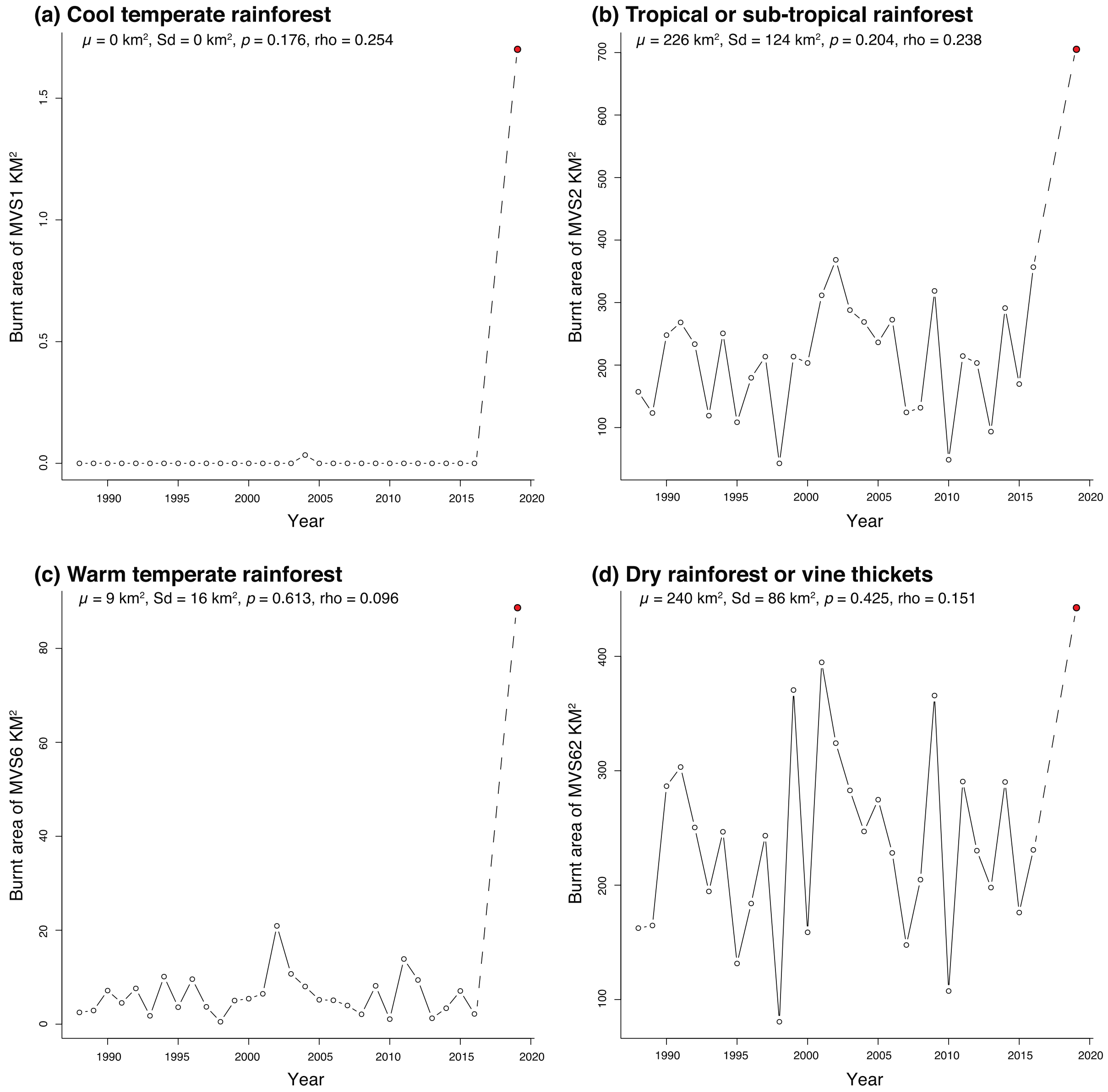

Figure S6. The area of Major Vegetation Subgroups (MVS) (a) one (cool temperate rainforest), (b) two (Tropical or Sub-Tropical Rainforest), (c) six (warm temperate rainforest), and (d) 62 (dry rainforest or vine thickets) burnt by year from 1988 to 2016 and the 2019-20 fire season (red). The mean (μ), standard deviation (Sd), p, and rho values from a two-sided Spearman's rank correlation test are included. Hashed lines indicates missing data from the 2017 and 2018 fire seasons.

General discussion

The results of this thesis develop the Fijian *Homalictus* bee fauna as a tractable model system for addressing evolutionary and ecological questions, particularly those that involve island biogeography. The insights gained from insular systems can be extended to continental systems with broader ecological and evolutionary implications.

Because taxonomy underpins most biological studies, my first chapter addressed the taxonomy of the Fijian *Homalictus* [99]. In chapter one I showed that there are many more Fijian *Homalictus* than initially recognized and which require formal description; but I did not attempt to describe all of these species. Instead, I only described all new species for which we currently have both sexes with the aim of laying the foundational work for the description of the remaining species which are, in large part, morphologically cryptic. I resolved this cryptic diversity by using a combination of mitochondrial DNA (mtDNA) — cytochrome c oxidase subunit I (COI) — and morphological (including genitalia) data. I also described the distribution of the highland-rich Fijian *Homalictus* diversity and its potential for extinction in a warming climate. My results here have implications for other Pacific islands which are poorly sampled for bees but likely also host high species richness and require examination. This foundational knowledge is critical for the complex ecological and evolutionary questions addressed in chapters two and three.

Once I completed initial species delimitations and descriptions, I could more-reliably differentiate between species for my second chapter. In this chapter, I used the framework of island biogeography to address how a single colonisation event for Fiji has led to at least 22 species of *Homalictus* in Fiji [32,232]. To accomplish this I used phylogenetic analyses of mtDNA and single nucleotide polymorphisms (SNPs). I found that very few of the 21 speciation events were associated with changes in elevational niches. This indicates that climatic niche shifts have not been a major driver of speciation in the Fijian *Homalictus*, which conflicts with the ‘taxon cycle’ model which was originally also based on Fijian hymenopterans (ants). My results provide empirical support for phylogenetic niche conservatism as a driver of speciation because elevational niches were broadly maintained across many speciation events. I suggest that the interactions between the narrow climatic tolerances of tropical ectotherms (i.e., phylogenetic niche conservatism), past climate cycles, and Fiji’s topographical complexity have all interacted, resulting in the current high species diversity [82]. Together, these factors could have driven repeated cycles of population isolation, as cool-adapted highland species were forced into the highlands during interglacial periods, and subsequent admixture during glacial maxima. This is supported by an absence of obvious phylogeographic signal in the group, indicating that inter-insular movement has been possible in the past (i.e., during glacial maxima). My results provide support for a strong role of phylogenetic niche conservatism and topographical complexity in the genesis of species. They also indicate clade-specific extinction risks under changing climates for the Fijian *Homalictus* and other similarly-derived clades in tropical insular systems.

My second chapter results drew implications that mostly relate to highland *Homalictus* species. However, it didn't address in detail the hyper-abundant lowland species, *H. fijiensis*. Because *H. fijiensis* is the only abundant endemic lowland bee in Fiji, it provides the best opportunity to examine how lowland bee populations have been variously impacted by past climates and anthropogenic modification of the environment.

My third chapter used phylogenetic analyses of mtDNA and SNPs to reconstruct the past demography of *H. fijiensis*, particularly on two major Fijian islands — Viti Levu and Kadavu. Groom, *et al.* [32] found that a recent and large population increase of *H. fijiensis* was associated with the end of the last glacial maximum. However, the then-unknown cryptic species diversity in Fiji and strong population structure compromised Groom, *et al.* [32]'s analyses. By using an expanded COI dataset and a new SNP dataset, I re-examined this question. I found that the *H. fijiensis* population on Viti Levu has undergone a rapid and recent population increase that began ~3 kya, perhaps followed by a founder event from Kadavu. The population increase on Viti Levu broadly coincides with the arrival and escalation of habitat clearing on that island by humans, rather than climate change. In contrast to Viti Levu, the Kadavu population has remained stable for the past 11,500 years. I found no evidence of human- or climate-induced demographic change of *H. fijiensis* on Kadavu. I attribute the former to low levels of human habitation on Kadavu. Hence, Kadavu acts almost as a control for the impact of human modification of the environment on *H. fijiensis* demography.

My third chapter showed that recent changes in population demography can be resolved in tropical ectotherms, particularly multivoltine species. This chapter also provided empirical evidence that human modification of the environment has had major impacts on bee demography in the past. Genetic data for population demographic analyses do not exist for most species, particularly rare invertebrate species that otherwise receive very little research or conservation attention. In such cases, other collection and ecological data must be used to infer potential past patterns and threats.

By their very nature, rare species are difficult to study. Perhaps the rarest Australian tropical bee genus is *Pharohylaeus*. In Australia, *Pharohylaeus* is represented by a single species, *P. lactiferus*, which was last collected in 1923 when only six specimens were known. In my fourth chapter, I provided the first biological information on the species and undertook exploratory analyses in an attempt to explain the rarity of *P. lactiferus* and its possible extinction risks. For this chapter, I sampled much of Australia's east coast for this rare bee species. I only uncovered three populations and all individuals were collected within 200 m of one major vegetation subgroup (MVS) — tropical or subtropical rainforest [201]. My exploratory GIS analyses found that, compared to pre-European habitats [200], this MVS has decreased in area and become more-fragmented in the bioregions where *P. lactiferus* has been found. I also found that this MVS is susceptible to bushfires and has burnt every year in Queensland for which records exist. So far, I have only found this species visiting two plant species that both exhibit bird-pollination syndromes, *Stenocarpus sinuatus* and *Brachychiton acerifolius*, to the exclusion of other available floral resources. Potential habitat and floral specialisation might contribute to the rarity of *P. lactiferus*. These factors raise concerns about the conservation status of the bee, but further research is required for formal assessments to be made.

While these chapters are all published and most caveats are discussed within each, there are some common caveats worth discussing together. Particularly for chapters one through three where I had to rely heavily on the mitochondrial gene fragment, COI. While I do incorporate other information, particularly genomic SNP and morphological data, to corroborate these analyses, COI data alone can sometimes give spurious results. Issues with the COI marker can include the following. First, because mitochondria are maternally-inherited, COI can show different trends to genomic data and this should be considered when making inferences. In this thesis, I have used additional data (e.g., SNPs and morphology) to verify my COI results. Second, mitochondrial DNA can undergo selection events independent of genomic DNA due to different inheritance pathways or co-inherited parasites such as the bacterial genus, *Wolbachia*. I am aware that *Wolbachia* is present, and somewhat widespread, in the

Fijian *Homalictus* clade; however, its impacts are uncertain in most species and likely very limited in the case of *H. fijiensis* as it is not common in that species. This is the topic of ongoing research. Third, COI sequences can sometimes represent nuclear copies of mitochondrial genes (numts) [233] or associated parasites (e.g., *Wolbachia*) [234]. I have avoided the former by checking for stop codons and the latter by using BLAST to compare my sequences with available bee and *Wolbachia* data. Fourth, multiple mitochondrial lineages can be present in a single individual, resulting in 'mitochondrial heteroplasmy' which could potentially lead to spurious results [234]. Mitochondrial heteroplasmy can be detected as multiple peaks in chromatograms and, because I excluded sequences with ambiguous bases, this is unlikely to be a major issue in my dataset. Fifth, because COI is a relatively quickly-evolving gene that is often used for relatively-recent divergences, older nodes can be poorly-resolved. This is an issue in several of my phylogenies; however, I used SNP and morphological data (across major lineages) to mitigate this problem. Additionally, active research using ultra-conserved elements (genomic data) derived from the Fijian *Homalictus* supports the current COI-derived topology. Sixth, our mutation rate from *Caenorhabditis elegans* might be perceived as an issue when a similar rate is available for *Drosophila melanogaster*. However, all species have a similar AT bias (*C. elegans* = 69.6%, *D. melanogaster* = 70.3, and *H. fijiensis* = 74%) [161], there were very few neutral mutations detected in the direct-estimate of the *D. melanogaster* mutation rate [235], and our rate is consistent with contemporary mutation rates [160]. Finally, the deep divergence time of *H. fijiensis* could potentially imply the existence of still further cryptic *Homalictus* species. At present, I do not believe that our data support the existence of additional cryptic species diversity. This is because (i) there is no clear clustering of the more-divergent *H. fijiensis* lineages (Chapter 3; Fig. 1) and (ii) the morphological data, particularly male genitalia, do not indicate cryptic species. This question will be addressed further in a planned complete revision of the Fijian *Homalictus*.

These four chapters, as well as some of my other papers published during my PhD [62,182,232,236-240], expand our knowledge of tropical bee diversity. They also highlight that the diversity of tropical bees can be used to answer fundamental and important evolutionary and ecological questions relevant to other taxa. I have taken substantial steps towards understanding the systematics, evolution, demography, ecology, and future risks of the endemic Fijian bee fauna [99,139,182,232,241]. I also begin to build the foundational work required to understand and assess the Australia tropical bee species, *P. lactiferus* [242].

However, these advances also highlight that our understanding of both the Fijian and Australian bee fauna is poor and requires much more research. They also indicate that research into the bee fauna of the broader Pacific region is currently very inadequate.

Future research in these regions should first focus on understanding species diversity through taxonomic examinations. Once diversity is better-understood, many theoretical biogeographical, evolutionary, and ecological questions can be addressed. Because bees are widespread, diverse, and ecologically and economically important, they are an ideal clade to study. For the same reasons, it is important to understand potential anthropogenic threats to their diversity and abundance. Genetic analyses, and particularly phylogenomics, will be an invaluable tool to address many of these questions.

References

1. Gallai N, Salles J-M, Settele J, Vaissière BE. 2009 Economic valuation of the vulnerability of world agriculture confronted with pollinator decline. *Ecol. Econ.* **68**, 810–821. (doi:http://dx.doi.org/10.1016/j.ecolecon.2008.06.014)
2. Abrol DP. 2012 *Pollination biology: biodiversity conservation and agricultural production*. Dordrecht, Netherlands, Springer Science+Business Media B.V; 812 p.
3. Delaplane KS, Mayer DF. 2000 Bee pollination. In *Crop Pollination by Bees*, pp. 8–17. Wallingford, UK, CABI.
4. Winfree R, Gross BJ, Kremen C. 2011 Valuing pollination services to agriculture. *Ecol. Econ.* **71**, 80–88. (doi:http://dx.doi.org/10.1016/j.ecolecon.2011.08.001)
5. McGregor SE. 1976 *Insect pollination of cultivated crop plants*. Washington, USA, Agricultural Research Service, US Department of Agriculture; 411 p.
6. Roubik DW. 2002 The value of bees to the coffee harvest. *Nature* **417**, 708–708. (doi:https://doi.org/10.1038/417708a)
7. Williams GR, Tarpy DR, Vanengelsdorp D, Chauzat MP, Cox-Foster DL, Delaplane KS, Neumann P, Pettis JS, Rogers RE, Shutler D. 2010 Colony collapse disorder in context. *Bioessays* **32**, 845–846. (doi:https://doi.org/10.1002/bies.201000075)
8. Michener CD. 2007 *The Bees of the World, 2nd edition*. Baltimore, USA, Hopkins University Press; 992 p.
9. Klein A-M, Vaissière BE, Cane JH, Steffan-Dewenter I, Cunningham SA, Kremen C, Tscharntke T. 2007 Importance of pollinators in changing landscapes for world crops. *Proc Biol Sci* **274**, 303–313. (doi:https://doi.org/10.1098/rspb.2006.3721)
10. Batley M, Hogendoorn K. 2009 Diversity and conservation status of native Australian bees. *Apidologie* **40**, 347–354. (doi:https://doi.org/10.1051/apido/2009018)
11. Groom SVC, Schwarz MP. 2011 Bees in the Southwest Pacific: Origins, diversity and conservation. *Apidologie* **42**, 759–770. (doi:https://doi.org/10.1007/s13592-011-0079-8)
12. Dorey JB, Stevens MI, Castrillon AV, Schwarz MP. 2017 Drivers of speciation in Fijian *Homalictus* — past climate cycles and geographic isolation. *Swainsona Supplement* **5**, 62.
13. Matthews C. 2018 The curious case of Fijian *Homalictus*: how the initially underestimated native bee genus has risen in diversity [Honours]. Adelaide, Flinders University.
14. Warren BH, et al. 2015 Islands as model systems in ecology and evolution: prospects fifty years after MacArthur-Wilson. *Ecol. Lett.* **18**, 200–217. (doi:https://doi.org/10.1111/ele.12398)
15. MacArthur RH, Wilson EO. 1963 An equilibrium theory of insular zoogeography. *Evolution* **17**, 373–387. (doi:https://doi.org/10.2307/2407089)
16. MacArthur RH, Wilson EO. 1967 *The theory of island biogeography*. Princeton, USA, Princeton University Press; 224 p.
17. Heaney LR. 1986 Biogeography of mammals in SE Asia - estimates of rates of colonization, extinction and speciation. *Biol. J. Linn. Soc.* **28**, 127–165. (doi:https://doi.org/10.1111/j.1095-8312.1986.tb01752.x)
18. Whittaker RJ, Fernández-Palacios JM. 2007 *Island Biogeography: Ecology, Evolution, and Conservation*. 2nd ed. Oxford, UK, Oxford University Press; 416 p.

19. Fernandez-Palacios JM, Rijsdijk KF, Norder SJ, Otto R, de Nascimento L, Fernandez-Lugo S, Tjorve E, Whittaker RJ. 2016 Towards a glacial-sensitive model of island biogeography. *Global Ecol. Biogeogr.* **25**, 817–830. (doi:https://doi.org/10.1111/geb.12320)

20. Wroe S, Field J, Grayson DK. 2006 Megafaunal extinction: climate, humans and assumptions. *Trends Ecol. Evol.* **21**, 61–62. (doi:https://doi.org/10.1016/j.tree.2005.11.012)

21. Lima-Ribeiro MS, Nogués-Bravo D, Marske KA, Fernandez FAS, Araujo B, Diniz-Filho JAF. 2012 Human arrival scenarios have a strong influence on interpretations of the late Quaternary extinctions. *Proc. Natl. Acad. Sci. U.S.A.* **109**, E2409. (doi:https://doi.org/10.1073/pnas.1206920109)

22. Saltré F, Chadoeuf J, Peters KJ, McDowell MC, Friedrich T, Timmermann A, Ulm S, Bradshaw CJA. 2019 Climate-human interaction associated with southeast Australian megafauna extinction patterns. *Nat. Commun.* **10**, 5311. (doi:https://doi.org/10.1038/s41467-019-13277-0)

23. Lombardo U, Iriarte J, Hilbert L, Ruiz-Pérez J, Capriles JM, Veit H. 2020 Early Holocene crop cultivation and landscape modification in Amazonia. *Nature* **581**, 190–193. (doi:https://doi.org/10.1038/s41586-020-2162-7)

24. Dearing JA, Jones RT, Shen J, Yang X, Boyle JF, Foster GC, Crook DS, Elvin MJD. 2008 Using multiple archives to understand past and present climate–human–environment interactions: the lake Erhai catchment, Yunnan Province, China. *J. Paleolimnol.* **40**, 3–31. (doi:https://doi.org/10.1007/s10933-007-9182-2)

25. Roos CI, Field JS, Dudgeon JV. 2016 Anthropogenic burning, agricultural intensification, and landscape transformation in post-Lapita Fiji. *Journal of Ethnobiology* **36**, 535–553, 519. (doi:https://doi.org/10.2993/0278-0771-36.3.535)

26. Nunn PD, Kumar R, Matararaba S, Ishimura T, Seeto J, Rayawa S, Kuruyawa S, Nasila A, Oloni B, Ram AR. 2004 Early Lapita settlement site at Bourewa, southwest Viti Levu Island, Fiji. *Archaeol. Ocean.* **39**, 139–143. (doi:https://doi.org/10.1002/j.1834-4453.2004.tb00571.x)

27. Clark G, Anderson A. 2009 Colonisation and culture change in the early prehistory of Fiji. In *Terra Australis*, pp. 413–443. Canberra, Australia, ANU E Press.

28. Sánchez-Bayo F, Wyckhuys KAG. 2019 Worldwide decline of the entomofauna: a review of its drivers. *Biol. Conserv.* **232**, 8–27. (doi:https://doi.org/10.1016/j.biocon.2019.01.020)

29. Lister BC, Garcia A. 2018 Climate-driven declines in arthropod abundance restructure a rainforest food web. *Proc. Natl. Acad. Sci. U.S.A.* **115**, E10397. (doi:https://doi.org/10.1073/pnas.1722477115)

30. Hallmann CA, et al. 2017 More than 75 percent decline over 27 years in total flying insect biomass in protected areas. *PLOS ONE* **12**, e0185809. (doi:https://doi.org/10.1371/journal.pone.0185809)

31. Haddaway NR, Grames EM, Boyes DH, Saunders ME, Taylor NG. 2020 What evidence exists on conservation actions to conserve insects? A protocol for a systematic map of literature reviews. *Environ. Evid.* **9**, 30. (doi:https://doi.org/10.1186/s13750-020-00214-8)

32. Groom SVC, Stevens MI, Schwarz MP. 2013 Diversification of Fijian halictine bees: Insights into a recent island radiation. *Mol. Phylogen. Evol.* **68**, 582–594. (doi:https://doi.org/10.1016/j.ympev.2013.04.015)

33. Saunders ME, Janes JK, O'Hanlon JC. 2019 Moving on from the insect apocalypse narrative: engaging with evidence-based insect conservation. *Bioscience* **70**, 80-89. (doi:https://doi.org/10.1093/biosci/biz143)

34. Cockerell T. 1919 The metallic-colored halictine bees of the Philippine Islands. *Philipp J. Sci.* **15**, 9–14. (doi:https://doi.org/10.5962/bhl.part.11763)

35. Danforth BN, Ji S. 2001 Australian *Lasioglossum* + *Homalictus* form a monophyletic group: resolving the "Australian Enigma". *Syst. Biol.* **50**, 268–283. (doi:https://doi.org/10.1093/sysbio/50.2.268)

36. Gibbs J, Brady SG, Kanda K, Danforth BN. 2012 Phylogeny of halictine bees supports a shared origin of eusociality for *Halictus* and *Lasioglossum* (Apoidea: Anthophila: Halictidae). *Mol. Phylogen. Evol.* **65**, 926–939. (doi:https://doi.org/10.1016/j.ympev.2012.08.013)

37. Niu ZQ, Oremek P, Zhu CD. 2013 First record of the bee genus *Homalictus* Cockerell for China with description of a new species (Hymenoptera: Halictidae: Halictini). *Zootaxa* **3746**, 393–400. (doi:https://doi.org/10.11646/zootaxa.3746.2.9)

38. Grieve AC, Barnden BL, Howell RM, Kanishka AM, Stevens MI, Schwarz MP, Parslow BA. 2018 Reproductive ethology of the Fijian predator-inquiline wasp *Pseudofoenus extraneus* (Hymenoptera: Gasteruptiidae: Hyptiogastrinae). *Trans. R. Soc. S. Aust.*, 1–8. (doi:https://doi.org/10.1080/03721426.2018.1483186)

39. Staines M, Vo C, Puiu N, Hayes S, Tuiwawa M, Stevens MI, Schwarz MP. 2017 Pollen larceny of the tropical weed *Solanum torvum* by a Fijian endemic halictine bee with implications for the spread of plants with specialized pollinator requirements. *J. Trop. Ecol.* **33**, 183–187. (doi:https://doi.org/10.1017/S0266467417000098)

40. Houston TF. 2018 *A guide to native bees of Australia*. Clayton, Australia, CSIRO Publishing; 280 p.

41. Pauly A, Donovan B, Munzinger J. 2015 Les abeilles du genre *Homalictus* Cockerell, 1919 en Nouvelle-Calédonie (Hymenoptera: Apoidea: Halictidae). *Belg. J. Entomol.* **34**, 1–30.

42. Gollan JR, Ashcroft MB, Batley M. 2011 Comparison of yellow and white pan traps in surveys of bee fauna in New South Wales, Australia (Hymenoptera: Apoidea: Anthophila). *Aust. J. Entomol.* **50**, 174–178. (doi:https://doi.org/10.1111/j.1440-6055.2010.00797.x)

43. Groom SV, Stevens MI, Ramage T, Schwarz MP. 2017 Origins and implications of apid bees (Hymentopera: Apidae) in French Polynesia. *Entomol. Sci.* **20**, 65–75. (doi:https://doi.org/10.1111/ens.12230)

44. Hall M. 2018 Blue and yellow vane traps differ in their sampling effectiveness for wild bees in both open and wooded habitats. *Agric. For. Entomol.* **20**, 487–495. (doi:https://doi.org/10.1111/afe.12281)

45. Danforth BN, Eardley C, Packer L, Walker K, Pauly A, Randrianambinintsoa FJ. 2008 Phylogeny of Halictidae with an emphasis on endemic African Halictinae. *Apidologie* **39**, 86–101. (doi:https://doi.org/10.1051/apido:2008002)

46. Murao R, Lee H-S, Tadauchi O. 2015 Bees of the *Lasioglossum* series (Hymenoptera: Halictidae) in South Korea, with an illustrated keys to species. *Zootaxa* **4044**, 511–534. (doi:https://doi.org/10.11646/zootaxa.4044.4.3)

47. Groom SVC, Stevens MI, Schwarz MP. 2014 Parallel responses of bees to Pleistocene climate change in three isolated archipelagos of the southwestern Pacific. *Proc Biol Sci* **281**. (doi:https://doi.org/10.1098/rspb.2013.3293)

48. Perkins RCL, Cheesman LE. 1928 *Insects of Samoa and other Samoan terrestrial arthropods pt. I: fasc. 1*. London, UK, British Museum of Natural History; 16 p.

49. Dorey JB. 2017 Drivers of speciation in endemic Fijian bees: past climate cycles provide an alternative to the 'Taxon Cycle' in island biogeography theory [Honours]. Adelaide, Australia, Flinders University.

50. Hebert PDN, Penton EH, Burns JM, Janzen DH, Hallwachs W. 2004 Ten species in one: DNA barcoding reveals cryptic species in the neotropical skipper butterfly *Astraptes fulgerator*. *Proc. Natl. Acad. Sci. U.S.A.* **101**, 14812–14817. (doi:https://doi.org/10.1073/pnas.0406166101)

51. Folmer O, Black M, Hoeh W, Lutz R, Vrijenhoek R. 1994 DNA primers for amplification of mitochondrial cytochrome c oxidase subunit I from diverse metazoan invertebrates. *Mol. Mar. Biol. Biotechnol.* **3**, 294–299.

52. Ivanova NV, Dewaard JR, Hebert PDN. 2006 An inexpensive, automation-friendly protocol for recovering high-quality DNA. *Mol. Ecol. Notes* **6**, 998–1002. (doi:https://doi.org/10.1111/j.1471-8286.2006.01428.x)

53. Kearse M, et al. 2012 Geneiouos basic: an integrated and extendable desktop software platform for the organization and analysis of sequence data. *Bioinformatics* **28**, 1647–1649. (doi:https://doi.org/10.1093/bioinformatics/bts199)

54. Grant WS. 2015 Problems and cautions with sequence mismatch analysis and Bayesian skyline plots to infer historical demography. *J. Hered.* **106**, 333–346. (doi:https://doi.org/10.1093/jhered/esv020)

55. Joly S, Stevens MI, Jansen van Vuuren B. 2007 Haplotype networks can be misleading in the presence of missing data. *Syst. Biol.* **56**, 857–862. (doi:https://doi.org/10.1080/10635150701633153)

56. Drummond AJ, Suchard MA, Xie D, Rambaut A. 2012 Bayesian phylogenetics with BEAUti and the BEAST 1.7. *Mol. Biol. Evol.* **29**, 1969–1973. (doi:https://doi.org/10.1093/molbev/mss075)

57. Drummond AJ, Ho SYW, Phillips MJ, Rambaut A. 2006 Relaxed phylogenetics and dating with confidence. *PLoS Biol.* **4**, e88–e88. (doi:https://doi.org/10.1371/journal.pbio.0040088)

58. Yule GU. 1925 A mathematical theory of evolution, based on the conclusions of Dr. J. C. Willis, F. R. S. *Phil. Trans. R. Soc. B* **213**, 21. (doi:https://doi.org/10.1098/rstb.1925.0002)

59. Gernhard T. 2008 The conditioned reconstructed process. *J. Theor. Biol.* **253**, 769–778. (doi:https://doi.org/10.1016/j.jtbi.2008.04.005)

60. Drummond AJ, Rambaut A, Shapiro B, Pybus OG. 2005 Bayesian coalescent inference of past population dynamics from molecular sequences. *Mol. Biol. Evol.* **22**, 1185–1192. (doi:https://doi.org/10.1093/molbev/msi103)

61. Rambaut A, Suchard MA, Xie D, Drummond AJ. 2014 Tracer version 1.6, Available from http://beast.bio.ed.ac.uk/Tracer. Edinburgh, Scotland.

62. Leijs R, Dorey JB, Hogendoorn K. 2018 Twenty six new species of *Leioproctus (Colletellus)*: Australian Neopasiphaeinae, all but one with two submarginal cells (Hymenoptera, Colletidae, *Leioproctus*). *ZooKeys* **811**, 109–168. (doi:https://doi.org/10.3897/zookeys.811.28924)

63. Houston TF. 1975 A revision of the Australian hylaeine bees (Hymenoptera : Colletidae). I. Introductory material and the genera *Heterapoides* Sandhouse, *Gephyrohylaeus* Michener, *Huleoides* Smith, *Pharohylaeus* Michener, *Hemirhiza*

Michener, *Amphylaeus* Michener and *Meroglossa* Smith. *Australian Journal of Zoology Supplementary Series* **23**, 1–135. (doi:https://doi.org/10.1071/AJZS036)

64. Harris R. 1979 *A glossary of surface sculpturing*. Sacramento, California, California Department of Food and Agriculture, Bureau of Entomology; 31 p.
65. Michener CD. 1979 Genus *Homalictus* in Fiji (Hymenoptera, Halictidae). *Pac. Insects* **21**, 227–234.
66. ESRI. 2011 ArcGIS Desktop: release 10. Redlands CA, Environmental Systems Research Institute.
67. FLIS. 2017 Fiji Land Information System: Fiji digital elevation model at 25 m resolution.
68. Michener CD. 1965 *A classification of the bees of the Australian and South Pacific Regions*. New York, American Museum of Natural History; 362 p.
69. Dew RM, Stevens MI, Schwarz MP. 2018 Taxonomy of the Australian allodapine bee genus *Exoneurella* (Apidae: Xylocopinae: Allodapini) and description of a new *Exoneurella* species. *Insect Systematics and Diversity* **2**. (doi:https://doi.org/10.1093/isd/ixx013)
70. Stevens MI, D'Haese CA. 2017 Morphologically tortured: taxonomic placement of an Antarctic springtail (Collembola: Isotomidae) misguided by morphology and ecology. *Zool. Scr.* **46**, 180-187. (doi:https://doi.org/10.1111/zsc.12204)
71. Zhang F, Greenslade P, Stevens MI. 2017 A revision of the genus *Lepidobrya* Womersley (Collembola: Entomobryidae) based on morphology and sequence data of the genotype. *Zootaxa* **4221**, zootaxa. 4221.4225. 4222-zootaxa. 4221.4225. 4222. (doi:https://doi.org/10.11646/zootaxa.4221.5.2)
72. Zhang F, Jantarit S, Nilsai A, Stevens MI, Ding Y, Satasook C. 2018 Species delimitation in the morphologically conserved *Coecobrya* (Collembola: Entomobryidae): a case study integrating morphology and molecular traits to advance current taxonomy. *Zool. Scr.* **47**, 342-356. (doi:https://doi.org/10.1111/zsc.12279)
73. Kami SK, Miller SE. 1998 Samoan insects and related arthropods: checklist and bibliography. Honolulu, USA, B. Museum; 121 p.
74. Cheesman LE, Perkins RCL. 1939 Halictine bees from the New Hebrides and Banks Islands. *Trans. R. Entomol. Soc. Lond.* **88**, 161–171. (doi:https://doi.org/10.1111/j.1365-2311.1939.tb00254.x)
75. Krombein KV. 1950 The aculeate Hymenoptera of Micronesia II. Colletidae, Halictidae, Megachilidae, and Apidae. *Proc. Hawaii. Entomol. Soc.* **14**, 101–142.
76. Krombein KV. 1951 Additional notes on the bees of the Solomon Islands (Hymenoptera: Apoidea). *Proc. Hawaii. Entomol. Soc.* **14**, 227–295.
77. Pauly A. 1986 Les Abeilles de la sous-famille des Halictinae en Nouvelle-Guinée et dans L'archipel Bismarck (Hymenoptera: Apoidea: Halictidae). *Zool. Verh* **227**.
78. Crosby JL. 1970 The evolution of genetic discontinuity: computer models of the selection of barriers to interbreeding between subspecies. *Heredity* **25**, 253–297. (doi:https://doi.org/10.1038/hdy.1970.30)
79. Whittaker RJ, Triantis KA, Ladle RJ. 2008 A general dynamic theory of oceanic island biogeography. *J. Biogeogr.* **35**, 977–994. (doi:https://doi.org/10.1111/j.1365-2699.2008.01892.x)

80. Ricklefs RE, Bermingham E. 2002 The concept of the taxon cycle in biogeography. *Global Ecol. Biogeogr.* **11**, 353–361. (doi:https://doi.org/10.1046/j.1466-822x.2002.00300.x)

81. Silvertown J. 2004 The ghost of competition past in the phylogeny of island endemic plants. *J. Ecol.* **92**, 168–173. (doi:https://doi.org/10.1111/j.1365-2745.2004.00853.x)

82. Wiens JJ. 2004 Speciation and ecology revisited: phylogenetic niche conservatism and the origin of species. *Evolution* **58**, 193–197. (doi:https://doi.org/10.1111/j.0014-3820.2004.tb01586.x)

83. Wiens JJ, et al. 2010 Niche conservatism as an emerging principle in ecology and conservation biology. *Ecol. Lett.* **13**, 1310–1324. (doi:https://doi.org/10.1111/j.1461-0248.2010.01515.x)

84. Flantua S, Henry H. 2018 Historical connectivity and mountain biodiversity (with special reference to the Northern Andes). In *Mountains, Climate and Biodiversity* eds. C. Hoorn, A. Perrigo & A. Antonelli), pp. 171–185, 1 ed. Amsterdam, The Netherlands, Wiley-Blackwell.

85. Stewart JR, Lister AM, Barnes I, Dalén L. 2010 Refugia revisited: individualistic responses of species in space and time. *Proc Biol Sci* **277**, 661–671. (doi:https://doi.org/10.1098/rspb.2009.1272)

86. Harter DEV, Irl SDH, Seo B, Steinbauer MJ, Gillespie R, Triantis KA, Fernández-Palacios J-M, Beierkuhnlein C. 2015 Impacts of global climate change on the floras of oceanic islands – Projections, implications and current knowledge. *Perspect. Plant Ecol. Evol. Syst.* **17**, 160–183. (doi:https://doi.org/10.1016/j.ppees.2015.01.003)

87. Wilson EO. 1961 The nature of the taxon cycle in the Melanesian ant fauna. *Am. Nat.* **95**, 169–193. (doi:https://doi.org/10.1086/282174)

88. Economo EP, Sarnat EM. 2012 Revisiting the ants of Melanesia and the taxon cycle: historical and human-mediated invasions of a tropical archipelago. *Am. Nat.* **180**, E1–E16. (doi:https://doi.org/10.1086/665996)

89. Weigelt P, Steinbauer MJ, Cabral JS, Kreft H. 2016 Late Quaternary climate change shapes island biodiversity. *Nature* **532**, 99. (doi:https://doi.org/10.1038/nature17443)

90. Magnacca KN, Danforth BN. 2006 Evolution and biogeography of native Hawaiian *Hylaeus* bees (Hymenoptera: Colletidae). *Cladistics* **22**, 393–411. (doi:https://doi.org/10.1111/j.1096-0031.2006.00119.x)

91. Janzen DH. 1967 Why mountain passes are higher in the tropics. *Am. Nat.* **101**, 233–249. (doi:https://doi.org/10.1093/icb/icj003)

92. Tewksbury JJ, Huey RB, Deutsch CA. 2008 Putting the heat on tropical animals. *Science* **320**, 1296–1297. (doi:https://doi.org/10.1126/science.1159328)

93. Kellermann V, Van Heerwaarden B, Sgrò CM, Hoffmann AA. 2009 Fundamental evolutionary limits in ecological traits drive *Drosophila* species distributions. *Science* **325**, 1244–1246. (doi:https://doi.org/10.1126/science.1175443)

94. Addo-Bediako A, Chown SL, Gaston KJ. 2000 Thermal tolerance, climatic variability and latitude. *Proc Biol Sci* **267**, 739–745. (doi:https://doi.org/10.1098/rspb.2000.1065)

95. Pagel M. 1997 Inferring evolutionary processes from phylogenies. *Zool. Scr.* **26**, 331–348. (doi:https://doi.org/10.1111/j.1463-6409.1997.tb00423.x)

96. Pagel M, Meade A, Barker D. 2004 Bayesian estimation of ancestral character states on phylogenies. *Syst. Biol.* **53**, 673–684. (doi:https://doi.org/10.1080/10635150490522232)
97. Harmon L. 2019 *Phylogenetic Comparative Methods: Learning From Trees*. Seattle, USA, Createspace Independent Publishing Platform; 234 p.
98. Crichton A, Francis N, Doherty S, Tuiwawa M, Hayes S, Stevens MI, Schwarz MP. 2018 Low endemic bee diversity and very wide host range in lowland Fiji: support for the pollinator super-generalist hypothesis in island biogeography. *Pac. Conserv. Biol.* **25**, 135–142. (doi:https://doi.org/10.1071/PC18037)
99. Dorey JB, Schwarz MP, Stevens MI. 2019 Review of the bee genus *Homalictus* Cockerell (Hymenoptera: Halictidae) from Fiji with description of nine new species. *Zootaxa* **4674**, 1–46. (doi:https://doi.org/10.11646/zootaxa.4674.1.1)
100. Lemey P, Rambaut A, Welch JJ, Suchard MA. 2010 Phylogeography Takes a Relaxed Random Walk in Continuous Space and Time. *Mol. Biol. Evol.* **27**, 1877–1885. (doi:https://doi.org/10.1093/molbev/msq067)
101. Ash J. 1992 Vegetation ecology of Fiji: past, present and future perspectives. *Pac. Sci.* **46**, 111–127.
102. Department of Environment Fiji. 2014 Fiji's fifth national report to the United Nations convention on biological diversity.
103. Huybers P, Wunsch C. 2004 A depth-derived Pleistocene age model: uncertainty estimates, sedimentation variability, and nonlinear climate change. *Paleoceanography* **19**, PA1028 1021–1024. (doi:https://doi.org/10.1029/2002PA000857)
104. Colwell RK, Rangel TF. 2010 A stochastic, evolutionary model for range shifts and richness on tropical elevational gradients under Quaternary glacial cycles. *Philos T R Soc B* **365**, 3695–3707. (doi:https://doi.org/10.1098/rstb.2010.0293)
105. Weng C, Hooghiemstra H, Duivenvoorden JF. 2007 Response of pollen diversity to the climate-driven altitudinal shift of vegetation in the Colombian Andes. *Philos T R Soc B* **362**, 253–262. (doi:https://doi.org/10.1098/rstb.2006.1985)
106. Huybers P, Wunsch C. 2005 Obliquity pacing of the late Pleistocene glacial terminations. *Nature* **434**, 491–494. (doi:https://doi.org/10.1038/nature03401)
107. Hua X, Wiens JJ. 2010 Latitudinal variation in speciation mechanisms in frogs. *Evolution* **64**, 429–443. (doi:https://doi.org/10.1111/j.1558-5646.2009.00836.x)
108. Wilson EO. 1959 Adaptive shift and dispersal in a tropical ant fauna. *Evolution* **13**, 122–144. (doi:https://doi.org/10.1111/j.1558-5646.1959.tb02996.x)
109. Deutsch CA, Tewksbury JJ, Huey RB, Sheldon KS, Ghalambor CK, Haak DC, Martin PR. 2008 Impacts of climate warming on terrestrial ectotherms across latitude. *Proc. Natl. Acad. Sci. USA* **105**, 6668–6672. (doi:https://doi.org/10.1073/pnas.0709472105)
110. Vinagre C, Leal I, Mendonça V, Madeira D, Narciso L, Diniz MS, Flores AAV. 2016 Vulnerability to climate warming and acclimation capacity of tropical and temperate coastal organisms. *Ecol. Indicators* **62**, 317–327. (doi:https://doi.org/10.1016/j.ecolind.2015.11.010)
111. Parmesan C, Yohe G. 2003 A globally coherent fingerprint of climate change impacts across natural systems. *Nature* **421**, 37–42. (doi:https://doi.org/10.1038/nature01286)

112. Parmesan C. 2006 Ecological and evolutionary responses to recent climate change. *Annu. Rev. Ecol., Evol. Syst.* **37**, 637–669. (doi:https://doi.org/10.1146/annurev.ecolsys.37.091305.110100)

113. Freeman BG, Lee-Yaw JA, Sunday JM, Hargreaves AL. 2018 Expanding, shifting and shrinking: the impact of global warming on species' elevational distributions. *Global Ecol. Biogeogr.* **27**, 1268–1276. (doi:https://doi.org/10.1111/geb.12774)

114. Polato NR, et al. 2017 Genetic diversity and gene flow decline with elevation in montane mayflies. *Heredity* **119**, 107–116. (doi:https://doi.org/10.1038/hdy.2017.23)

115. Parmesan C, Galbraith H. 2004 *Observed ecological impacts of climate change in North America*. Arlington, VA, Pew Center on Global Climate Change.

116. Smith AT. 1974 The distribution and dispersal of pikas: influences of behavior and climate. *Ecology* **55**, 1368–1376. (doi:https://doi.org/10.2307/1935464)

117. Descimon H, Bachelard P, Boitier E, Pierrat V. 2005 Decline and extinction of *Parnassius apollo* populations in France-continued. *Studies on the Ecology and Conservation of Butterflies in Europe* **1**, 114–115.

118. Duarte H, Tejedo M, Katzenberger M, Marangoni F, Baldo D, Beltrán JF, Martí DA, Richter-Boix A, Gonzalez-Voyer A. 2012 Can amphibians take the heat? Vulnerability to climate warming in subtropical and temperate larval amphibian communities. *Global Change Biol.* **18**, 412–421. (doi:https://doi.org/10.1111/j.1365-2486.2011.02518.x)

119. Huey RB, Kearney MR, Krockenberger A, Holtum JAM, Jess M, Williams SE. 2012 Predicting organismal vulnerability to climate warming: roles of behaviour, physiology and adaptation. *Philos T R Soc B* **367**, 1665–1679. (doi:https://doi.org/10.1098/rstb.2012.0005)

120. Patiño J, et al. 2017 A roadmap for island biology: 50 fundamental questions after 50 years of the theory of island biogeography. *J. Biogeogr.* **44**, 963–983. (doi:https://doi.org/10.1111/jbi.12986)

121. Lanfear R, Calcott B, Ho SY, Guindon S. 2012 PartitionFinder: combined selection of partitioning schemes and substitution models for phylogenetic analyses. *Mol. Biol. Evol.* **29**, 1695–1701. (doi:https://doi.org/10.1093/molbev/mss020)

122. Lanfear R, Frandsen PB, Wright AM, Senfeld T, Calcott B. 2016 PartitionFinder 2: new methods for selecting partitioned models of evolution for molecular and morphological phylogenetic analyses. *Mol. Biol. Evol.* **34**, 772–773. (doi:https://doi.org/10.1093/molbev/msw260)

123. Guindon S, Dufayard JF, Lefort V, Anisimova M, Hordijk W, Gascuel O. 2010 New algorithms and methods to estimate maximum-likelihood phylogenies: assessing the performance of PhyML 3.0. *Syst. Biol.* **59**, 307–321. (doi:https://doi.org/10.1093/sysbio/syq010)

124. Bouckaert R, et al. 2019 BEAST 2.5: An advanced software platform for Bayesian evolutionary analysis. *PLoS Comp. Biol.* **15**. (doi:https://doi.org/10.1371/journal.pcbi.1006650)

125. Baele G, Lemey P, Bedford T, Rambaut A, Suchard MA, Alekseyenko AV. 2012 Improving the accuracy of demographic and molecular clock model comparison while accommodating phylogenetic uncertainty. *Mol. Biol. Evol.* **29**, 2157–2167. (doi:https://doi.org/10.1093/molbev/mss084)

126. Excoffier L, Laval LG, Schneider S. 2005 Arlequin ver. 3.0: An integrated software package for population genetics data analysis. *Evol. Bioinform. Online* **1**, 47–50. (doi:https://doi.org/10.1177/117693430500100003)

127. Jaccoud D, Peng K, Feinstein D, Kilian A. 2001 Diversity arrays: a solid state technology for sequence information independent genotyping. *Nucleic Acids Res.* **29**, E25–E25. (doi:https://doi.org/10.1093/nar/29.4.e25)

128. Gruber B, Unmack PJ, Berry OF, Georges A. 2018 dartr: An r package to facilitate analysis of SNP data generated from reduced representation genome sequencing. *Mol. Ecol. Resour.* **18**, 691–699. (doi:https://doi.org/10.1111/1755-0998.12745)

129. Paradis E, Schliep K. 2018 ape 5.0: an environment for modern phylogenetics and evolutionary analyses in R. *Bioinformatics* **35**, 526–528. (doi:https://doi.org/10.1093/bioinformatics/bty633)

130. Jombart T. 2015 A tutorial for discriminant analysis of principal components (DAPC) using adegenet 2.0.0. *London: Imperial College London, MRC Centre for Outbreak Analysis and Modelling*.

131. Jombart T. 2008 Adegenet: a R package for the multivariate analysis of genetic markers. *Bioinformatics* **24**, 1403–1405. (doi:https://doi.org/10.1093/bioinformatics/btn129)

132. Prescott GW, Williams DR, Balmford A, Green RE, Manica A. 2012 Quantitative global analysis of the role of climate and people in explaining late Quaternary megafaunal extinctions. *Proc. Natl. Acad. Sci. U.S.A.* **109**, 4527–4531. (doi:https://doi.org/10.1073/pnas.1113875109)

133. Prather CM, Pelini SL, Laws A, Rivest E, Woltz M, Bloch CP, Del Toro I, Ho CK, Kominoski J, Newbold TS. 2013 Invertebrates, ecosystem services and climate change. *Biol Rev* **88**, 327–348. (doi:https://doi.org/10.1111/brv.12002)

134. Mora C, Tittensor DP, Adl S, Simpson AG, Worm B. 2011 How many species are there on Earth and in the ocean? *PLoS Biol.* **9**, e1001127. (doi:https://doi.org/10.1371/journal.pbio.1001127)

135. Lorenzen ED, Nogués-Bravo D, Orlando L, Weinstock J, Binladen J, Marske KA, Ugan A, Borregaard MK, Gilbert MTP, Nielsen R. 2011 Species-specific responses of Late Quaternary megafauna to climate and humans. *Nature* **479**, 359-364. (doi:https://doi.org/10.1038/nature10574)

136. Bickel DJ. 2009 The first species described from Cape York amber, Australia: *Chaetogonopteron bethnorrisae* n. sp.(Diptera: Dolichopodidae). *Denisia* **86**, 35-39.

137. Labandeira CC, Sepkoski JJ. 1993 Insect diversity in the fossil record. *Science* **261**, 310-315. (doi:https://doi.org/10.1126/science.11536548)

138. Karr JA, Clapham ME. 2015 Taphonomic biases in the insect fossil record: shifts in articulation over geologic time. *Paleobiology* **41**, 16-32. (doi: https://doi.org/10.1017/pab.2014.3)

139. Dorey JB, Groom SVC, Freedman EH, Matthews CS, Davies OK, Deans EJ, Rebola C, Stevens MI, Lee MSY, Schwarz MP. 2020 Radiation of tropical island bees and the role of phylogenetic niche conservatism as an important driver of biodiversity. *Proc Biol Sci* **287**, 20200045. (doi:https://doi.org/10.1098/rspb.2020.0045)

140. Stevens GC. 1989 The latitudinal gradient in geographical range: how so many species coexist in the tropics. *Am. Nat.* **133**, 240–256. (doi:https://doi.org/10.1086/284913)

141. Taylor GK, Gascoyne J, Colley H. 2000 Rapid rotation of Fiji: paleomagnetic evidence and tectonic implications. *J. Geophys. Res.* **105**, 5771–5781. (doi:https://doi.org/10.1029/1999JB900305)

142. Kumar R, Nunn PD. 2003 Inland and coastal Lapita settlement on Vitilevu island, Fiji: new data. *Domodomo* **16**, 15–20.

143. Field JS. 2006 The prehistory of the interior of Viti Levu. *Domodomo* **19**, 7–19.

144. Anderson A, Roberts R, Dickinson W, Clark G, Burley D, de Biran A, Hope G, Nunn P. 2006 Times of sand: sedimentary history and archaeology at the Sigatoka Dunes, Fiji. *Geoarchaeology* **21**, 131–154. (doi:https://doi.org/10.1002/gea.20094)

145. Draper JT, et al. 2021 Extreme host range in an insular bee supports the super-generalist hypothesis with implications for both weed invasion and crop pollination. *Arthropod Plant Interact*. (doi:https://doi.org/10.1007/s11829-020-09799-w)

146. Pante E, Simon-Bouhet B. 2013 marmap: a package for importing, plotting and analyzing bathymetric and topographic data in R. *PLoS ONE* **8**, e73051. (doi:https://doi.org/10.1371/journal.pone.0073051)

147. Dorey JB, Groom SVC, Freedman EH, Matthews CS, Davies OK, Deans EJ, Rebola C, Stevens MI, Lee MSY, Schwarz MP. 2020 Radiation of tropical island bees and the role of phylogenetic niche conservatism as an important driver of biodiversity, v3, Dryad, Dataset.

148. Shams F, Dyer F, Thompson R, Duncan RP, Thiem JD, Kilian A, Ezaz T. 2019 Application of DArT seq derived SNP tags for comparative genome analysis in fishes; an alternative pipeline using sequence data from a non-traditional model species, *Macquaria ambigua*. *PLOS ONE* **14**, e0226365. (doi:https://doi.org/10.1371/journal.pone.0226365)

149. O'Leary SJ, Puritz JB, Willis SC, Hollenbeck CM, Portnoy DS. 2018 These aren’t the loci you’e looking for: Principles of effective SNP filtering for molecular ecologists. *Mol. Ecol.* **27**, 3193-3206. (doi:https://doi.org/10.1111/mec.14792)

150. Bandelt H-J, Forster P, Röhl A. 1999 Median-joining networks for inferring intraspecific phylogenies. *Mol. Biol. Evol.* **16**, 37–48. (doi:https://doi.org/10.1093/oxfordjournals.molbev.a026036)

151. Leigh JW, Bryant D. 2015 PopART: full-feature software for haplotype network construction. *Methods Ecol. Evol.* **6**, 1110–1116. (doi:https://doi.org/10.1111/2041-210X.12410)

152. Rogers AR, Harpending HC. 1992 Population growth makes waves in the distribution of pairwise genetic differences. *Mol. Biol. Evol.* **9**, 552–569. (doi:https://doi.org/10.1093/oxfordjournals.molbev.a040727)

153. Heller R, Chikhi L, Siegismund HR. 2013 The confounding effect of population structure on Bayesian skyline plot inferences of demographic history. *PloS one* **8**, e62992. (doi:https://doi.org/10.1371/journal.pone.0062992)

154. Ermolaeva MD. 2001 Synonymous codon usage in bacteria. *Curr. Issues Mol. Biol.* **3**, 91-97.

155. Altekar G, Dwarkadas S, Huelsenbeck JP, Ronquist F. 2004 Parallel Metropolis coupled Markov chain Monte Carlo for Bayesian phylogenetic inference. *Bioinformatics* **20**, 407–415. (doi:https://doi.org/10.1093/bioinformatics/btg427)

156. Rambaut A, Drummond AJ, Xie D, Baele G, Suchard MA. 2018 Posterior summarization in Bayesian phylogenetics using Tracer 1.7. *Syst. Biol.* **67**, 901–904. (doi:https://doi.org/10.1093/sysbio/syy032)

157. Bouckaert R, Vaughan TG, Barido-Sottani J, Duchêne S, Fourment M, Gavryushkina A, Heled J, Jones G, Kühnert D, De Maio N. 2019 BEAST 2.5: An advanced software platform for Bayesian evolutionary analysis. *PLoS Comp. Biol.* **15**, e1006650.

158. Denver DR, Morris K, Lynch M, Vassilieva LL, Thomas WK. 2000 High direct estimate of the mutation rate in the mitochondrial genome of *Caenorhabditis elegans*. *Science* **289**, 2342–2344. (doi:https://doi.org/10.1126/science.289.5488.2342)

159. Gratton P, Konopiński MK, Sbordoni V. 2008 Pleistocene evolutionary history of the Clouded Apollo (*Parnassius mnemosyne*): genetic signatures of climate cycles and a 'time-dependent' mitochondrial substitution rate. *Mol. Ecol.* **17**, 4248–4262. (doi:https://doi.org/10.1111/j.1365-294X.2008.03901.x)

160. Papadopoulou A, Anastasiou I, Vogler AP. 2010 Revisiting the insect mitochondrial molecular clock: the mid-Aegean trench calibration. *Mol. Biol. Evol.* **27**, 1659–1672. (doi:https://doi.org/10.1093/molbev/msq051)

161. BOLD. 2020 Barcode of Life System, https://www.boldsystems.org/index.php accessed on 19/Jun/2020.

162. Drummond AJ. 2016 FigTree version 1.4.3, available from http://tree.bio.ed.ac.uk/software/figtree/.

163. Colwell RK. 2013 EstimateS : Statistical estimation of species richness and shared species from samples. Version 9.1.0. User's Guide and application. *http://purl.oclc.org/estimates*.

164. Collin F-D, Durif G, Raynal L, Lombaert E, Gautier M, Vitalis R, Marin J-M, Estoup A. Submitted Extending approximate Bayesian computation with supervised machine learning to infer demographic history from genetic polymorphisms using DIYABC Random Forest. *Mol. Ecol. Resour.* (doi:https://doi.org/10.1111/1755-0998.13413)

165. Durif G, Collin F-D. 2021 diyabcGUI: Graphical User Interface for DYIABC-RF software. R package version 1.0.12. https://github.com/diyabc/diyabcGUI.

166. Ashfaq M, Hebert PDN, Mirza MS, Khan AM, Mansoor S, Shah GS, Zafar Y. 2014 DNA barcoding of *Bemisia tabaci* complex (Hemiptera: Aleyrodidae) reveals southerly expansion of the dominant whitefly species on cotton in Pakistan. *PLoS ONE* **9**. (doi:https://doi.org/10.1371/journal.pone.0104485)

167. López-Uribe MM, Cane JH, Minckley RL, Danforth BN. 2016 Crop domestication facilitated rapid geographical expansion of a specialist pollinator, the squash bee *Peponapis pruinosa*. *Proc Biol Sci* **283**, 20160443. (doi:https://doi.org/10.1098/rspb.2016.0443)

168. Papadopoulou A, Anastasiou I, Spagopoulou F, Stalimerou M, Terzopoulou S, Legakis A, Vogler AP. 2011 Testing the species–genetic diversity correlation in the Aegean archipelago: toward a haplotype-based macroecology? *Am. Nat.* **178**, 241-255. (doi:https://doi.org/10.1086/660828)

169. Johnson KP, Adler FR, Cherry JL. 2000 Genetic and phylogenetic consequences of island biogeography. *Evolution* **54**, 387-396. (doi:https://doi.org/10.1111/j.0014-3820.2000.tb00041.x)

170. McGlaughlin ME, Wallace LE, Wheeler GL, Bresowar G, Riley L, Britten NR, Helenurm K. 2014 Do the island biogeography predictions of MacArthur and Wilson hold when examining genetic diversity on the near mainland California Channel Islands? Examples from endemic *Acmispon* (Fabaceae). *Bot. J. Linn. Soc.* **174**, 289-304. (doi:https://doi.org/10.1111/boj.12122)

171. Fu Y-X. 1997 Statistical tests of neutrality of mutations against population growth, hitchhiking and background selection. *Genetics* **147**, 915-925. (doi:https://doi.org/10.1093/genetics/147.2.915)
172. Tajima F. 1989 Statistical method for testing the neutral mutation hypothesis by DNA polymorphism. *Genetics* **123**, 585–595. (doi:https://doi.org/10.1093/genetics/123.3.585)
173. Ray N, Currat M, Excoffier L. 2003 Intra-deme molecular diversity in spatially expanding populations. *Mol. Biol. Evol.* **20**, 76-86. (doi:https://doi-org.ezproxy.flinders.edu.au/10.1093/molbev/msg009)
174. Waples RK, Larson WA, Waples RS. 2016 Estimating contemporary effective population size in non-model species using linkage disequilibrium across thousands of loci. *Heredity* **117**, 233-240. (doi:https://doi.org/10.1038/hdy.2016.60)
175. Charlesworth B. 2009 Effective population size and patterns of molecular evolution and variation. *Nat. Rev. Genet.* **10**, 195-205. (doi:https://doi.org/10.1038/nrg2526)
176. Pulido-Santacruz P, Aleixo A, Weir JT. 2020 Genomic data reveal a protracted window of introgression during the diversification of a neotropical woodcreeper radiation. *Evolution* **74**, 842–858. (doi:https://doi.org/10.1111/evo.13902)
177. Peltier WR, Fairbanks RG. 2006 Global glacial ice volume and last glacial maximum duration from an extended Barbados sea level record. *Quat. Sci. Rev.* **25**, 3322–3337. (doi:https://doi.org/10.1016/j.quascirev.2006.04.010)
178. Stott L, Cannariato K, Thunell R, Haug GH, Koutavas A, Lund S. 2004 Decline of surface temperature and salinity in the western tropical pacific ocean in the holocene epoch. *Nature* **431**, 56–59. (doi:https://doi.org/10.1038/nature02903)
179. Morrison R, Clarke W. 1990 Soil erosion in Fiji-problems and perspectives. *Journal of the Japan Society of Erosion Control Engineering* **43**, 52–59. (doi:https://doi.org/10.11475/sabo1973.43.2_52)
180. Cronin SJ, Ferland MA, Terry JP. 2004 Nabukelevu volcano (Mt. Washington), Kadavu – a source of hitherto unknown volcanic hazard in Fiji. *J. Volcanol. Geotherm. Res.* **131**, 371–396. (doi:https://doi.org/10.1016/S0377-0273(03)00414-1)
181. Cockerell T. 1929 Descriptions and records of bees. — CXVIII. *Annals and Magazine of Natural History* **4**, 142-152. (doi:https://doi.org/10.1080/00222932908673036)
182. da Silva CRB, et al. 2021 Climate change and invasive species: a physiological performance comparison of invasive and endemic bees in Fiji. *J. Exp. Biol.* **224**, jeb230326. (doi:https://doi.org/10.1242/jeb.230326)
183. Friese H. 1914 *Die bienenfauna von Java*. Amsterdam, Nederlandse Entomologische Vereniging.
184. Silva CS, Cordeiro EMG, de Paiva JB, Dourado PM, Carvalho RA, Head G, Martinelli S, Correa AS. 2020 Population expansion and genomic adaptation to agricultural environments of the soybean looper, *Chrysodeixis includens*. *Evol Appl* **13**, 2071-2085. (doi:https://doi.org/10.1111/eva.12966)
185. Peltier WR. 2004 Global glacial isostasy and the surface of the ice-age Earth: the ICE-5G (VM2) model and GRACE. *Annu. Rev. Earth Planet. Sci.* **32**, 111–149. (doi:https://doi.org/10.1146/annurev.earth.32.082503.144359)
186. Vie J-C, Hilton-Taylor C, Stuart SN. 2009 Wildlife in a changing world: an analysis of the 2008 IUCN Red List of Threatened Species. Gland, Switzerland, IUCN; 180 p.

187. Bradshaw CJA. 2012 Little left to lose: deforestation and forest degradation in Australia since European colonization. *J. Plant. Ecol.* **5**, 109–120. (doi:https://doi.org/10.1093/jpe/rtr038)
188. Evans MC. 2016 Deforestation in Australia: drivers, trends and policy responses. *Pac. Conserv. Biol.* **22**, 130–150. (doi:https://doi.org/10.1071/PC15052)
189. Reside AE, Beher J, Cosgrove AJ, Evans MC, Seabrook L, Silcock JL, Wenger AS, Maron M. 2017 Ecological consequences of land clearing and policy reform in Queensland. *Pac. Conserv. Biol.* **23**, 219–230. (doi:https://doi.org/10.1071/PC17001)
190. Hurlbert AH, Jetz W. 2007 Species richness, hotspots, and the scale dependence of range maps in ecology and conservation. *Proc. Natl. Acad. Sci. USA* **104**, 13384. (doi:https://doi.org/10.1073/pnas.0704469104)
191. Crisp MD, Laffan S, Linder HP, Monro A. 2001 Endemism in the Australian flora. *J. Biogeogr.* **28**, 183–198. (doi:https://doi.org/10.1046/j.1365-2699.2001.00524.x)
192. Orme CDL, et al. 2005 Global hotspots of species richness are not congruent with endemism or threat. *Nature* **436**, 1016–1019. (doi:https://doi.org/10.1038/nature03850)
193. Smith T. 2018 *The Australian bee genera: an annotated, user-friendly key*. Armidale, Australia, The Radar Community Ecology Lab; 116 p.
194. Cockerell TDA. 1910 Descriptions and records of bees. XXX. *Ann. Mag. Nat. Hist.* **6**, 17–31. (doi:https://doi.org/10.1080/00222931008692817)
195. Hirashima Y, Roberts H. 1986 Discovery of the bee genus *Pharohylaeus* Michener from Papua New Guinea, with description of a new species (Hymenoptera, Colletidae). *Esakia* **24**, 63–66.
196. ALA. 2019 Apiformes — Atlas of Living Australia occurrence download at https://biocache.ala.org.au/occurrences/search?q=lsid%3Aurn%3Alsid%3Abiodiversity.org.au%3Aafd.taxon%3A6992b8f3-0ac3-4631-90d1-a2feec592659 accessed on Fri Oct 25 23:39:58 AEDT 2019.
197. QGIS Development Team. 2020 QGIS geographic information system. Open Source Geospatial Foundation Project. http://qgis.osgeo.org.
198. R Development Core Team. 2019 R: a language and environment for statistical computing. Vienna, Austria.
199. Wickham H. 2016 *ggplot2: Elegant graphics for data analysis*. New York, Springer-Verlag; 226 p.
200. NMD. 2003 Vegetation - Pre-European Settlement (1788).
201. NMD. 2003 Vegetation - Post-European Settlement (1988).
202. DEE. 2017 Interim biogeographic regionalisation for Australia (IBRA), version 7 (Regions) - states and territories.
203. Floyd AG. 1978 *NSW rainforest trees part VII: Families Proteaceae, Santalaceae, Nyctaginaceae, Gyrostemonaceae, Annonaceae, Eupomatiaceae, Monimiaceae*. Sydney, NSW, Forestry Commission of NSW; 78 p.
204. Foreman DB. 2020 *Stenocarpus sinuatus,* in (ed.), Flora of Australia. Australian Biological Resources Study, Department of Agriculture, Water and the Environment. Accessed on 04/Dec/2020 from https://profiles.ala.org.au/opus/foa/profile/Stenocarpus%20sinuatus
205. Guymer G. 1988 A taxonomic revision of *Brachychiton* (Sterculiaceae). *Aust. Syst. Bot.* **1**, 199–323. (doi:https://doi.org/10.1071/SB9880199)

206. Beck HE, Zimmermann NE, McVicar TR, Vergopolan N, Berg A, Wood EF. 2018 Present and future Köppen-Geiger climate classification maps at 1-km resolution. *Scientific Data* **5**, 180214. (doi:https://doi.org/10.1038/sdata.2018.214)

207. Almeida EAB. 2008 Colletidae nesting biology (Hymenoptera: Apoidea). *Apidologie* **39**, 16–29. (doi:https://doi.org/10.1051/apido:2007049)

208. Hearn LR, Williams KA, Stevens MI, Schwarz MP, Davies OK, Parslow BA. 2019 Description and novel host records for a new species of Australian mutillid wasp (Hymenoptera: Mutillidae) from hylaeine bee nests (Hymenoptera: Colletidae). *Austral Entomol.* **58**, 524–532. (doi:https://doi.org/10.1111/aen.12414)

209. Dew R, Schwarz M. 2013 Distribution of the native South Australian bee *Exoneurella tridentata i*n Western Myall (*Acacia papyrocarpa*) woodlands. *S. Aust. Nat.* **87**, 70–74.

210. Williams G, Adam P. 2010 *The Flowering of Australia's Rainforests: A Plant and Pollination Miscellany*. Collingwood, Victoria, CSIRO Publishing; 217 p.

211. Nicolson SW, Van Wyk B-E. 1998 Nectar Sugars in Proteaceae: Patterns and Processes. *Aust. J. Bot.* **46**, 489–504. (doi:https://doi.org/10.1071/BT97039)

212. Shrestha M, Dyer AG, Boyd-Gerny S, Wong BBM, Burd M. 2013 Shades of red: bird-pollinated flowers target the specific colour discrimination abilities of avian vision. *New Phytol.* **198**, 301-310. (doi:https://doi.org/10.1111/nph.12135)

213. Dyer AG, Garcia JE, Shrestha M, Lunau K. 2015 Seeing in colour: a hundred years of studies on bee vision since the work of the Nobel laureate Karl von Frisch. *Proc. R. Soc. Vic.* **127**, 66–72. (doi:https://doi.org/10.1071/RS15006)

214. Peitsch D, Fietz A, Hertel H, de Souza J, Ventura DF, Menzel R. 1992 The spectral input systems of hymenopteran insects and their receptor-based colour vision. *J. Comp. Physiol. A Neuroethol. Sens. Neural. Behav. Physiol.* **170**, 23–40. (doi:https://doi.org/10.1007/BF00190398)

215. Horridge A. 1998 Bees see red. *Trends Ecol. Evol.* **13**, 87-88. (doi:https://doi.org/10.1016/S0169-5347(97)01315-3)

216. Roubik DW. 1993 Tropical pollinators in the canopy and understory: field data and theory for stratum “preferences”. *J. Insect Behav.* **6**, 659–673. (doi:https://doi.org/10.1007/BF01201668)

217. Tucker BNIJ. 2000 Linkage restoration: interpreting fragmentation theory for the design of a rainforest linkage in the humid Wet Tropics of north-eastern Queensland. *Ecol. Manage. Restor.* **1**, 35–41. (doi:https://doi.org/10.1046/j.1442-8903.2000.00006.x)

218. Sutherland W, Dicks L, Showler D. 2010 *Bee Conservation: evidence for the effects of interventions*. Exeter, UK, Pelagic Publishing; 147 p.

219. Cockerell T. 1910 Descriptions and records of bees. XXXI. *Annals and Magazine of Natural History* **8**, 160–168.

220. Fabricius JC. 1775 *Systema entomologiae, sistens insectorum classes, ordines, genera, species, adjectis synonymis, locis, descriptionibus, observationibus*, Flensbvrgi et Lipsiae: In Officina Libraria Kortii; 832 p.

221. Keys RN, Buchmann SL, Smith SE. 1995 Pollination Effectiveness and Pollination Efficiency of Insects Foraging *Prosopis velutina* in South-Eastern Arizona. *J. Appl. Ecol.* **32**, 519–527. (doi:10.2307/2404649)

222. Ballantyne G, Baldock KCR, Rendell L, Willmer PG. 2017 Pollinator importance networks illustrate the crucial value of bees in a highly speciose plant community. *Scientific Reports* **7**, 8389. (doi:10.1038/s41598-017-08798-x)
223. DSITI. 2017 Landsat fire scars (1988-2016) Queensland.
224. DAWE. 2020 National Indicative Aggregated Fire Extent Dataset v20200525.
225. Jung M. 2016 LecoS — A python plugin for automated landscape ecology analysis. *Ecol. Inform.* **31**, 18–21. (doi:http://dx.doi.org/10.1016/j.ecoinf.2015.11.006)
226. DNRME. 2019 Baseline roads and tracks - Queensland.
227. Ewers RM, Didham RK. 2006 Confounding factors in the detection of species responses to habitat fragmentation. *Biol Rev* **81**, 117–142. (doi:https://doi.org/10.1017/S1464793105006949)
228. Forbes T, Tatham H. 2018 From rainforest to cinders: national park may take 'hundreds of years' to recover from bushfire disaster. ABC Tropical North. (https://www.abc.net.au/news/2018-12-04/eungella-rainforest-future-questioned-by-expert/10578802)
229. CSIRO and BOM. 2015 Climate change in Australia information for Australia’s natural resource management regions: Technical report. 222 p.
230. ALA. 2020 *Brachychiton acerifolius* — Atlas of Living Australia occurrence download at https://biocache.ala.org.au/occurrences/search?q=qid:1589866722024 accessed on Tue May 19 15:39:03 AEST 2020.
231. ALA. 2020 *Stenocarpus sinuatus* — Atlas of Living Australia occurrence download at https://biocache.ala.org.au/occurrences/search?q=qid:1589866831488 accessed on Tue May 19 15:40:44 AEST 2020.
232. Ibalim S, Groom SVC, Dorey JB, Velasco-Castrillon A, Schwarz MP, Stevens MI. 2020 Origin and dispersal of *Homalictus* (Apoidea: Halictidae) across Australia, Papua New Guinea and Pacific. *Trans. R. Soc. S. Aust.*, 1–14. (doi:https://doi.org/10.1080/03721426.2020.1740957)
233. Buhay JE. 2009 “COI-like” Sequences Are Becoming Problematic in Molecular Systematic and DNA Barcoding Studies. *J. Crust. Biol.* **29**, 96-110. (doi:10.1651/08-3020.1)
234. Davies OK. 2021 Mitochondrial heteroplasmy in Australian native bee *Amphylaeus morosus* and its association with the parasite *Wolbachia*. Adelaide, Australia, Flinders University.
235. Haag-Liautard C, Coffey N, Houle D, Lynch M, Charlesworth B, Keightley PD. 2008 Direct estimation of the mitochondrial DNA mutation rate in *Drosophila melanogaster*. *PLoS Biol.* **6**, 1706–1714. (doi:10.1371/journal.pbio.0060204)
236. Leijs R, Dorey JB, Hogendoorn K. 2020 The genus *Amegilla* (Hymenoptera, Apidae, Anthophorini) in Australia: a revision of the subgenus *Asaropoda*. *ZooKeys* **908**, 45–122. (doi:https://doi.org/10.3897/zookeys.908.47375)
237. Dorey JB, Fagan-Jeffries EP, Stevens MI, Schwarz MP. 2020 Morphometric comparisons and novel observations of diurnal and low-light-foraging bees. *J. Hymenoptera Res.* **79**, 117–144. (doi:https://doi.org/10.3897/jhr.79.57308)
238. Dorey JB. 2018 *Bees of Australia: A Photographic Exploration*. Clayton, Australia, CSIRO Publishing; 224 p.
239. Dorey JB, et al. 2021 Continental risk assessment for understudied taxa post catastrophic wildfire indicates severe impacts on the Australian bee fauna. *Global Change Biol.* **27**. (doi:https://doi.org/10.1111/gcb.15879)

240. Naaz ZT, Bibi R, Dorey JB. 2021 Current status of bees in Fiji; geographical distribution and role in pollination of crop plants. *Orient. Insects* **Taylor & Francis**, 1-27. (doi:https://doi.org/10.1080/00305316.2021.1982043)

241. Dorey JB, Groom SVC, Velasco-Castrillón A, Stevens MI, Lee MSY, Schwarz MP. 2021 Holocene population expansion of a tropical bee coincides with early human colonisation of Fiji rather than climate change. *Mol. Ecol.* **30**. (doi:https://doi.org/10.1111/mec.16034)

242. Dorey JB. 2021 Missing for almost 100 years: the rare and potentially threatened bee *Pharohylaeus lactiferus* (Hymenoptera, Colltidae). *J. Hymenoptera Res.* **81**, 165-180. (doi: https://doi.org/10.3897/jhr.81.59365)

Thesis appendices

Introduction to thesis appendices

My thesis appendices include the email responses, or licences, from journals confirming permission to reproduce parts of publications. Supplementary materials, or links to them, can be found near the end of the relevant thesis chapters.

Thesis appendix 1: permissions to reproduce publications

Permission to reproduce “Review of the bee genus *Homalictus* Cockerell (Hymenoptera: Halictidae) from Fiji with description of nine new species”

On 19 April 2021 at 12:23:12 pm, Zhi-Qiang Zhang (zhangz@landcareresearch.co.nz) wrote:

Dear James:

I herein grant your permission to reproduce the images/text from Zootaxa* on two conditions. In addition to citing the paper, you will need to indicate that the reproduction of text/image is permitted, e.g. mention “reproduced with permission from copyright holder” in your thesis.

*Requested materials:
Review of the bee genus Homalictus *Cockerell (Hymenoptera: Halictidae) from Fiji with description of nine new species* (https://doi.org/10.11646/zootaxa.4674.1.1

Please keep this letter for legal purpose.

Zhi-Qiang Zhang
Chief editor/publisher of Magnolia Press

Permission to reproduce “Radiation of tropical island bees and the role of phylogenetic niche conservatism as an important driver of biodiversity”

On 19 April 2021 at 4:17:18 pm, proceedingsb (proceedingsb@royalsociety.org) wrote:
Dear James,

You are not permitted to publish our typeset version of the paper but you are able to publish your own version.

Best wishes

Jennifer

Permission to reproduce “Holocene population expansion of a tropical bee coincides with early human colonisation of Fiji rather than climate change”

JOHN WILEY AND SONS LICENSE
TERMS AND CONDITIONS

Jul 17, 2021

This Agreement between Flinders University -- James Dorey ("You") and John Wiley and Sons ("John Wiley and Sons") consists of your license details and the terms and conditions provided by John Wiley and Sons and Copyright Clearance Center.

License Number: 5111260463113
License date: Jul 17, 2021
Licensed Content Publisher: John Wiley and Sons
Licensed Content Publication: Molecular Ecology
Licensed Content Title: Holocene population expansion of a tropical bee coincides with early human colonization of Fiji rather than climate change
Licensed Content Author: James B. Dorey, Scott V. C. Groom, Alejandro Velasco-Castrillón, et al
Licensed Content Date: Jul 16, 2021
Licensed Content Volume: 0
Licensed Content Issue: 0
Licensed Content Pages: 18
Type of use Requestor type Format Portion: Dissertation/Thesis
Will you be translating? No
Title: The systematics, evolution and extinction risks of tropical bees Flinders University
Institution name: Flinders University
Expected presentation date: Aug 2021

Permission to reproduce “Missing for almost 100 years: the rare and potentially threatened bee, *Pharohylaeus lactiferus* (Hymenoptera, Colletidae)”

On 19 April 2021 at 5:18:51 pm, Editorial Office (journals@pensoft.net) wrote:
Dear James,

You suspect right - there is no need to ask for permission, as JHR publishes under the **Creative Commons Attribution License (CC BY 4.0)**. (it is indicated in this on the website: https://jhr.pensoft.net/about#CopyrightNotice). Moreover, according to it "Copyright on any article is retained by the author(s)." So feel free to use it and all the best with your PhD thesis!

Best wishes,
Boriana
--
Boriana Ovcharova
Managing Editor
Pensoft Publishers
ARPHA Journal Publishing Platform
12 Prof. Georgi Zlatarski Street
1700 Sofia, Bulgaria
Tel +359-2-8704281
Fax +359-2-8704282
Publishing services for journals: https://arphahub.com/about/services
Books published by Pensoft: https://pensoft.net/books
Services for scientific projects: https://pensoft.net/projects
Find us on: Facebook, Twitter